



Università degli Studi di Ferrara

DOTTORATO DI RICERCA IN
"FISICA"

CICLO **XXIX**

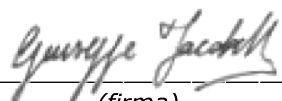
COORDINATORE **Prof. VINCENZO GUIDI**

**Higgs connections:
Electroweak Vacuum Stability and Cosmology**

Settore Scientifico Disciplinare **FIS/02**

Dottorando

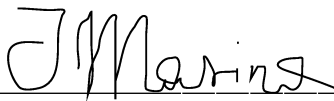
Dott. **IACOBELLIS GIUSEPPE**



(firma)

Tutore

Prof. **MASINA ISABELLA**



(firma)

Anni 2014/2016

*Nature uses the longest threads to weave her patterns,
so that each small piece of her fabric reveals
the organization of the entire tapestry.*

— Richard P. Feynman

DECLARATION

The work presented in this thesis was carried out at the **Dipartimento di Fisica e Scienze della Terra, Università di Ferrara (Italy)**, funded by a three-year scholarship of the **Agenzia Spaziale Italiana (ASI)**.

An additional financial support was provided by the **Istituto Nazionale di Fisica Nucleare (INFN) - section of Ferrara**, through the **PRIN** project "Theoretical Astroparticle Physics" (TASP).

The work done led to the publication of one paper and one proceeding:

1. **G. Iacobellis** and I. Masina, "*Stationary configurations of the Standard Model Higgs potential: Electroweak stability and rising inflection point*", **Phys.Rev.D 94 (2016) no.7, 073005 [1]**.
2. **G. Iacobellis**, "*Next-to-Next-to-Leading Order analysis of the electroweak vacuum stability and rising inflection point*", 28th Rencontres de Blois Proceedings, Conference: 16-05-29, **arXiv:1609.09228**.

On the content of these works are based **Chapter 3** and **Chapter 4**. **Chapter 5** and **Chapter 6** are instead based on unpublished work, carried out in collaboration with dr. Isabella Masina. It led to a substantial confirmation of the results already present in the literature.

Ferrara, march 2017

Giuseppe Iacobellis

Higgs connections: Electroweak Vacuum Stability and Cosmology

Giuseppe Iacobellis

March 19, 2017

Short abstract

The Higgs boson discovery carries with it the possibility to study the Standard Model up to the edge of its validity, deciding whether the actual configuration of the theory is absolutely stable or metastable, with the appearance of a second vacuum that could be more or less energetic, respectively, than the the electroweak one.

We provide an accurate up-to-date analysis, taking advantage of the updated experimental data, of the Standard Model stability, wondering if, by means of different configurations within and beyond the Standard Model (anyhow keeping the extensions on a minimal ground), the Higgs field could play the role of the inflaton in the early Universe.

Keywords: *Standard Model, Higgs boson, Stability, Criticality, Top Mass, Cosmology, Inflation, Planck, Inflection point, Non-minimal coupling, B-L.*

SOMMARIO

La scoperta del bosone di Higgs a LHC e la determinazione del valore della sua massa ha aperto la possibilità di studiare il Modello Standard fino ad alte energie, rendendo possibile la verifica della consistenza della teoria e del suo range di validità, dal momento che lo consideriamo come un modello effettivo.

In questo scenario, facendo uso dei dati sperimentali più aggiornati, molto interesse è stato riposto nello studio della stabilità del vuoto elettrodebole del Modello Standard e le sue particolari implicazioni sia nella fisica delle particelle che, soprattutto, in cosmologia.

Il nostro lavoro [1] si inserisce in questo contesto con un doppio fine: da un lato, proviamo a raffinare i più recenti calcoli dei vincoli di stabilità, alla luce dei dati sperimentali e degli approcci teorici più aggiornati, soprattutto relativi alla tecnica del potenziale effettivo; mentre, dall'altro lato, usiamo i risultati di questa analisi per studiare e porre vincoli ad alcune realizzazioni di inflazione cosmica nel contesto del puro Modello Standard e di sue estensioni minime.

In particolare, abbiamo studiato alcune osservabili *gauge*-indipendenti legate a due configurazioni stazionarie del potenziale del Modello Standard, estrapolato ad alte energie grazie all'approccio che fa uso del potenziale effettivo e delle equazioni del gruppo di rinormalizzazione, nella loro forma più aggiornata, vale a dire il NNLO: il valore della massa del quark top in corrispondenza del quale si ha la stabilità del vuoto elettrodebole (criticality) e il potenziale valutato nel suo punto di flesso.

Dimostrata l'indipendenza dalla scelta del *gauge* di queste osservabili, sono state stimate le incertezze relative. Il primo risultato rilevante, in accordo con [2] e, con qualche piccola discrepanza, con [3, 4], è che la stabilità assoluta del Modello Standard non è completamente esclusa, data l'attuale finestra sperimentale: è, in linea di principio, possibile assumere il Modello Standard valido fino alla scala di Planck, dove ci aspettiamo che l'interazione gravitazionale cominci a diventare rilevante, senza alcuna inclusione di nuova fisica a basse scale energetiche ("*desert scenario*").

Partendo da questo punto, abbiamo provato a spiegare la fase inflazionaria primordiale all'interno del puro Modello Standard, sfruttando la configurazione del punto di flesso. Tuttavia, mostriamo che diventa in questi casi molto difficile riprodurre gli attuali vincoli sul rapporto tensore/scalare.

Vista la necessità di introdurre nuovi gradi di libertà per includere nella teoria un ragionevole meccanismo per l'inflazione cosmica e, in maniera consistente, una stabilizzazione per il potenziale del Modello Standard, proviamo a passare in rassegna le principali caratteristiche di una delle possibili estensioni minime al Modello Standard, attraverso una simmetria globale $U(1)_{B-L}$, e a porre dei vincoli ai parametri propri del nuovo modello, in maniera tale da riuscire a raggiungere entrambi gli obiettivi. Lo scalare extra associato alla rottura di questa nuova simmetria, oltre a garantire la stabilizzazione mediante un effetto di soglia al *tree-level*, sarebbe responsabile della generazione della massa di un neutrino *right-handed*, che, a sua volta, fornisce, attraverso il meccanismo *see saw* di tipo I, le masse dei neutrini di bassa energia. In questo

contesto, troviamo la finestra dei parametri accessibile sia per una fase inflazionaria funzionale, guidata dallo stesso scalare massivo, che per la stabilizzazione del modello: confermiamo i risultati riportati in letteratura [5, 6, 7], nonostante i lavori rilevanti svolgono le loro analisi o in configurazioni leggermente differenti, oppure raffrontano i loro risultati con vincoli sperimentali più datati, giungendo poi dunque a conclusioni diverse. Ad ogni modo, il risultato globale sembra essere perfettamente compatibile: facendo riferimento allo stato dell'arte attuale dal punto di vista sperimentale, questa semplice realizzazione di estensione con nuova fisica del Modello Standard sembra non essere sufficiente, evidenziando le difficoltà a voler risolvere i nostri due obiettivi primari in un solo colpo.

L'altra modifica al Modello Standard che consideriamo è basata sull'inclusione di un accoppiamento non minimale tra il campo di Higgs, che ancora una volta ricopre il ruolo di inflatone, e la gravità: questa idea era stata proposta diversi anni fa ed è ancora molto discussa. Qui proviamo a porre qualche vincolo sul rapporto tensore/scalare nel modello di *Higgs inflation* originario, in questo rivisto alla luce dei recenti sviluppi sulla scelta della prescrizione di rinormalizzazione: in maniera tale da aggirare le difficoltà intrinseche della teoria a livello di unitarietà, analizziamo lo spazio dei parametri relativo ai bassi ξ , sfruttando la già citata configurazione di punto di flesso. I nostri risultati, oltre a confermare la robustezza delle predizioni inflazionarie del modello al variare delle correzioni radiative, già mostrata nel recente passato [8], mostrano qualche problema a spingere l'accoppiamento non minimale verso valori piccoli, lasciando invariate le altre osservabili ormai ben note. Queste conclusioni non aggiungono nulla a quanto noto dalla letteratura più recente [si veda ancora, ad esempio [8]].

ABSTRACT

The discovery of the Higgs boson at LHC and the determination of its mass value have opened up the possibility to study the SM up to very high energies, in order to probe the consistency of the theory and its range of validity, considering the model as an effective one.

In this framework, equipped with the latest experimental data, a lot of interest has been devoted to the study of the stability of the Standard Model electroweak vacuum and the peculiar implications both in particle physics and, mostly, in cosmology.

Our work [1] fits in this scenario with a two-fold aim: on one side, we try to refine the latest calculations of the stability bounds, in the light of updated experimental data and new theoretical approaches in the improved effective potential technique; while, on the other side, we take advantage of this analysis in order to investigate and constrain some realisation of the primordial inflationary phase within the pure SM and its some minimal extensions.

In particular, we studied the gauge-independent observables related to two interesting stationary configurations of the SM potential, extrapolated up to high energies by means of the state-of-the-art RGE-improved effective potential approach, namely the NNLO: the value of the top quark mass which ensures the electroweak vacuum stability (criticality) and the potential evaluated at the inflection point.

Proved the gauge independence of these observables, there were estimated in detail the uncertainties related. The first main result, in agreement with [2] and, with some minor discrepancies [3, 4], is that the SM absolute stability is not completely excluded, given the current experimental data: it is possible to assume the theory valid up to the Planck scale, at which we suppose that the gravitational interaction starts to be relevant, without any inclusion of new physics at low energy (“desert scenario”).

Starting from this point, we tried to explain the inflationary phase embedded in a pure SM scenario, exploiting the inflection point configuration. However, we showed that it turns out to be impossible to reproduce the most recent bounds on the primordial tensor-to-scalar-ratio in the sight of SM inflection point models.

Being necessary the introduction of new degrees of freedom, in order to include a reasonable inflationary expansion and, consistently, the stabilisation of the SM potential, we try to review the main features of a minimal extension of the SM, through a global $U(1)_{B-L}$ symmetry and try to constrain its parameters so as to achieve both our goals. The extra scalar singlet associated with the breaking of this new symmetry, granting the stabilisation through an induced tree-level threshold effect, would be responsible of the generation of the right-handed neutrino mass, which in turn would provide, via the type I see-saw mechanism, the masses of the low-energy neutrinos. In this framework, we found the parameter window attainable for both a successfully inflationary phase, driven by the same heavy scalar, and the stabilisation of the model: we confirm the results reported in the literature [5, 6, 7], although the related works carry out the analysis in slightly different setups and often comparing the results to different experimental bounds, leading to different conclusions. However, the overall

outcome is perfectly compatible: sticking with the current experimental state-of-the-art, this very simple realisation of new-physics extension of the SM seems to be insufficient, and we stress the troubles which arise if we try to achieve our initial tasks in one single shot.

The other modification of the SM that we consider deals with the inclusion of a non-minimal coupling between the Higgs field, still playing the role of inflaton, and gravity: this proposal was made years ago and it is still much debated. Here, we put some constraints on the tensor-to-scalar-ratio in the original Higgs inflation model, here revised up to the present developments on the renormalisation prescriptions choice: in order to evade the intrinsic unitarity issues of the theory, we investigate the low- ξ parameter space, taking advantage of the above-mentioned inflection point configuration. Our results, as well as confirm the robustness of the inflationary predictions of the model against radiative corrections, already shown in the recent past [8], display some problems to push the non-minimal coupling towards small values, keeping unchanged all the other well-established observables. These conclusions add nothing to what is known from the very recent literature [see, for instance, again [8]].

*I would rather have
questions that can't be answered
than answers that can't be questioned.*

— Richard P. Feynman

ACKNOWLEDGEMENTS

First, I would like to thank Isabella Masina for introducing me in the world of research, broadening my mind in the Particle Physics field. I value her willingness to accept to supervise me and her valuable collaboration in carrying out the main part of the work.

I would also like to thank the Cosmology Group in Ferrara, which, although it was not directly involved in my work, has always shown support and interest. In particular, special thanks to Paolo Natoli and Massimiliano Lattanzi, with their precious advice both on scientific and human level, always available to help me in several occasions during my PhD.

Thanks obviously to the INFN - section of Ferrara and ASI, for the financial support.

Finally, I have to say that I could not have made it without the hospitality and lightheartedness of my new friends and colleagues here in Ferrara, and, above all, the unconditional love and support from my family.

The very last words can only be dedicated to Micaela, my brightest star.

Ferrara, March 2017

G. I.

CONTENTS

1	THE STANDARD MODEL OF FUNDAMENTAL INTERACTIONS	1
1.1	Electroweak gauge theory: The Weinberg–Salam model	1
2	STANDARD MODEL AT HIGH ENERGIES: EXTRAPOLATION AND PROPERTIES	9
2.1	Effective potential	9
2.1.1	RGE and β -functions	10
2.1.2	Matching	11
2.1.3	RG-improved effective potential	15
2.2	Theoretical issues: Bounds and scale-dependent properties	17
2.2.1	Unitarity bound	17
2.2.2	Triviality bound	19
2.2.3	Hierarchy problem	20
3	ELECTROWEAK VACUUM STABILITY	23
3.1	Stability and metastability	23
3.1.1	Metastability scenario	25
3.2	Stationary configurations of the SM: Vacuum stability analysis	27
3.2.1	Criticality: Calculation	28
3.2.2	Criticality: Results	30
3.3	Gauge (in)dependences	35
4	THE INFLATIONARY FRAMEWORK: THE INFLECTION POINT CONFIGURATION	39
4.1	General notes on inflation	39
4.1.1	Issues of the Standard Cosmological Model: flatness problem and horizon problem	40
4.1.2	Solving the issues: Hubble flow and amount of inflation	42
4.1.3	Slow-roll dynamics	44
4.1.4	Inflationary observables	47
4.2	Inflection point analysis	53
5	$U(1)_{B-L}$ EXTENSION OF THE STANDARD MODEL: STABILITY AND INFLATION	59
5.1	The model	60
5.2	Stabilisation of the potential	64
5.2.1	Tree-level threshold relations	67
5.2.2	RGE	68
5.3	Inflation	68
5.4	Stability vs Inflation	72
5.5	Reheating	74
6	HIGGS ξ -INFLATION	79
6.1	Non-minimal coupling	80

6.2	Adding quantum corrections	81
6.2.1	RGE	82
6.2.2	Effective potential	82
6.3	Numerical analysis: inflationary observables	86
6.4	Unitarity	92
Conclusions		95
A	FORMULÆ FOR THE RG RUNNING AT NNLO	99
A.1	The SM gauge couplings β -functions for $n_f = 5$	99
A.2	The SM β -functions for $n_f = 6$	100
A.3	The β -functions in the $U(1)_{B-L}$ extension	102
A.4	The SM β -functions with the suppression factor $s(\phi)$	105
B	MATCHING PROCEDURES	107
B.1	Strong coupling matching	107
B.2	Higgs quartic coupling matching	107
B.3	Top Yukawa matching	109
C	TWO-LOOP EFFECTIVE POTENTIAL	113

LIST OF FIGURES

Figure 1	Spontaneous symmetry breaking for a toy-potential of a real scalar field	3
Figure 2	“Mexican hat” potential	4
Figure 3	Three-loop RG evolution of the SM couplings	10
Figure 4	Zoom-in of the RG evolution of the Higgs quartic coupling	12
Figure 5	Triviality and stability bounds on the Higgs boson mass	20
Figure 6	Instability scale as a function of m_H and m_t	24
Figure 7	Second vacuum configurations	25
Figure 8	SM phase diagram	26
Figure 9	Stability phase diagram: near-criticality	31
Figure 10	Scale dependence of the top critical value m_t^c	32
Figure 11	Stability diagram for a lower top quark mass central value	33
Figure 12	Shape of the SM effective potential for different values of the top quark mass	36
Figure 13	Sketch of the horizon problem solution	41
Figure 14	Sketch of a typical slow-roll inflationary potential	45
Figure 15	Planck 2015 results: CMB power spectrum	48
Figure 16	Sketch of the inflationary and post-inflationary evolution: CMB window	49
Figure 17	Planck 2015 results: constraints on inflation	51
Figure 18	BICEP2/Keck Array analysis on inflationary parameters	52
Figure 19	Inflection point configuration of the Higgs potential: dependence on m_H and r	54
Figure 20	Scale dependence of the height of the potential at inflection point	55
Figure 21	Shape of the potential at inflection point and its scale dependence	56
Figure 22	Tensor-to-scalar ratio in a SM inflection point scenario	57
Figure 23	Shape of the two-field potential	62
Figure 24	Stabilisation of the potential through a singlet scalar	65
Figure 25	Inflationary predictions in the $U(1)_{B-L}$ model	70
Figure 26	Inflationary predictions: running of n_s and r vs. v' in the $U(1)_{B-L}$ model	72
Figure 27	Scale dependence of the tree-level potential at inflection point for some ξ values	85
Figure 28	Scale dependence of the one-loop and two-loop potential for some ξ values	86

Figure 29	ξ values allowed within the current bounds on r	87
Figure 30	Critical regime for low- ξ scenario: m_t, m_H, α_s window	88
Figure 31	Inflationary predictions in the Higgs ξ -inflation model	91

LIST OF TABLES

Table 1	SM coefficients for the Coleman-Weinberg correction	15
Table 2	Particle content of the minimal B – L extension	61

INTRODUCTION

The discovery of the Higgs boson at the Large Hadron Collider (LHC) [9, 10] has sanctioned the triumph of the Standard Model (SM) as a successful theory of fundamental interactions in Nature. This particle was the only one, among the explicitly predicted by the model, without an experimental feedback: its revelation and the lack of signals of physics beyond the SM so far, has opened a new era for the investigation in particle physics and even beyond, with the chance to explain fundamental problems, only in terms of the SM, and their connection to other fields of study, *e.g.* early-Universe cosmology.

The precise determination of the Higgs mass gives us all the properties of the SM Higgs boson [11], such as its production cross section and decay widths, and provides an estimation of its quartic coupling λ in the SM. In particular, the study of the behaviour of this coupling, and more generally of the Higgs potential at high energies, proved to be quite interesting because of the fact that λ , depending on the other SM parameters, can in principle become negative at some high-energy scale Λ_I , below the Planck scale, where the gravitational effects are supposed to become relevant. This suggests a possible instability of the SM electroweak vacuum. In this case, the Higgs potential may become unbounded from below or it might develop a second minimum, which now would become the true one, for very large field values. In the first scenario or, if the decay time from the electroweak vacuum towards the true one turns out to be smaller than the age of the Universe, we talk of absolute instability, otherwise, if that tunnelling rate is greater than the age of the Universe, we say that we are in the metastable configuration. Thus, from a cosmological point of view, the question is: why Nature, in early Universe, should favour the electroweak minimum rather than a less energetic one at large field values?

The vacuum stability problem is deeply connected with these issues and it can be addressed only after a careful analysis of the behaviour of the SM up to high energies, in order to be sure to be able to discriminate between a stable or unstable (metastable) scenario [see the well-known works [3, 4, 12, 2]]. This study turns out to be heavily tied up with the precise determination of the top quark mass: small variation in its value could push the electroweak vacuum towards the stability or instability region. If the electroweak vacuum reveals itself as metastable (as the current central values of the top mass, along with the Higgs mass and the strong coupling, currently better constrained from experiments, seem to suggest), the electroweak vacuum is intended to decay into the less energetic true one, with a lifetime that exceeds the age of the Universe.

In this case a possible solution may be the introduction of new physics in-between the electroweak and the instability scale, given the inability of the SM of handling some still unexplained observations, like neutrino masses, the dark universe and the baryon asymmetry, just to name a few. Indeed, the presence of an instability at an intermediate scale might be seen as a sign of a threshold of physics beyond the SM around Λ_I : this could be the reason for a matching condition $\lambda \approx 0$ at a scale near Λ_I , which is going to drive some of our considerations.

The task we try to address in this thesis is to perform a careful extrapolation of the SM up to high energies, at the present state of the art, namely the Next-to-Next-to-Leading Order (NNLO) [see our work [1] and the Chap. 3, based on it], taking advantage of the most updated tools in dealing with:

- the running of the couplings, via the Renormalisation Group Equations (RGE);
- the matching conditions at the different regimes;
- the effective potential expansion, including new theoretical approaches in addressing some peculiar issues related to this approximation.

We stress that the whole analysis is carried out at zero temperature and assuming the SM valid up to the Planck scale: the inclusion of gravitational effects, finite-temperature effects and, in general, new physics could spoil the entire framework [for more details, see the discussion drawn in the partial conclusions of Chap. 3]. In any case, the electroweak vacuum stability imposes severe constraints on possible SM extensions: any physics beyond the SM should reproduce it as a low-energy effective theory.

Beyond the stability issue, our goal is to investigate also its interplay with the early-Universe physics, with a particular interest in the inflationary framework.

Inflation, as it is well known, is, so far, the most elegant and reliable mechanism, although without a “smoking gun” proof of its existence yet, which can explain the flatness and the homogeneity on large scales of our Universe we measure today. The fact is that it needs a scalar field able to drive this explosive expansion and, at the same time, to generate the correct amount of primordial curvature perturbations survived until today.

Up to now, the Higgs boson is the only elementary scalar known in Nature so far, thus, it seems natural (and tempting) to wonder if it could be involved actively in the primordial inflationary phase of the very early Universe.

Originally, it was common to assume that the Higgs field remains inert during inflation, being its vacuum expectation value fixed at the very low value of $v = 246$ GeV: inflation should proceed through slow roll along a potential which extend in another field direction, confining the Higgs to the role of mere spectator of the dynamics.

In models where the Higgs is not playing any role, the inflationary process might be anyway affected, because a violent quasi-exponential expansion, like inflation, can generate large fluctuations of the Higgs field, inducing a possible destabilisation. Assuming “desert” up to the Planck scale and believing in metastability, the instability region could be easily reached by the Higgs during inflation, posing the bothersome issue of how the Higgs is not ended in its true minimum [see, for instance [13]]. Of course, post-inflationary physics and reheating need to be taken into account for such an analysis [14]: we know for sure that the matter content of the Universe started forming when inflation ended, so, if the inflationary framework is the right one, a sort of coupling between the inflationary sector and the SM Higgs must exist [15].

Even the first attempts to explore the possibility of the SM Higgs as the inflaton failed, due to the insufficient e-folds gained in the parameter space related, or, if this last constraint was satisfied, due to the inability to achieve the correct primordial curvature perturbations given by the measured power spectrum [see, for instance [16], for

a recent review about this possibility]. This failure is imputable to the Higgs potential behaviour, which grows too fast: possible solutions are connected to some mechanisms able to flatten the potential at large field values.

The first try, which we discuss also in this thesis in Chap. 4, consists in setting up a plateau arising for tuned values of the top quark mass, finding the so-called inflection point in the SM Higgs potential [12].

Related to this possibility, is the case of Higgs false vacuum inflation [17, 18, 19], in which a tuning of the top mass could allow the appearance of a shallow false vacuum at high energies, able to drive inflation. In this scenario the Higgs is not necessarily dynamical during inflation, but essential in setting up the energy scale. Unfortunately, the inflationary expansion gained in this case, in order to come to an end and reproduce the correct amount of scalar perturbations, needs new dynamical degrees of freedom, able to provide an additional escape way for the inflaton (via some specific mechanisms) and maybe to generate the curvature perturbations.

Another popular approach is based on a non-minimal coupling of the Higgs field to gravity [20]. We will review all the aspects of the original model and some of its developments, stressing both the simplicity of the idea and also its difficulties, related to the very large value of the non-minimal coupling required, from which some concerns about the consistency of the theory descend. In the context of effective theories, the model suffers of unitarity issues and it turns out to be difficult to find a viable ultraviolet (UV) completion [see Chap. 5 and references therein].

In this thesis we investigate, besides the inflection point configuration, which is still in the pure SM framework, two additional scenarios, characterised by minimal extensions to the SM.

The first relies on a model, known for a long time, which aspires to give a reasonable explanation in one single shot to inflation, electroweak stability and neutrino masses (with some possible hints related to dark matter and leptogenesis). It deals with an additional global gauge symmetry, based on the conservation of the quantum number $B - L$ (“baryon number minus lepton number”): here the heavy Higgs of this new symmetry is supposed to play the role of the inflaton, while the SM Higgs is involved only in the post-inflationary phase. From the symmetry breaking of the large gauge group, the right-handed neutrinos are generated, responsible, through the type I see-saw scheme, of the low-energy neutrino masses.

The second follows the path of the non-minimally coupled scheme, called here Higgs ξ -inflation, in which we try to lower the non-minimal coupling value in some critical configurations, such as the inflection point pattern.

The thesis is organised as follows.

CHAPTER 1 We provide a self-consistent introduction to the SM of fundamental interactions, focussing on the spontaneous symmetry breaking via the Higgs mechanism and on the full Lagrangian of the theory, setting up conventions, symbols and framework.

CHAPTER 2 The chapter is devoted to the extrapolation of the SM up to very high energies: we look over the effective potential expansion, the running of the couplings and the matching conditions. Furthermore, we remember that the value of the Higgs mass is also connected to the high-energy cutoff of the theory, where the

SM is supposed to break down (unitarity bound), along with another high-scale theoretical property, known as triviality. At the end of the chapter, we try to present the hierarchy problem and some possible solutions proposed in literature.

CHAPTER 3 We introduce the vacuum stability problem and propose our own analysis, focussing on motivations, methodologies and results. The final section is based on possible gauge-dependence issues which can be encountered in the proposed calculation.

CHAPTER 4 All the main aspects of the inflationary model are reviewed. Then, we outline our inflection point analysis. The results have been compared to the current experimental data.

CHAPTER 5 We move away from pure SM and we analyse the above-mentioned $U(1)_{B-L}$ model, starting from its formulation. Then, we try to scan the viable parameter space in order to achieve a suitable inflationary expansion, taking into account the electroweak stability constraints.

CHAPTER 6 We try to review the main ideas related to the Higgs ξ -inflation theory. Our contribution concerns a numerical analysis of the lower bound of the non-minimal coupling in the inflection point configuration and a simple calculation of the inflationary observables, taking into account the radiative corrections. A final summary on the unitarity issues of the theory is provided at the end of the chapter.

CONCLUSIONS Lastly, some overall conclusions and possible future developments are drawn.

APPENDIX A All the RGE for each different model and regime studied are contained.

APPENDIX B It is shown the formal matching procedure.

APPENDIX C It is displayed the two-loop effective potential used in our calculations.

The aim of this chapter is to summarise, briefly, the main features of the Standard Model of elementary particles and fundamental interactions (as a reference point, see the three seminal works by Sheldon L. Glashow, Steven Weinberg and Abdus Salam [21, 22, 23]), which is, up to now, the most satisfactory theoretical framework for the description of all the matter constituents and their fundamental interactions, excluding gravity. For this short review we will vaguely follow, as a matter of choice, the introductory textbook [24].

Throughout this work, the Greek indexes go from 0 to 4, while the Latin ones from 1 to 3. The γ matrices in the Dirac equation satisfy the anticommutation relations

$$\gamma^\mu \gamma^\nu + \gamma^\nu \gamma^\mu = 2g^{\mu\nu}, \quad (1)$$

where $g^{\mu\nu}$ is the metric tensor. The representation used is

$$\gamma^0 = \begin{pmatrix} \mathbf{1} & 0 \\ 0 & -\mathbf{1} \end{pmatrix} \quad \gamma^i \equiv \gamma = \begin{pmatrix} 0 & \vec{\sigma} \\ -\vec{\sigma} & 0 \end{pmatrix}, \quad (2)$$

where

$$\sigma^1 = \begin{pmatrix} 0 & 1 \\ 1 & 0 \end{pmatrix}, \quad \sigma^2 = \begin{pmatrix} 0 & -i \\ i & 0 \end{pmatrix}, \quad \sigma^3 = \begin{pmatrix} 1 & 0 \\ 0 & -1 \end{pmatrix}, \quad (3)$$

are the usual Pauli matrices and $\mathbf{1}$ stands for the 2×2 unit matrix. A recurrent combination is

$$\gamma^5 \equiv i\gamma^0\gamma^1\gamma^2\gamma^3 = \gamma_5 = \begin{pmatrix} 0 & \mathbf{1} \\ \mathbf{1} & 0 \end{pmatrix}. \quad (4)$$

In terms of the adjoint spinors, we define $\bar{\psi} \equiv \psi^\dagger \gamma^0$.

1.1 ELECTROWEAK GAUGE THEORY: THE WEINBERG–SALAM MODEL

In order to write down the complete SM Lagrangian, it is needed to determine the adequate gauge symmetry for electroweak interactions. Let us present the full Lagrangian first, in order to explain later all the contributions:

$$\mathcal{L} = \mathcal{L}_g + \mathcal{L}_H + \mathcal{L}_Y, \quad (5)$$

where, respectively, we have a gauge sector, in which are described the vector bosons and fermions interactions; a Higgs part, which triggers electroweak symmetry breaking and a Yukawa sector, which account the coupling between the Higgs field and the fermions, giving rise to SM flavour physics. Let us inspect all of these in turn.

GAUGE SECTOR. The strong, electromagnetic and weak interactions are all embedded in a gauge theory established on the group symmetry

$$SU(3)_C \times SU(2)_L \times U(1)_Y. \quad (6)$$

From now on we will neglect the $SU(3)$ colour part, decoupled from the electroweak sector and beyond the scope of this work. We recall the QED Lagrangian, displaying explicitly the charge operator¹ in order to comprise also all the quarks and lepton fields:

$$\mathcal{L}_{\text{QED}} = \bar{\psi}(i\gamma^\mu \partial_\mu - m)\psi + e\bar{\psi}\gamma^\mu Q A_\mu \psi - \frac{1}{4}F_{\mu\nu}F^{\mu\nu}, \quad (7)$$

where the second term can be recast in the usual $U(1)_{em}$ interaction term

$$-iej_{em}^\mu A_\mu = -ie(\bar{\psi}\gamma^\mu Q\psi)A_\mu. \quad (8)$$

If we want to incorporate the weak processes too, we should replace (8) with

$$-ig\bar{\chi}_L^\mu \cdot \vec{W}_\mu = -ig\bar{\chi}_L \gamma^\mu \vec{T} \cdot \vec{W}_\mu \chi_L \quad \boxed{SU(2)_L}, \quad (9)$$

$$-ig' \frac{j_Y^\mu}{2} B_\mu = -ig' \bar{\psi} \gamma^\mu \frac{Y}{2} \psi B_\mu \quad \boxed{U(1)_Y}, \quad (10)$$

where \vec{T} and Y are the generators of the groups $SU(2)_L$ and $U(1)_Y$ respectively. The left-handed fermions are isospin doublets χ_L , while the right-handed ones are isospin singlets ψ_R . Quarks, differently from neutrinos², have a non-zero mass and hence have both right- and left-handed components.

The interaction (8) is contemplated in both (9): the generators of the three groups involved satisfy the Gell-Mann–Nishijima formula

$$Q = T_3 + \frac{1}{2}Y, \quad \text{so that} \quad j_{em}^\mu = J_3^\mu + \frac{1}{2}j_Y^\mu, \quad (11)$$

this means that the electromagnetic current is a combination of the two neutral currents present in the second relation of (11). Hence the two neutral gauge fields A_μ and Z_μ are orthogonal combinations of W_μ^3 and B_μ , ruled by a mixing angle θ_W , called Weinberg angle and whose updated experimental value is $\sin^2 \theta_W = 0.23126 \pm 0.00005$ [see table 10.2 of [25]³]. Finally, the neutral interaction can be rewritten in terms of only physical fields:

$$-igJ_3^\mu W_{3,\mu} - ig' \frac{j_Y^\mu}{2} B_\mu = -iej_{em}^\mu A_\mu - ie \frac{e}{\sin \theta_W \cos \theta_W} \underbrace{[J_3^\mu - \sin^2 \theta_W j_{em}^\mu]}_{J_{NC}^\mu} Z_\mu, \quad (12)$$

¹ The local gauge transformation from which the Lagrangian is obtained is $\psi(x) \rightarrow e^{i\rho(x)Q}\psi$.

² Remaining in the SM framework, neutrinos are massless, although oscillations experimental data state quite the contrary. We will come back to this point in Chap. 6.

³ Note that this experimental value, as the following masses below, are given in the \overline{MS} scheme. Where present, the last digits in parenthesis after the values stands for the 1σ uncertainties.

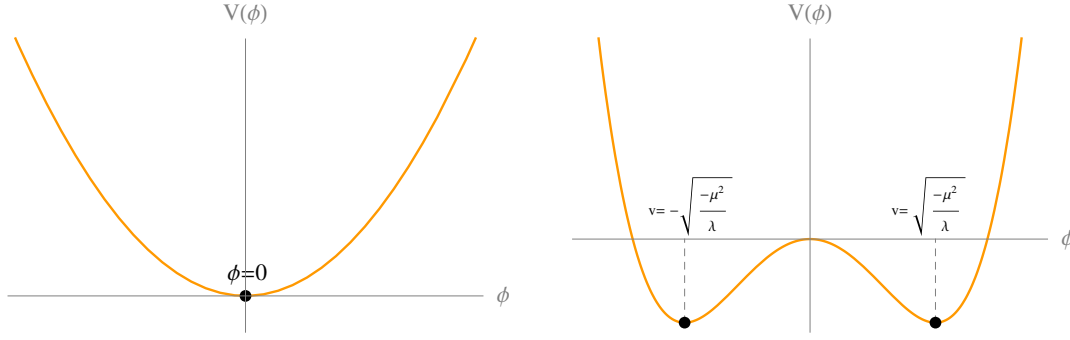


Figure 1: The potential $V(\phi) = \frac{1}{2}\mu^2\phi^2 + \frac{1}{24}\lambda\phi^4$, with $\lambda > 0$ and $\mu^2 > 0$ (left panel, a self-interacting field of mass μ), $\mu^2 < 0$ (right panel, the same potential with two degenerate minima).

where J_{NC}^μ is the global neutral current. All the couplings are forced to satisfy the fundamental SM relation

$$e = g \sin \theta_W = g' \cos \theta_W, \quad (13)$$

where $e = 1.602176565(35) \times 10^{-19}$ C is the electric charge [25].

Lastly, we can write down the definitive gauge part of the full Lagrangian (5), obtained, as usual, imposing the invariance under the group symmetry $SU(2)_L \times U(1)_Y$:

$$\mathcal{L}_g = -\frac{1}{4}\vec{W}_{\mu\nu} \cdot \vec{W}^{\mu\nu} - \frac{1}{4}B_{\mu\nu}B^{\mu\nu} \quad (14a)$$

$$+ \bar{L}\gamma^\mu \left(i\partial_\mu - g\frac{1}{2}\vec{\tau} \cdot \vec{W}_\mu - g'\frac{Y}{2}B_\mu \right) L \quad (14b)$$

$$+ \bar{R}\gamma^\mu \left(i\partial_\mu - g'\frac{Y}{2}B_\mu \right) R, \quad (14c)$$

where in (14a) are displayed the W^\pm , Z^0 and photon kinetic energies and self-interactions: in particular, they are defined as

$$\vec{W}_{\mu\nu} \equiv \partial_\mu \vec{W}_\nu - \partial_\nu \vec{W}_\mu - g\vec{W}_\mu \times \vec{W}_\nu \quad (15)$$

$$B_{\mu\nu} \equiv \partial_\mu B_\nu - \partial_\nu B_\mu, \quad (16)$$

where, the last term in the first equation, as in the simple QCD case, is due to the non-Abelian character of the symmetry group, because the \vec{T} s do not commute with each other. In (14b) and (14c) we have respectively the left-handed and right-handed quarks and leptons kinetic energies and interactions with gauge bosons. Note that we represented the left-handed fermion doublet with L, while R stands for the right-handed fermion singlet.

This Lagrangian is a singlet under the transformation of each gauge group: verifying, for example, the invariance under $U(1)_{em}$ will led to charge conservation. Up to now the model is completely massless, because any mass term can not be added, because it would break gauge invariance: as we already know, we need the Higgs mechanism.

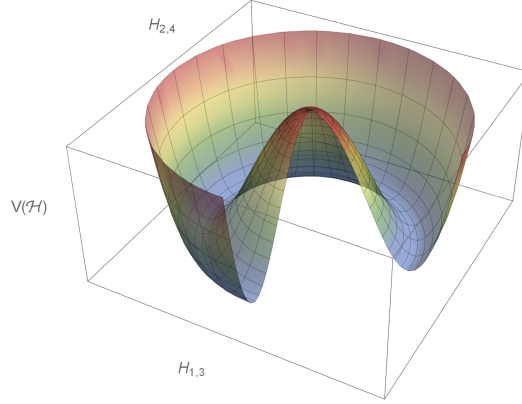


Figure 2: The “mexican hat” potential $V(\mathcal{H}) = \mu^2 \mathcal{H}^\dagger \mathcal{H} + \frac{\lambda}{6} (\mathcal{H}^\dagger \mathcal{H})^2$, with $\lambda > 0$ and $\mu^2 < 0$ (circle of minima). For the definitions of the axes, see (18).

HIGGS SECTOR. Repeating the spontaneous symmetry breaking procedure, illustrated in Fig. 1 for a general scalar field with quartic potential, now for the $SU(2)_L \times U(1)_Y$ group, we will led to a gauge invariant Lagrangian

$$\mathcal{L}_H = \left| \left(i\partial_\mu - g\vec{T} \cdot \vec{W}_\mu - g' \frac{Y}{2} B_\mu \right) \mathcal{H} \right|^2 - V(\mathcal{H}), \quad (17a)$$

$$V(\mathcal{H}) = -\frac{1}{2} m_h^2 \mu^2 \mathcal{H}^\dagger \mathcal{H} + \frac{\lambda}{6} (\mathcal{H}^\dagger \mathcal{H})^2, \quad (17b)$$

where the squared modulus is intended as the product between the hermitian conjugate of the argument and the argument itself. \mathcal{H} is the complex Higgs doublet [26, 27], made of four real fields H_i , $i = 1, 2, 3, 4$, that must belong to $SU(2)_L \times U(1)_Y$ multiplets. The minimal choice in this sense is to arrange these fields in an isospin doublet with weak hypercharge $Y = 1$:

$$\mathcal{H} = \begin{pmatrix} H^+ \\ H^0 \end{pmatrix}, \quad H^{+,0} \equiv \frac{1}{\sqrt{2}} (H_{1,3} + iH_{2,4}). \quad (18)$$

$V(\mathcal{H})$ is the usual “mexican hat” Higgs potential [see Fig. 2] on which we will focus throughout the thesis: to generate gauge boson masses we put ourselves in the case $\lambda > 0$ and $\mu^2 < 0$; choosing one vacuum configuration for \mathcal{H} and expanding about it, we have

$$\mathcal{H}_0 = \frac{1}{\sqrt{2}} \begin{pmatrix} 0 \\ v + \phi_H(x) \end{pmatrix}. \quad (19)$$

It can be shown that the vacuum expectation value v is related to the Fermi constant $G \sim g^2/m_W^2$ by the relation $1/(2v^2) = G_\mu/\sqrt{2}$ and so, its value is fixed at

$v \simeq 246.221 \text{ GeV}$ [25], where G_μ is the Fermi constant from muon decay: $G_\mu = 1.1663787(6) \times 10^{-5} \text{ GeV}^{-2}$. All the other H_i are the Nambu–Goldstone bosons and are “eaten up” by the combinations of gauge bosons W^\pm and Z^0 , which get masses⁴ [25]

$$m_W = \frac{1}{2}gv = 80.385 \pm 0.015 \text{ GeV}, \quad (20)$$

$$m_Z = \frac{1}{2}v\sqrt{g^2 + g'^2} = \frac{m_W}{\cos\theta_W} = 91.1876 \pm 0.0021 \text{ GeV}. \quad (21)$$

The photon remains massless, as required by the residual unbroken $U(1)_{em}$ symmetry: the breaking is done by means of the neutral part of the Higgs field (eigenvalue of zero electric charge) to guarantee invariance. This is the main reason for the choice (19): in other words, due to the conservation of the electric charge, only neutral scalars are allowed to acquire a vacuum expectation value. The last scalar degree of freedom survived corresponds indeed to the Higgs boson. Its mass $m_H^2 = -2\mu^2 = 2\lambda v^2$ is a free parameter of the theory and must be determined by experiments: more on this in the following chapters.

The same Higgs isospin doublet is the one suitable for the generation of fermion masses, as we are going to see, in the so-called “Higgs mechanism” [26, 27].

YUKAWA SECTOR. As stated before, in the Lagrangian (14) a fermion mass term is forbidden by gauge invariance. However, exactly the same Higgs doublet which gives rise to gauge bosons masses is also enough to generate masses for quarks and leptons: through a Yukawa interaction, we have to couple left-handed doublets and right-handed singlets. In other words, we need a $SU(2)_L$ singlet with $Q = Y = 0$: the Higgs doublet considered previously has the required $SU(2)_L \times U(1)_Y$ quantum numbers to couple to a $\bar{L}R$ pair.

For example, to generate the electron mass, we should include the following term in the global SM Lagrangian:

$$\mathcal{L}_Y^{\text{leptons}} = -g_e \left[(\bar{\nu}_e \quad \bar{e})_L \begin{pmatrix} H^+ \\ H^0 \end{pmatrix} e_R + \bar{e}_R (H^- \quad \bar{H}^0) \begin{pmatrix} \nu_e \\ e \end{pmatrix}_L \right], \quad (22)$$

where e_R is the electron right-handed singlet, coupled *à la* Yukawa to the electron left-handed lepton doublet by the Higgs doublet. g_e is the generic coupling to be fixed in order to define the electron mass [see just below].

⁴ Further details on the derivation of these formulæ and the mixing between the gauge fields can be found in any introductory particle physics textbook, for instance [24].

Then we spontaneously break the symmetry via the usual procedure (19). After the substitution, the electron part (22) becomes⁵

$$\begin{aligned}\mathcal{L}_Y^{\text{leptons}} &= -\frac{1}{\sqrt{2}}g_e v (\bar{e}_L e_R + \bar{e}_R e_L) - \frac{1}{\sqrt{2}}g_e (\bar{e}_L e_R + \bar{e}_R e_L) \phi_H \\ &= -m_e \bar{e}e - \frac{m_e}{v} \bar{e}e \phi_H, \quad \text{with } m_e = \frac{g_e v}{\sqrt{2}}.\end{aligned}\quad (23)$$

It is worth mentioning that the electron mass is not a prediction of the model, due to the arbitrariness of the electron coupling g_e . Furthermore, the last term turns out to be very small, since v is of order $\mathcal{O}(10^2 \text{ GeV})$.

For the quarks masses the prescription is the same: the only difference is in the generation of the mass of the upper member of the doublet, for which we have to construct a suitable Higgs doublet from \mathcal{H} :

$$\mathcal{H}_c \equiv -2i\tau_2 \mathcal{H}^* = \begin{pmatrix} -\bar{H}^0 \\ H^- \end{pmatrix} \rightarrow \frac{1}{\sqrt{2}} \begin{pmatrix} v + \phi_H(x) \\ 0 \end{pmatrix}. \quad (24)$$

\mathcal{H}_c has the same transformation properties of \mathcal{H} (but has opposite weak hypercharge, $Y = -1$)⁶, hence it looks perfect to build a gauge-invariant contribution for the full Lagrangian:

$$\begin{aligned}\mathcal{L}_Y^{\text{quarks}} &= -g_d (\bar{u} \quad \bar{d})_L \begin{pmatrix} H^+ \\ H^0 \end{pmatrix} d_R - g_u (\bar{u} \quad \bar{d})_L \begin{pmatrix} -\bar{H}^0 \\ H^- \end{pmatrix} u_R + \text{h.c.} \\ &= -m_d \bar{d}d - m_u \bar{u}u - \frac{m_d}{v} \bar{d}d \phi_H - \frac{m_u}{v} \bar{u}u \phi_H.\end{aligned}\quad (25)$$

Obviously the expression can be extended to the other quark flavour eigenstates.

The Higgs coupling does not spoil the flavour conservation, but, also in this case, all the masses generated can not be predicted, because they depend on arbitrary couplings.

Merging (23) and (25), the global flavour contribution can be synthesised in the following form:

$$\boxed{\mathcal{L}_Y = -G_1 \bar{L} \mathcal{H} R - G_2 \bar{L} \mathcal{H}_c R + \text{h.c.}} \quad (26)$$

Putting together (14), (17) and (26), we obtain the full SM Lagrangian (5).

The introduction of the Higgs field, besides the generation of the heavy boson masses, is required also to guarantee renormalisability: when we consider, for example, the scattering of W bosons, we found that each individual diagram diverge as s^2/m_W^4 , where s is the growing energy. Although we can introduce neutral processes mediated

⁵ The implied step for the second equality is

$$\begin{aligned}-m_e (\bar{e}_R e_L + \bar{e}_L e_R) &= -m_e \bar{e} \left(\frac{1}{2}(1 + \gamma^5) \frac{1}{2}(1 + \gamma^5) \right) e \\ &= -m_e \bar{e} \left(\frac{1}{2}(1 - \gamma^5) + \frac{1}{2}(1 + \gamma^5) \right) e = -m_e \bar{e}e.\end{aligned}$$

⁶ \mathcal{H} is an element of $SU(2)$, which can be proven to be the universal covering group of $SO(3)$, *i.e.* a simply-connected group, homomorphic to $SO(3)$, which does not contain any simply-connected subgroup homomorphic to $SO(3)$. This means that the element \mathcal{H}_c , result of a particular rotation, has the same transformation properties of the $SU(2)$ doublet. For a pedagogical review, see [28].

by the Z^0 , which diverge in a more gentle way $\sim s/m_W^2$, the sum of all diagrams still diverge as s/m_W^2 : seen that heavy leptons can not help, the only solution is to introduce a scalar particle which cancels these residual divergences: just the Higgs boson. Already conjectured by Weinberg and Salam, this feature was rigorously proven by Gerald 't Hooft in 1971 [29, 30]. Further details on this issue are drawn in Sec. 2.2.1.

The first Large Hadron Collider (LHC) run has confirmed that the Higgs boson does exist [9, 10], produced via the gluon-fusion process and decayed in the $\phi_H \rightarrow ZZ$, $\phi_H \rightarrow WW$ and $\phi_H \rightarrow \gamma\gamma$ channels, and it is surprisingly light: the most updated mass measurement, coming from a combined analysis of the Atlas and CMS collaborations [31], gives the following value

$$m_H = 125.09 \pm 0.21(\text{stat}) \pm 0.11(\text{syst}) \text{ GeV}. \quad (27)$$

Measurements on this new neutral resonance showed also that its dominant spin and parity, and its SM-like couplings to fermions and bosons were compatible within available statistics with expectations of the Standard Model Higgs boson [11] and opens up several questions regarding the Higgs sector, the Higgs potential and more fundamental issues related to the SM structure, consistency and reliability.

2

STANDARD MODEL AT HIGH ENERGIES: EXTRAPOLATION AND PROPERTIES

In this chapter we want to introduce the mathematical and conceptual tools used in our analysis [1], contextualising the extrapolation of the SM to high energies: we are going to eviscerate the standard technique for the evolution of the SM couplings up to the Planck scale via the RGE as long as the matching between the initial conditions of the theory and its high-energy regime. We emphasise the crucial role covered by the quantum radiative corrections to the SM potential, giving rise to the RG-improved effective potential, exploited up to two loops. Some gauge-dependence issues are also discussed.

In this framework, we mention, at the end of the chapter, some important scale-dependent properties of the SM, able to weakly constrain the Higgs mass. Few words on the well-known hierarchy problem are also drawn in the last part.

2.1 EFFECTIVE POTENTIAL

Resuming Sec. 1.1, we write the potential for the physical Higgs field ϕ_H , already presented in a general form in (17b), which is given, at tree level, by

$$V_0(\phi_H) = \frac{\lambda(\mu)}{6} \left(|\mathcal{H}|^2 - \frac{v^2}{2} \right)^2 \approx \frac{\lambda(\mu)}{24} \phi_H^4, \quad (28)$$

where $\mathcal{H} = (0 \quad (\phi_H + v)/\sqrt{2})^T$ is the Higgs doublet, introduced previously in (18) and, in unitary gauge, in (19). The superscript T stands for the transposition operator, while v is the usual Higgs vacuum expectation value introduced before. μ will be, from now on, if not specified differently, the renormalisation scale: here we emphasised the μ -dependency of λ , in order to underline its running nature with energy. The approximation in the second equality holds when considering large field values, regime that will prove of interest to us: as we are going to see in Chap. 3, when one is interested in studying the shape of the potential at large values of the classical field, the quadratic term can be ignored, because of its monotonic damping when the energy scale grows beyond the instability scale.

According to our normalisation, the physical Higgs mass satisfies the tree-level relation

$m_H^2 = \lambda v^2/3$. In addition, the mass of a generic fermion f reads, at tree level, $m_f = h_f v/\sqrt{2}$, where h_f denotes the associated Yukawa coupling.

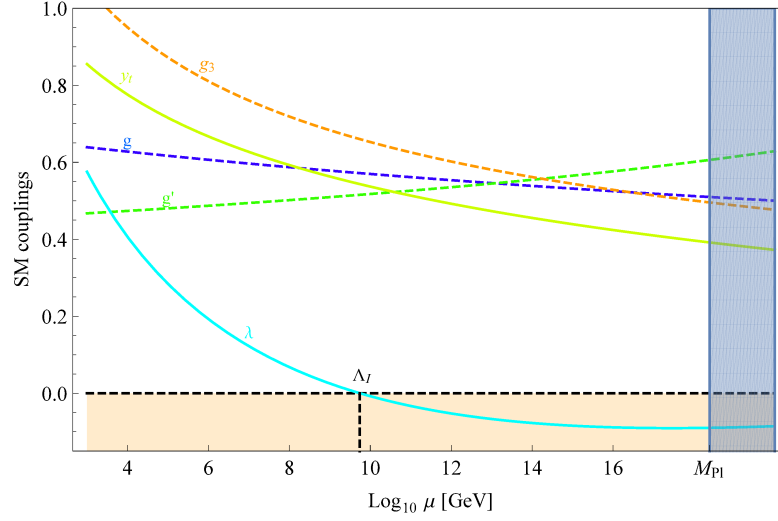


Figure 3: Three-loop RG evolution in the $\overline{\text{MS}}$ scheme, of the SM gauge couplings, the top Yukawa coupling and the Higgs quartic coupling, from the Fermi scale to the Planck scale. The instability scale Λ_I (the energy at which λ crosses zero, evaluated for central experimental values of the strong coupling constant $\alpha_s^{(5)} = 0.1181$, the Higgs boson mass $m_H = 125.09$ GeV and the top quark mass $m_t = 173.34$ GeV) and the quantum gravity regime (the shaded area beyond the Planck scale) are also pointed out. The figure, done by the author, is inspired to the corresponding one in [4].

In order to extrapolate the behaviour of the Higgs potential at very high energies, we adopt the mass-independent subtraction scheme, *i.e.* the $\overline{\text{MS}}$ scheme and consider the RG evolution for the relevant couplings which, in addition to the Higgs quartic coupling λ , are the gauge couplings g , g' , g_3 , the top Yukawa coupling h_t and the anomalous dimension of the Higgs field γ , which we are going to define in a while.

Each time we will present our specific analyses, we will particularise the precision and the loop-order we are working at. Normally, throughout this work, we perform the calculations according to the present state of the art, namely the NNLO.

2.1.1 RGE and β -functions

It is customary to introduce the dimensionless time parameter $t = \ln(\mu/m_t)$, where μ stands for the renormalisation scale and m_t is used as a conventional reference scale.

The RGE for the relevant couplings can be written as a sum of contributions with increasing loop numbers:

$$\frac{d}{dt}\lambda_i(t) = \kappa\beta_{\lambda_i}^{(1)} + \kappa^2\beta_{\lambda_i}^{(2)} + \kappa^3\beta_{\lambda_i}^{(3)} + \dots, \quad (29)$$

where $\kappa = 1/(16\pi^2)$ and the apex on the β -functions represents the loop order.

We are interested in the RGE-dependence of the couplings $\lambda_i = g, g', g_3, h_t, \lambda, \gamma$. See Fig. 3 for the running of the SM couplings and, in particular, for the Higgs quartic

coupling behaviour in Fig. 4, where we also show the effect on λ of varying the most relevant input parameters, *i.e.* the strong coupling constant, the Higgs and top quark mass.

The one-loop and two-loop expressions for the β -functions are well known and can be found, for instance, in [32] [see also [33, 34, 35, 36, 37, 38, 39, 40, 41, 42, 43, 44, 45, 46, 47]].

The complete three-loop β -functions for the SM have been computed quite recently:

- as for the SM gauge couplings, they have been presented by Mihaila, Salomon and Steinhauser in [48]¹;
- as for the leading three-loop terms in the RG evolution of λ , h_t and the Higgs anomalous dimension have been computed by Chetyrkin and Zoller in [50]².

The dominant four-loop contribution to the running of the strong gauge coupling has been computed quite recently, see [56, 57]. In our NNLO analysis, we include all these contributions, neglecting the four-loop contribution to the Higgs self-coupling, anomalous dimension of the Higgs field and top Yukawa β -functions, calculated very recently by Chetyrkin and Zoller [58]. A numerical estimate of these terms by the same authors leads to the conclusion that they are negligible with respect to the other sources of uncertainty.

For the sake of completeness, the expressions of the β -functions up to three loops and four loops for the strong gauge coupling are collected in App. A.2.

2.1.2 Matching

We present here the general updated matching procedure for the gauge couplings, the top Yukawa coupling and the quartic coupling that could be found in literature. In our analysis, as we are going to see in Chap. 3, we used directly the inputs given in a recent work by Bednyakov *et al.* [2]. For all the details, go to Sec. 3.2.1.

GAUGE COUPLINGS' MATCHING AT m_Z AND RUNNING UP TO m_t . The matching of the running gauge couplings is usually done at the Z boson pole mass, m_Z [see (20)]. The procedure is the following one.

Exploiting the $\overline{\text{MS}}$ scheme all orders relations

$$\alpha(\mu) = e^2(\mu)/4\pi, \quad e(\mu) = g(\mu) \sin \theta_W, \quad (30)$$

¹ Another work by the same authors appeared later [49]: results are compatible with [48] because the new contributions considered, due to the others Yukawa couplings not taken into account previously, are sub-dominant.

² Also in this case a more updated reference by the same authors appeared later [51]. The new full three-loop expression here is the same of [50] in the limit $g', g, h_b, h_\tau \rightarrow 0$: from a numerical estimate by the same authors, it has been proved that the only dominant contributions are due to g_s , h_t and λ , confirming the goodness of the approximation used. Next to these works, some papers by Bednyakov, Pikelner and Velizhanin [52, 53, 54, 55] came out, with some negligible correction to the Chetyrkin and Zoller expressions.

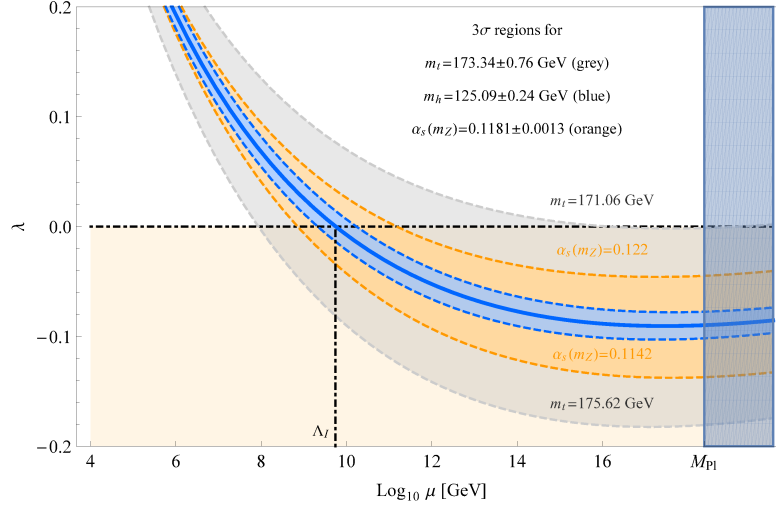


Figure 4: Three-loop RG evolution of the Higgs quartic coupling λ , accounting for the variation by $\pm 3\sigma$ of the top mass m_t (grey), of the Higgs mass m_H (blue) and of the strong coupling α_s (orange). Again, the instability scale and the quantum gravity regime are emphasised. The figure, done by the author, is inspired to the corresponding one in [4].

where the Weinberg angle value is given in Sec. 1.1 and the experimental value for the fine structure constant at m_Z is $\alpha_{em}(m_Z)^{-1} = 127.944 \pm 0.015$ [see [25]], we obtain

$$g(m_Z) = \frac{\sqrt{4\pi\alpha(m_Z)}}{\sin\theta_W} = 0.65171 \pm 0.00001, \quad (31)$$

$$g'(m_Z) = g(m_Z) \tan\hat{\theta}_W = 0.35745 \pm 0.00004. \quad (32)$$

Crucial for the sake of our calculation is the strong coupling constant α_s , whose current world average at m_Z , where there are just five quark flavours, is [59]

$$\alpha_s^{(5)}(m_Z) = 0.1181 \pm 0.0013. \quad (33)$$

It has been recognised that the error displayed in the above formula is nearly doubled with respect to the old value given in the Particle Data Group (PDG) database [25], because of a previous underestimation of the uncertainty in the lattice results. This will be one of our driving motivations in the forthcoming analyses.

From the strong coupling constant at m_Z , displayed in (33), we get

$$g_3^{(5)}(m_Z) = \sqrt{4\pi\alpha_s^{(5)}(m_Z)} = 1.2182 \pm 0.0067. \quad (34)$$

The errors shown are obtained by the simple error propagation formula.

Then one should perform the running of the SM gauge couplings from m_Z to m_t by means of the β -functions in the presence of five flavours. The updated running has to be done by including the full three-loop β -functions [49, 48] and the pure QCD

dominant term for the four-loop contribution [33, 34]. All these β -functions can be found in App. A.1.

Thus, the five-flavour strong coupling constant has to be matched with the six-flavour one at m_t . When the fraction of number n_f of the quark flavours is considered light ($m_q \ll \mu$), the remaining $n_l = n_f - 1$ heavier quark flavours decouple from the theory: for this reason, it is recommended to relate the coupling for the effective theory with $n_f + 1$ light flavours to that with n_f . In particular, it is needed a matching relation between the strong coupling in the $n_f = 6$ scenario, $\alpha_s^{(6)}$ and the same coupling in presence of $n_l = n_f - 1 = 5$ flavours, namely $\alpha_s^{(5)}$, decoupling the top quark from the theory. This decoupling equation is given in a general form in the most updated PDG review on QCD [59] or, for instance, in the review [60]) [see the App. B.1]: we show here a simplified version, written up to the two-loop matching

$$\begin{aligned} \alpha_s^{(6)}(\mu^2) &= \alpha_s^{(5)}(\mu^2) \left[1 + c_{10} \alpha_s^{(5)}(\mu^2) + c_{11} \alpha_s^{(5)}(\mu^2) \ln \frac{\mu^2}{m_t^2} \right. \\ &\quad + c_{20} \left(\alpha_s^{(5)}(\mu^2) \right)^2 + c_{21} \left(\alpha_s^{(5)}(\mu^2) \right)^2 \ln \frac{\mu^2}{m_t^2} \\ &\quad \left. + c_{22} \left(\alpha_s^{(5)}(\mu^2) \right)^2 \ln^2 \frac{\mu^2}{m_t^2} \right] \end{aligned} \quad (35)$$

where the first c_{nm} coefficients³ are:

$$\begin{aligned} c_{10} &= 0, & c_{11} &= \frac{1}{6\pi}, \\ c_{20} &= \frac{7}{24\pi^2}, & c_{21} &= \frac{19}{24\pi^2}, & c_{22} &= c_{11}^2 = \frac{1}{(6\pi)^2}. \end{aligned} \quad (36)$$

Full terms up to c_{4m} can be found in [61, 62].

In a previous work [12] the six-flavour running was considered: the correction that came out by running with five flavours up to the top mass is very small and could be neglected at the time, as discussed in [63]. But now that the value of the strong coupling constant is better known, it is worth considering it. The effect is that $\alpha_s(m_t)$ gets smaller with respect to the previous analyses, which goes in the direction of destabilising the Higgs potential. More on this in Chap. 3.

It is customary to write the gauge couplings at the top mass value, using the three-loop RG running up to m_t and matching the theory with five or six flavours. For the strong coupling, we obtain [2]:

$$g_3(m_t) = 1.2182 + 0.0134 \left(\frac{\alpha_s^{(5)}(m_Z) - 0.1181}{0.0013} \right) - 0.00046 \left(\frac{m_t}{\text{GeV}} - 173.34 \right). \quad (37)$$

MATCHING OF λ . To match the $\overline{\text{MS}}$ running quartic coupling $\lambda(\mu)$ with the Higgs pole mass m_H , one requires to exploit an expansion

$$\lambda(\mu) = \sum_{n=1,2,3,\dots} \lambda^{(n)}(\mu) = 3 \frac{m_H^2}{v^2} \left(1 + \delta_t^{(1)}(\mu) + \delta_t^{(2)}(\mu) + \dots \right), \quad (38)$$

³ The index n stands here for the loop order: for our purposes a two-loop matching is enough. The m -index runs from 0 to n .

which is known at present at NLO: $\delta_t^{(1)}(\mu)$ is the one-loop $\mathcal{O}(\alpha)$ result of Sirlin and Zucchini [64], while $\delta_t^{(2)}(\mu)$ is the recently calculated two-loop result, composed of a QCD contribution of $\mathcal{O}(\alpha\alpha_3)$ [63, 3, 65] and a Yukawa contribution [3]. More details can be found in App. B.2.

As it is well known, there is some arbitrariness in the choice of the matching scale μ in Eq. (38), which introduces a “theoretical” error in the RG procedure. In this work, we choose to perform the matching of the Higgs quartic coupling λ at the scale $\mu = m_t$. The theoretical uncertainty will be estimated by performing the matching also at different scales and by evolving $\lambda(\mu)$ via RG running until $\mu = m_t$. The spread in the numerical values obtained for $\lambda(m_t)$ can then be used to infer the magnitude of this theoretical error. See Sec. 3.2.1.

MATCHING OF h_t . It is common to extrapolate the $\overline{\text{MS}}$ top Yukawa coupling $h_t(\mu)$ from the matching condition with the running top mass $\bar{m}_t(\mu)$ [66, 12] and the top pole mass m_t :

$$h_t(\mu) \frac{v}{\sqrt{2}} = \bar{m}_t(\mu) = m_t (1 + \delta_t(\mu)), \quad \delta_t(\mu) = \delta_t^W(\mu) + \delta_t^{\text{QED}}(\mu) + \delta_t^{\text{QCD}}(\mu), \quad (39)$$

where $\delta_t^W + \delta_t^{\text{QED}}$ represent the electroweak contribution, which is known at one-loop [67], while δ_t^{QCD} is the QCD one. The QCD one-loop result is known since many years [67]; the QCD two-loop and three-loop results as a function of the matching scale μ are given for instance in [68, 69, 70]. We also include the four-loop result, following [71, 72].

There is also a strong-weak mixed contribution, known at two-loop [73] and evaluated at m_t : its effect is of order of the three-loop contribution.

The updated reference values for the top quark mass and its uncertainty are those of the first joint Tevatron and LHC analysis [74], $m_t^{\text{exp}} = 173.34$ GeV and $\Delta m_t^{\text{exp}} = 0.76$ GeV. However, since the top mass is extracted by fitting Monte Carlo (MC) computed distributions to experimental data, what is really measured is a MC parameter, m_t^{MC} and this could be source of further uncertainties.

According to some authors [75], although it is common to identify the top quark pole mass m_t with m_t^{MC} , the uncertainty in the translation from the MC mass definition to a theoretically well-defined short distance mass definition at a low scale should currently be estimated to be of order of 1 GeV [76]; if this were the case [66, 12, 2], the customary confidence ellipses with respect to m_t^{MC} and m_H [more on this in Sec. 3.2.2] should be taken with a grain of salt.

Other authors [77, 78] argued that measurements relying on the reconstruction of top-decay products yield results which are actually close to the top quark pole mass, although there are theoretical uncertainties due to the approximations contained in the MC shower models, namely missing loop and width corrections and colour-reconnection effects. The discrepancy between MC and pole masses was estimated in [79], by identifying the MC mass as a SCET (Soft Collinear Effective Theory) jet mass, evaluated at a scale given by the shower infrared cutoff, i.e. $\mathcal{O}(1$ GeV), in $e^+e^- \rightarrow t\bar{t}$ collisions. As discussed in [78], such a discrepancy amounts to about 200 MeV. In addition, the renormalon ambiguity affecting the pole mass, was recently estimated [77] as the size of the last converging term in the $\overline{\text{MS}}$ /pole relation, obtained extrapolating to higher orders the four-loop computation in [71], and amounting to less than 100 MeV. The

p	t	W	Z	ϕ_H	χ
N_p	-12	6	3	1	3
C_p	3/2	5/6	5/6	3/2	3/2
κ_p	$h^2/2$	$g^2/4$	$(g^2 + g'^2)/4$	3λ	λ

Table 1: Coefficients for Eq. (42) in the Landau gauge.

four-loop correction was also obtained in semi-analytical form in [72], finding agreement with [71].

The matching is usually done at the top pole mass scale and the theoretical error associated with the arbitrariness of the matching scale can be estimated as said before, namely by comparing the values of $h_t(m_t)$ obtained with different matching scales. For all the details see App. B.3, while, for our results, go to Sec. 3.2.1.

2.1.3 RG-improved effective potential

In order to carefully study the shape of the Higgs potential at high energy, one should consider the renormalisation improved effective potential, which is a truncated expansion, starting from the tree-level SM potential (28), that consider the quantum radiative corrections at some order, having in mind that all the couplings and running parameters of the theory have to be evolved by means of the RG equations, from App. A. We will follow here our work [1]. As already stressed, t can be chosen in such a way that the convergence of perturbation theory is improved. Without sticking, for the time being, to any specific choice of renormalisation scale μ , the RG-improved effective potential at high field values can be rewritten as [80]

$$V_{\text{eff}}(\phi_H, t) \approx \frac{\lambda_{\text{eff}}(\phi_H, t)}{24} \phi_H^4, \quad (40)$$

where $\lambda_{\text{eff}}(\phi_H, t)$ can be thought as a sum of tree-level plus increasing loop contributions:

$$\lambda_{\text{eff}}(\phi_H, t) = \left[\lambda(t) + \lambda^{(1)}(\phi_H, t) + \lambda^{(2)}(\phi_H, t) + \dots \right]. \quad (41)$$

In particular, the one-loop radiative correction, induced by the SM fields, take the well-known Coleman-Weinberg form [81]:

$$\lambda^{(1)}(\phi_H, t) = \frac{6}{(4\pi)^2} \sum_p N_p \kappa_p^2(t) \left(\log \frac{\kappa_p(t) e^{2\Gamma(t)} \phi_H^2}{\mu(t)^2} - C_p \right), \quad (42)$$

where $\mu(t) = e^t \mu$ and, generically, p runs over the top quark, W , Z , Higgs and Goldstone bosons contributions. The coefficients N_p , C_p , κ_p are listed in the Table 1 in the Landau gauge [see e.g. Table 2 of [82] for a general R_ξ gauge].

Due to the wave function renormalisation for the Higgs field, the following replacement have to be considered:

$$\phi_H \rightarrow e^{\Gamma(t)} \phi_H, \quad (43)$$

where

$$\Gamma(t) = - \int_0^t \gamma(\lambda(t')) dt', \quad (44)$$

and $\gamma(\lambda) \equiv -d \ln \phi_H / d \ln \mu$ is the anomalous dimension of the scalar field ϕ_H . This redefinition results in a $e^{4\Gamma(t)}$ overall factor in front of (41).

In order to minimise the logarithms effect from higher-loop corrections it is common to consider the identification⁴

$$\mu(t) = \alpha \phi_H(t), \quad (45)$$

where here α represents the theoretical uncertainty in the choice of the renormalisation scale. Usually, for simplicity, this constant of proportionality is chosen to be 1: in Chap. 3 will be studied its variation and the related effects on physical observables.

The two-loop contribution $\lambda^{(2)}(\phi_H, t)$ was originally derived by Ford, Jack and Jones in [32] and, in the limit $\lambda \rightarrow 0$, was recast in a more compact form in [3] and later in [4], see App. C. We verified, consistently with these works, that the error committed in this approximation is less than 10% and can thus be safely neglected.

The Higgs and the Goldstone part are heavily suppressed in the instability region ($\lambda \sim 0$) and so we can neglect them. Actually, there is a deeper argument thank to which we should discard these two terms from the analysis.

There are a couple of issues related to a general effective potential.

- i. An effective potential is not gauge-invariant [83]. The traditional approach is based on a Landau gauge treatment with the strong assumption that all the approximations used are self-consistent: in other words, the physical quantities extracted from the effective potential have to be gauge-invariant. We know from the Nielsen identity [84]

$$\left(\xi \frac{\partial}{\partial \xi} + C(\phi, \xi) \frac{\partial}{\partial \phi} \right) V(\phi, \xi) = 0, \quad (46)$$

(where ξ is a gauge parameter, $C(\phi, \xi)$ a calculable function and $V(\phi, \xi)$ the effective potential under exam) that the value of the scalar field ϕ , if we exclude the values taken at the extrema, can never be physical: any rescaling of the field can be compensated for by a gauge-change. Furthermore, the value of V at an extremum in ϕ is gauge-invariant.

- ii. The other issue is related to the scale-dependence of the effective potential. We know that the effective potential satisfies the so-called Callan–Symanzik equation [81]

$$\left(\mu \frac{\partial}{\partial \mu} - \gamma \phi \frac{\partial}{\partial \phi} + \beta_i \frac{\partial}{\partial \lambda_i} \right) V = 0. \quad (47)$$

The dependence on a renormalisation scale μ can be compensated for by a rescaling of the couplings λ_i of the theory according to their β -functions β_i and the rescaling of the field ϕ according to its anomalous dimension γ (RGE). Physical quantities extracted from V should be independent of field rescaling: the additional freedom of choosing μ tells us that even in a fixed gauge, field values are

⁴ A result in Quantum Field Theory states that it is always possible to formulate and Effective Field Theory, where only one logarithm term remains relevant in the effective potential, while the others decouple, resulting only in an unphysical shift in the definition of the parameters of the theory. For a high-energy analysis like ours, the fruitful strategy to minimise this term is to consider the renormalisation scale proportional to the scalar field, which is going to assume high values and hence, to dominate on the remaining particle content.

still unphysical. It can be said that V at any extremum is both gauge-invariant and independent of the scale where it is calculated.

Usual loop expansion turns out to be inappropriate for effective potential near quantum-generated vacua [85]: for instance, a classical potential like $V_0 \sim \lambda\phi^4$ can only turn over due to one-loop corrections like $V_1 \sim \lambda_{\text{eff}}\phi^4 = \frac{g^2}{(4\pi)^2}\hbar\phi^4$. Since $\lambda \sim \hbar$, each factor of λ in a diagram changes its effective loop order: this approach may still be correct, but another complication is present. There could be terms scaling with inverse powers of \hbar , so, since λ counts as \hbar , they contribute to loop order terms which could be of order lower than expected.

Including all relevant terms according to this modified power counting, truncating the expansion to order \hbar , we obtain a leading-order gauge-invariant effective potential [86], which takes into account both tree- and one-loop contributions and has the form of the sum between (28) and (42). However, the Higgs and Goldstone part are no more present, because they contribute to higher-order corrections: for the NLO, one contribution comes from the \hbar^2 terms in one-loop potential and another from the λ^0 and $\ln\lambda$ terms in two-loop potential. Finally, there is the contribution from three-loop and higher, proportional to inverse powers of λ : now the potential at each extremum is gauge invariant. Furthermore in Landau gauge some parts of the NLO contribution vanish, leaving an expression compatible with the formula given in App. C.

2.2 THEORETICAL ISSUES: BOUNDS AND SCALE-DEPENDENT PROPERTIES

The light Higgs boson mass (27) observed at LHC raises some concerns about the consistency of the theory: the electroweak scale turns out to be many orders of magnitude lower than the very next physical regime, the one which marks the beginning of the quantum gravity non-negligible influence. This discrepancy, which goes under the name of naturalness problem, will be addressed in Sec. 2.2.3. Together with that, we mention a couple of theoretical bounds which can be put on the Higgs mass, here considered as a free parameter. They rely on some interesting structure features of the SM, *i.e.* the unitarity (Sec. 2.2.1) and triviality (Sec. 2.2.2) arguments.

2.2.1 Unitarity bound

As we already sketched in the end of Sec. 1.1, the introduction of the Higgs field is theoretically motivated by the cancellation of the divergences in some kind of processes. Starting from this point, we are going to see that it is possible to obtain a Higgs mass bound, in order to preserve the unitarity of the theory, following broadly the lecture [87].

Let us consider a process involving the W and Z bosons: this would possibly lead to cross sections which increase indefinitely with the energy, and violate probability

conservation at some stage. We can see that decomposing the scattering amplitude \mathcal{M} into partial waves a_ℓ of orbital angular momentum ℓ , we obtain

$$\mathcal{M} = 16\pi \sum_{\ell=0}^{\infty} (2\ell + 1) \mathcal{P}_\ell(\cos \theta) a_\ell, \quad (48)$$

where the \mathcal{P}_ℓ are the Legendre polynomials and θ the scattering angle. Calling s the centre-of-mass energy, the simple cross section for a $2 \rightarrow 2$ process is

$$\frac{1}{2\pi} \frac{d\sigma}{d(\cos \theta)} = \frac{|\mathcal{M}|^2}{64\pi^2 s} \rightarrow \sigma = \frac{16\pi}{s} \sum_{\ell=0}^{\infty} (2\ell + 1) |a_\ell|^2. \quad (49)$$

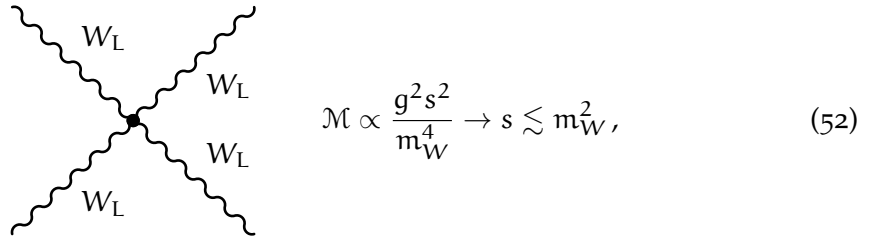
From the conservation of probability it is possible to derive the so-called optical theorem, which relates the cross section with the forwards scattering amplitude

$$\sigma = \frac{1}{s} \Im\{\mathcal{M}(\theta = 0)\}, \quad (50)$$

from which

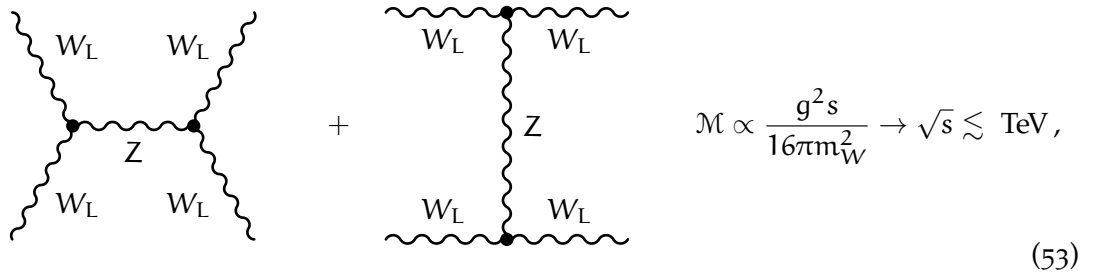
$$\begin{aligned} |a_\ell|^2 = \Im\{a_\ell\} &\rightarrow (\Re\{a_\ell\})^2 + (\Im\{a_\ell\})^2 = \Im\{a_\ell\} \\ &\rightarrow (\Re\{a_\ell\})^2 + \left(\Im\{a_\ell\} - \frac{1}{2}\right)^2 = \frac{1}{4} \\ &\rightarrow |\Re\{a_\ell\}| < \frac{1}{2}. \end{aligned} \quad (51)$$

If we consider the longitudinal components of W and Z , for instance, it can be shown that the related longitudinal polarisation, after a boost in that direction, becomes proportional to the boson momentum, so at very high energy the longitudinal amplitudes will dominate, growing possibly to infinite. The unitarity condition (2.2.1) drawn before is hence badly violated by the quartic interaction of the longitudinal part of the gauge boson W :



$$\mathcal{M} \propto \frac{g^2 s^2}{m_W^4} \rightarrow s \lesssim m_W^2, \quad (52)$$

that is, as we anticipated before, partly cured by adding other SM gauge neutral interactions, *i.e.* Z and γ contributions, from which



$$\mathcal{M} \propto \frac{g^2 s}{16\pi m_W^2} \rightarrow \sqrt{s} \lesssim \text{TeV}, \quad (53)$$

where also the diagrams mediated by the photon, instead of the Z , are understood. The issue is fully addressed with the inclusion of Higgs interactions:

$$\mathcal{M} \propto \frac{g^2 m_H^2}{32\pi m_W^2} \rightarrow m_H \lesssim 875 \text{ GeV}, \quad (54)$$

Considering all the possible contributions to this process, involving couplings to other neutral channels, *e.g.* $Z_L Z_L$, HH , $Z_L H$, or charged ones, *e.g.* $W_L^+ H$, WZ_L , the unitarity constraint weakens up to $m_H \lesssim 710 \text{ GeV}$. As we are going to see, this bound is widely conservative: other theoretical arguments will lead us to narrower value windows.

2.2.2 Triviality bound

The triviality argument [88] states that the SM must be a perturbative theory at all energy scales: all coupling constants must remain small (less than unity) up to high energies. The issue, as a matter of fact, rely on the finiteness of the running of the self-coupling $\lambda(\mu)$ at very high energies. From the RGE

$$\frac{d\lambda}{d \ln \mu} = \beta_\lambda(g, g', g_3, h_t, \lambda, \dots), \quad (55)$$

for very large values of the Higgs mass (and consequently of λ), it can be obtained the following approximate solution for a generic high-energy scale Λ :

$$\lambda(\Lambda) \simeq \lambda(\mu_0) \left[1 - \frac{\beta_\lambda}{\lambda(\mu_0)} \ln \left(\frac{\Lambda^2}{\mu_0^2} \right) \right]^{-1} \approx \frac{\lambda(\mu_0)}{1 - \frac{3}{4\pi^3} \lambda(\mu_0) \ln \left(\frac{\Lambda^2}{\mu_0^2} \right)}, \quad (56)$$

taking the β -function as a constant and $\mu_0 \ll \Lambda$ as a reference scale, *e.g.* the vacuum expectation value v . As the energy grows, the quartic coupling becomes larger and, possibly, infinite, regardless the initial condition for λ : in this case, we will say that the running $\lambda(\mu)$ has a pole at the scale Λ_L , called Landau pole:

$$\Lambda_L = \mu_0 e^{\frac{\lambda(\mu_0)}{2\beta_\lambda}}. \quad (57)$$

For energies $\mu \gtrsim \Lambda_L$ the theory can not be described perturbatively any more. The scalar sector of the SM is a ϕ^4 -theory, hence to remain perturbative at all scales, one needs to have all zero couplings, which means a massless Higgs boson, thus making the theory non-interacting, *i.e.* trivial.

Fixing the Higgs mass and using the RGE evolution, it is possible to establish the energy domain up to which the SM is valid, *i.e.* the cut off Λ below which the self-coupling λ remains finite; or, alternatively, fixing the scale Λ and determine the bound

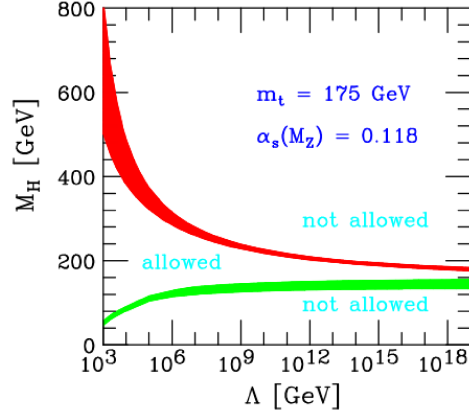


Figure 5: The triviality bound (upper red) and the stability one (lower green, see Sec. 3.1) on the Higgs boson mass as a function of the cut off scale Λ , with a nominal fixed top quark mass $m_t = 175 \pm 6 \text{ GeV}$ and $\alpha_s(m_Z) = 0.118 \pm 0.002$. Figure taken from [89], in agreement with [90].

on the Higgs mass for the theory to be still perturbative. For instance, if we assume $\Lambda \sim 10^{19} \text{ GeV}$, the upper bound for the Higgs would be $m_H \lesssim 145 \text{ GeV}$ at $\mu_0 = v$: this constraint evolve with the cut off scale as Fig. 5.

Since the measured Higgs mass at the electroweak scale is not too large [see 27], there is no problem with the triviality bound for any value of the cut off $\Lambda \lesssim M_P$: actually, from a rough estimation, we infer that $\Lambda_L \gtrsim 10^{38} \text{ GeV}$. This gives us freedom of choosing the energy scale where new physics can occur, or, alternatively, consider no new physics at all up to the Planck scale, giving rise to the so-called “desert scenario”.

2.2.3 Hierarchy problem

For this section, we are going to follow the approach adopted in [91].

The lightness of the observed Higgs boson remains unexplained. In the SM, as we said, the mass terms for fermions and vectors are not allowed by the symmetry $SU(2)_L \times U(1)_Y$, so they must vanish when the symmetry is restored. This means that all the masses are proportional to the Higgs vacuum expectation value v , also including higher orders in perturbation theory, because the renormalisation procedure leaves the symmetries unbroken. So we will say that any gauge boson or fermion masses are protected by symmetry: in other words, the point $m = 0$ is stable under quantum corrections. In general, if we have an enhanced symmetry for a point in the parameter space, this would be stable under renormalisation group evolution.

This property is no longer valid for scalar particles: for instance, the Higgs boson mass m_H is a free parameter of the theory, unprotected by any symmetry, which implies a tower of radiative corrections proportional to the mass of any particle which the Higgs is coupled to. It is said that the point $m_H = 0$ is UV-unstable.

Driven by the motivation according to which some new physics has to appear at least at the Planck scale⁵, where gravity effects become relevant, we are now supposed to modify the SM at some scale $\Lambda_{\text{BSM}} > \Lambda_{\text{SM}}$, where conventionally we take $\Lambda_{\text{SM}} \sim m_W$. If the Higgs boson is coupled to the new physics sector, then it has to face corrections also due to these new heavy particles, quadratic in their mass $M \sim \Lambda_{\text{BSM}}$. Any UV-completion of this kind would be problematic for the predictability of the Higgs mass. In other words, this means that the Higgs particle, in order to preserve its light mass, has to accommodate many fine-tuned cancellations between unrelated physical observables, giving rise to the well-known hierarchy⁶ or naturalness problem [92].

It is possible to quantify the amount of fine-tuning required, fixing the boundary conditions for the RGE at the scale Λ_{BSM} , where the UV-completion intervenes in the determination of the masses and couplings [93]:

$$m_{\text{H}}^2(\Lambda_{\text{SM}}) = m_{\text{H}}^2(\Lambda_{\text{BSM}}) - C\Lambda_{\text{BSM}}^2 \ln\left(\frac{\Lambda_{\text{BSM}}}{\Lambda_{\text{SM}}}\right) \rightarrow \delta \sim \frac{\Lambda_{\text{BSM}}^2}{m_{\text{H}}^2 \Lambda_{\text{SM}}}, \quad (58)$$

where C is a generic function of the coupling constants and δ stands for the precision to which the initial conditions at the high scale must be fixed, in order to obtain the low-energy phenomenology. An arrangement of about 34 digits is required in case the new physics appear at the Planck scale, for example, in order to have an Higgs mass of 125 GeV. Of course, the lower the fine-tuning, the smaller the new physics scale: as reference numbers, an arrangement of percent level implies a new physics scale of order of TeV.

There exists a certain number of attempt in order to solve or, at least, soften the issue. Trivially, if we trust the SM as the complete description of Nature, without any new effects to take into account, then there would be no hierarchy problem: the (renormalised) Higgs mass remains an observable that must be determined by experiments only, unpredicted by the theory, which can provide only lower and upper bounds. The lack of naturalness in the ratio of the relevant physical scales is then relegated to a merely aesthetic matter. Another philosophical attitude counts on simply ignoring the problem and accept the SM as a fine-tuned model, as many other models in Nature: naturalness would be substituted by another guiding principle, for example, following [3, 4], the near-criticality of the Higgs quartic coupling (and of its β -function), between the stable and metastable configuration, or, alternatively, between the broken and unbroken electroweak phases [94].

Turning to actual solutions proposed, we have to mention first the supersymmetric approach: the power-law divergences of the radiative corrections to the Higgs mass could be removed if we have to consider, above the scale of supersymmetry-breaking particle mass, also the contributions coming from the superpartners of the SM particles, which carry the most important corrections to the Higgs mass [95]. In this way, due to the spin-statistic correlation, we have an opposite sign which gives rise to an exact cancellation of the ill-defined terms, making this solution the most attractive one. Cur-

⁵ There are many indirect hints of new physics coming from different fields of research: just to mention a few of that, we have dark matter observations, baryon asymmetry of the Universe, smallness of neutrino masses, hierarchies in flavour physics, inflation and dark energy puzzles.

⁶ By extension, the hierarchy problem is also referred to the large discrepancy between the strength of the weak force and gravity, 10^{32} times weaker than the former.

rently, supersymmetry and its effects are being tested at LHC, although no evidence in any direction has been found so far.

In a no-supersymmetric scenario, limiting us in a pure SM background, another solution to the hierarchy problem has been proposed: since that the uncontrolled radiative correction on renormalisation is referred to the quadratic Higgs term, it can be supposed that Higgs field has initially no mass, in order to avoid the problem. Then, an alternative method has to be found in order to recover the dynamical generation of the electroweak scale, via a non-null vacuum expectation value. The original method, known as Coleman–Weinberg mechanism [81], takes advantage of the conformal anomaly in order to introduce a mass scale from a symmetry breaking, induced by radiative corrections. However, the Higgs mass obtained in this way is far too small than the accepted experimental value.

Less minimalistic models, involving, for instance, extended supersymmetric scenarios (*e.g.* [96]), a cosmological Higgs-axion interplay as a source of electroweak symmetry breaking [97], a R^2 curvature correction responsible of dimensional transmutation [98], a conformal conspiracy cancellation [see [93] and related more recent works] and composite Higgs models [99] are now under scrutiny. In composite models, in particular, the Higgs is a resonance of some new sector: in this case, there is no point in considering the Higgs particle itself above its compositeness scale, and so it is automatically protected from any UV-corrections. Again, no experimental hints so far give us any confidence on these hypothesis.

Also several extra-dimensions approaches were taken to tackle the problem: for instance, it can be shown that the fundamental Planck mass (obtained in n -dimensional scenario) could be actually small, compensating the strength of the gravitational interaction by the number of extra dimensions and their size. These theories are currently severely constrained by LHC.

Obviously, the Higgs mass could be protected from UV-effects through some unknown mechanisms: any phenomenon below the Planck scale can be sufficiently decoupled from the SM to make its correction irrelevant.

3

ELECTROWEAK VACUUM STABILITY

The main aim of this chapter is to study the vacuum absolute stability conditions for the SM, starting from the knowledge of the behaviour of the Higgs quartic coupling λ up to high-energy scales. Relying on the current central experimental data, we are led to a negative value of λ at a scale $\Lambda_I \sim 10^{10}$ GeV [100, 3, 63, 66, 12, 4], which means that, for central values of the input parameters, the electroweak vacuum of the theory is metastable. A more refined study, as we are going to see, leaves some room (within few σ s) for absolute stability, avoiding dangerous tunnellings of the theory towards possible less energetic true vacua.

3.1 STABILITY AND METASTABILITY

The study of the scale-dependent properties of the Higgs effective potential with no new physics at sub-Planckian regimes can shed light on some very interesting features of the SM, revealing intriguing effects on the early-universe physics [101, 102]. On one hand, the SM can be considered valid up to some energy scale only if the electroweak minimum is stable, or, at least, metastable. On the other hand, the shape of the Higgs potential at high energy could have some impact on cosmology, *e.g.* on the inflationary dynamics or the reheating stage.

Adopting the usual RG-evolution of the Higgs quartic coupling, we can infer, for energies higher than the electroweak scale, the behaviour of the SM vacuum, whose stability is put under pressure by the current central values of the Higgs and top quark masses, along with the strong coupling constant value. A naïve extrapolation would led to a negative value for the Higgs quartic coupling at some energy scale below the Planck mass, making the Higgs potential metastable. We already saw that, according to the Higgs mass measured value, we are in a parameter window in which the SM can be safely extrapolated up to the Planck scale, avoiding any consistency issue: the fact that an instability could arise anyway, make a high-precision analysis for the vacuum stability compulsory.

With the correct estimation of all the experimental and theoretical errors which plague such a precision analysis, and considering the inclusion of the three-loop RG equations and two-loop matching conditions, the instability scale, for the central values of the strong coupling and the top and Higgs masses, occurs at $\Lambda_I \sim 10^{11}$ GeV

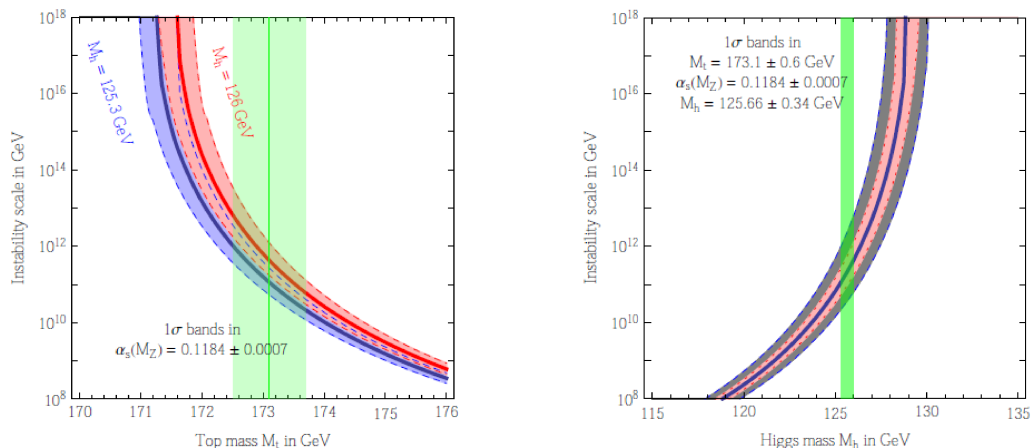


Figure 6: The instability scale Λ_I at which the Higgs quartic coupling becomes negative as a function of the Higgs boson mass m_H (*left panel*) and of the top quark mass m_t (*right panel*). The values used are displayed in the diagrams. Figure taken from [4].

(see Fig. 4), meaning that, at that scale, a non-trivial tunnelling probability to the true minimum which arise could appear (metastability) [100, 14].

The guiding assumption throughout the work is that new physics possibly shows up only at a very high-energy scale, at least the Planck scale. Despite the presence of this new contributions, we assume that they would be suppressed, which implies that the possible tunnelling rate in the metastable scenario can be calculated from SM interactions only [4]. Another opposite approach [103, 104, 105] relies on the fact that any stability analysis would be ineluctably spoiled by the eventual Planck-scale physics beyond the SM. We will spend few words on that in the partial conclusions at the end of the chapter.

The SM, as we are going to see in detail, seems to lie on the border between the absolute stability and the metastability regimes, in the so-called near-criticality scenario [4], where the coupling λ and its β -function β_λ seem to vanish around the Planck scale. However, as stated in [4], the smallness of β_λ might be due to an accidental cancellation between different large contributions, making the near-criticality scenario a matter of coincidence. We can wonder if the fact that the Higgs potential is so close to a configuration with two degenerate vacua is telling us something deep [pointed out for the first time by [106], and resumed, among the others, for instance, by [14]: maybe, the SM proximity to the critical border may be the most important thing we have learnt so far from experimental data on the Higgs particle, in the absence of any new physics hint at low-energy.

The very peculiar value of the Higgs boson mass revealed experimentally could be explained, in alternative, as the outcome of a threshold relation related to some more fundamental high-energy theory at the Planck scale: thus it is needed a model able to drive $\lambda(M_P)$ (and its β -function) to zero [4].

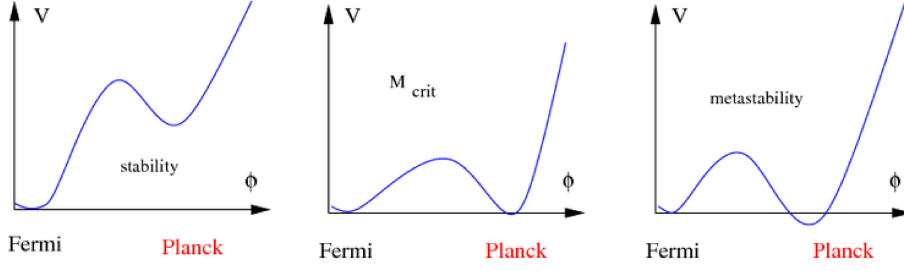


Figure 7: Different configurations for the second minimum that arises at the Planck scale. *Left panel:* the absolute stable potential, where the second vacuum is more energetic than the electroweak one. In this case we can safely extrapolate the SM up to the Planck scale. *Central panel:* critical scenario, in which the two vacua are degenerate in energy. *Right panel:* metastable configuration. The second minimum is less energetic than the low-energy one, and hence a non-zero tunnelling probability appears. The unstable configuration can be imagined by a potential unbounded from below: any extrapolation in this case is forbidden. Figure taken from [63].

3.1.1 Metastability scenario

We saw that the RG-improved effective potential might develop a second minimum at $\phi_c \gg v$: depending on the SM parameters, this new vacuum can be more or less energetic than the electroweak one [see Fig. 7]. In the first case, the electroweak vacuum is said to be stable, otherwise it is metastable¹, and then turns out to be useful to consider the lifetime of the false electroweak vacuum τ and compare it to a known time scale. It happens that nucleation of bubbles of true vacuum within the space of our Universe should lead to a decay of the electroweak vacuum to the state of lowest energy. If τ results very large, even though the electroweak vacuum is not the true one, our Universe would be steady stable on a metastable minimum. This is the main difference with the absolute instability configuration, which would lead to a dreadful sudden breakdown of the theory.

Following [91, 4], we can infer that in semi-classical approximation, the quantum tunnelling rate Γ , *i.e.* the quantum probability per unit time, has been computed [107]:

$$\frac{\Gamma}{dV} \approx A e^{-B/\hbar} [1 + \mathcal{O}(\hbar)] \approx A e^{-S(\ell_B)}, \quad (59)$$

where dV is the space volume and $S(\ell_B)$ is the Euclidean action of the bounce against the barrier, of size $R_B = \ell_B^{-1}$, evaluated in the saddle-point approximation at the solution of the classical field equation

$$\partial_\mu \partial^\mu \phi_H - V'(\phi_H) = \frac{d^2 \phi_H}{dr^2} + \frac{3}{r} \frac{d\phi_H}{dr} - V'(\phi_H) = 0. \quad (60)$$

¹ When the two vacua are degenerate, we found ourselves in the critical configuration, which delimits the border between the stable and metastable scenarios.

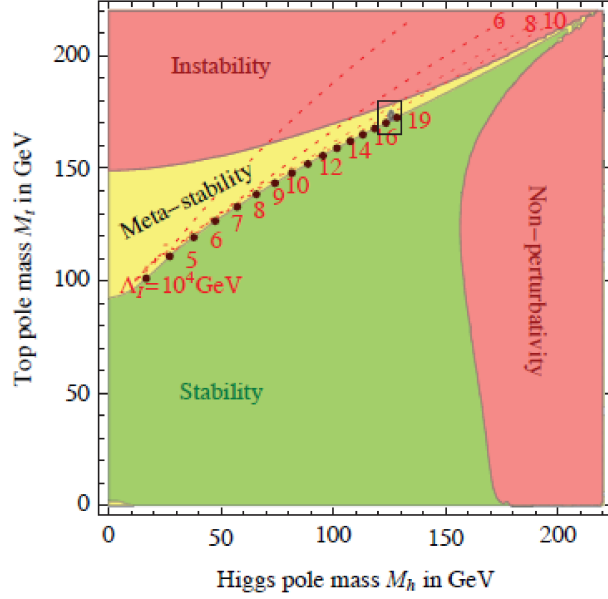


Figure 8: SM phase diagram in the m_t vs. m_H plane, obtained in [3], divided into the absolute stability, metastability and absolute instability regions of the electroweak vacuum and the regime of non-perturbativity of the Higgs quartic coupling. The dashed lines represent the instability scale in GeV.

The spatial coordinate r runs from the false vacuum v up to the true one. The prime stands for the first derivative of the effective potential with respect to ϕ_H . The boundary conditions are

$$\phi'_H(0) = 0, \quad \phi_H(\infty) = v \rightarrow 0. \quad (61)$$

The analytical solution, for negative λ , to obtain the tree-level bounce is

$$\phi_H(r) = \sqrt{\frac{2}{|\lambda|} \frac{R_B}{R_B^2 + r^2}}. \quad (62)$$

The bounce action is hence given by

$$S(\ell_B) = \frac{8\pi^2}{3} \frac{1}{|\lambda(\ell_B)|}. \quad (63)$$

At tree level, the theory is function of the only quartic coupling and is scale invariant, with an arbitrary size of the bounce. This scale is evaluated when Γ/dV is maximised: this means that $\lambda(\ell_B)$ has to be minimised, condition satisfied when $\beta_\lambda(\ell_B) = 0$. The degeneracy is broken when we consider the radiative corrections, going to the one-loop action: the RG flow breaks scale invariance, then the coefficient A can be calcu-

lated [108]: it is equal to $\tau_U \ell_B^4$, where $\tau_U \simeq 13.8$ Gyr is the age of the Universe, used as reference time scale². The one-loop tunnelling rate becomes

$$\frac{\Gamma}{dV} = \frac{1}{4\pi^2 \tau_U} \left(\frac{\tau_U^4 \mathcal{S}(\ell_B)}{R_B^4} e^{-\mathcal{S}(\ell_B)} \right) \times e^{-\Delta \mathcal{S}^{(1)}}, \quad (64)$$

where $\Delta \mathcal{S}^{(1)}$ is the one-loop correction to the bounce action. Substituting the solution (62) in Eq. (64) and constraining the probability to be less than one, we obtain a lower bound for λ , which can be translated in a lower bound for the Higgs mass, approximately given by [110]

$$m_H > 117 \text{ GeV} + \Delta m_t + \Delta \alpha_s + 0.1 \ln \left(\frac{\tau_U}{10^{10} \text{ yr}} \right). \quad (65)$$

This metastability constraint, along with the other theoretical bounds mentioned in Sec. 2.2.1 and in Sec. 2.2.2, helps to build the global stability phase diagram [for the well-known result from Degraffi *et al.* [3], see Fig. 8]: the differences between this work and ours [1] are going to be discussed in the next sections. The instability-metastability line is drawn imposing $\tau = \tau_U$ dealing with the bound above, while our interests are focussed on the stability-metastability line.

As long as $\ell_B \ll M_P$, the analysis is independent on gravitational effects. When we take into account also gravitational corrections (namely whenever $\ell_B > M_P$), it is possible to obtain a lower bound on the tunnelling probability by setting $\lambda(\ell_B) = \lambda(M_P)$. The results, beyond the scope of this thesis, are contained in [111].

It is possible to evaluate the total probability of vacuum decay Γ/dV integrating Eq. (59) over space-time of our past light-cone, to know if it have occurred up to now (in a matter-dominated cosmology) and in a cosmological constant-dominated scenario, in order to have a feeling of how much the false vacuum is likely to decay in the future. The first result is that the probability is independent of the early cosmology history: Γ/dV is very small, as a consequence of the near-criticality regime of the SM parameters [4]. In the other case, the electroweak vacuum is again likely to survive for times hugely longer than the age of the Universe.

The smallness of β_λ at high energies allows to assume no-physics thresholds around the instability scale and hence the SM to be valid beyond Λ_I and up to the Planck scale, since tunnelling probability remains small.

3.2 STATIONARY CONFIGURATIONS OF THE SM: VACUUM STABILITY ANALYSIS

Two stationary configurations of the SM Higgs potential turn out to be particularly relevant: the case of two degenerate vacua [106], that is the condition for electroweak vacuum stability, and the case of a rising inflection point at high energy [19], close to the Planck scale, which is going to be detailed in Chap. 4, where we are going to present our analysis [1].

Our goal is to perform a detailed and updated study of the gauge-independent observables associated with such stationary configurations, building on the recent

² This number is extrapolated from the latest Planck data [109].

progress made in both the theoretical and the experimental sides. We extrapolate the SM Higgs potential up to high energy according to the present state of the art, namely the NNLO, and study in particular:

- i. the value of the top mass ensuring the stability of the SM electroweak minimum;
- ii. the value of the Higgs potential at the rising inflection point.

We examine in detail and reappraise in a critical way the experimental and theoretical uncertainties which plague their determination.

The inputs necessary to carry out the extrapolation are: the low energy values of the three gauge couplings, the top quark and the Higgs masses. Since the discovery of the Higgs boson, a lot of work has been done in the direction of refining the calculation of the RGE-improved Higgs effective potential at high energy. We use now the tools presented in Chap. 2³, together with a better understanding of how to extract gauge-invariant observables [82, 14] from the (gauge-dependent) effective potential.

On the experimental side, we already mentioned the crucial improvements in the measurements of the top and Higgs mass, as long as the updated determination of the strong coupling constant.

Taking into account all these developments, we update the analyses [3, 63, 4, 66, 12, 112, 2], reappraising in a critical way the experimental and theoretical uncertainties which plague the determination of the top mass value ensuring the stability of the SM electroweak minimum.

3.2.1 Criticality: Calculation

The state of the art of the NNLO stability analyses in the SM involves the RGE of all coupling constants up to three-loop level and the threshold corrections at the weak scale up to two-loop order. The reason for that is that we are working with the improved effective potential and, as it was proved in [113], the L-loop effective potential improved by $(L + 1)$ -loop RGE resums all the L^{th} -to-leading logarithm contributions. Therefore, for the vacuum stability analysis at L-loop, the threshold value at L-loop also will be needed. The first point is achieved by imposing the renormalisation group equation to the effective potential in an appropriate choice of coordinates, defined in the space of fields and parameters. By imposing the RG equation to the new parametrised version of the effective potential, one is able to reconstruct the full potential since the leading logarithms have coefficients determined by the tree-level potential and the one-loop result for the β - and γ -functions. An analogous approach is intended for the sub-leading logarithms. The crucial point is that the improved potential is obtained in terms of running parameters in the fields space. For the last point we consider the improved effective potential, in which, for large fields, λ_{eff} has the same loop order of the effective potential as of its threshold value.

In order to derive the values of the relevant parameters $(g, g', g_3, h_t, \lambda)$ at the top pole mass m_t , at which the boundary conditions we use are given, we exploit, in our work [1], the results of one of the most recent analyses about the matching procedure,

³ As concerns the matching, although the full theoretical procedure has been presented, we only use, as anticipated, the inputs from [2].

performed by Bednyakov *et al.* [2]. This paper uses as input parameters at m_Z those from the 2014 release of the PDG [25]. Such parameters are evolved in the context of the SM as an effective theory with five flavours, and then matched to the six-flavours theory at m_t . The procedure is carried out by including corrections up to $\mathcal{O}(\alpha_{em}^2)$, $\mathcal{O}(\alpha_{em}\alpha_s)$, $\mathcal{O}(\alpha_s^4)$, as in general explained in Sec. 2.1.2. The theoretical uncertainties in the results due to unknown higher-order corrections are estimated considering both scale variations and truncation errors. The matching is thus carried out at the NNLO (actually even slightly beyond, because of the strong gauge coupling contribution).

Although in our analysis we use the complete results of [2] (see in particular their Eq. (6) and table I therein), we provide here some simplified expressions which capture the dominant dependences and sources of uncertainty. It is well known that, for the sake of the present calculation, the most significant uncertainties are those associated with the determination of $g_3(m_t)$, $\lambda(m_t)$, $h_t(m_t)$, while uncertainties in the matching of $g(m_t)$, $g'(m_t)$ are negligible. Let us consider the former three couplings in turn, updating the work above, when necessary, by means of the latest (September 2015) release of the PDG [59].

GAUGE COUPLINGS. The uncertainty in the value of $g_3(m_t)$ is mainly dominated by the experimental error on the $\alpha_s^{(5)}$ value, the strong coupling constant at m_Z in the SM with five flavours:

$$g_3(m_t) \simeq 1.1636 + 5.8 \times 10^{-3} \frac{\alpha_s^{(5)} - \alpha_s^{(5,exp)}}{\Delta\alpha_s^{(5,exp)}}, \quad (66)$$

where the present world average experimental value, already given in (33), is $\alpha_s^{(5,exp)} = 0.1181$, and its associated 1σ error $\Delta\alpha_s^{(5,exp)} = 0.0013$ have been used as reference values. Notice that in [2] it is used instead as reference value $\alpha_s^{(5,exp)} = 0.1185$, with 1σ error given by $\Delta\alpha_s^{(5,exp)} = 0.0006$ [25]; previous analyses like *e.g.* [3, 63, 4], used $\alpha_s^{(5,exp)} = 0.1184$, with 1σ error given by $\Delta\alpha_s^{(5,exp)} = 0.0007$ [114].

HIGGS QUARTIC COUPLING. The uncertainty on $\lambda(m_t)$ is dominated by the experimental uncertainty on the Higgs mass m_H and by the theoretical uncertainty associated with the matching procedure (scale variation and truncation, here added in quadrature)

$$\lambda(m_t) \simeq 0.7554 + 2.9 \times 10^{-3} \frac{m_H - m_H^{exp}}{\Delta m_H^{exp}} \pm 4.8 \times 10^{-3}, \quad (67)$$

where we used as reference values the most recent ATLAS and CMS combination⁴, as anticipated in (27), $m_H^{exp} = 125.09$ GeV, with 1σ error given by $\Delta m_H^{exp} = 0.24$ GeV [31]. Notice that in Eq. (67) the theoretical error is pretty large, being equivalent to a 1.6σ variation in m_H . In the previous literature there is some difference about the size of the theoretical error: for instance, the theoretical error of the recent analysis by Bednyakov *et al.* [2] is about the half of the one quoted in the well-known analysis by Degrandi *et al.*

⁴ Again, we update the result of [2] by using the most recent LHC data, instead of $m_H^{exp} = 125.7$ GeV and $\Delta m_H^{exp} = 0.4$ GeV, quoted in the 2014 version of the PDG [25]. Notice also that within our normalisation the value of λ is six times the one of [2].

al. [3], due to the inclusion of all corrections up to $\mathcal{O}(\alpha_{em}^2)$, $\mathcal{O}(\alpha_{em}\alpha_s)$, $\mathcal{O}(\alpha_s^4)$. On the other hand, Buttazzo *et al.* [4] quote an error which is five times smaller than the one of [3]. According to another previous similar analysis [12], the upper error is as small as the one of [4], but the lower error is indeed consistent with [3]. Clearly, it would be worth assessing and further refining the present error in the matching of λ .

TOP YUKAWA COUPLING. The uncertainty on $h_t(m_t)$ is essentially affected by the experimental error on the top pole mass m_t itself, but also the theoretical uncertainty associated with the matching procedure (scale variation and truncation, here added in quadrature) is sizable

$$h_t(m_t) \simeq 0.9359 + 4.4 \times 10^{-3} \frac{m_t - m_t^{\text{exp}}}{\Delta m_t^{\text{exp}}} \pm 1.4 \times 10^{-3}, \quad (68)$$

where we used as reference value for the top mass $m_t^{\text{exp}} = 173.34$ GeV, with an error $\Delta m_t^{\text{exp}} = 0.76$ GeV. The theoretical uncertainty in Eq. (68) is consistent with the one of [3, 4]⁵.

It is clear that when $\lambda(t)$ becomes negative, the Higgs and Goldstone contributions in Eq. (42) are small but complex, and this represents a problem in the numerical analysis of the stability of the electroweak vacuum. Indeed, in [3, 4] the potential was calculated at the two-loop level, but setting to zero the Higgs and Goldstone contributions in Eq. (42). In [12] it was decided to calculate the potential only at the tree-level because, for the sake of the analysis of the electroweak vacuum stability, the numerical difference with respect to the previous method was negligible.

As clarified, in general, at the end of Sec. 2.1.3, some authors [115, 86] recently showed that the procedure of [3, 4] is actually theoretically justified when λ is small (say $\lambda \sim \hbar$): in this case, the sum over p does not have to include the Higgs and Goldstone's contributions, which rather have to be accounted for in the two-loop effective potential, which practically coincides with the expression derived in [3, 4].

For the stationary configurations we are interested in – two degenerate minima and a rising point of inflection – it happens that λ is small (and could be negative): we thus adopt the procedure outlined in [86].

3.2.2 Criticality: Results

As discussed in the previous section, once m_H and $\alpha_s^{(5)}$ have been fixed, the value of the top mass for which the SM displays two degenerate vacua, m_t^c , is a gauge-invariant quantity. This value is however plagued by experimental and theoretical errors, which we now discuss in turn.

The experimental error is the one associated with the precision at which we know the input parameters at the matching scale m_t . The uncertainty on m_t^c due to varying $\alpha_s^{(5)}$ in its 1σ range is ± 0.37 GeV, while the uncertainty due to varying m_H in its 1σ range is ± 0.12 GeV. This can be graphically seen in Fig. 9, where m_t^c is displayed as

⁵ The latter quotes an error on the matching of h_t which is three times smaller than the one in Eq. (68), but includes an error of $\mathcal{O}(\Lambda_{\text{QCD}})$, *i.e.* about 0.3 GeV, in the definition of m_t , to account for non-perturbative uncertainties associated with the relation between the measured value of the top mass and the actual definition of the top pole mass, issue already discussed in Sec. 2.1.2.

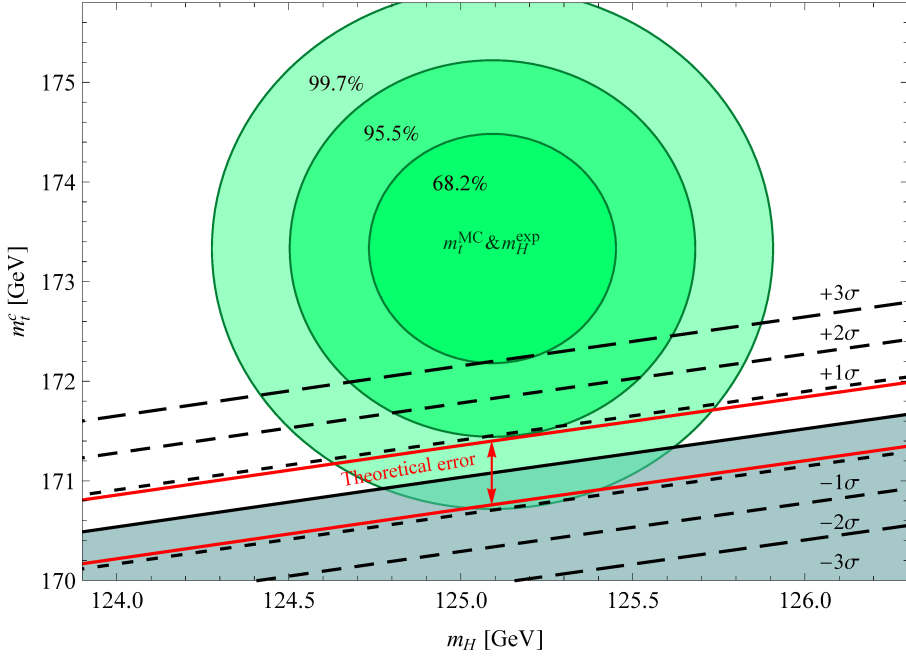


Figure 9: Lines for which the Higgs potential develops a second degenerate minimum at high energy. The solid line corresponds to the central value of $\alpha_s^{(5)}$; the dashed lines are obtained by varying $\alpha_s^{(5)}$ in its experimental range, up to 3σ . The (red) arrow represents the theoretical error in the position of the lines. The (green) shaded regions are the covariance ellipses obtained combining $m_t^{\text{MC}} = 173.34 \pm 0.76$ GeV and $m_H^{\text{exp}} = 125.09 \pm 0.24$ GeV; the probability of finding m_t^{MC} and m_H inside the inner (central, outer) ellipse is equal to 68.2% (95.5%, 99.7%). The shaded area at the bottom of the figure is the parameter space where absolute stability takes place. The figure is contained in [1].

a function of m_H for selected values of $\alpha_s^{(5)}$; in particular, the solid line refers to its central value, while the dotted, short and long dashed lines refer to the 1σ , 2σ and 3σ deviations respectively. In the region below (above) the line the potential is stable (metastable).

Theoretical errors come from the approximations done in the three steps of the calculation: matching at m_t , running from m_t up to high scales, effective potential expansion.

- As already seen in Sec. 3.2.1, the theoretical error in the NNLO matching (scale variation and truncation) of λ is equivalent to a variation in m_H by about 1.6σ (± 0.38 GeV), which in turn means an error on m_t^c of about ± 0.19 GeV. The theoretical error in the NNLO matching (scale variation and truncation) of h_t is equivalent to a variation in m_t by about 0.3σ , which translates into an uncertainty of about ± 0.25 GeV on m_t^c . Combining in quadrature, the theoretical uncertainty on m_t^c due to the NNLO matching turns out to be about ± 0.32 GeV: this means

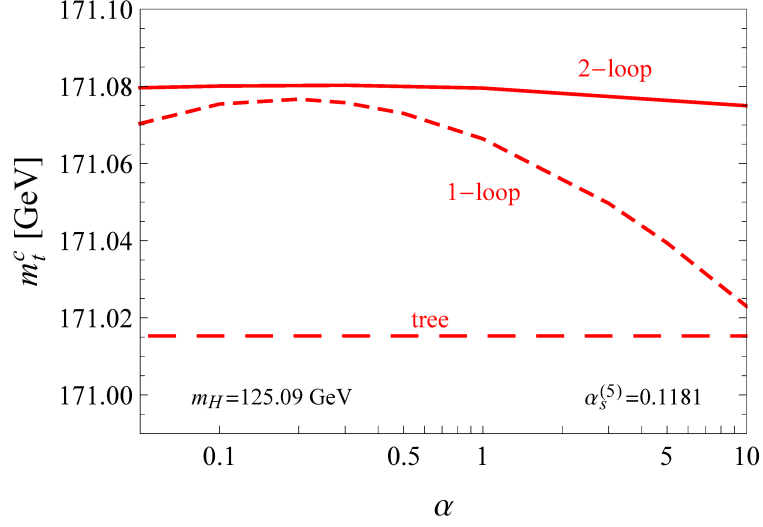


Figure 10: Dependence of m_t^c on α , for the increasing level of the effective potential expansion. We choose the central values for m_H and $\alpha_s^{(5)}$. The figure is contained in [1].

that the position of the straight lines in Fig. 9 can be shifted up or down by about 0.32 GeV, as represented by the (red) arrow for the central value of $\alpha_s^{(5)}$.

- The theoretical uncertainty associated with the order of the β -functions in the RGE can be estimated by adding the order of magnitude of the unknown subsequent correction. For the NNLO, it turns out that the impact of the subsequent four-loop correction on m_t^c is of order 10^{-5} GeV, thus negligible.
- A way to estimate the theoretical uncertainty on m_t^c associated with the order of the expansion of the effective potential is to study its dependence on α . In Fig. 10 we show this dependence by varying α in the interval 0.1 – 10, while keeping the other parameters fixed at their central values. For comparison, we display the dependence obtained by performing the calculation of the effective potential at the tree- (long-dashed), one-loop (short-dashed) and two-loop (solid) levels. A few comments are in order here. The renormalisation scale $\mu(t)$ depends on α via Eq. (45) so that, at the tree level, the Higgs potential does not depend explicitly on $\mu(t)$, but only implicitly via the dependence of the running couplings; for this reason, in Fig. 10, the dependence on α for tree level is negligible, and we find $m_t^c \simeq 171.02$ GeV. At one-loop the dependence on α is explicit, but the variation is anyway small, being about 0.05 GeV. The two-loop order further improves the independence on α : we can conclude that the error on m_t^c at the NNLO is very small, ± 0.005 GeV.

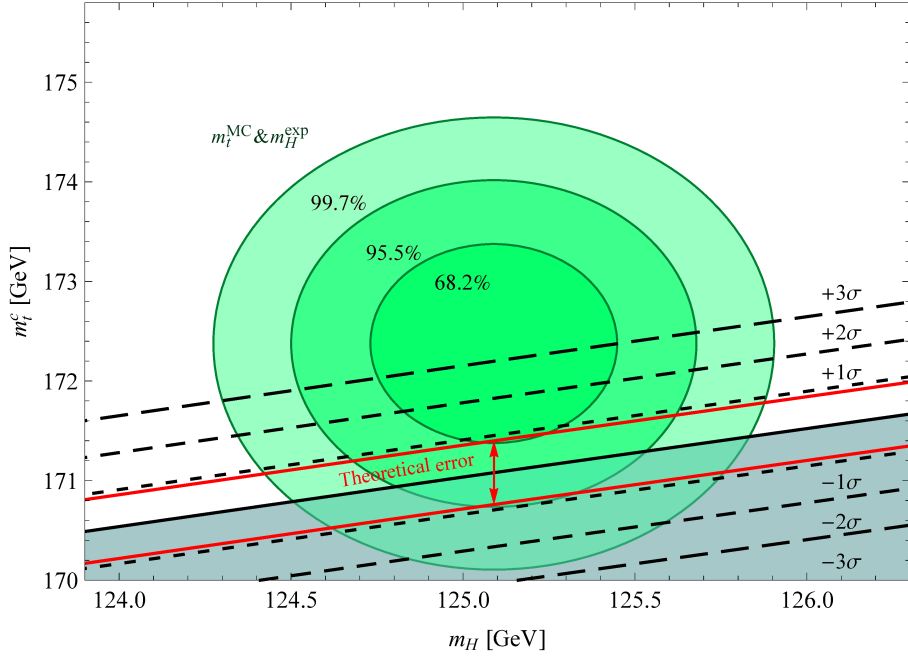


Figure 11: Lines for which the Higgs potential develops a second degenerate minimum at high energy. The solid line corresponds to the central value of $\alpha_s^{(5)}$; the dashed lines are obtained by varying $\alpha_s^{(5)}$ in its experimental range, up to 3σ . The (red) arrow represents the theoretical error in the position of the lines. The (green) shaded regions are the covariance ellipses obtained combining $m_t^{\text{CMS}} = 172.38 \pm 0.66$ GeV [116] and $m_H^{\text{exp}} = 125.09 \pm 0.24$ GeV. Again the shaded area at the bottom of the plot is the absolute stability region. The figure is contained in [1].

Summarising, the theoretical error that mostly affects the NNLO calculation of m_t^c is the one in the matching, while those in the truncation of the loop expansion in the β -functions and in the effective potential expansions are negligible.

We can conclude that the result of the NNLO calculation is

$$\boxed{m_t^c = 171.08 \pm 0.37_{\alpha_s} \pm 0.12_{m_H} \pm 0.32_{\text{th}} \text{ GeV},} \quad (69)$$

where the first two errors are the 1σ variations of $\alpha_s^{(5)}$ and m_H .

Our results for the value of m_t^c update and improve⁶ and, modulo the doubling of the experimental error in $\alpha_s^{(5)}$, are essentially consistent with, those of the most recent literature [3, 63, 66, 12, 4, 2].

The above value of m_t^c has to be compared with the experimental determination of the top pole mass, m_t . The present value of the MC top mass is $m_t^{\text{MC}} = 173.34 \pm 0.76$ GeV [74] and would imply a difference with m_t^c at the level of about 1.7σ . This

⁶ The calculation of the theoretical error associated with the truncation at the two-loop order has (to our knowledge) not been shown so far.

can be graphically seen in Fig. 9, where the (shaded) ellipses are the covariance ellipses for a two-valued Gaussian density, obtained by combining the present experimental values of the MC top mass and Higgs mass, so that the probability of being inside the smaller, central and larger ellipses, is respectively 68.2%, 95.5% and 99.7%. However, as discussed in Sec. 3.2.1, the uncertainty in the identification between the pole and MC top mass is currently estimated to be of order 200 MeV [77, 78] (or even 1 GeV for the most conservative groups [75]): this would further reduce the difference, say at the 1.5σ level. Statistically speaking, a tension at the 1.5σ level supports stability and metastability at the 14% and 86% C.L. respectively. Physically speaking, in our opinion, it is even too strong to use the term “tension” in such a scenario.

CONCLUSIONS. As a result, the updated calculation of the experimental and theoretical uncertainties on m_t^c , in addition to the uncertainty in the identification of the MC and pole top masses, lead us to conclude that the configuration with two degenerate vacua is at present compatible with the experimental data.

Our conclusions agree with those of [2]. Previous claims that stability is disfavored at more than the 95% level [3, 4] are due, in our opinion, to the previous underestimation of two uncertainties – the experimental one in the determination of $\alpha_s^{(5)}$ and the theoretical one in the identification of the MC and pole top masses –, together with a less conservative interpretation (with respect to ours) of the significance of the results. For the same reasons, we do not feel confident in strongly excluding stability, as claimed in other works like [13, 117].

It is clear that, in order to discriminate in a robust way between stability and metastability, it would be crucial to reduce the experimental uncertainties in both m_t and $\alpha_s^{(5)}$. A reduction of the theoretical error in the matching would also be welcome.

As a final remark, notice that a recent measurement of the top pole mass by the CMS Collaboration suggest a value of $m_t^{\text{CMS}} = 172.38 \pm 0.66$ GeV [116]. The shaded ellipses in this case would change as shown in Fig. 11, and the discrepancy with m_t^c would thus further decrease, at less than 1σ . It will be very interesting to see if such a low value will be confirmed by future LHC data. Also some more rumors about some refined recent Higgs mass measurements, amounting to slightly lower values with respect the current central one, seem to suggest a tenuous shift towards the stability regime. Official future data are welcome.

Throughout this analysis we assumed the SM to be valid all the way up to the Planck scale⁷ and we noticed how the stability of the SM can be very sensitive to the higher-order radiative corrections. Near the cutoff of the theory, large Planckian effects are possible, but without a satisfactory comprehension of quantum gravity effects (with a reliable UV-completion of the theory) there is no hope to calculate them. The usual approach in this sense is to consider a tower of a non-renormalisable operators suppressed by the cutoff in an effective theory scenario below M_P [103, 104, 105, 118, 119, 14], leading to a modification of the SM Higgs potential, *e.g.*:

$$V(\phi) = \frac{\lambda}{24} \phi^4 + \frac{\lambda_6}{6} \frac{\phi^6}{M_P^2} + \frac{\lambda_8}{8} \frac{\phi^8}{M_P^4} + \mathcal{O}\left(\frac{\phi^{10}}{M_P^6}\right). \quad (70)$$

⁷ The scale at which gravitational effects become non-negligible is conventionally assumed to be the Planck scale, as we are going to do throughout this thesis, but some recent works has shown that this energy is model dependent.

Without any protecting symmetry, these corrections have to be taken into account. In this way, assuming $\mathcal{O}(1)$ values for the new unknown couplings, here represented by λ_6 and λ_8 , treated as free parameters, it is in principle possible to estimate the impact of gravitational physics. The effects of these higher-order operators turn out to be heavily dependent on the choice of the free couplings towards both stability and instability: it is not clear why gravitational physics should make the potential more unstable or vice versa. The theory, when predictions happen to depend on a number of parameters larger than the number of predictions themselves, ceases to be predictive. This philosophical attitude (see [103, 104, 105] and related works) is actually based on the belief according to which a high-precision vacuum stability analysis, as the one performed here, is, by its nature, not conclusive, because severely limited by our ignorance about the physics beyond the SM. The approach of Eq. (70) has however raised some concerns [120], as the method is based on an effective theory expansion that breaks down when $\phi_H \sim M_P$. The use of an effective theory close to its cutoff might not be fully reliable.

3.3 GAUGE (IN)DEPENDENCES

In order to deal with the two particular stationary configurations considered, we have to handle the well-known gauge dependence of the RGE-improved effective potential. For instance, we know that the value of the top mass corresponding to the stability bound does not suffer from this issue [4]. We want to provide a general proof of this result, generalising it also to any stationary point in the potential.

Let us start from the argument presented by Di Luzio and Mihaila [82] for the case of two degenerate vacua (here we focus on m_t instead of m_H).

We assume that all the parameters of the SM are precisely determined, except for the top mass. After choosing the renormalisation scale μ , the RGE-improved effective potential (2.1.3), $V_{\text{eff}}(\phi, m_t; \xi)$, is a function of ϕ , the top mass m_t , and the gauge-fixing parameters, collectively denoted by ξ . m_t is actually a free parameter, whose variation modifies the shape of the effective potential, as sketched in Fig. 12 for the Landau gauge. Starting from top to bottom, the shape of the Higgs potential changes, going from stability to instability by increasing the top mass.

The absolute stability bound on the top mass can be obtained by defining a critical mass top mass m_t^c , for which the value of the effective potential at the electroweak minimum ϕ_{ew} , and at a second minimum, $\phi_c > \phi_{ew}$, are the same:

$$\left. \frac{\partial V_{\text{eff}}}{\partial \phi} \right|_{\phi_{ew}, m_t^c} = \left. \frac{\partial V_{\text{eff}}}{\partial \phi} \right|_{\phi_c, m_t^c} = 0, \quad V_{\text{eff}}(\phi_{ew}, m_t^c; \xi) - V_{\text{eff}}(\phi_c, m_t^c; \xi) = 0. \quad (71)$$

Slightly lowering m_t , one finds another particular value of the top mass, m_t^i , such that the Higgs potential displays an inflection at $\phi_i > \phi_{ew}$:

$$\left. \frac{\partial V_{\text{eff}}}{\partial \phi} \right|_{\phi_{ew}, m_t^i} = \left. \frac{\partial V_{\text{eff}}}{\partial \phi} \right|_{\phi_i, m_t^i} = 0, \quad \left. \frac{\partial^2 V_{\text{eff}}}{\partial \phi^2} \right|_{\phi_i, m_t^i} = 0. \quad (72)$$

Due to the explicit presence of ξ in both the conditions, it is not obvious *a priori* which are the physical (gauge-independent) observables which we could work out in the analysis.

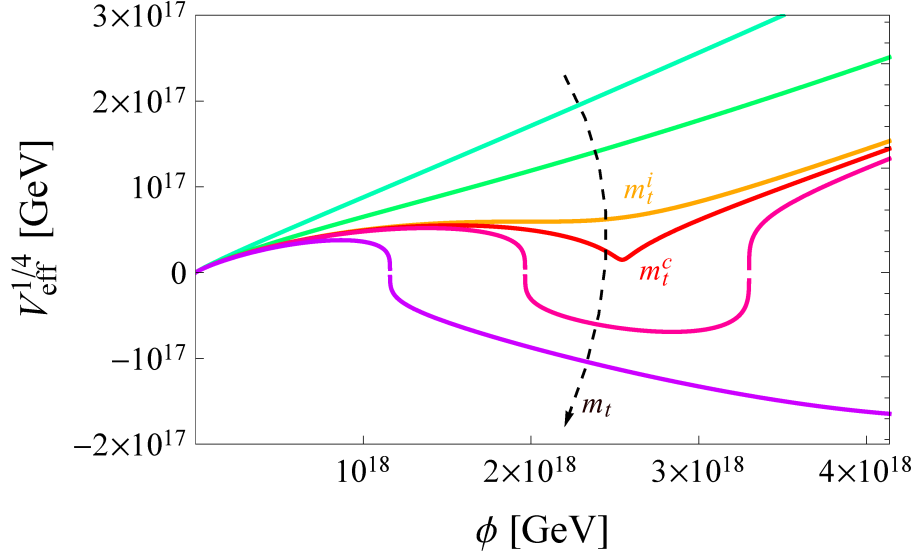


Figure 12: Sketch of the shape of SM effective potential at high energy in the Landau gauge, for increasing values of the top mass, from top to bottom. Two peculiar stationary configurations can be identified: two degenerate vacua (criticality) and a rising point of inflection, associated respectively with the values m_t^c and m_t^i . The figure is contained in [1].

The guideline in capturing the gauge-invariant content of the effective potential, is given by the Nielsen identity (46), where we leave the correlator $C(\phi, \xi)$ undefined, because it will not be needed for our argument. The identity tells us that $V_{\text{eff}}(\phi, \xi)$ is constant along the characteristics of the equation, which are the curves in the (ϕ, ξ) plane for which

$$d\xi = \frac{\xi}{C(\phi, \xi)} d\phi. \quad (73)$$

In particular, we can conclude that the effective potential is gauge independent where it is stationary. Due to the fact that the value of the effective potential at any stationary point ϕ_s (as it is the case for ϕ_{ew} , ϕ_c and ϕ_i) is gauge invariant

$$\left. \frac{\partial V_{\text{eff}}(\phi, \xi)}{\partial \phi} \right|_{\phi_s, m_t} = 0 \rightarrow \left. \frac{\partial V_{\text{eff}}(\phi, \xi)}{\partial \xi} \right|_{\phi_s, m_t} = 0, \quad (74)$$

its value at the extremum can be calculated working in any gauge, *e.g.* the Landau gauge

$$V_{\text{eff}}(\phi_s, m_t; \xi) = V_{\text{eff}}(\phi_s^L, m_t; 0), \quad (75)$$

where ϕ_s^L is the field evaluated at a stationary point, in Landau gauge.

We want to check explicitly that, contrary of ϕ_s , the particular values of m_t ensuring the criticality m_t^c , and an inflection point m_t^i , are gauge independent. Let us call them

collectively m_t^s ($s = c, i$), and denote by \bar{V}_s the associated value of the effective potential in the Landau gauge:

$$V_{\text{eff}}(\phi_s, m_t^s; \xi) = V_{\text{eff}}(\phi_s^L, m_t^s; 0) \equiv \bar{V}_s. \quad (76)$$

Inverting Eq. (76) (together with the stationary condition) would yield gauge-dependent field and top mass values: $\phi_s = \phi_s(\xi)$ and $m_t^s = m_t^s(\xi)$. We apply a total derivative with respect to ξ to Eq. (75) and obtain

$$\left. \frac{\partial V_{\text{eff}}}{\partial \xi} \right|_{\phi_s, m_t^s} + \left. \frac{\partial V_{\text{eff}}}{\partial m_t} \right|_{\phi_s, m_t^s} \frac{\partial m_t^s}{\partial \xi} + \left. \frac{\partial V_{\text{eff}}}{\partial \phi} \right|_{\phi_s, m_t^s} \frac{\partial \phi_s}{\partial \xi} = 0, \quad (77)$$

where the third and first terms in the left-handed side (lhs) vanish because of the stationary condition and the Nielsen identity, respectively. Since in general $\left. \frac{\partial V_{\text{eff}}}{\partial m_t} \right|_{\phi_s, m_t^s} \neq 0$, we obtain that

$$\boxed{\frac{\partial m_t^s}{\partial \xi} = 0}. \quad (78)$$

We can conclude that the peculiar values of m_t ensuring the stationary configurations, like two degenerate vacua or an inflection point, are gauge independent.

Notice that the above argument can be easily generalised to the case in which we treat as free parameters not only the top mass, but all other input parameters entering in the calculation of the effective potential, as, for instance, the Higgs mass and α_s . Let us call them $\vec{f} = (m_t, m_H, \alpha_s, \dots)$, so that $V_{\text{eff}}(\phi, \vec{f}; \xi)$. In this case, the generalisation of Eq. (77) is simply:

$$\left. \frac{\partial V_{\text{eff}}}{\partial \xi} \right|_{\phi_s, \vec{f}^s} + \sum_i \left. \frac{\partial V_{\text{eff}}}{\partial f_i} \right|_{\phi_s, \vec{f}^s} \frac{\partial f_i^s}{\partial \xi} + \left. \frac{\partial V_{\text{eff}}}{\partial \phi} \right|_{\phi_s, \vec{f}^s} \frac{\partial \phi_s}{\partial \xi} = 0. \quad (79)$$

As before, the last and the first terms in the lhs vanish because of the stationary condition and the Nielsen identity, respectively. Since in general $\left. \frac{\partial V_{\text{eff}}}{\partial f_i} \right|_{\phi_s, \vec{f}^s} \neq 0$, we obtain again $\frac{\partial f_i^s}{\partial \xi} = 0$. Hence, the result remains valid for any input parameter.

Working in the Landau gauge is thus perfectly consistent in finding the value of the effective potential at a stationary point, \bar{V}_s , or the value of the top mass which ensures it. Nevertheless, one has to be aware that the truncation of the effective potential loop expansion at some loop order, introduces an unavoidable theoretical error both in \bar{V}_s and in m_t^s . For this sake, as shown explicitly in Sec. 3.2.2 and in the next chapter 4.2, we studied the dependence of \bar{V}_s and m_t^s on the α parameter, introduced in (45). From Fig. 10, the higher the order of the loop expansion, the less the dependence on α . In the next chapter, we are going to study in detail the case of another stationary point of interest: a rising inflection point at high energies, in the context of a pure SM inflationary scenario.

4

THE INFLATIONARY FRAMEWORK: THE INFLECTION POINT CONFIGURATION

Besides the critical configuration in the stability analysis of the SM, performed in the previous chapter, we want to repeat the calculation for another stationary point in the pure SM scenario. The Higgs potential, tuning properly the top quark mass, being fixed the Higgs mass value, could develop an inflection point at high energy: it is tempting to take advantage of this feature for a possible realisation of an inflationary phase [19, 18, 17, 121]. The Higgs boson, here playing the role of the inflaton, rolls down gently along its well-shaped high-energy potential, giving us some hope in providing a suitable amplitude of scalar perturbation and a long enough expansion phase, in order to solve the early Universe issues related to its initial conditions.

This inflationary model has to face, obviously, the experimental constraints on the cosmological observables, introduced in the first part of the present chapter.

In Sec. 4.1 we will review the main aspects of inflation, included its historical development, introducing all the relevant physical quantities and their related current experimental windows. When all the useful tools are settled, in the last part of the chapter [Sec. 4.2] we will propose a detailed analysis of the inflection point configuration, reappraising all the experimental and theoretical errors which have to be taken into account in the proper determination of this stationary point [1]. The final attempt to build inflation on this shape of the SM potential will be given then at the end of the chapter, including some partial conclusions.

4.1 GENERAL NOTES ON INFLATION

We recap here the most important concepts related to the inflationary framework, starting from the motivations for its introduction, following the approach used in [122]: in Sec. 4.1.1 we summarise briefly the two most problematic issues of the early stages of the Universe, the flatness and horizon problems, and try to solve them with an inflationary phase [Sec. 4.1.2], characterised by a slow-roll dynamics [Sec. 4.1.3]. In the second part of the section we define the fundamental inflationary observables, outlining the experimental state of the art [Sec. 4.1.4].

4.1.1 Issues of the Standard Cosmological Model: flatness problem and horizon problem

Despite its astonishing success, the Standard Cosmological Model (SCM) has some problematic aspects. Some of them are related to the present era, as the dark matter and the dark energy puzzles (which are beyond the scope of this thesis), and others are referred to the very early universe. We will focus on the latter, intimately connected to the inflationary model.

FLATNESS. The first problem, called “flatness problem”, refers to the spatial curvature scale and its evolution in the SCM. Let us consider the ratio

$$\rho(t) \equiv \frac{\text{spatial curvature}}{\text{space-time curvature}} = \frac{L_H(t)}{L_\kappa(t)} = \frac{\sqrt{\kappa}}{aH}, \quad (80)$$

where $L_H(t) = |H|^{-1}$ is the proper length associated with the Hubble radius and controls the space-time curvature, and $L_\kappa(t) = (|\kappa|/a^2)^{-1/2}$ is the proper length which controls the radius of the three-dimensional space part of the Friedmann-Lemaître-Robertson-Walker (FLRW) metric (the inverse of curvature). a is the scale factor of the universe evolution, κ the curvature parameter and H the Hubble parameter, defined as $H \equiv \dot{a}/a$. We can notice that

$$\rho(t)^2 = \Omega_\kappa = \frac{\kappa}{a^2 H^2}, \quad (81)$$

where Ω_κ is the usual symbol to identify the spatial curvature contribution to the total energy density of the Universe, in unit of critical density. Experimentally, from the updated PDG data [25], we know that $0 \lesssim \kappa/(a_0 H_0) \lesssim 0.012$ (the subscript stands for the epoch in which the quantity is measured: “0” defines the current era) and this means that the current spatial curvature is less than the space-time one: $\rho_0 \lesssim 0.1$. If we try to extrapolate the ratio $\rho(T)$ down with the past, it is easy to obtain that, within the SCM, it has to be smaller and smaller, leading to highly non-symmetric initial state for our Universe. At the Planck time (about 10^{-44} GeV), for instance, when $H_P = M_P$ (Planck epoch), according to the SCM, we know that the evolution laws for radiation and matter are, respectively

$$\text{radiation: } a \sim t^{1/3} \sim H^{-1/2}, \quad \text{matter: } a \sim t^{2/3} \sim H^{-2/3}, \quad (82)$$

from which

$$\frac{r_P}{r_0} = \frac{a_0 H_0}{a_P H_P} = \frac{a_0 H_0 a_{eq} H_{eq}}{a_{eq} H_{eq} a_P H_P} = \left(\frac{H_0}{H_{eq}} \right)^{1/3} \left(\frac{H_{eq}}{M_P} \right)^{1/2}, \quad (83)$$

where with the subscript “eq” is intended as the radiation-matter equilibrium epoch. Substituting the experimental values [25]

$$H_0 \simeq 3.2h \times 10^{-18} \text{ s}^{-1} \simeq 8.7h \times 10^{-61} M_P, \quad \text{with } h = 0.673 \pm 0.006, \quad (84)$$

$$H_{eq} \simeq \left(\frac{3.36\pi^2}{90} \right)^{1/2} \frac{T_{eq}^2}{M_P} \simeq 1.8 \times 10^{-55} M_P, \quad \text{with } T_{eq} \simeq 1.47 \times 10^4 \text{ K} \simeq 1.3 \text{ eV}, \quad (85)$$

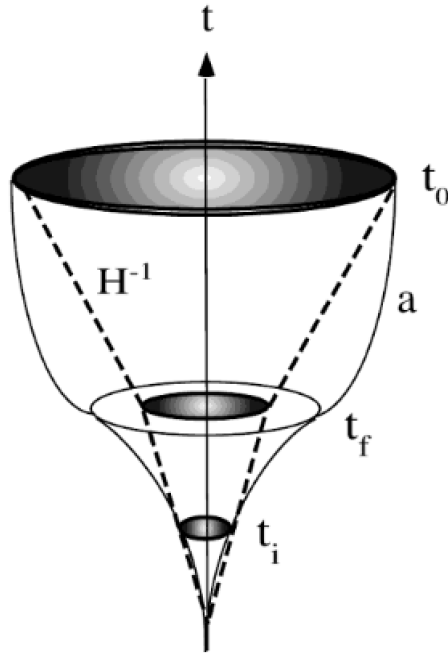


Figure 13: Space-time diagram in which the evolution of the Hubble horizon H^{-1} (dashed lines) and the scale factor a (solid lines) are shown. The vertical axis is the time dimension, while the horizontal plane represents a bi-dimensional section with $t = \text{const}$. The inflationary phase goes from t_i to t_f , the standard one from t_f to t_0 and the shaded areas are the causally-connected regions at different epochs. Today, at t_0 , the observable portion of Universe is contained in the Hubble radius H_0^{-1} , but, at the beginning of the standard phase t_f that region was larger than the horizon H_f^{-1} : the solution to this paradox resides in the fact that the causally-connected area was born from a initial portion of space completely contained in the Hubble horizon H_i^{-1} and so, causally connected at the beginning of inflation. Figure taken from [122].

we obtain

$$\rho_p \sim 10^{-30} \rho_0 \lesssim 10^{-31}. \quad (86)$$

Thus, the SCM requires very fine-tuned initial conditions, with a spatial curvature incredibly suppressed with respect to the space-time one.

A possible solution is the introduction of a special initial phase, inflation, in which $\rho(t)$ decreases (instead of growing) with time. Then it is possible to start from natural initial conditions, *i.e.* $\rho \sim 1$, and suppress ρ in order to match the initial stage of the subsequent standard evolution.

HORIZON. A very similar issue, which could be solved by an inflationary phase, is the so-called “horizon problem”. We consider again a ratio $\rho(t)$, now defined as

$$\rho(t) \equiv \frac{\text{horizon radius}}{\text{inner space radius}} = \frac{H^{-1}}{a} = \frac{1}{\dot{a}} \sim t^{1-\beta} \xrightarrow{t \rightarrow 0} 0. \quad (87)$$

For the SCM ($a \sim t^\beta$, $t > 0$ and $0 < \beta < 1$), there is a particle horizon of radius $d_p(t_0)$, defined as the spherical surface centred in the observer position at present time. This particle horizon divides the unobserved space regions from the already observed ones: the points outside, with $d > d_p(t_0)$, are not causally connected with the origin at the time t_0 , but they may become so at later stages $t > t_0$.

It can be shown that, still within the SCM, $d_p(t_0) \sim \beta H^{-1}/(1 - \beta)$, while the inner portion of space has a volume which scales as a^3 . These are the reasons according to which the ratio (87) becomes smaller and smaller, going towards the early universe. Follows that the portion of space currently inside our observational area was much larger, in the past, than the horizon d_p : it contained for sure space regions not causally connected.

The initial conditions that emerge from this scenario push us to wonder why the portion of Universe we observe today is so homogeneous and isotropic, or, equivalently, why the cosmic radiation temperature is nearly the same in every point of the space. According to the SCM, the different space regions which we can observe today were unable to interact and thermalise in such a uniform way.

The solution, again, could be found in a trend inversion in the evolution of the ratio (87), putting by hand an inflationary phase before the standard one: if $\rho(t)$ decreases in time during inflation, the space portion contained initially in the particle horizon would expand faster than the horizon itself and, at the end of the inflationary phase, the causally-connected region is much larger than the horizon radius at that epoch. In other words, we restored the apparently non-natural initial conditions required by the following standard evolution [see Fig. 13].

4.1.2 Solving the issues: Hubble flow and amount of inflation

The basic idea is to assume an accelerated phase ($\ddot{a} > 0$), which implies that the Universe was filled with some kind of vacuum energy of negative pressure, satisfying

$$\rho + 3p < 0, \quad (88)$$

where ρ and p are the energy density and the pressure of the dominant cosmic fluid, respectively. This new field should suppress the contribution of radiation and matter at very early times, fact that is not in contrast with the SM, due to the very high energy regime. In order to solve this two problems, mentioned in the previous section (along with others, less relevant), the inflationary phase has to last for a sufficient period, in which the expansion has to be efficient enough: during inflation, the ratio ρ should decrease from an initial value ρ_i up to a final value $\rho_f < \rho_i$, large enough to accomplish the subsequent increase from ρ_f to ρ_0 , due to the standard phase. The necessary condition is

$$\frac{\rho_f}{\rho_i} \lesssim \frac{\rho_f}{\rho_0} \rightarrow \left| \frac{\eta_f}{\eta_i} \right| \lesssim \left| \frac{\eta_f}{\eta_0} \right|, \quad (89)$$

where it is shown the same relation expressed in terms of the conformal time η , in which the ratio ρ is linear¹. The absolute values of the two fractions are taken, because the inflationary parameters are usually parametrised as power of the conformal time on a window of negative values ($\infty < \eta_i < \eta_f < 0$).

The acceleration condition implies

$$\ddot{a} > 0 \rightarrow \frac{d}{dt}(aH)^{-1} < 0 \rightarrow \frac{1}{a}(\epsilon_1 - 1) < 0, \quad \text{with } \epsilon_1 \equiv -\frac{\dot{H}}{H^2} = \frac{d \ln H}{dN}, \quad (90)$$

where N is the e-fold number, defined as

$$dN \equiv d \ln a = -H dt. \quad (91)$$

Then, inflation takes place as long as $\epsilon_1 < 1$. When this ϵ_1 parameter reaches one, inflation must end in order to give rise to the standard cosmological evolution. The condition (89) can be expressed as

$$N = \ln \left(\frac{a_f}{a_i} \right) \gtrsim \ln \left[\frac{a_{eq}}{a_f} \left(\frac{a_0}{a_{eq}} \right)^{1/2} \right] = \ln \left(\frac{T_f}{T_{eq}} \right) + \frac{1}{2} \ln \left(\frac{T_{eq}}{T_0} \right), \quad (92)$$

where the behaviour of the temperature T is given by the relation $T \sim a^{-1}$, and the numerical values are in Eq. (84) for T_{eq} and $T_0 = 2.73$ K. The only unknown term is related to the epoch of transition between the inflationary expansion and the standard evolution. Taking for T_f , as a reference value, a typical temperature of the grand unification scale, of order $T_f \sim 10^{16}$ GeV, from the Eq. (92), we have the constraint

$$N \gtrsim \ln 10^{27} \simeq 62, \quad (93)$$

which is the minimal value that the e-fold parameter must assume in order to solve the flatness and horizon problem. Indeed, such a phase allows the largest scale we observe today to be inside the horizon at early times. In general, a total number $N \gtrsim 50 - 60$ is enough to explain the thermalisation of the largest observational scale at present. The flatness problem is faced by means of the same mechanism: a decreasing comoving Hubble radius $(aH)^{-1}$ drives Ω_κ to unity: after inflation, the curvature will start diverging, as it happens in a universe filled with ordinary matter. Notice that the same amount of inflation needed to solve the horizon problem is needed to retrieve the flatness we measure today.

A second important parameter which controls the amount of inflation is

$$\epsilon_2 \equiv \frac{d \ln \epsilon_1}{dN}. \quad (94)$$

We can see that the condition $|\epsilon_2| < 1$ implies a small variation of ϵ_1 , guaranteeing enough duration for the process.

In principle, it is possible to construct an infinite number of these Hubble flow functions ϵ_i , taking iteratively the logarithmic derivate of the $(i - 1)$ -Hubble function [123].

¹ The conformal time is related to the usual (cosmic) time via the relation $dt = a(\eta)d\eta$, and so $a \sim \eta^\beta$ and $d\ln a/d\ln \eta = \beta/\eta$. In the radiation-dominated epoch hence we have $a \sim \eta$, while in the matter-dominated era $a \sim \eta^2$.

The first of these quantities is conventionally taken as the Hubble parameter itself: $\epsilon_0 \equiv H$.

The first proposal of inflationary model [124] relies on a perfect fluid as a source of the expansion, with equation of state $p = -\rho$. From the equation of motion of the standard cosmology $\dot{\rho} + 3H(\rho + p) = 0$, we obtain $\dot{\rho} = 0$, from which $p = -\rho = -\Lambda = \text{const.}$, where Λ can be identified with the cosmological constant. For this type of source, the Friedmann equation² has an exact solution, called de Sitter solution, according to which the scale factor satisfies the following evolution rule

$$a(t) = e^{H_\Lambda t}, \quad \text{with } H_\Lambda \equiv \left(\frac{\Lambda}{3M_p^2} \right)^{1/2}, \quad (95)$$

valid for any value of the cosmic time and in the case of flat space-time ($\kappa = 0$). This solution gives an expanding universe with constant acceleration

$$H = H_\Lambda, \quad \dot{H} = 0, \quad \frac{\ddot{a}}{a} = H_\Lambda^2, \quad (96)$$

which admit an event horizon of radius H^{-1} . The condition of enough inflation, in this case, leads to a lower bound for the e-fold number: $N = \ln e^{H_\Lambda(t_f - t_i)} = H_\Lambda \Delta t \gtrsim 62$, from which we notice the huge exponential growth of the scale factor in a time interval, relatively small with respect to the evolution scale H_Λ^{-1} of that epoch.

4.1.3 Slow-roll dynamics

The de Sitter model, however, is not satisfactory from a phenomenological point of view: the inflationary phase must stop at some stage and there should be, already included in the model, a transition to the standard cosmological phase. According to de Sitter, in fact, inflation is eternal [125], and the attempts in order to permit a “graceful exit” have not proven themselves convincing.

Much more success is reserved to inflationary models in which the expansion is only quasi-exponential, the curvature is not constant, but slightly decreasing and the scalar field, source of the metric, rolls down slowly along a stretch of a gently sloping potential, instead of remain trapped in a minimum. These models, called slow-roll inflationary models, are capable of sustain an accelerated expansion phase and, simultaneously, to lead the system towards the standard cosmological phase. The scalar field which drives the accelerated phase is also called inflaton.

² Starting from the Einstein equations of General Relativity and limiting to FLRW geometries, we found:

$$\begin{aligned} H^2 + \frac{\kappa}{a^2} &= \frac{8}{3}\pi G\rho, \\ 2\dot{H} + 3H^2 + \frac{\kappa}{a^2} &= -8\pi Gp, \end{aligned}$$

along with the energy conservation already used

$$\dot{\rho} + 3H(\rho + p) = 0.$$

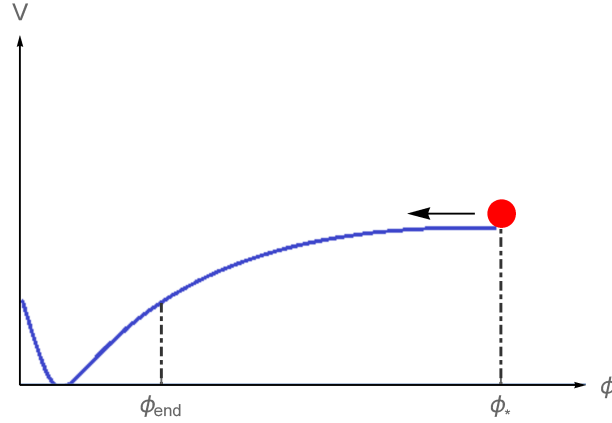


Figure 14: The inflaton slowly rolls down and stops at ϕ_* , starting from ϕ_{end} , at least around 60 e-folds before the end, giving rise to a quasi-exponential expansion. When the scalar field reaches the minimum, inflation ends and the standard evolution starts to dominate.

It is easy to verify that a slow evolution of the scalar field and of the geometry lead to an efficient inflationary phase. Let us suppose that the variation of the first Hubble function ϵ_1 is small and constant, such that

$$\epsilon_1 = \frac{\dot{H}}{H^2} \ll 1, \quad \epsilon_1 \simeq 0. \quad (97)$$

We have that $\epsilon_1 dt = -dH/H^2 \rightarrow \epsilon_1 t \simeq H^{-1} = a/\dot{a}$, from which, integrating again,

$$a(t) \sim t^{1/\epsilon_1}, \quad \text{where } \frac{1}{\epsilon_1} \gg 1. \quad (98)$$

Hence, this scale factor describes a power-law inflationary phase. Eq.(97) is named slow-roll condition.

Let us now better characterise the slow-roll model, obtaining the constraints on the scalar field ϕ and its potential $V(\phi)$. The action of a scalar field minimally coupled to gravity is

$$S = \int d^4x \sqrt{-g} \left[-\frac{M_{\text{P}}^2}{2} R + \frac{1}{2} g^{\mu\nu} \partial_\mu \phi \partial_\nu \phi - V(\phi) \right], \quad (99)$$

where g stands for the determinant of the metric $g^{\mu\nu}$. The variation of the action with respect to the metric gives the field equations, while, with respect to ϕ , gives the equations of motion for the scalar field:

$$\nabla_\mu \nabla^\mu \phi + V' = 0, \quad (100)$$

where ∇_μ is the covariant derivative in General Relativity (GR)³, from which we can define the covariant divergence $\nabla_\mu \nabla^\mu \phi = \nabla_\mu (g^{\mu\nu} \partial_\nu \phi)$.

Finding solutions embedded in a FLRW metric $ds^2 = dt^2 - a(t)^2 |d\vec{x}|^2$, spatially flat, we assume that the inflaton is homogeneous: the components of the energy-momentum tensor T_μ^ν are

$$T_0^0 = \rho(t) = \frac{1}{2} \dot{\phi}^2 + V(\phi), \quad T_i^j = -p(t) \delta_i^j = -\delta_i^j \left(\frac{1}{2} \dot{\phi}^2 - V(\phi) \right). \quad (101)$$

For a constant field $\dot{\phi} = 0$, we retrieve the de Sitter solution $p = -\rho = -V = \text{const.}$ Manipulating the Friedmann equations [see footnote n.2 of this chapter], we obtain, from (100), the equation of motion for the inflaton

$$\ddot{\phi} + 3H\dot{\phi} + V' = 0. \quad (102)$$

A slow evolution implies the following conditions:

$$|\dot{H}| \ll H^2, \quad |\ddot{\phi}| \ll |H\dot{\phi}|, \quad \dot{\phi}^2 \ll |V|, \quad (103)$$

from which we can work out two fundamental approximated relations

$$3H^2 = \frac{V}{M_{\text{P}}^2}, \quad (104)$$

$$3H\dot{\phi} = -V'. \quad (105)$$

The goal is to relate the ϵ_1 parameter with the slope of the potential: taking the derivative with respect to ϕ of (104) and dividing by $3H^2$, we have

$$\frac{H'}{H} = \frac{1}{2} \frac{V'}{V} \rightarrow \epsilon_1 = -\frac{H'}{H} \frac{\phi}{H} = -\frac{1}{2} \frac{V'}{V} \frac{\phi}{H}. \quad (106)$$

Furthermore, dividing by $3H^2$ Eq. (105), we have

$$\frac{\dot{\phi}}{H} = -M_{\text{P}}^2 \frac{V'}{V}, \quad (107)$$

from which, putting together with Eq. (106), we can define

$$\epsilon_1 \simeq \epsilon \equiv 2M_{\text{P}}^2 \left(\frac{V'}{V} \right)^2, \quad (108)$$

called (first) slow-roll parameter, only approximately equal to the Hubble function ϵ_1 : the main difference is that the former relies on the specific form of the inflationary potential, while the latter is simply proportional to the Hubble parameter⁴. In any

³ In general, for a generic four-vector A^μ , it is defined $\nabla_\alpha A^\mu = \partial_\alpha A^\mu + \Gamma_{\alpha\beta}^{\mu} A^\beta$, while for a scalar field $\nabla_\alpha (A^\mu A_\mu) = \partial_\alpha (A^\mu A_\mu)$. With $\Gamma_{\alpha\beta}^{\mu}$ we represent the Christoffel connection of the metric, *i.e.* a combination of derivatives of the metric.

⁴ Strictly within the slow-roll approximation, the slow-roll parameters are related to the Hubble flow functions through the relations

$$\epsilon_0 \simeq (V/3)^{1/2}, \quad \epsilon_1 \simeq \epsilon, \quad \epsilon_2 \simeq -4\epsilon + 2\eta.$$

case, the logarithmic variation of the potential must be very small on scales of order of the Planck length, equal to the reciprocal of the Planck mass, in natural units.

It is customary to introduce a second slow-roll parameter η (not to be confused with the conformal time: unfortunately, following the usual conventions, they are both indicated by the same symbol) which controls the second derivative of the potential V'' :

$$\eta \equiv M_{\text{p}}^2 \left(\frac{V''}{V} \right). \quad (109)$$

The conditions $\epsilon, |\eta| \ll 1$ guarantee that the inflaton acceleration $\ddot{\phi}$ is small with respect to the inertial term $3H\dot{\phi}$, due to the gravitational interactions. When this term starts to be dominant, the two slow-roll parameters become of order one and inflation stops.

It is useful to define also a third slow-roll parameter:

$$\zeta \equiv M_{\text{p}}^4 \left(\frac{V'''V'}{V} \right). \quad (110)$$

One of the first simple slow-roll models proposed, considers a generic power-law behaviour for the potential $V(\phi) \sim \phi^n$, with $n > 0$. In this case the slow-roll conditions for ϵ and η are satisfied if

$$\phi^2/M_{\text{p}}^2 \gg 1. \quad (111)$$

If $n = 2$, the model is quadratic in the potential and it was originally proposed as a typical example of slow-roll inflation [126]. It is known as “chaotic” model, because it deals with a primordial cosmological system in which the starting values of the inflaton are casually distributed in different regions of space. Only in the space portions where the condition $\phi^2 \gg M_{\text{p}}^2$ is satisfied, the universe inflates and slow-roll takes place.

The success of these models resides in the fact that the condition (111) assures a duration long enough for solving the horizon and flatness problem simultaneously: if we compute the number of e-folds in the framework described above, we obtain

$$N = \frac{1}{2n} \left(\frac{\phi_i^2}{M_{\text{p}}^2} - \frac{\phi_f^2}{M_{\text{p}}^2} \right), \quad (112)$$

we see that the condition of sufficient inflation $N \gg 1$ is easily achieved (the smaller n , the better).

The other strength point of this way of thinking refers to the fact that ϵ and η are not constant here, but grow slowly during inflation $\epsilon \sim \eta \sim \phi^{-2}$, as long as the inflaton goes towards the minimum of the potential. Near the minimum, the velocity increases and the slow-roll conditions are no more valid: inflation ends and the effective mass term V'' becomes comparable to H^2 . This means that the solution for ϕ turns out to be suddenly oscillating: physically speaking, in a process called reheating [for a review see [127]], the inflaton can, in principle, decay, producing the SM particles and radiation, which are going to become dominant in the following standard evolution.

4.1.4 Inflationary observables

The discovery of the Cosmic Microwave Background (CMB) in 1965 [128], began a new scientific era, where (almost) all speculations about the Universe and its evolution found scientific validation.

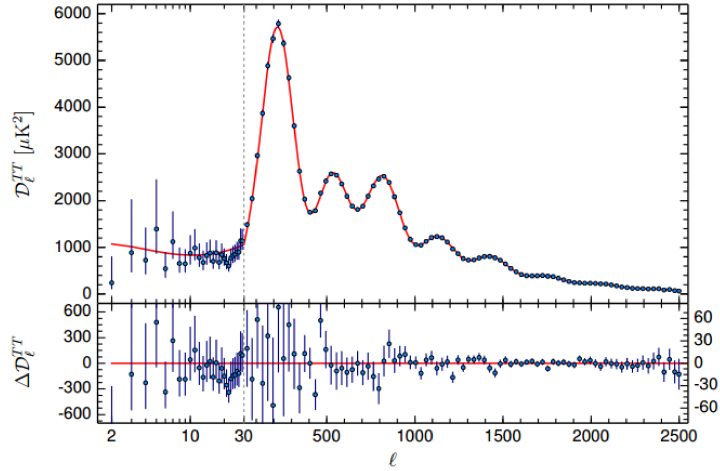


Figure 15: CMB angular power spectrum of temperature anisotropy measured by Planck, in the 2015 release [109]. As we can see, the SCM fits extraordinarily the experimental data, and so, from every peak in the spectrum we can extrapolate a lot of information about our Universe evolution. l stands for the angular coordinate: an angle θ in the sky is identified as π/l , so low l means large scales and *viceversa*. The quantity \mathcal{D}_l^{TT} in the plot is defined as $\mathcal{D}_l^{TT} = \ell(\ell + 1)C_\ell/(2\pi)$, where the coefficients C_ℓ stands for the proper angular power spectrum and they are basically a variance, *i.e.* a sum of the difference in temperature in different directions.

The CMB is the farthest surface we can push our observations to: beyond this isotropic snapshot, nothing can directly reach our measurement instruments. The homogeneity and isotropy of CMB, together with its peculiar temperature spatial anisotropy [see Fig. 15], makes us think of inflation as a period that goes beyond this last scattering surface, reaching the very first instants of life of our Universe, where the space and time started to exist (the usual estimation is that inflation lasted from 10^{-36} s after the initial singularity, to sometime between 10^{-33} s – 10^{-32} s after the singularity itself).

However, through CMB measurements, we have indirect stringent constraints on the inflationary dynamical mechanism: fluctuations produced during inflation freeze outside the horizon, providing a link between two separated moments in time [see Fig. 13 and 16], from which we can extrapolate restrictions on the form of the scalar potential $V(\phi)$.

We skip all the procedure which would lead to the extrapolation of these information from the CMB temperature power spectrum [for an introductory proper treatment see, for instance, the textbook [129]]: in few words, we can say that the spectrum contains all the details of the evolution of the initial fluctuations from the moment they re-enter the horizon at the decoupling, and then, of their projection in the sky. The result is the theoretical prediction (red line) in Fig. 15. The large damping of the spectrum at small

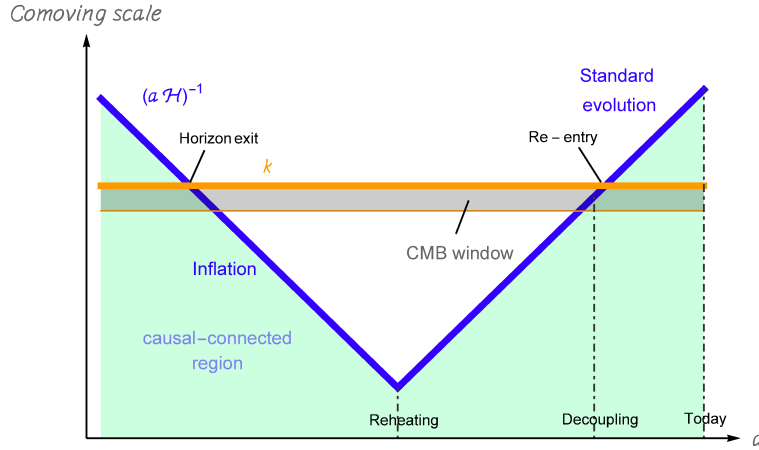


Figure 16: The causal-connected region changes with time, because of the variation of the comoving Hubble radius $(aH)^{-1}$ for all typical scales. Inflation is then needed to explain the thermalisation of furthest points, which, in principle, would not have been in contact in the past. With k is represented a generic mode of quantum fluctuations produced during inflation, which exits the horizon, freezes and then re-enters when the standard evolution has begun, after the reheating stage, sourcing acoustic oscillations of the cosmic fluid. At decoupling time, CMB photons come towards us through free streaming: we can measure their power spectrum in the CMB window, denoted here by the grey shaded area. The figure, done by the author, is inspired to the corresponding one in [132].

angular scales reflects the fact that we are able to probe just a very small window of the inflationary era.

Inflation generates a scalar perturbation density, responsible for the growth of large scale structures. From the theory of cosmological primordial perturbations and their evolution after inflation [see the seminal work of Mukhanov *et al.* [130, 131]] we can work out the related scalar power spectrum

$$\Delta_{\zeta}(k)^2 = \frac{H^4}{4\pi^2 \dot{\phi}^2} \simeq \frac{1}{24\pi^2 M_p^4} \frac{V}{\epsilon}, \quad (113)$$

where the second approximated equality is valid in the slow-roll regime and evaluated at horizon crossing.

Inflation, besides scalar quantum fluctuations, excite tensor perturbations as well, from which it would be generated the primordial gravitational waves background. The dimensionless power spectrum, in this case, turns out to be

$$\Delta_h(k)^2 = 2 \times \left(\frac{H}{2\pi} \right)^2, \quad (114)$$

where the factor 2 is due to the two photon polarisations.

These two power spectra of perturbations are obtained in a perfect de Sitter and massless approximation ($H \approx \text{const.}$, $V'' \approx 0$), but, as we know, during inflation, the energy scale controlled by H , has to change slightly with time and the inflaton mass is non-zero. In order to parametrise the deviation from scale invariance, it is customary to define the scalar and tensor spectral index, respectively

$$n_s - 1 \equiv \frac{d \ln \Delta_\zeta^2}{d \ln k}, \quad n_t - 1 \equiv \frac{d \ln \Delta_h^2}{d \ln k}, \quad (115)$$

which means that, with a pivot scale k_* and stopping at the first order of scale dependence:

$$\Delta_\zeta(k)^2 \sim \left(\frac{k}{k_*}\right)^{n_s-1}, \quad \Delta_h(k)^2 \sim \left(\frac{k}{k_*}\right)^{n_t}. \quad (116)$$

In terms of slow-roll parameters, we can rewrite the spectral indexes in the following way:

$$n_s - 1 = 2\eta - 6\varepsilon, \quad n_t = -2\varepsilon. \quad (117)$$

Finally, the tensor-to-scalar ratio is defined as

$$r \equiv \frac{\Delta_h(k_*)^2}{\Delta_\zeta(k_*)^2} \simeq 16\varepsilon, \quad (118)$$

and stands for the suppression of the tensor perturbations with respect to the scalar ones.

Lastly, it is customary to consider the running of the spectral index, which is related to the slow-roll parameters by the following relation

$$\frac{dn_s}{d \ln k} = 24\varepsilon^2 - 16\varepsilon\eta + 2\zeta^2. \quad (119)$$

All the slow-roll parameters must be evaluated at the field value assumed at the beginning of inflation ϕ_* .

EXPERIMENTAL STATE OF THE ART. The Planck mission has scanned all the sky with unprecedented accuracy [109, 133]: in particular, we have, up to now, stringent constraints on the inflationary parameters [for a collection of the inflationary predictions of the most important inflationary models, compared with the Planck constraints, see Fig. 17].

The experimental value for the amplitude of scalar perturbations, measured at the pivot scale $k_* = 0.05 \text{ Mpc}^{-1}$ is

$$\Delta_\zeta(k_*)^2 = (2.14 \pm 0.1) \times 10^{-9}. \quad (120)$$

As concerns the scalar spectral index, Planck [133] and, later on, the Planck and BICEP2/Keck Array collaborations joint analysis [134] provided the value

$$n_s = 0.968 \pm 0.006 \text{ (68\% CL)}, \quad (121)$$

while for the tensor-to-scalar ratio, due to lack of direct or indirect revelation of B-modes for the CMB polarisation⁵ (the only way, up to now, to reveal a tensor contribution from the cosmic relic radiation), we have only an upper bound. The most updated

⁵ The claim of direct detection of B-modes by the BICEP2 collaboration [135] did not survive on the subsequent validation tests: the signal observed was mainly due to dust polarisation [134].

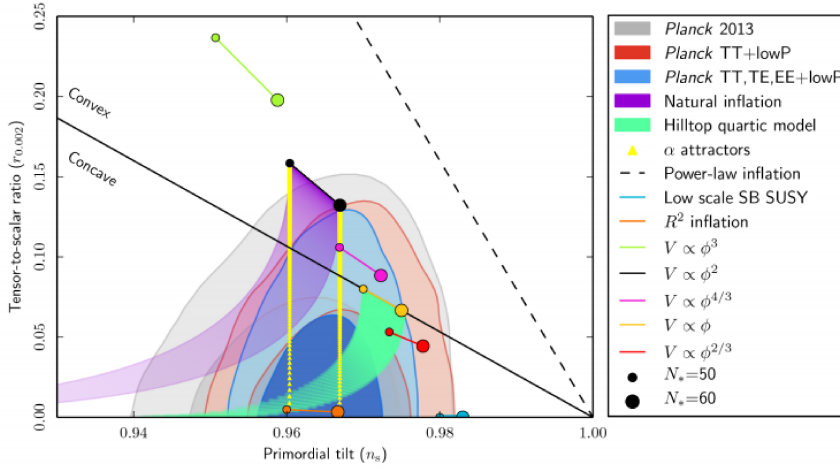


Figure 17: Spectral index and tensor-to-scalar ratio from the 2015 release of the Planck collaboration, evaluated for the pivot scale $k_* = 0.002 \text{ Mpc}^{-1}$ [109, 133]. A bunch of popular inflationary models predictions are also displayed.

one is that given by the BICEP2/Keck Array collaboration, which added the 95 GHz channel and used the Planck public data as an external dataset [136] [see Fig. 18]:

$$r < 0.08 \text{ (95\% CL)}. \quad (122)$$

It is well known that the detection of a primordial gravitational wave signal would directly determine the height of the potential V and its slope at the moment of horizon crossing of the relevant scales during the expansion phase. Furthermore, such a detection would also infer that the inflaton field excursion $\Delta\phi$ during inflation is at least of order of the Planck scale, satisfying the so-called Lyth bound [137] (valid for a detectable tensor-to-scalar-ratio)

$$\Delta\phi \gtrsim \frac{M_{\text{P}}}{2}. \quad (123)$$

In general, considered 0.08 a reference value for r , the bound says that

$$\frac{\Delta\phi}{M_{\text{P}}} \simeq \frac{1}{2} \left(\frac{r}{0.08} \right)^{1/2}. \quad (124)$$

Since we have observed, so far, a non-vanishing scalar spectral index but no tensor homologous, we can convince ourselves to have discovered a new hierarchy, this time related to the slow-roll parameters: $\epsilon \ll \eta$. Considering the ongoing quest for primordial gravitational waves by CMB experiments (both in space and ground-based), as long as persists this lack of evidence for tensor modes, the upper bound on r gets stronger and this hierarchy becomes more evident. Sometimes this regime $\epsilon \ll \eta$ is called inflationary conformal limit: it describes all viable single-field and slow-roll

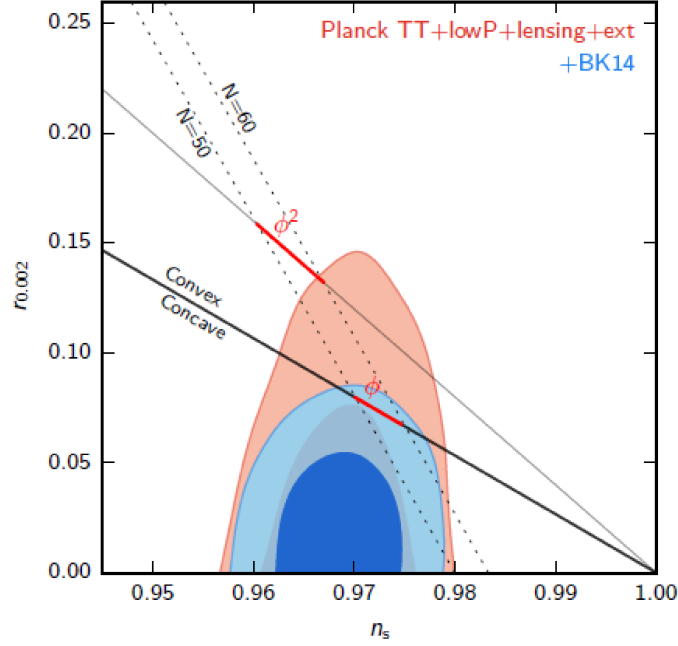


Figure 18: Improved constraints on the spectral index and the tensor-to-scalar ratio from the BICEP2/Keck Array collaboration, using the public Planck data as an external dataset, for the pivot scale $k_* = 0.002 \text{ Mpc}^{-1}$ [136].

models. For instance, a model with a sub-Planckian excursion $\Delta\phi \ll M_{\text{P}}$ is a specific example of the hierarchy mentioned before:

$$\varepsilon \lesssim \left(\frac{\Delta\phi}{M_{\text{P}}}\right)^2 \frac{1}{N^2} \lesssim \frac{1}{N^2} \lesssim \eta^2, \quad (125)$$

where it was used the Lyth bound (124) and, assuming $N \sim 60$, the relation $\eta \simeq 1 - n_s$. The formal treatment of the conformal symmetry classification for the inflationary models goes beyond the scope of this work.

The running of the scalar spectral index turns out to be compatible with zero, supposedly, tinely negative [133]:

$$\boxed{\frac{dn_s}{d \ln k} = -0.008 \pm 0.008.} \quad (126)$$

A useful parametrisation allows us to get an estimate of the value of the inflationary potential energy at horizon crossing:

$$\boxed{V^{1/4} \simeq 1.93 \times 10^{16} \left(\frac{r}{0.12}\right)^{1/4} \text{ GeV}.} \quad (127)$$

We can see that inflation should have taken place at very high energies (around the 10^{16} GeV), and, also for very small values for r , the decrease in energy is still not relevant.

4.2 INFLECTION POINT ANALYSIS

We wonder now if the SM Higgs boson, the only scalar particle revealed in Nature so far, could play the role of the inflaton, taking advantage of the shape of its potential at high energy, and, at the same time, generate the anisotropies in the scalar power spectrum, seeding the large scale structures we see nowadays.

The answer is probably already known [138] and it deals with the unlikely eventuality of the Higgs boson responsible of both the tasks we mentioned. The basic issue is that we need enough e-folds of inflation and this is reflected on a need of a adequate flatness of the SM potential: this requirement seems to be in conflict with the hope of generating the correct amount of scalar anisotropies, thought as being produced by the quantum fluctuations of the Higgs field. The height of the SM Higgs potential in its flat regime can not be freely adjusted in order to match the correct value of Δ_{ζ}^2 and this put a hard constraint on the idea of a Higgs boson as a single actor in the play.

An interesting approach, developed in [139], lowers the ambition of an unified description of the phenomenon, investing the Higgs field with the only role of source of the scalar perturbations (also known as “curvaton”), thinking to another singlet scalar, which would drive the inflationary phase. The scenario turns out to be robustly viable. Here, we limit ourselves to a phenomenological analysis, trying to study the situation in which we have a very shallow false vacuum near the Planck scale and understand to what extent it could be relevant for inflation. This is a pure SM scenario, in which the Higgs boson returns to play both the roles, but now in a tuned, featured configuration of its potential at high energies.

We assume, as usual, that the potential at the electroweak minimum is zero.

It is worth mentioning that, defined as μ_i the renormalisation scale where the Higgs potential has an inflection point, both the conditions

$$\lambda(\mu_i) = 0, \quad \beta_{\lambda}(\mu_i) = 0, \quad (128)$$

have to be fulfilled [12]. As we anticipated, such a configuration could be relevant for the class of models of primordial inflation in which the Higgs is trapped in a shallow false minimum [19, 18, 17, 121]: in particular, the height of the effective potential at an inflection point, let us call it \bar{V}_i , could be directly linked to the tensor-to-scalar-ratio r , via the slow-roll relation

$$\bar{V}_i^{1/4} \simeq \left(\frac{3\pi^2}{2} r \Delta_{\zeta}^2 \right)^{1/4} M_{\text{P}}, \quad (129)$$

where the amplitude of scalar perturbations is shown in Eq. (120). It is thus important for models of primordial inflation to assess the size of the experimental and theoretical errors in the calculation of \bar{V}_i .

Experimental uncertainties on \bar{V}_i can be estimated as follows, as done in [1]. We let m_{H} vary in its 3σ experimental range and, for fixed values of $\alpha_s^{(5)}$, we determine m_{t}^{i} , the value of the top mass needed to have an inflection point (which is so close to m_{t}^{c}

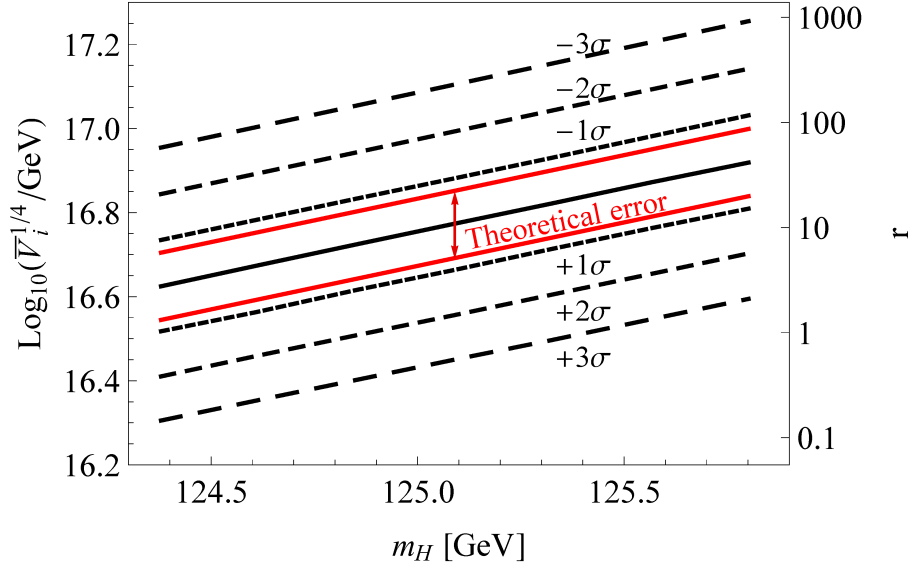


Figure 19: Dependence of $\bar{V}_i^{1/4}$ on m_H , for fixed values of $\alpha_s^{(5)}$. The (red) arrow and solid lines show the theoretical error due to the matching of λ (positive contribution to λ for the upper line, negative for the lower one). The right vertical axis displays the associated value of the tensor-to-scalar ratio r , according to Eq. (129). The figure is contained in [1].

that one can read it from the stability line of Fig. 9). We then evaluate the effective potential at this point, \bar{V}_i . The result is displayed in Fig. 19: one can see that $\bar{V}_i^{1/4}$ spans one order of magnitude, as it varies from 2×10^{16} GeV up to 2×10^{17} GeV, for decreasing values of $\alpha_s^{(5)}$; the dependence on m_H is less dramatic but still relevant, being about 50%.

We divide the theoretical errors in three categories, as done before in Sec. 3.2.1.

- The theoretical errors associated with the matching of λ at NNLO have an impact on m_t^c of about ± 0.19 GeV (see Fig. 9 in Sec. 3.2.2) and an impact on $\log_{10}(\bar{V}_i^{1/4}/\text{GeV})$ of about ± 0.08 , namely a 20% variation of $\bar{V}_i^{1/4}$. As for the NNLO matching of h_t , the impact on m_t^c is of about ± 0.25 GeV, but there is no significant impact on \bar{V}_i . As a consequence of the theoretical error in the matching, the lines in Fig. 19 could be shifted up or down by about 0.08; for the central value of $\alpha_s^{(5)}$, this is represented in Fig. 19 by the (red) arrow and solid lines. The theoretical error due to the NNLO matching is thus slightly smaller than the experimental error due to the 1σ variation of $\alpha_s^{(5)}$.

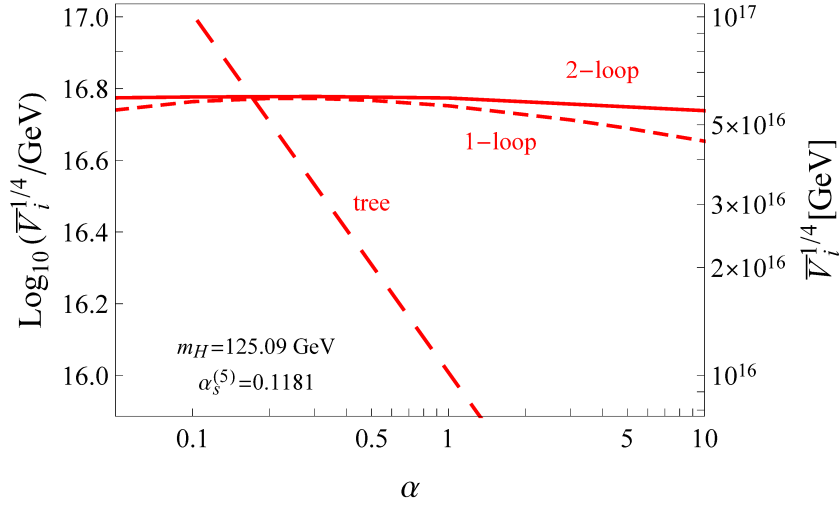


Figure 20: Dependence of $\bar{V}_i^{1/4}$ on α . For definiteness, $\alpha_s^{(5)}$ and m_H are assigned to their central values. The figure is contained in [1].

- The order of magnitude of the theoretical errors associated with the β -functions at NNLO can be estimated by studying the impact of the subsequent correction; it turns out that $\bar{V}_i^{1/4}$ changes at the per mil level. Such error is thus negligible.
- The theoretical uncertainty associated with the fact that we truncate the effective potential at two-loop can be estimated by studying the dependence of \bar{V}_i on α . We fix $\alpha_s^{(5)}$ and m_H at their central values and display in Fig. 20 the resulting value of $\bar{V}_i^{1/4}$ by means of the solid line; for comparison, we display also the dependences obtained at tree⁶ (long-dashed) and one-loop (short-dashed) levels. Notice that the dependence of \bar{V}_i on α at the tree-level is implicit⁷, but significant: the tree-level calculation of $\bar{V}_i^{1/4}$ is uncertain by more than one order of magnitude. The one-loop corrections flattens the dependence on α so that the uncertainty on $\bar{V}_i^{1/4}$ gets reduced down to about 20%; this uncertainty is comparable to the theoretical one due to the matching. The two-loop correction further flattens the dependence on α and allows to estimate $\bar{V}_i^{1/4}$ with a 5% precision [for the explicit shape of the potential at inflection point and its dependence on α , see also Fig. 21].

Summarising, the theoretical error that mostly affects the calculation of \bar{V}_i at the NNLO is the one associated with the matching. The theoretical error in the truncation

⁶ We checked that our results for the tree level with $\alpha = 1$ agree with those obtained in [12, 121]. In these works, the potential was indeed calculated only at the tree-level, without providing any estimate for the theoretical uncertainty because of neglecting higher loops.

⁷ Indeed, $V_{\text{eff}} \propto \lambda [\ln(\alpha\phi_H/m_t)]$.

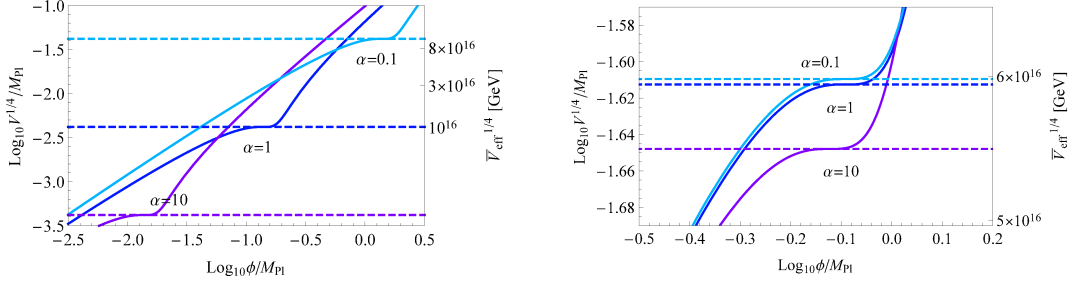


Figure 21: Explicit shape of the potential $V^{1/4}$ at inflection point and its dependence on α at tree level (*left panel*) and two loop (*right panel*). Again, for definiteness, $\alpha_s^{(5)}$ and m_H are assigned to their central values. As we can see, the higher the loop order, the less the dependence on α of the inflection point position.

of the effective potential is smaller than the theoretical error in the matching only including the two-loop correction to the effective potential.

We can conclude that the result of the NNLO calculation is

$$\boxed{\log_{10} \bar{V}_i^{1/4} = 16.77 \pm 0.11_{\alpha_s} \pm 0.05_{m_H} \pm 0.08_{\text{th}} \text{ GeV},} \quad (130)$$

where the first two errors refer the 1σ variations of $\alpha_s^{(5)}$ and m_H respectively, while the theoretical error is essentially dominated by the one in the matching.

As anticipated, a precise determination of \bar{V}_i is important for models of inflation based on the idea of a shallow false minimum [19, 18, 17, 121] as, in these models, \bar{V}_i and r are linked via Eq. (129). In view of such application, the right axis of Fig. 19 reports the corresponding value of r . Notice that the dependence of r on $\alpha_s^{(5)}$ and m_H is extremely strong: when the latter are varied in their 3σ range, r spans about four orders of magnitude, from 0.1 to 1000. In addition, the theoretical error in the matching implies an uncertainty on r by a factor of about 2.

According to the 2015 analysis of the Planck Collaboration, the present upper bound on the tensor to scalar ratio is $r < 0.12$ at 95% C.L. [133], as also confirmed by the recent joint analysis with the BICEP2 Collaboration [134]. Due to Eq. (129), this would translate into to the bound $\log_{10} \bar{V}_i^{1/4} < 16.28$ GeV at 95% C.L.; this implies a tension with Eq. (130) at about 3σ .

This can be graphically seen in Fig. 22, where the contour levels of r in the plane $(m_H, \alpha_s^{(5)})$ are shown. Even invoking the uncertainty due to the matching (red-dashed lines), a value for r as small as 0.12 (red-solid line), could be obtained only with $\alpha_s^{(5)}$ in its upper 3σ range, while the values of m_H , and also m_t (see Fig. 9), could stay inside their 1σ interval. This tension, was, in a more qualitative way, already pointed out in [16].

CONCLUSIONS. A value for r close to 0.2, as claimed by BICEP2 in 2013 [135], would have been compatible at about 2σ with a model based on a shallow false minimum.

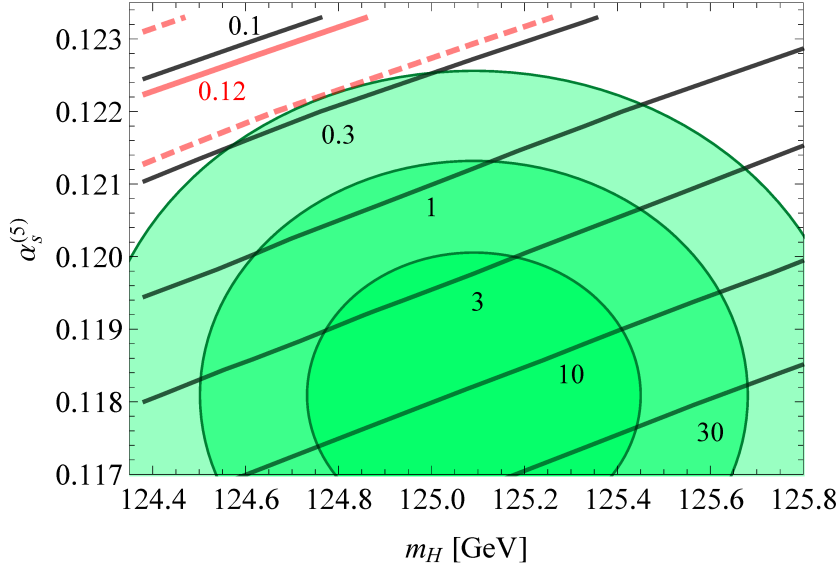


Figure 22: Contour levels of r in the plane $(m_H, \alpha_s^{(5)})$. The theoretical uncertainty corresponding to $r = 0.12$ is shown by means of the (red) dashed lines. The shaded regions are the covariance ellipses indicating that the probability of finding the experimental values of m_H and $\alpha_s^{(5)}$ inside the ellipses are respectively 68.2%, 95.4%, 99.7%. The figure is contained in [1].

However, as we know, that reference value is now ruled out by observations [134]. With the inclusion of the theoretical error and the slight changes in the central values of the input parameters, the present calculation supersedes the results obtained in the previous paper [121], where the calculation of the effective potential was done only at tree level (due to the yet unsolved problem of the inclusion of the one-loop correction when λ turns negative [86]).

The present results have to be compared with those of the most recent detailed analysis on the inflection point configuration, performed by Ballesteros *et al.* [7]. The latter includes the two-loop correction to the Higgs effective potential but, to our understanding, do not include the theoretical error in the matching (which is actually, according to us, the dominant one). This may justify their stronger exclusion of the inflection point configuration. Apart from this detail, the results of the two analysis are in substantial agreement. The even stronger exclusion of the inflection point configuration found in [140], might be also due to an underestimation of the theoretical errors, together with the previous underestimation of the experimental uncertainty on $\alpha_s^{(5)}$.

Lastly, the shallow false minimum idea seems in trouble: in order to embed inflation in a SM-like framework, new physics has to be introduced. Two minimal extension to the SM are then presented here in turn: first, a U(1) extension of the SM gauge group, in order to take into account, together with inflation and stability, the small neutrino

masses [see Chap. 6]; second, the very well-known path of a non-minimal coupling between the Higgs field and gravity [see Chap. 5].

The inclusion of new physics beyond SM appears mandatory also in the metastable scenario [see, for instance [14]]. The electroweak vacuum stability during (or after) inflation is threatened by the field fluctuations $\delta\phi_H$, which are proportional to

$$\delta\phi_H \sim H \frac{\sqrt{N}}{2\pi} \sim H, \quad (131)$$

approximately comparable to a scale of order 10^{14} GeV.

When the field reaches values above the instability scale, the Higgs evolves to the true minimum at high energy⁸: after inflation, the Higgs field is spread in causally-disconnected space regions, with values either above or below the scale of the second minimum. The consequent evolution of the field should lead to observable effects like the appearance of bubbles or domain walls. For this reason it would be better, in the case of metastable vacuum, to think at some new physics beyond the SM able to stabilise the potential. We will try to pursue this task, albeit without any ambition in formulating a complete unified theory, following two different paths in the last two chapters.

⁸ In this scenario, at the (p)reheating stage, the high temperature thermal effects could become relevant. For instance, it was proposed a scenario with the Higgs driving inflation in a metastable vacuum thanks to thermal correction to the effective potential: a symmetry restoration after inflation due to high temperature effects could lead to the (temporary) disappearance of the vacuum at Planck values of the Higgs field [141]. For a pedagogical review on finite temperature field theory, see [142].

5

$U(1)_{B-L}$ EXTENSION OF THE STANDARD MODEL: STABILITY AND INFLATION

The SM, as we saw in Chap. 1, is based on the gauge symmetry $SU(3)_C \times SU(2)_L \times U(1)_Y$, and it is, by far, in excellent agreement with the current experimental results. Nevertheless, we have, among the others which we are going to ignore in this work, at least three unambiguous observational evidences of new physics beyond SM: neutrino masses, the baryon asymmetry and the dark Universe (dark matter and dark energy).

Furthermore, according to the updated electroweak vacuum stability analysis, presented in Chap. 3 and based on [1], a new-physics extension of the SM is needed, in principle, to stabilise the SM Higgs potential below the Planck scale (in case the upcoming experimental data will lead us towards a metastable scenario) and, for sure, give a reasonable physical realisation of the inflationary phase, for example in order to eradicate the tension between the false vacuum-based inflationary models and the current experimental data [see Chap. 4].

One of the examples of a minimal extension of the SM is the inclusion of a $B - L$ global gauge symmetry (baryon number minus lepton number, which is a conserved quantum number), introducing three singlet fermions (right-handed neutrinos), an extra gauge boson, known as Z' in phenomenology, and an extra singlet scalar, in the role of a heavy Higgs field. With such an extension, it could be possible, in principle, to stabilise the potential and provide an inflationary scenario, generating, in the same framework, the low-energy neutrino masses through the type I see-saw mechanism [143, 144, 145], accounting, possibly, for the baryon asymmetry of the Universe through leptogenesis. Citing Weinberg, “a neutral vector boson somewhat heavier than the Z_0 and coupled to $B - L$ seems like the most plausible addition to the SM” [146].

This is, of course, not a new idea. First attempts of constraining the Higgs mass in scenarios of type I see-saw, in which the neutrino masses are dynamically generated, can be found in [147], together with various applications of the $B - L$ extension of the SM [148, 149, 100, 150, 151, 152, 12, 153, 154], in which also some SM stability analyses were performed. The general theoretical framework of these kind of models is well summarised in [155] and, with particular care to the Z' phenomenology, in [156, 157, 158]. The effects of the inverse see-saw [159] and type II see-saw mechanism on the stability of the electroweak vacuum, with some forecasts on the value of the Higgs mass [152, 160], go beyond the scope of our work.

The inflationary dynamics in $B - L$ extended scenarios was also widely studied [see, for example [161, 5, 6]]: we try here to review and update these results. Although there are also some analyses in non-minimal coupled scenarios, in which the $B - L$ scalar,

playing the role of the inflaton, presents a non-minimal coupling to gravity [162, 163], we will focus here on the minimally-coupled case. Some overviews on the status of the phenomenological and experimental state of the art in the search of the Z' can be found in [164, 165].

Starting from the mentioned state of the art, we provide here our simple study of the viable parameter window for both stabilisation and primordial inflationary expansion in the so-called $B - L$ scenario, in the light of the updated experimental bounds from cosmology.

First, in Sec. 5.1, we are going to introduce the model in its minimal formulation, focussing on the stability issue of the full potential, compared to the pure SM one. Then, in Sec. 5.2, we actually try to address the stabilisation mechanism, introducing the relevant physical scales and providing the analytical tree-level threshold relations generated from the inclusion of the new scalar singlet [see, in particular, Sec. 5.2.1], along with the modified RGE [see Sec. 5.2.2], relevant for our analysis. In Sec. 5.3 we are going to look over the inflationary phase, driven by the heavy extra scalar singlet, with the SM Higgs field acting as a spectator, giving rise to a simple single-field inflationary model, currently favoured by data. Few words are spent also on the reheating phase [Sec. 5.5]. The final qualitative joint analysis of the parameter window, putting together the viable parameter space from stability and inflation, is carried out in Sec. 5.4, and afterwards, in the last part of the chapter, we are going to draw the conclusions of our reanalysis, in agreement with the literature, with some possible studies that could be done in the future.

5.1 THE MODEL

We introduce here the Abelian extension to the SM by the $U(1)_{B-L}$ group, in order to try to stabilise the electroweak vacuum of our particle physics model and build a reasonable connection with the inflationary phase. For this theoretical snapshot of the model, we follow [6, 155]

The extended full-symmetry group can be represented by

$$\mathcal{G}_{B-L} \equiv \underbrace{SU(3)_C \times SU(2)_L \times U(1)_Y}_{\text{Standard Model}} \times \underbrace{U(1)_{B-L}}_{\text{Extension}}, \quad (132)$$

which contains one extra gauge boson C_μ (also denoted by Z' in phenomenology), in order to ensure the invariance of the full Lagrangian under this gauge symmetry. Besides the usual SM content, we have also three singlet fermions, identified with three right-handed neutrinos and denoted from now on by ν_R^i , $i = 1, 2, 3$, to cancel all the gauge and gravitational anomalies, making the $U(1)_{B-L}$ group anomaly-free. In this framework, the breaking scale of this global $B - L$ symmetry could provide a natural identification to the so-called see-saw scale [143, 144, 145].

	$SU(3)_C$	$SU(2)_L$	$U(1)_Y$	$U(1)_{B-L}$
q_L^i	3	2	+1/6	+1/3
u_R^i	3	1	+2/3	+1/3
d_R^i	3	1	-1/3	+1/3
L^i	1	2	-1/2	-1
ν_R^i	1	1	0	-1
R^i	1	1	-1	-1
\mathcal{H}	1	2	-1/2	0
X	1	1	0	+2

Table 2: Quantum numbers of the particles in the $B-L$ model. Besides the well-known SM particle contents, the right-handed neutrinos ν_R^i , where $i = 1, 2, 3$ is the generation index, and the $B-L$ scalar singlet X are also listed.

The Lagrangian of the $B-L$ sector is given by:

$$\begin{aligned}
\mathcal{L}_{B-L} = & \imath \bar{L} D_\mu \gamma^\mu L + \imath \bar{R} D_\mu \gamma^\mu R + \imath \bar{\nu}_R D_\mu \gamma^\mu \nu_R + \\
& - \left(h_i^e \bar{L}_i \phi_H R + h_{ij}^{\nu_L} \bar{L}_i \tilde{\phi}_H \nu_{Rj} + \frac{1}{2} h_{ij}^{\nu_R} \bar{\nu}_{Ri}^c \chi \nu_{Rj} + \text{h.c.} \right) + \\
& + (D^\mu \phi_H)^\dagger (D_\mu \phi_H) + (D^\mu \chi)^\dagger (D_\mu \chi) - \frac{1}{4} C_{\mu\nu} C^{\mu\nu} - V(\phi_H, \chi), \quad (133)
\end{aligned}$$

where $C_{\mu\nu} \equiv \partial_\mu C_\nu - \partial_\nu C_\mu$ is the field strength tensor of the $U(1)_{B-L}$, whose kinetic term is given by the last but one term in (133) and L, R are the usual SM lepton doublet and right-handed singlet, respectively. We are going to identify all the terms in this Lagrangian throughout the section.

The covariant derivative D_μ is now generalised in the following way:

$$D_\mu \equiv \partial_\mu + \imath g \frac{\tau^a}{2} W_\mu^a + \imath g' Y_{B-L} + \imath (g'_{B-L} Y + g_{B-L} Y_{B-L}) C_\mu, \quad (134)$$

where g_{B-L} is the $U(1)_{B-L}$ gauge coupling constant, the Y_{B-L} charge is the $B-L$ quantum number and g'_{B-L} the gauge coupling which identifies the Abelian mixing at tree level. For the values of the Y_{B-L} number for quarks, leptons and scalars, see the Table 2. It is possible to define an effective coupling Y_{eff} and an effective charge g_{eff} , so that $g_{\text{eff}} Y_{\text{eff}} \equiv g'_{B-L} Y + g_{B-L} Y_{B-L}$: in the following we will assume a generic mixing between the $U(1)_Y$ and $U(1)_{B-L}$ gauge groups, where the new C_μ boson couples to one such linear combination. Usually it is customary to impose a tiny mixing between Z' and Z^0 (small g'_{B-L}), giving rise to the so-called ‘‘pure’’ $B-L$ model. We will follow this path, although some g'_{B-L} -dependent terms emerges in the RGE [see App. A.3]. The h^e, h^{ν_L} and h^{ν_R} refer to the 3×3 Yukawa coupling matrices.

As concerns the scalar sector, the model contains one $SU(2)_L$ singlet complex scalar X , which is a singlet under the SM, that, carrying a non-zero $B-L$ charge, once it has acquired a vacuum expectation value $\langle \chi \rangle = v'/\sqrt{2}$, whose value is not fixed, it can spontaneously break the $U(1)_{B-L}$ symmetry, possibly just above the inflationary scale. In our scenario, after the symmetry breaking, it is obtained $X = \chi/\sqrt{2} + v'$, where the phase part leading to Goldstone modes has been neglected. The real part of X , denoted by χ , can be decomposed in a background contribution $\chi^{(0)}$, which will be

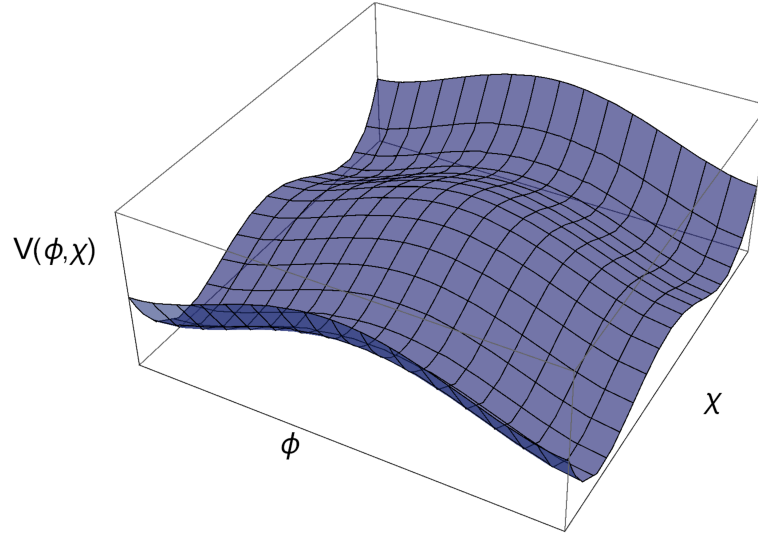


Figure 23: Sketch of the two-field potential (135) after the two symmetry breakings, in which are clear the B – L and electroweak symmetry breaking minima.

identified with the inflaton, and a fluctuation part $\delta\chi$, responsible for the production of primordial perturbations during inflation. The other scalar of the model \mathcal{H} is the usual SM Higgs $SU(2)_L$ doublet, which guarantees the electroweak symmetry breaking down to $U(1)_{em}$ at the measured vacuum expectation value $\langle\phi_H\rangle = v/\sqrt{2} \simeq 246$ GeV. In total we have six scalar degrees of freedom: after both the symmetry breakings, four of them are eaten by the Z' , Z^0 and W^\pm bosons and two of them (ϕ_H , χ) remain as physical degrees of freedom.

After the B – L breaking, the scalar potential $V(\mathcal{H}, \chi)$ of this extended theory is given by:

$$V(\mathcal{H}, \chi) = \frac{\lambda_{\phi_H}}{6} (\mathcal{H}^\dagger \mathcal{H})^2 + \frac{\lambda_\chi}{24} (|\chi|^2 - v'^2)^2 + \frac{\lambda_{\phi_H\chi}}{2} (\mathcal{H}^\dagger \mathcal{H}) (|\chi|^2 - v'^2), \quad (135)$$

from which $m_\chi^2 = \lambda_\chi v'^2/6$ is the B – L singlet mass, while λ_{ϕ_H} , λ_χ and $\lambda_{\phi_H\chi}$ are the SM Higgs quartic coupling, the B – L singlet self-coupling and the portal coupling between ϕ_H and χ , respectively. The SM Higgs mass term and the v contribution are not taken into account in this formula yet, because, with $\lambda_{\phi_H\chi} > 0$, it is possible to generate a non-zero vacuum expectation value v' , while $v = 0$: this means that the two phases of symmetry breaking happen at very different energy scales $v' \gg v$.

We can notice that we have now three new terms in the scalar part of the Lagrangian: $\lambda_{\phi_H\chi} v'^2 \mathcal{H}^\dagger \mathcal{H}$ redefines the Higgs mass parameter, $\lambda_{\phi_H\chi} v' \mathcal{H}^\dagger \mathcal{H} \chi^{(0)}$ makes viable the decay of the inflaton into two SM Higgs fields during reheating [see Sec. 5.5] and $\lambda_{\phi_H\chi} \mathcal{H}^\dagger \mathcal{H} \chi^{(0)} \chi^{(0)}$ takes into account the scattering between the SM Higgs and the inflaton during the inflationary phase. From now on, if not specified, the “(0)” superscript for the background part of the scalar field $\chi^{(0)}$ will be dropped.

The potential (135) must be stable: in other words, in order to be bounded from below, the following condition¹ must be satisfied at first (in the $\lambda_{\phi_H\chi} > 0$ case):

$$\lambda_{\phi_H\chi} > \sqrt{\frac{\lambda_{\phi_H}\lambda_\chi}{27}}, \quad \lambda_{\phi_H}, \lambda_\chi \geq 0. \quad (136)$$

Furthermore, as in the usual Higgs mechanism, the vacuum expectation values v and v' cannot be non-zero unless negative square mass $m_\chi^2 < 0$ is assumed. In addition, we do not want a local minimum in $\langle \phi_H \rangle = \langle \chi \rangle = 0$, so we have to require another condition on the quartic couplings: $\lambda_{\phi_H\chi}^2 < 4\lambda_{\phi_H}\lambda_\chi$. It should be noticed that, if we reduce the problem to an additional real singlet instead of a complex one, the Abelian symmetry has to be replaced by a \mathbb{Z}_2 symmetry, under which the SM fields are even and χ is odd: in this way all the linear and cubic terms in χ are prevented to appear, so the field χ is stable and can not decay into SM particles, preserving the well-established low-scale SM phenomenology.

Below the electroweak symmetry breaking scale, as we already said, the Higgs field is redefined, in unitary gauge, as $\mathcal{H} = (0 \ v + \phi_H)^\top / \sqrt{2}$ and the scalar fields get mixed. The physical light and heavy fields (ϕ_l and ϕ_h , respectively) are obtained diagonalising the mass matrix:

$$\mathcal{M}^2(\phi_H, \chi) = \begin{pmatrix} \lambda_{\phi_H} v^2 & \frac{1}{2} \lambda_{\phi_H\chi} v v' \\ \frac{1}{2} \lambda_{\phi_H\chi} v v' & \lambda_\chi v'^2 \end{pmatrix}, \quad (137)$$

which gives:

$$m_{\phi_l, \phi_h}^2 = \frac{1}{2} \left(\lambda_{\phi_H} v^2 + \lambda_\chi v'^2 \pm \sqrt{(\lambda_{\phi_H} v^2 - \lambda_\chi v'^2)^2 + \lambda_{\phi_H\chi}^2 v^2 v'^2} \right). \quad (138)$$

It is possible to parametrise the mass eigenstate fields ϕ_l and ϕ_h in the following way:

$$\begin{pmatrix} \phi_l \\ \phi_h \end{pmatrix} = \begin{pmatrix} \cos \theta & -\sin \theta \\ \sin \theta & \cos \theta \end{pmatrix} \begin{pmatrix} \phi_H \\ \chi \end{pmatrix}, \quad (139)$$

where the mixing angle is given by

$$\tan 2\theta = \frac{|\lambda_{\phi_H\chi}| v v'}{\lambda_{\phi_H} v^2 - \lambda_\chi v'^2}. \quad (140)$$

Clearly, with $\lambda_{\phi_H\chi} = 0$ there is no mixing and we recover the expressions given before. For $\lambda_{\phi_H\chi} \neq 0$, the light Higgs mass becomes smaller than the SM prediction.

After the B – L symmetry breaking, the gauge boson Z' acquires a mass $m_{Z'}^2 \sim g_{B-L}^2 v'^2$. It might be useful to stress that, given the possible tree-level mixing mentioned earlier, Z^0 and Z' may be not mass eigenstates. However, no hints, so far, have been revealed by LHC in relation to the existence of a TeV particle compatible with this scenario [for a related recent work, see, for instance [165]].

The second line in (133) takes into account the relevant contributions for the see-saw mechanism, involving, apart from the SM fermions, the three right-handed neutrinos: the second term in the parenthesis generates the Dirac neutrino mass term after electroweak symmetry breaking, while the third one gives rise to the right-handed

¹ See Sec. 5.2.1 for further details.

neutrino Majorana mass term, related to the $B - L$ gauge symmetry breaking. These are the only allowed gauge invariant terms, being $Y_{B-L}^X = 2$. The $\tilde{\phi}_H$ operator stands for $i\sigma_2\phi_H^*$, being σ_2 the second Pauli matrix. The $h_{\nu_R}\chi\nu_R\nu_R$ term in the Lagrangian, appeared after the $U(1)_{B-L}$ symmetry breaking, leads to a right-handed neutrino mass $m_{\nu_R} = h_{\nu_R}v'/\sqrt{2}$, while the electroweak symmetry breaking implies a Dirac neutrino mass term $m_D = h_\nu v$. The condition $m_{\nu_R} \gg m_D$ is typical of a type I see-saw scenario, automatically implemented in this model, characterised by a mass matrix

$$\mathcal{M}^2 \sim \begin{pmatrix} 0 & m_D \\ m_D & m_{\nu_R} \end{pmatrix}, \quad (141)$$

where the first row and the first column are referred to the left-handed neutrino ν_L , while the others to the right-handed component ν_R . Being aware of the see-saw condition, we can diagonalise the matrix and obtain the light and heavy mass eigenstates:

$$m_{\nu, \text{light}} \simeq -m_D m_{\nu_R}^{-1} m_D^T = h_\nu h_{\nu_R}^{-1} h_\nu^T \frac{v^2}{v'}, \quad m_{\nu, \text{heavy}} \simeq m_{\nu_R}. \quad (142)$$

Different parametrisations of the mass matrix are obviously allowed.

The relation (142) accounts for small neutrino masses of order $\mathcal{O}(10^{-1})$ eV. In our analysis, for simplicity, we consider only a one-generation neutrino see-saw scheme: if the right-handed neutrinos corresponding to the two lighter neutrinos have masses lighter than the one we take into account m_{ν_R} , the associated h_ν are consequently smaller with a negligible effect in the stabilisation mechanism of λ_{ϕ_H} , as we are going to stress later. The $B - L$ scale and hence m_{ν_R} remain anyway arbitrary: it is common, for instance, to put $m_{\nu_R} \sim 10^{15}$ GeV in order to reproduce the correct pattern of light neutrino masses, sticking with the atmospheric and solar neutrinos data [166].

5.2 STABILISATION OF THE POTENTIAL

For this introduction on the relevant physical scales, we take inspiration from the very detailed work by Ballesteros and Tamarit [7] and the subsequent papers, by the same authors (with others) [168, 169].

In the pure SM, for the central values of the top quark mass and the Higgs boson mass (along with the strong coupling), adopting the procedure of [1], we obtain the scale at which the potential becomes negative, also called instability scale: $\Lambda_I \sim 10^{10}$ GeV, already defined in Chap. 2. This scale is approximately the one identified when the Higgs quartic coupling $\tilde{\lambda}_{\phi_H}$ crosses zero (from now on the pure SM parameters will be denoted by a tilde, in order to distinguish them from the extended model ones). We said ‘‘approximately’’, because of the RGE-improved effective potential approach: anyway we will assume Λ_I as the physically meaningful one, following the definition of absolute stability as the one related to the positiveness of the potential everywhere.

The scalar and the mixing couplings are not involved in this effect, not having in their β -functions the top-Yukawa contributions which bring the running down towards negative values, besides the high-energy contribution due to right-handed neutrinos.

The inclusion of a high-scale $U(1)_{B-L}$ gauge symmetry is aimed, for now, to make the quartic couplings of the theory bounded from below at all energy scales, restoring

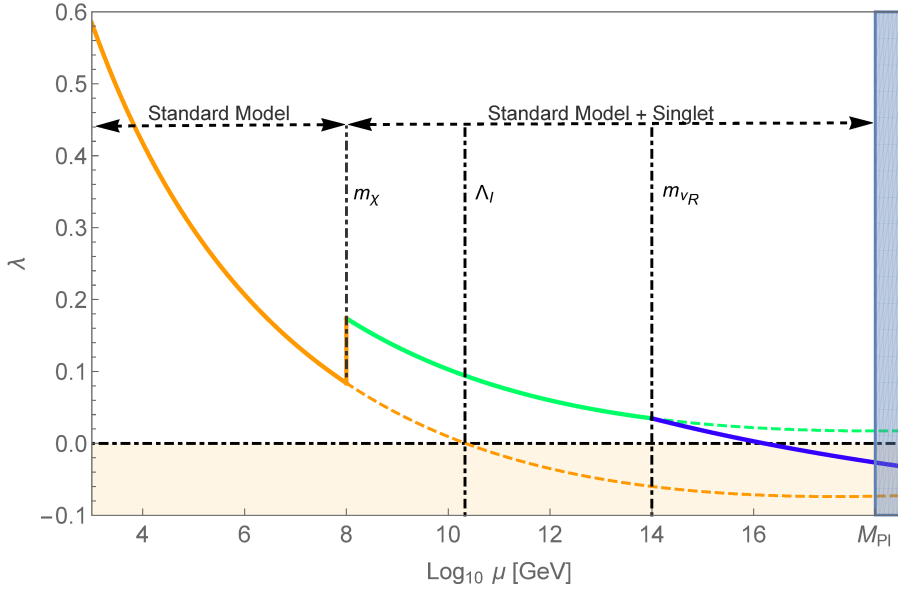


Figure 24: Running of the Higgs quartic coupling as a function of the energy scale, from the SM to the model with a scalar singlet (with positive portal coupling $\lambda_{\phi_{\text{HX}}} > 0$), here assumed to have mass $m_\chi = 10^8$ GeV, up to the full model, including also the right-handed neutrino, supposed to set in at a mass scale $m_{\nu_R} = 10^{14}$ GeV. The tree-level threshold shift at $\mu = m_\chi$ helps the quartic coupling to remain positive beyond the instability scale Λ_I , here at $\sim 10^{10}$ GeV, as the analysis related to the central values of the top quark mass, the Higgs mass and the strong coupling suggests. When the Yukawa coupling of the heavy neutrino becomes relevant in the β -functions, for $\mu \geq m_{\nu_R}$, the running is pulled down towards the negative region. As usual, the shaded area represents the quantum-gravity regime. The first figure of this kind of running was shown in [167].

the sufficient condition of vacuum stability all the way up to the Planck scale. At a first glance, giving the big difference in energy of the two symmetry breakings considered (the low energy effective theory, which is just the SM and the $U(1)_{B-L}$ gauge extended SM), one might think at a manifestation of a sort of “decoupling theorem”, according to which the effect of the new heavy physical states would not affect the behaviour of the quartic coupling at lower scales, dominated by the SM only. Actually, as already stated in [167], the presence of a heavy scalar does influence also the physics at lower scales, generating a tree-level threshold effect in the evolution of the λ_{ϕ_H} quartic coupling:

$$\lambda_{\phi_H} = \tilde{\lambda}_{\phi_H} + 9 \frac{\lambda_{\phi_{\text{HX}}}^2}{\lambda_\chi}. \quad (143)$$

This helps in the stabilisation of the electroweak vacuum, as long as, as we naively expect, the mass scale of the heavy scalar is lower than the instability scale, typically around 10^{10} GeV [see Fig. 24].

The threshold correction would be effective in the stabilisation if $\Lambda_T < \Lambda_I$, where the scale $\Lambda_T^2 \sim \frac{9\lambda_{\phi_H\chi}}{2\lambda_{\phi_H}\lambda_\chi} |m_\chi^2|$ is the one associated with the extra singlet scalar, keeping all the factors in front of the dimensionless couplings². This coincides with the mass scale of the scalar, which gives the limit of validity of the SM, only if all the couplings are the of the same order $2\lambda_{\phi_H}\lambda_\chi \sim 9\lambda_{\phi_H\chi}$, but if they are not, the factors should be kept: it means that Λ_T represents here the regime in which the stability condition is given by $\lambda_{\phi_H} > 9\frac{\lambda_{\phi_H\chi}^2}{\lambda_\chi}$, instead of the SM condition $\lambda_{\phi_H} > 0$, which turns out to be restored again for high-field values, or, in other words, for energies much higher than Λ_T . Summarising: if $\lambda_{\phi_H\chi} > 0$, the instability region near the scale introduced by the new scalar singlet is raised up till the threshold correction value contained in (143), then it decays rapidly to the usual SM condition of positiveness of the Higgs quartic coupling. If the scale Λ_I is larger enough than Λ_T , the relevant stability condition would be the simple SM one.

Let us give a closer look to the threshold effect structure: a big threshold inevitably can cure the instability problem and this could be accomplished pushing the values of $\lambda_{\phi_H\chi}$ and λ_{ϕ_H} towards very small positive values, keeping the ratio unchanged. Apparently, the only important thing is that instability occurs beyond the scale Λ_T . In this way the new physics term would be actually decoupled from the SM theory, but, at the same time, the stabilisation issue would be unexpectedly solved. Furthermore, if we consider $\lambda_{\phi_H\chi} \rightarrow 0$, at some point the Λ_T will then become larger than the instability scale, making the stabilisation impossible. This means that the mixing term is essential in the mechanism and it can not be made small indefinitely.

Another relevant scale could be retrieved if we analyse the potential obtained after we integrate out the χ field, now dependent only on ϕ_H : it reproduces the SM potential and the consequent stability condition, *i.e.* $\tilde{\lambda}_{\phi_H} > 0$, is reliable for the field range $\phi_H^2 \lesssim 2|m_\chi^2|/\lambda_{\phi_H\chi}$, that could be redefined as new scale Λ'_T . This range represents the scales for which the valley of minima for χ does exist. Asking that $\partial V/\partial\chi = 0$, the tree-level solution is

$$\lambda_\chi\chi^2 + 3\lambda_{\phi_H\chi}\phi_H^2 - 6m_\chi^2 = 0 \quad (\chi\text{-minima}), \quad (145)$$

from which we have the constraints $0 \leq \chi^2 \leq 6m_\chi^2/\lambda_\chi$ and $0 \leq \phi_H^2 \leq 2m_\chi^2/\lambda_{\phi_H\chi}$, which is the scale Λ'_T .

The global stability condition can thus be written in the following way:

$$\Lambda_I \gtrsim \Lambda, \quad (146)$$

where Λ stands for the greatest scale among Λ_T and Λ'_T , related between each other through the factor $9\lambda_{\phi_H\chi}^2/4\lambda_\chi\lambda_{\phi_H}$.

Thus, the condition (146) is violated as well in the case in which the instability scale is intermediate between the singlet mass scale and Λ_T : $\Lambda_T < \Lambda_I < |m_s^2|^{1/2}$. Here the

² If we consider the full potential (135) along the $\chi = 0$ direction, we can determine for which values of the Higgs field it becomes zero (the criticality limit). Solving for ϕ_H^2 , we find

$$\phi_H^2 = \frac{9\lambda_{\phi_H\chi}|m_\chi^2|}{2\lambda_{\phi_H}\lambda_\chi} \left(1 \pm \sqrt{1 - \frac{16\lambda_{\phi_H}\lambda_\chi}{9\lambda_{\phi_H\chi}^2}} \right), \quad (144)$$

for instance, for very small λ_χ , as it the case, we retrieve the scale Λ_T^2 .

correct hierarchy is $\Lambda \sim \Lambda_I' > \Lambda_I$, making stabilisation impossible again. Summarising, stabilisation is not achievable (remaining in the perturbative regime) whenever $|m_\chi^2| \gtrsim \Lambda_I^2$.

5.2.1 Tree-level threshold relations

Being the singlet decoupled at low energies, we need the matching conditions between the two regimes and, in this brief section, we try to summarise all the tree-level threshold equations obtained, useful to determine the relation between the parameters in the extended model and in the pure SM. As shown in [7], the tree-level description is sufficient to describe the inflationary dynamics.

We start from the potential (135), considering only the real part of the B – L scalar (after the symmetry breaking) and neglecting the field-independent pieces of the function:

$$V(\mathcal{H}, \chi) = m_{\text{H}}^2 (\mathcal{H}^\dagger \mathcal{H}) - \frac{m_\chi^2}{2} \chi^2 + \frac{\lambda_{\Phi\text{H}}}{6} (\mathcal{H}^\dagger \mathcal{H})^2 + \frac{\lambda_\chi}{24} \chi^4 + \frac{\lambda_{\Phi\text{H}\chi}}{2} (\mathcal{H}^\dagger \mathcal{H}) \chi^2, \quad (147)$$

where $m_\chi^2 < 0$.

It is possible now to integrate out the field χ through its equation of motion³:

$$\left. \frac{\partial V(\mathcal{H}, \chi)}{\partial \chi} \right|_{\chi=\chi_{\min}(\mathcal{H})} = 0 \rightarrow \chi^2 = \frac{6}{\lambda_\chi} \left(m_\chi^2 - \lambda_{\Phi\text{H}\chi} (\mathcal{H}^\dagger \mathcal{H}) \right). \quad (148)$$

The new potential, in terms of the SM parameters, is given by

$$V(\mathcal{H}, \chi) = \tilde{m}_{\text{H}}^2 (\mathcal{H}^\dagger \mathcal{H}) + \frac{\tilde{\lambda}_{\Phi\text{H}}}{6} (\mathcal{H}^\dagger \mathcal{H})^2 + V_0, \quad \tilde{m}_{\text{H}}^2 < 0, \quad (149)$$

where

$$\tilde{m}_{\text{H}}^2 \equiv m_{\text{H}}^2 + \frac{3\lambda_{\Phi\text{H}\chi}}{\lambda_\chi} m_\chi^2, \quad \tilde{\lambda}_{\Phi\text{H}} \equiv \lambda_{\Phi\text{H}} - 9 \frac{\lambda_{\Phi\text{H}\chi}^2}{\lambda_\chi}, \quad V_0 \equiv \frac{1}{2} \left(\frac{\tilde{m}_{\text{H}}^4}{\tilde{\lambda}_{\Phi\text{H}}} - 3 \frac{m_\chi^4}{\lambda_\chi} \right). \quad (150)$$

V_0 stands for the cosmological constant, irrelevant for our studies. We can see that we retrieve the threshold effect (143) mentioned earlier. Notice that the value of the Higgs mass m_{H}^2 in the full model can become quite different from its homologous in SM \tilde{m}_{H}^2 , given the correction proportional to $|m_\chi|^2 \gg m_{\text{H}}^2$. This shift in the mass value is compatible with the Higgs properties, experimentally observed: the matching conditions make possible the emergence of the electroweak scale through an adequate value for the portal coupling $\lambda_{\Phi\text{H}\chi}$.

As concerns the stability condition (136), after the electroweak symmetry breaking as well, it can be obtained finding the minimum of the potential in the χ -valley:

$$\left. \frac{\partial V(\Phi\text{H}, \chi)}{\partial \Phi\text{H}} \right|_{\Phi\text{H}=\Phi\text{H}, \min(\chi)} = 0 \rightarrow \Phi_{\text{H}}^2 = 3 \frac{\lambda_{\Phi\text{H}\chi}}{\lambda_{\Phi\text{H}}} \chi^2, \quad (151)$$

from which, substituting in the original potential, we find the sought condition.

³ The full high-energy potential of the extended model along the line of minima of the field χ , reduces itself as the SM one. This is of course valid neglecting higher-order non-renormalisable terms.

Finally, we can extract the vacuum expectation values of the two scalar fields, which are

$$v^2 = -6 \frac{\tilde{m}_H^2}{\lambda}, \quad v'^2 = -\frac{6}{\lambda_\chi} \left(3 \frac{\lambda_{\Phi_H \chi}}{\lambda} \tilde{m}_H^2 + m_\chi^2 \right). \quad (152)$$

These relations have been useful in the determination of the range of values reached by the scalar fields during the inflationary phase, constraining the parameters of the model.

5.2.2 RGE

The inclusion of a new scalar field and neutrinos modifies the renormalisation group evolution of the SM couplings. All the relevant RGE above the scale m_χ up to two loops can be found in [167, 170, 171] and are given in detail within our normalisation in App. A.3. As it can be seen, stopping at one loop in this case, we added the additional terms coming from the specific $U(1)_{B-L}$ model we are studying, *i.e.* the terms involving the g'_{B-L} and g_{B-L} gauge couplings and the right-handed neutrino Yukawa coupling h_{ν_R} (only one generation has been considered). Also their own running is displayed. The impact of h_ν and h_{ν_R} in the running is not negligible, in principle, due to the high $U(1)_{B-L}$ breaking scale. Besides the tree-level threshold effect mentioned before, these new contributions in the RGE represent another source of stabilisation for the potential, preventing the λ_{Φ_H} quartic coupling from becoming negative [see the green line in Fig. 24, which appears less steep than the running of the SM Higgs quartic coupling, and would show a growing behaviour at high energies]. Nevertheless, it must be said that this effect is sub-dominant and that the right-handed neutrino contribution in the β -functions, dominated by its Yukawa coupling, goes against stabilisation, pulling down the running of the Higgs quartic coupling. A threshold effect strong enough is required to win over these terms [see the partial conclusions at the end of the chapter].

5.3 INFLATION

Let us focus now on dynamics. We start again from the scalar potential (135), bearing in mind that we are now in the inflationary regime, so we have to take into account that $v \ll v'$ and $\lambda_{\Phi_H \chi} \ll 1$: it emerges a simple single-field inflationary scenario, in which the heavy singlet plays the role of the inflaton, as already anticipated. See Sec. 5.4 for further motivations on the actual “decoupling” of the high-scale physics from the electroweak regime. Following [161], in order to take into account quantum corrections to the tree-level potential, at leading-log order, we can rewrite V with a parametrisation in which the renormalisation scale is chosen to be fixed at v' :

$$V(\chi) = \lambda_\chi \left[\frac{1}{24} (\chi^2 - v'^2)^2 + a \log \left(\frac{\chi}{v'} \right) \chi^4 \right], \quad (153)$$

where the parameter $a \equiv \beta_{\lambda_\chi}^{(1)} / (16\pi^2 \lambda_\chi)$ takes into account the right-handed neutrino effect on the quartic coupling and estimates the relevance of the Coleman-Weinberg log-correction to the tree-level potential: in other words, it determines whether the

$U(1)_{B-L}$ symmetry is broken by the radiative logarithmic term or simply by the tree-level potential. Neglecting the sub-leading contributions, the α parameter is approximately given by [see App. A.3 for the full expression]

$$\alpha \approx \frac{1}{16\pi^2\lambda_\chi} \left(12\lambda_{\Phi_{HX}}^2 + \frac{10}{3}\lambda_\chi^2 + \frac{4}{3}\lambda_\chi h_{\nu_R}^2 - 48\lambda_\chi g_{B-L}^2 - 576g_{B-L}^4 - 6h_{\nu_R}^4 \right). \quad (154)$$

It will be seen that this running is dependent only on the right-handed neutrino Yukawa coupling and the value of g_{B-L} , $\beta_{\lambda_\chi}^{(1)} \approx g_{B-L}^4 - h_{\nu_R}^4$, given that $\lambda_\chi \ll h_{\nu_R}$, g_{B-L} [see the results shown at the end of the section].

As already seen in Chap. 4, the inflationary phase happens when the inflaton slowly rolls down along the potential towards the minimum for a period long enough to solve the early-cosmology issues in the SCM.

Here we have two possibilities, in which the scalar field can travel from “above” the vacuum expectation value of the heavy scalar ($\chi > v'$) or from “below” ($\chi < v'$). In general, the analysis is accomplished picking out time after time a value for v' in Planck units and find a suitable value for the quartic coupling λ_χ , in order to reproduce the correct amount of primordial scalar perturbations $\Delta_\zeta(k_*)^2$.

At this stage, h_{ν_R} and consequently the quantum parameter α should be estimated. We will return on this referring to each particular scenario.

Inflation ends conventionally when one of the slow-roll parameters reaches the unity, then, enforcing this condition, it is possible to determine the end-value for the inflaton χ_{end} . Thus, the field value χ_* at the pivot scale has to be calculated, imposing the desired number of e-folds, *i.e.* $N = 50 - 60$. Finally, at χ_* , the potential and all the primordial inflationary observables can be inferred.

Summarising, we have to fit five physical observables ($\Delta_\zeta(k_*)^2$, n_s , r , $\frac{dn_s}{d\ln k}$ and m_ν) with four free parameters (v' , λ , h_ν and α), related to each other. Sticking with the inflationary constraints on $\Delta_\zeta(k_*)^2$ and on the duration of the expansion phase, we can infer that the predicted values of n_s , r and $\frac{dn_s}{d\ln k}$ depend on the parameter α (*i.e.* h_{ν_R}) and the vacuum expectation value v' of the heavy scalar.

The followed approach consists in looking over two regimes, in which v' is either super-Planckian or sub-Planckian. Let us consider this two limits in turn.

$v' > M_P$. In this regime the Majorana Yukawa coupling, in order to reproduce the correct order of magnitude for the low-energy neutrino mass, is heavily suppressed: for a $v' \sim 10^3 M_P$, corresponds $h_{\nu_R} \sim 10^{-6}$. For this reason, in this case the quantum corrections are negligible and the whole analysis can be carried out only on the tree-level potential, from which it is possible to draw simplified relations for the inflationary observables, starting from the number of e-folds

$$N \simeq \frac{1}{4M_P^2} \left(\frac{1}{2}\chi^2 - v'^2 \log \chi \right), \quad (155)$$

and ending with the slow-roll parameters

$$\varepsilon \simeq \frac{8M_P^2\chi_*^2}{(\chi_*^2 - v'^2)^2}, \quad \eta \simeq \frac{4M_P^2(3\chi_*^2 - v'^2)}{(\chi_*^2 - v'^2)^2}, \quad \zeta \simeq \frac{96M_P^4\chi_*^2}{(\chi_*^2 - v'^2)^3}. \quad (156)$$

The inflationary parameters are obtained using (117), (118) and (119).

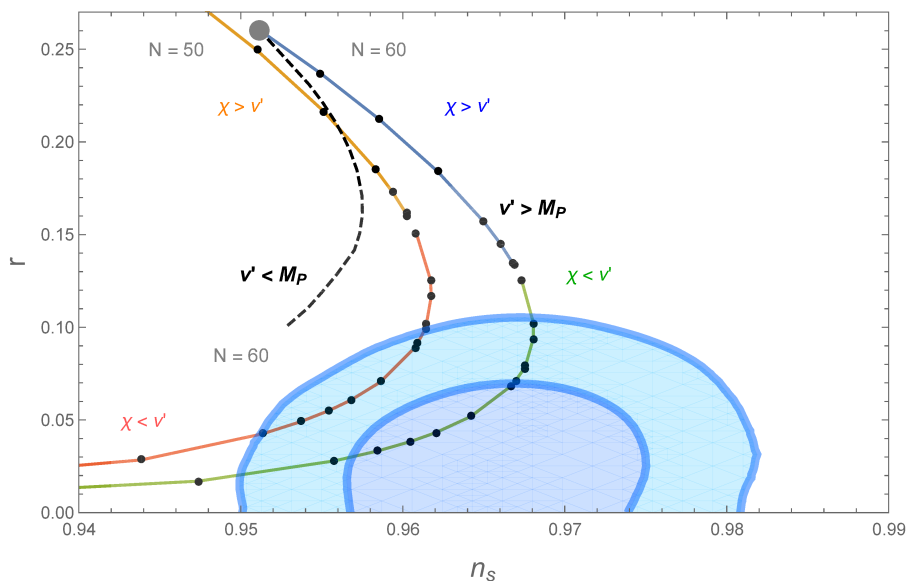


Figure 25: (r, n_s) plane in this B – L framework. The $v' > M_P$ case, in which the radiative corrections can be neglected, is shown with solid lines: the blue branch refers to the solutions above the vacuum expectation value of the scalar singlet, for $N = 60$. Just below we have the green one, representing the points obtained in the case of the inflaton rolling down from below, again for $N = 60$. The orange and the red branches are again for the $\chi > v'$ and $\chi < v'$ cases, respectively, but this time for a number of e-folds equal to $N = 50$. The region in between the two corresponding branches is filled with all the allowed points for the case under examination. We see how, for a fixed number of e-folds, both branches converge towards the quadratic inflation predictions, *i.e.* $(r, n_s) = (0.967, 0.13)$ for the $N = 60$ case. The small black points on each branch, starting from the top downwards, indicate the values $v'/M_P = 1, 5, 10, 20, 50, 100, 500, 1000$ for the upper branch (the last two points are nearly superimposed), and, starting from below upwards, $v'/M_P = 13, 15, 16, 17, 18, 20, 25, 26, 29, 30, 40, 50, 200, 500, 1000$ for the lower branch, with an increased density of points analysed where the curve bends (the first two points exceed the plot range). The contours are the 1σ and 2σ allowed regions, from the latest constraints put by the joint analysis of the Planck and BICEP2/Keck Array collaborations [134]: it is clear that it is possible to have viable values for r and n_s for sufficiently low v' in the so-called “hilltop” configuration. For comparison, also the $v' < M_P$ case is shown, by the dashed line: it is obtained varying the α parameter in the window $[-0.011, -0.013]$ for $N = 60$. It is clear that the radiatively corrected quartic potential, although very popular at the time of the BICEP2 claim [135], does not fit the current experimental constraints. It is worth noting that the quantum corrections contribute to deviate from the standard quartic inflationary potential predictions (the big grey point in the upper part of the plot), to which both the branches converge. The analysis broadly follows the one did for a slightly different scenario in [5].

As concerns the quartic coupling, it is not involved in the dynamics, but it must satisfy the condition on the amplitude of primordial perturbations, which reads, in this case:

$$\Delta_{\zeta}(k_*) \simeq \frac{\lambda_{\chi}(\chi_*^2 - v'^2)^4}{768\pi^2 M_{\text{P}}^6 \chi^2} = 2.15 \times 10^{-9}. \quad (157)$$

The values obtained are in the range $\lambda_{\chi} \approx 10^{-17} - 10^{-14}$, which justifies the approximation used for Eq. (154).

In Fig. 25 are displayed the results for the predicted values of the tensor-to-scalar ratio and the spectral index, represented by the solid lines and obtained varying the vacuum expectation value of the heavy scalar and fixing the number of e-folds at $N = 50$ and $N = 60$. In both cases we display some particular values for v' , seen as small black points and the two different scenarios, which we told about earlier, related to the starting position of the inflaton in its rolling: $\chi < v'$ when it rolls from smaller to larger values until it reaches its minimum at v' (where, in principle, the field is at rest and the universe reheats) and the opposite, where the field rolls down along the steeper part of the “Mexican hat” potential towards the vacuum. Both branches converge towards the predictions of the standard quadratic inflationary model, $(n_s, r) = (0.967, 0.13)$ [126]. For $v' \simeq M_{\text{P}}$, instead, the predictions go towards the big grey circle, which stands for the quartic inflation potential $(n_s, r) = (0.951, 0.26)$. The results are compared with the current experimental bounds put by the joint analysis of the Planck and BICEP2/Keck Array collaborations [134]: it seems clear that the “hilltop” configuration⁴ is preferred ($\chi < v'$), with a B-L scalar vacuum expectation value of order $v' \simeq 20M_{\text{P}} - 30M_{\text{P}}$, with respect to the standard chaotic quartic model, which gives too large values for r , as already expected. Nevertheless, it can be seen that a lower bound for r emerges: if future experiments will be able to detect a tensor-to-scalar ratio smaller than $r \lesssim 0.03$, this model would be in trouble. In Fig. 26 are also displayed the running of the spectral index and the dependence of r on the vacuum expectation value: very tiny negative values for $\frac{dn_s}{d \ln k}$ are correctly predicted and suitable predictions on r are achieved in the window $v' \simeq 20M_{\text{P}} - 30M_{\text{P}}$.

$v' < M_{\text{P}}$. The sub-Planckian configuration, in the large $v' \simeq M_{\text{P}}$ limit, converges to the quartic potential scenario. Going down with v' , the radiative corrections are now relevant, given that $h_{\nu_{\text{R}}}$ can become large: the coupling between the heavy scalar and the right-handed neutrino, as already said, estimates the departure from the standard textbook predictions. The result, for $N = 60$ is displayed in Fig. 25 as a dashed line: it is obtained fixing $g_{\text{B-L}} \simeq 10^{-5}$ [6] and by varying α in the range $[-0.011, -0.013]$ (for larger values of α the potential becomes unbounded from below): it shows predictions quite distant from the experimental contours. The radiatively corrected scenario could be suitable for a high- r detection [5, 6], but now seems to be a ruled out possibility. We report it as a comparison.

⁴ Configuration proposed for the first time in [172].

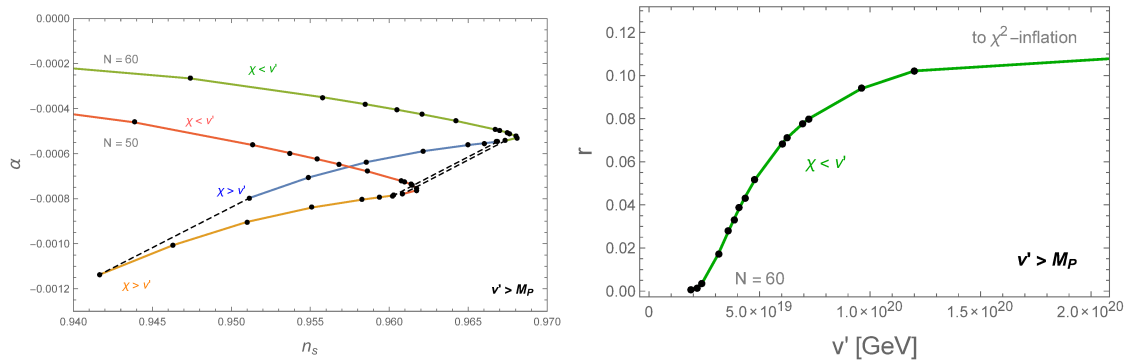


Figure 26: *Left panel:* running of the scalar spectral index (here denoted by the common symbol $\alpha \equiv \frac{dn_s}{d \ln k}$) vs. the spectral index itself. For all the details see the caption of Fig. 25. *Right panel:* tensor-to-scalar ratio as a function of v' in the case $\chi < v'$. Again, for the graphic representation details see the caption of Fig. 25. The curve is obtained for a constant N equal to 60 and shows how values of r compatible with data are achieved for $v' \lesssim 30M_P$. For higher-field values, r converges to the quadratic inflation prediction, by now excluded by observations. The figures are unpublished, done by the author.

5.4 STABILITY VS INFLATION

We have seen that the stabilisation through the threshold mechanism could be effective only if the condition $|m_\chi^2| < \Lambda_I^2$ is satisfied. Actually, in our scenario, the mass of the scalar singlet is not a free parameter, but is fixed in order to reproduce a suitable inflationary phase. As we found in Sec. 5.3, inflation is viable for a vacuum expectation value of the inflaton of order $v' \sim 20M_P$ and the correct amount of primordial scalar perturbations is reproduced thanks to a very tiny quartic coupling $\lambda_\chi \sim 10^{-14}$. Collecting this parameter estimations, we can say that the required mass scale for the inflaton is

$$|m_\chi^2| = \frac{1}{6}\lambda_\chi v'^2 \sim 10^{25} \text{ GeV}^2, \quad (158)$$

larger than the instability scale $\Lambda_I^2 \sim 10^{20} \text{ GeV}^2$, found in Chap. 2 for the central values of top and the Higgs masses. The threshold effect turns out to be useless for stability at this level.

Another constraint could come from the portal coupling $\lambda_{\phi_H \chi}$, wondering if the quantum fluctuations generated during inflation would cause Higgs instability, or, in other words, if the Higgs field, during the inflationary phase, acquires values that trespass in the instability region, being comparable with Λ_I^2 . We investigate now the values reached by the field ϕ_H in its valley of minima, whose maximum is obtained

in the $\chi = 0$ case ($\lambda_{\phi_{\text{HX}}} > 0$ and $\phi_{\text{H}}, \chi \geq 0$). The procedure is similar to that used for Eq. (145), now requiring $\frac{\partial V}{\partial \phi_{\text{H}}} = 0$. The tree-level solution is:

$$\begin{aligned} \lambda_{\phi_{\text{H}}} \phi_{\text{H}}^2 + \frac{1}{3} \lambda_{\phi_{\text{HX}}} \chi^2 + 6m_{\text{H}}^2 &= 0 \quad (\phi\text{-minima}), \\ \phi_{\text{H}} = 0: \quad 0 \leq \chi^2 &\leq -\frac{18m_{\text{H}}^2}{\lambda_{\phi_{\text{HX}}}}, \\ \chi = 0: \quad 0 \leq \phi_{\text{H}}^2 &\leq -\frac{6m_{\text{H}}^2}{\lambda_{\phi_{\text{H}}}}, \end{aligned} \quad (159)$$

Taking the mass threshold relation (150), we have

$$m_{\text{H}}^2 = \tilde{m}_{\text{H}}^2 - \frac{3\lambda_{\phi_{\text{HX}}}}{\lambda_{\chi}} m_{\chi}^2 \approx -\frac{3\lambda_{\phi_{\text{HX}}}}{\lambda_{\chi}} m_{\chi}^2 = -\frac{1}{2} \lambda_{\phi_{\text{HX}}} v'^2, \quad (160)$$

where the SM Higgs mass has been neglected and the mass formula for the heavy scalar has been used. Now, from (159), the highest value reachable by the Higgs field is

$$\phi_{\text{H}}^2 \leq 3 \frac{\lambda_{\phi_{\text{HX}}}}{\lambda_{\phi_{\text{H}}}} v'^2, \quad (161)$$

and so, if we want that it remains much smaller than Λ_{I}^2 , the condition approximately becomes

$$\lambda_{\phi_{\text{HX}}} \ll \tilde{\lambda}_{\phi_{\text{H}}} \frac{\Lambda_{\text{I}}^2}{3v'^2} \sim 10^{-19}, \quad (162)$$

given that at the electroweak scale $\tilde{\lambda}_{\phi_{\text{H}}} \simeq \lambda_{\phi_{\text{H}}} \simeq 0.27$. The identification of the Higgs quartic coupling in the SM with the one in the extended model is safe, being valid the threshold relation (150) and $\lambda_{\phi_{\text{HX}}}^2$ a higher-order correction. In presence of values of the portal coupling larger than about 10^{-19} , for the central values for the top and Higgs masses, the inflationary trajectory could be spoiled and the Higgs field could fall into the (less energetic) true vacuum. Furthermore, even with a very tiny portal coupling, fluctuations of the Higgs field during inflation have to be taken into account, of order of the Hubble parameter, could in principle forbid inflation [14].

Thus, if the top Yukawa coupling leads to an instability for the Higgs field, in any case (even for not too small values for $\lambda_{\phi_{\text{HX}}}$) the model has to be stabilised in the extended model, even not taking care of quantum fluctuations of the Higgs during inflation.

The only chance, at this stage, is to consider values for m_{t} lower than its central values, in order to push the instability scale towards higher values (at least of order of the heavy scalar singlet mass scale) and make the stabilisation possible via the threshold mechanism.

Taking the heavy singlet mass at $m_{\chi} \sim 3.16 \times 10^{12}$ GeV and the scalar quartic coupling $\lambda_{\chi} \sim 10^{-14}$ as required by inflation, we see that the scale Λ depends now only on $\lambda_{\phi_{\text{HX}}}$ [see (146)]. Ignoring the bound (162), we impose a weaker constraint from reheating, that will be clear in the following section, $\lambda_{\phi_{\text{HX}}} \lesssim 10^{-6}$, from which we can infer the new minimum instability scale $\sim 10^{16}$ GeV, needed to have a stabilisation from the threshold mechanism. Assuming the central values for the Higgs mass and the strong coupling in the SM background, this configuration is accomplished for a $m_{\text{t}}^{\wedge} \simeq 171.10$ GeV.

Seen that the critical top mass m_t^c which ensures absolute stability is given by $m_t^c \simeq 171.08$ GeV [see Eq. (69)], our viable window $m_t^c \lesssim m_t \lesssim m_t^\wedge$ turns out to be extremely narrow, making vain almost all our hopes to find a comfortable parameter space, in which inflation and stability could cohabit. Thus, if the SM parameters, in the light of more precise future measurements, are such that the SM potential will appear to be metastable, the threshold mechanism for stabilisation is not compatible with our inflationary scenario for almost all the parameter window. All these results are in agreement with [7] and [6, 5], although these two last works are driven in their conclusions by the BICEP2 claim, ending with different considerations. Further extensions or a change of perspective will be needed.

5.5 REHEATING

After the inflationary phase, any scenario, in order to be successful, should guarantee a transition to the well-known Standard Model phenomenology: when the inflaton starts oscillating around its minimum, produces the decay products which can reheat the universe. This particular era in the history of the Universe, if inflation is the correct framework to deal with, is characterised by a very complicated phenomenon, not fully understood yet. Here, we limit ourselves to few words about reheating in our particular scenario at a basic level⁵, just to mention the calculability, in principle, of the reheating temperature T_R . For all the details on the reheating process, see, for instance, the review [127].

The inflaton starts oscillating with a frequency of order of its mass. The portal coupling $\lambda_{\phi_H\chi}$ between the inflaton and the SM Higgs field allows the decay of our scalar singlet into a pair of SM Higgs. The rate of this process can be computed via the usual standard field theory tools and is given by [161]

$$\Gamma_{\chi \rightarrow \phi_H \phi_H} = \frac{\lambda_{\phi_H\chi}^2 v'^2}{32\pi m_\chi}. \quad (163)$$

Taking into account the expansion of the Universe, this particle decay emerges as an additional friction term in the inflaton equation of motion⁶ besides the standard gravitational term $3H\dot{\chi}$ [see footnote n. 2 of Chap. 4]:

$$\ddot{\chi} + 3H\dot{\chi} + \Gamma\dot{\chi} + m_\chi^2\chi = 0. \quad (164)$$

The reheating phase is considered complete when the Hubble expansion rate H drops below Γ . At that time the energy density is $\rho(t_R) = 3M_p^2\Gamma^2$ (t_R identifies the reheating epoch). We assume that we are in thermodynamic equilibrium (or that it can be reached quickly), so we can finally relate the decay rate to the reheating temperature:

$$\rho(t_R) = \frac{\pi^2 g_*}{30} T_R^4 \rightarrow T_R^2 = \left(\frac{\pi^2 g_*}{90} \right)^{-1/2} M_p \Gamma \simeq 0.3 M_p \Gamma, \quad (165)$$

⁵ Concepts as parametric resonance or Bose-Einstein enhancement of the reheating process go beyond the scope of this work and were discarded.

⁶ This naïve approach has however raised some concerns, for the details see [173].

where $g_* \sim 100$ is the number of effective degrees of freedom for relativistic particles at that time⁷. From big-bang nucleosynthesis, a model-independent lower bound on T_R can be taken, given by $T_R \gtrsim 1$ MeV [174]. If also the CMB is taken into account, the limit is a bit higher: $T_R \gtrsim 4.7$ MeV [175].

Thus, the reheating process is made possible in this case thanks to the portal coupling $\lambda_{\phi_H\chi}$ between the SM Higgs and the scalar singlet, assumed small from previous considerations. Given the smallness of the inflaton quartic coupling too, the decay to SM particles naturally prefers to happen through the mixing $\lambda_{\phi_H\chi}$. In our case

$$T_R^2 \simeq 9.5 \times 10^{-4} M_P \lambda_{\phi_H\chi}^2 v'^2. \quad (166)$$

We have seen that an estimation of λ_χ and m_χ is affordable under the assumption of small $\lambda_{\phi_H\chi}$: although we have some suitable values for v' , coming from inflationary constraints, we only dispose of an upper bound for $\lambda_{\phi_H\chi}$ related to stability arguments. In principle, relying on observations, the portal coupling could even be zero, but, if we want to build a reasonable mechanism of exit from the inflationary phase, its presence turns out to be obligatory, if there are no other fields in the game. Obviously, any hope to probe this coupling by means of a particle physics experiment is vain, since the low-energies signatures of the heavy scalar singlet behave as \tilde{m}_H^2/m_χ^2 , which is practically zero.

However, just to have a feeling of the numbers involved, and bearing in mind that we can evade the bound (162) considering a lower value for m_t and pursuing the stabilisation in the extended case, we could simply demand that the dominant decay rate $\Gamma_{\chi \rightarrow \phi_H \phi_H}$ is at least smaller than the inflaton mass, in order to avoid instability of the inflaton during inflation, which means, from (163), that $\lambda_{\phi_H\chi}^2 \lesssim 32\pi\lambda_\chi$. Taking as a reference a value a portal coupling of order $\sim 10^{-6}$, we obtain

$$T_R \sim 1.3 \times 10^{13} \text{ GeV}. \quad (167)$$

Another possibility is that the inflaton decay into two heavy right-handed neutrinos, whose rate $\Gamma_{\chi \rightarrow \nu_R \nu_R}$ is proportional to $h_{\nu_R}^2 m_\chi$. For not too small $\lambda_{\phi_H\chi}$, this process is suppressed compared to the two-Higgs decay: it would yield a lower reheating temperature, and thus we consider this process as a sub-dominant one.

CONCLUSIONS. We analysed a possible minimal extension of the SM, adding a $U(1)$ global gauge symmetry, related to the conservation of the $B - L$ quantum number, with an additional gauge boson, three right-handed neutrinos and a new scalar singlet, responsible of the symmetry breaking at a scale not far from the inflationary one.

In principle, this model, already proposed some years ago, could account for the masses of the low-energy neutrinos through the minimal type I see-saw mechanism and act as a reasonable framework for an inflationary scenario, in which the real part of the additional scalar (also known as “majoron”⁸ in literature [176]) plays the role of the inflaton.

Here, we tried to address a simple combined analysis of the viable parameter space taking into account both the stability of the SM electroweak vacuum in the extended

⁷ For any details on this formulae see any introductory cosmology textbook, e.g. [122].

⁸ Actually, the “majoron” term was attached to the Goldstone boson related to the $U(1)_{B-L}$ symmetry breaking. It is common, however, to find this name in relation to the real part of the scalar singlet.

model and the inflationary constraints coming from every possible configuration with the fields at our disposal and the values which the couplings can acquire.

Inflation, now compatible with a single-field realisation, turns out to predict inflationary observables within the current experimental bounds in the “hilltop” configuration, in which the field starts rolling down from values lower than its vacuum expectation value, which reaches super-Planckian values, in relation to which, radiative corrections can be safely neglected. In the window $v' \sim 20M_P - 30M_P$, with a scalar self-coupling of order $\lambda_\chi \sim 10^{-17} - 10^{-14}$ we can have a suitable inflationary expansion, which lasts enough to solve the early-cosmology problems and reproduces the correct amount of primordial scalar perturbations.

Unfortunately, while adopting a value for the portal coupling which takes into account the constraint $\lambda_{\phi_H\chi} \ll 10^{-18}$, coming from the highest value reachable by the Higgs field during inflation, safely lower than the instability scale Λ_I , for the central values of the strong coupling and the top and the Higgs masses, the SM potential can not be stabilised through a threshold mechanism as long as the mass scale of the heavy scalar singlet appears beyond Λ_I .

A lower m_t than its central value seems necessary, in order to push the instability scale towards higher values and make the stabilisation possible. Remaining above the m_t^c which ensures absolute stability [see Chap. 3], we can rely only on an extremely narrow window.

Due to the narrowness of the feasible parameter space, a very accurate numerical analysis of stability and running of the couplings is required, taking into account every source of uncertainty, which could in principle spoil the scenario. We then conclude that a minimal extension, like the one treated in this chapter, seems not completely satisfying in describing a reasonable inflationary phase, compatible with the stability requirements of the electroweak vacuum.

This conclusion is common to any other model in which the radiative corrections do not interfere with the shape of the inflationary potential (like in our viable branch $v' > M_P$ and $\chi < v'$). Instead, if the sub-Planckian regime $v < M_P$, in which the radiative corrections are responsible of the symmetry breaking, had provided good inflationary predictions, stabilisation would have been possible, due to the coupling of the inflaton with the fermions (right-handed neutrinos) and the new gauge field. Unluckily, this scheme overproduces primordial gravitational waves, and, more subtly, is exposed to the risk of an instability on the inflaton direction, because of the dependence of the potential on λ_χ . Our results are in agreement with the related literature, *e.g.* [7] and [6, 5], net of final certain considerations connected to the experimental state of the art at the time these works were written *i.e.* BICEP2 claim [135].

The model may also provide a possible dark matter candidate and act as a good backdrop for a leptogenesis scheme. For the former, there exists some suggestions in which the $B - L$ scalar singlet could be seen as a viable dark matter candidate [177], giving some signatures in the CMB temperature power spectrum [178] and acceptable decaying schemes for adequate mass ranges [179], *e.g.* considering, for the low values of h_{ν_R} and $\lambda_{\phi_H\chi}$, freeze-in [180].

As concerns leptogenesis, the presence of right-handed neutrinos, directly coupled with the inflaton, could be a good starting point in building feasible scenarios [181]. We do not deal with these two possibilities here.

Starting from this minimal set up, it may be interesting a further investigation of the connection between inflation and neutrino masses, seeing for instance the dependence of the Majorana Yukawa coupling on the vacuum expectation value of the inflaton, for a given Dirac coupling. Furthermore, it can be possible to extend the analysis done in the last section of [12] in this new scenario: from the requirement of electroweak stability after the inclusion of the see-saw, to what extent the upper bound on the right-handed neutrino mass m_{ν_R} , as a function of the top quark mass, can be influenced by the presence of an extra scalar singlet? Moreover, it could be left as a future investigation the estimation of the m_{ν_R} required to retrieve the inflection point configuration studied in the pure SM scenario in Chap. 4, now in presence of the heavy singlet scalar, generalising the analysis done in [12]. As a last idea for a further development, the non-minimal coupling between both the scalars and gravity can be embedded in the $U(1)_{B-L}$ scenario, in order to perform a full numerical analysis for stability and inflation [see, for instance [162]].

The first minimal extension to the SM we look over is the well-known Higgs inflation model, initially proposed by Bezrukov and Shaposhnikov some years ago [20]: it is based on considering a non-minimal coupling ξ between the Higgs field, again playing the role of inflaton, and gravity. This coupling should be required in a complete renormalisable model and can make the Higgs potential suitable for an inflationary phase. The model, in its tree-level version, is briefly presented in Sec. 6.1.

This model, along with Starobinsky inflation¹ [182, 183], is one of the most attractive either on the motivation side, seen that it does not involve any physics beyond the SM, either on the phenomenological side, because of its standard predictions for the CMB inflationary parameters, well within the latest experimental bounds. We will review, at the end of Sec. 6.3, the main differences and similarities between the model in exam and Starobinsky inflation, including the theoretical reasons driving their degeneracy in the predictions.

The value of ξ required for reproducing the amplitude of scalar perturbations in the original model turns out to be very large, and have some problematic implications for the unitarity of the theory. We will reappraise this issue in Sec. 6.4.

In order to consider a lower value for ξ , we will analyse some critical configurations of the effective potential, in order to probe the viability of the inflationary phase and its dependence on the renormalisation scale.

First, we are going to consider quantum corrections, starting from the RGE in the extended case [see Sec. 6.2.1 and App. A.4] and then we will obtain the effective poten-

¹ The Starobinsky model relies basically on a modification of gravity, in which it is considered the quadratic term of the scalar curvature in the perturbation expansion:

$$S = \int d^4x \sqrt{-g} \left(\frac{M_P^2}{2} R + c_1 R^2 \right), \quad (168)$$

where c_1 is the Wilson coefficient related to the mass of the hidden scalar, sometimes called “scalaron” (which can be made manifest in the so-called linear representation), through the relation $c_1 = 1/(6M^2)$. In order to reproduce the correct value for Δ_{ζ} , it should be $c_1 \sim 10^9$ (equivalent to $M \sim 10^5$). Going to the Einstein frame, one can get the scalar field version of the model. The theory leads to inflation with the following scalar index and tensor-to-scalar ratio:

$$n_s - 1 \approx -\frac{2}{N}, \quad r \approx \frac{12}{N^2}. \quad (169)$$

The additional $1/N$ suppression on r helps to produce a tiny amount of primordial gravitational waves.

tial [see Sec. 6.2.2]. After that we will study its dependence on the α parameter, at each loop order.

In Sec. 6.2.2 we will outline the issue related to the renormalisation prescription, *i.e.* the procedure of quantisation of the effective action, deciding in which frame (the Jordan or the Einstein one, in which the field is respectively non-minimally and minimally coupled to gravity, related via a conformal transformation with each other) should be done. We will try to solve the question in a non-ambiguous analytical way, showing the underlying equivalence of the two approaches.

Following the literature, putting an upper bound for the height of the potential in relation to the experimental upper bound on the tensor-to-scalar ratio, we can rule out some values for ξ . At the same time, we are going to provide the inflationary predictions for the model, including all the quantum corrections, confirming the robustness of the tree-level results. This analysis will be carried out in Sec. 6.3.

6.1 NON-MINIMAL COUPLING

We consider a model with a non-minimal gravitational coupling ξ between the SM Higgs doublet \mathcal{H} and the scalar curvature R [20]². In general, ξ is a free parameter of the model: no direct measurements so far have been provided and the discovery of the Higgs boson, as the expected last SM particle, implies only a very weak upper bound $\xi < 2.6 \times 10^{15}$ [185]. There exists one preferred value $\xi = -1/6$, related to conformal invariance, but, so far, no hints connected to conformal symmetry as a symmetry of Nature were revealed. The general action is given by:

$$\mathcal{S} = \int d^4x \sqrt{-g} \left[\mathcal{L}_{SM} - \frac{M_P^2}{2} R - \xi \mathcal{H}^\dagger \mathcal{H} R \right], \quad (170)$$

where \mathcal{L}_{SM} is the full Standard Model Lagrangian (5).

The relevant part of the action (170), from a cosmological point of view, is:

$$\mathcal{S}_J = \int d^4x \sqrt{-g} \left[(\partial_\mu \mathcal{H})^\dagger (\partial^\mu \mathcal{H}) - \frac{M_P^2}{2} R - \xi \mathcal{H}^\dagger \mathcal{H} R - V \right], \quad (171)$$

where $V = \frac{\lambda}{6} (\mathcal{H}^\dagger \mathcal{H} - v^2/2)^2$ is the SM potential (17b) and the subscript J means that the action is evaluated in the frame where physical distances are measured and the inflationary model is defined, called *Jordan frame*.

In order to remove the non-minimal coupling, we introduce a conformal (Weyl) transformation:

$$g_{\mu\nu} \rightarrow \tilde{g}_{\mu\nu} = \Omega^2 g_{\mu\nu}, \quad \text{with } \Omega^2 \equiv 1 + 2\xi \frac{\mathcal{H}^\dagger \mathcal{H}}{M_P^2}. \quad (172)$$

The resulting action is:

$$\begin{aligned} \mathcal{S}_E = & \int d^4x \sqrt{-\tilde{g}} \left[\frac{1}{\Omega^2} (\partial_\mu \mathcal{H})^\dagger (\partial^\mu \mathcal{H}) - \frac{M_P^2}{2} \tilde{R} \right. \\ & \left. + \frac{3\xi^2}{\Omega^4 M_P^2} \partial_\mu (\mathcal{H}^\dagger \mathcal{H}) \partial^\mu (\mathcal{H}^\dagger \mathcal{H}) - \frac{V}{\Omega^4} \right], \end{aligned} \quad (173)$$

² A term like this is required by the renormalisation properties of the scalar field in a curved space-time background [184].

where \tilde{R} is calculated from the metric \tilde{g} and the subscript E denotes that now we are in the Weyl-transformed frame, called *Einstein frame*.

If we consider the unitary gauge, like the original choice made in (19), in which the only scalar field is the radial mode ϕ_H

$$\mathcal{H} = \frac{1}{\sqrt{2}} \begin{pmatrix} 0 \\ \phi_H \end{pmatrix}, \quad (174)$$

we can simplify the (173) in the following way:

$$S_E = \int d^4x \sqrt{-\tilde{g}} \left[-\frac{M_P^2}{2} \tilde{R} + \frac{K}{2} \partial_\mu \phi_H \partial^\mu \phi_H - \frac{V}{\Omega^4} \right], \quad (175)$$

where

$$K \equiv (\Omega^2 + 6\xi^2 \bar{\phi}_H^2) / \Omega^4, \quad V = \frac{\lambda(\mu)}{24} (\phi_H^2 - v^2)^2, \quad \Omega^2 = 1 + \xi \bar{\phi}_H^2. \quad (176)$$

The bar over the fields indicates, from now on, that they are defined in Planck units: $\bar{\phi}_H \equiv \frac{\phi_H}{M_P}$.

It is useful to get rid of the non-canonical kinetic term for the Higgs field in (175) by a redefinition of the fields: $\phi_H = \phi_H(\chi)$, where χ is a new scalar, which satisfy the following relation:

$$\frac{d\chi}{d\phi_H} \equiv \sqrt{\frac{\Omega^2 + 6\xi \bar{\phi}_H^2}{\Omega^4}}, \quad \phi_H(\chi = 0) = 0. \quad (177)$$

One can obtain also a closed analytical relation between the two fields:

$$\begin{aligned} \chi(\phi_H) &= M_P \sqrt{\frac{1+6\xi}{\xi}} \sinh^{-1} \left(\frac{\sqrt{\xi(1+6\xi)} \phi_H}{M_P} \right) \\ &\quad - \sqrt{6} M_P \tanh^{-1} \left(\frac{\sqrt{6\xi} \phi_H}{\sqrt{M_P^2 + \xi(1+6\xi)\phi_H^2}} \right). \end{aligned} \quad (178)$$

The final expression for the Einstein frame action is:

$$S_E = \int d^4x \sqrt{-\tilde{g}} \left[\frac{1}{2} \partial_\mu \chi \partial^\mu \chi - \frac{M_P^2}{2} \tilde{R} - u(\chi) \right], \quad (179)$$

where the potential is given by

$$u(\chi) \equiv \frac{V(\chi)}{\Omega(\chi)^4} = \frac{\lambda(\mu)}{24} \frac{(\phi_H(\chi)^2 - v^2)^2}{(1 + \xi \bar{\phi}_H(\chi)^2)^2}, \quad (180)$$

and the last equality holds only at tree level. We can notice that the potential is exponentially flat for large field values and can in principle provide a slow-roll inflationary phase, driven by the Higgs field itself.

6.2 ADDING QUANTUM CORRECTIONS

Now we turn on quantum corrections. This will take into account both the running of the couplings (now including also the running of the non-minimal coupling ξ , see in particular App. A.1 and A.4) and loop corrections to the effective potential.

6.2.1 RGE

In the small field regime the running of the couplings is described by the usual SM RGE, used in the analyses of the previous chapters. However, as we evaluate the field ϕ_H in the Einstein frame with a canonical gravity sector, we notice that the kinetic sector is non-canonical. On a spatial hypersurface, the canonical momentum of ϕ_H is

$$\pi_H \equiv \frac{\partial \mathcal{L}}{\partial \dot{\phi}_H} = \sqrt{-\tilde{g}}(\tilde{g}^{\mu\nu} n_\mu \partial_\nu \phi_H) \left(\frac{d\chi}{d\phi_H} \right)^2, \quad (181)$$

where n_μ is a time-like vector. So, imposing standard commutation relations for ϕ_H and the canonical momentum π_H , we obtain [186]:

$$[\phi_H(\vec{x}), \dot{\phi}_H(\vec{y})] = i\hbar s(\phi_H) \delta^{(3)}(\vec{x} - \vec{y}), \quad (182)$$

with

$$s(\phi_H) = \frac{1 + \xi \bar{\phi}_H^2}{1 + (1 + 6\xi)\xi \bar{\phi}_H^2}. \quad (183)$$

For small field values $\phi_H \ll M_P/\xi$, $s \simeq 1$, recovering the SM case, while in the inflationary regime $\phi_H \gg M_P/\xi$, we see a suppression in the commutator: then, quantum loops involving the Higgs field are heavily suppressed and hence the RG equations differ from those of the SM. For this reason, the prescription adopted is to introduce a $s(\phi_H)$ factor for each off-shell Higgs that runs in a quantum loop in the RG equations³ [188, 189] [see App. A.4 for more details].

6.2.2 Effective potential

Following the approach adopted in Sec. 2.1.3, the total RG-improved effective potential is given by

$$\mathcal{U}_{\text{eff}} = \mathcal{U}_0 + \mathcal{U}_1 + \mathcal{U}_2 + \dots, \quad (184)$$

where $\mathcal{U}_0, \mathcal{U}_1, \mathcal{U}_2$ are the tree-, one-loop and two-loop contributions, respectively, with the running of all the couplings involved, evaluated at some renormalisation scale μ , conveniently chosen in order to minimise the effect of the logarithms, as done in the pure SM case.

The tree-level RGE-improved SM potential in the Einstein frame in the large field regime⁴ is:

$$\mathcal{U}_0(\phi_H) = \frac{\lambda(\mu)}{24} \frac{e^{4\Gamma(\mu)} \bar{\phi}_H^4}{\Omega^4}, \quad \text{where } \Omega^2 = 1 + \xi e^{2\Gamma(\mu)} \bar{\phi}_H^2. \quad (185)$$

Renormalisation prescriptions

There exist two inequivalent options for the quantisation of the classical theory and, for this reason, the effective potential can not be defined unambiguously [190].

³ This is not the only method of dealing with this effect: another one [187] is to view the effect as a suppression of the effective Higgs coupling to other SM fields and, for large ξ , neglect the physical Higgs field in the region $\phi_H \gtrsim M_P/\xi$. The resulting theory with a frozen radial Higgs mode, known as chiral electroweak theory, gives slightly different results.

⁴ The v^2 -term in the potential does not play any role during inflation and can be safely neglected.

One can compute quantum corrections to the potential *after* the transformation (172), in the Einstein frame (prescription I) [20, 187] or *before*, directly in the Jordan frame and then go to the Einstein one (prescription II) [191]. Even if the two frames are related through an harmless conformal transformation, it is not universally accepted that they describe the same physics. Furthermore, without a satisfying UV completion of the theory at the Planck scale, in principle it is not clear which prescription should be used [192]: the first has been connected to a possible quantum scale invariance in an interesting hierarchy problem solution [193, 194, 195, 196]; the second is thought to be preferable simply because the Jordan frame is the “natural” one, free of possible trouble sources originated by the conformal transformation [191].

Nevertheless, for sufficiently large λ_{eff} , in a large ξ scenario, the choice of renormalisation prescription should be irrelevant from a practical point of view, as stated in [190, 3].

The equivalence of the two frames was made explicit in a certain number of works, e.g. considering, in the action, only dimensionless quantities, invariant under conformal transformation [197], or works essentially based on case-by-case checks, involving the curvature perturbation during inflation [198], or the on-shell effective action [199]. Unfortunately, the issue is not completely clarified, leaving the choice of the renormalisation scale still confusing.

We try here to review a careful step-by-step calculation, in order to show that no ambiguities should arise when the two frames are considered, reaching the same conclusions of [197, 200]. In addition, we remark that the recent findings on how to deal with the one- and two-loop corrections to the effective potential mentioned before [see again Sec. 2.1.3] imply that the two prescriptions are *de facto* equivalent [8].

We assume that we stop at the first loop order in quantum perturbations and that we want to end up always in the Einstein frame, for simplicity, regardless the prescription used.

PRESCRIPTION I. We go in the Einstein frame and then we turn on the quantum corrections to the potential \mathcal{U} :

$$V_0 \rightarrow \mathcal{U}_0 \quad \text{then} \quad \mathcal{U}_{\text{eff}}^{(\text{I})} = \mathcal{U}_0 + \mathcal{U}_1 = \frac{V_0}{\Omega^4} + \mathcal{U}_1, \quad (186)$$

where the one-loop correction induced by the SM fields takes the usual Coleman-Weinberg form

$$\begin{aligned} \mathcal{U}_1(\chi) = & \frac{1}{(4\pi)^2} \left[\frac{3m_W^4}{2} \left(\ln \frac{m_W^2}{\mu^2} - \frac{5}{6} \right) + \frac{3m_Z^4}{4} \left(\ln \frac{m_Z^2}{\mu^2} - \frac{5}{6} \right) - 3m_t^4 \left(\ln \frac{m_t^2}{\mu^2} - \frac{3}{2} \right) \right. \\ & \left. + \frac{m_H^4}{4} \left(\ln \frac{m_H^2}{\mu^2} - \frac{3}{2} \right) + \frac{3m_\sigma^4}{4} \left(\ln \frac{m_\sigma^2}{\mu^2} - \frac{3}{2} \right) \right]. \end{aligned} \quad (187)$$

The particle content is computed expanding the Higgs doublet (including the Nambu-Goldstone bosons σ) in the full expression for the tree-level potential to quadratic order in the fields, giving, in Landau gauge [201]:

$$\begin{aligned} m_W^2 = & \frac{g^2 e^{2\Gamma(\mu)} \bar{\Phi}_H^2}{4\Omega^2}, \quad m_Z^2 = \frac{(g^2 + g'^2) e^{2\Gamma(\mu)} \bar{\Phi}_H^2}{4\Omega^2}, \quad m_t^2 = \frac{h_t^2 e^{2\Gamma(\mu)} \bar{\Phi}_H^2}{2\Omega^2}, \\ m_H^2 = & \frac{s(\Phi_H) \lambda e^{2\Gamma(\mu)} \bar{\Phi}_H^2}{2\Omega^4} \left(\frac{1 - \xi \bar{\Phi}_H^2}{1 + \xi \bar{\Phi}_H^2} \right), \quad m_\sigma^2 = \frac{\lambda e^{2\Gamma(\mu)} \bar{\Phi}_H^2}{6\Omega^4}. \end{aligned} \quad (188)$$

So, in general, all the mass scales (including the Planck mass, cutoff scale and renormalisation scale) are rescaled by a Ω factor:

$$m_J \rightarrow m_E = \frac{m_J}{\Omega}, \quad (189)$$

Besides the conformal factor at the denominator, using the asymptotically flat tree-level potential to determine the particle masses, rather than the Jordan-frame potential, leads also to the appearance of additional factors in the physical Higgs and Nambu-Goldstone boson masses, responsible of a suppression of these two contributions (with respect to the W , Z and t ones) to the effective potential during inflation. This is in agreement with the reasons exposed in Sec. 2.1.3 in the treatment of the RG-improved effective potential [86].

The two-loop radiative correction \mathcal{U}_2 can be found in the same way, operating on the explicit form given in App. C.

PRESCRIPTION II. We add the Coleman-Weinberg correction to the Jordan-frame potential and then go in the Einstein frame:

$$V_0 + V_1 \rightarrow \mathcal{U}_{\text{eff}}^{(\text{II})} = \frac{V_0}{\Omega^4} + \frac{V_1}{\Omega^4}. \quad (190)$$

Following one of the two paths, will lead, in principle, to different results: this is because degrees of freedom that are fixed in one frame become dynamical in the other and *viceversa*.

Looking at (187) and focussing on the top quark term, for instance, we notice that the logarithm will be minimised for $\mu_E = m_{t,E}$. This is the renormalisation choice for prescription I: in the Higgs inflation scenario this is translated in the usual approach according to which the renormalisation scale is chosen to be exactly the typical energy scale involved in the process, *i.e* the field value.

In the prescription II approach, the condition for the minimisation of the logarithms is $\mu_J = m_{t,J}$. Expressing it in Planck units and using (189), we obtain

$$\frac{\mu_J}{M_{P,J}} = \frac{m_{t,J}}{M_{P,J}} = \frac{\Omega m_{t,E}}{\Omega M_{P,E}} = \frac{\mu_E}{M_{P,E}}, \quad (191)$$

hence, it is the same prescription as in the Einstein frame: there is no ambiguity in the choice of the renormalisation scale, which is correctly given by prescription I. Even the expression of the potential turns out to be the same: the conformal factors arising from the Jordan-frame masses in the Coleman-Weinberg piece compensate the ones in the denominators of the Einstein frame expression, so $\mathcal{U}^{(\text{II})} = \mathcal{U}^{(\text{I})}$.

We will use, coherently with the choice (45):

$$\boxed{\mu(t) = \frac{\alpha \phi_H(t)}{\Omega(\phi_H(t), \xi)}}. \quad (192)$$

Dependence on α

As showed for the pure SM case in Sec. 3.2.2 and in Sec. 4.2, also in this case, when we include all the loops corrections, there is independence of the effective potential on

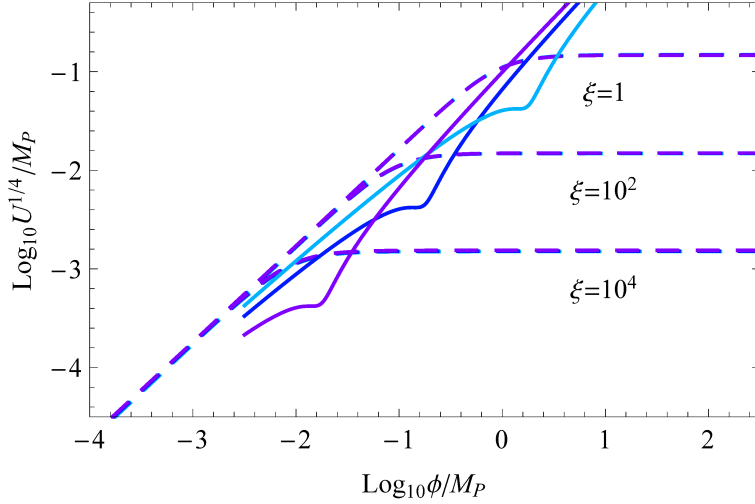


Figure 27: Dependence of the tree-level potential \mathcal{U} on the renormalisation scale through the α parameter. With the light blue, blue and purple lines are represented the shapes of the effective potential at the inflection point for $\alpha = 0.3$, $\alpha = 1$ and $\alpha = 10$, respectively. Fixing the non-minimal coupling to the reference values $\xi = 1$ (minimally coupled scenario), $\xi = 10^2$ and $\xi = 10^4$, we can notice the emergence of the plateau for high field values, one for each α value: the lines are pretty much indistinguishable.

the α parameter. Again, two loops are enough to enlight this behaviour and to make the errors on the predictions small: we can rely on the effective potential expansion, providing a description which is robust enough.

To this extent it is useful to look at the variation with α of the RG-improved effective potential for particular values of m_t and ξ (central for m_H and α_s) for each loop order.

In Fig. 27 we display the scale dependence of the tree-level Einstein frame potential \mathcal{U} , for three particular values of the non-minimal coupling: $\xi = 1$, $\xi = 10^2$ and $\xi = 10^4$. As done before, for clarity, we put ourselves in a stationary configuration, *i.e.* the inflection point configuration, tuning adequately the top mass: for comparison, together with the potentials in the non-minimally coupled scenario, also the pure SM curves are displayed, one for each reference value for α : $\alpha = 0.3$ (light blue), $\alpha = 1$ (blue) and $\alpha = 10$ (purple). We can easily notice that the curves related to the different values of α are practically indistinguishable.

Going further with the loop corrections, we display in Fig. 28 the same configuration for the one-loop (first row, long-dashed curves) and two-loop (second row, short-dashed curves) effective potential. With the solid lines are described the tree-level results. The plot columns are obtained for $\xi = 1$, $\xi = 100$ and $\xi = 1000$, respectively. It is now more evident that as long as we increase the loop order, the less is the dependence on the renormalisation choice, confirming what inferred in Sec. 3.2.2 and in

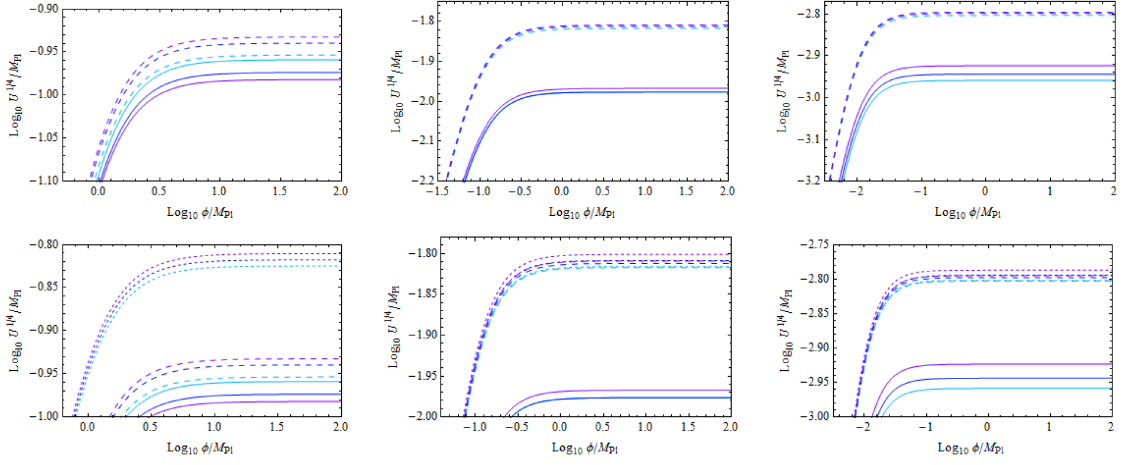


Figure 28: Dependence of the effective potential, up to the two-loop radiative corrections, on the α parameter at the inflection point configuration. In the first row are showed the one-loop results (long-dashed curves), while in the second row the two-loop ones (short-dashed curves). The first column is obtained for $\xi = 1$, the second for $\xi = 100$ and the third for $\xi = 1000$. The solid lines represent the tree-level results. The higher the loop order considered, the less the dependence on the renormalisation scale, almost regardless the non-minimal coupling value.

Sec. 4.2. The result seems to be insensitive to the particular value of the non-minimal coupling chosen.

6.3 NUMERICAL ANALYSIS: INFLATIONARY OBSERVABLES

For the same values of m_t , α_s and m_H , we now vary ξ in order to have a better understanding of the magnitude of \mathcal{U} , working at two loop in the effective potential, trying to bear in mind a reasonable order of magnitude for the inflationary energy scale.

In Fig. 29, we show the height of the potential in relation of the three reference values of ξ considered before, for fixed values of m_t (tuned to ensure stability), α_s and m_H . With the thick red line we represent the upper bound on \mathcal{U} , coming from the current experimental bound on the tensor-to-scalar ratio, $r < 0.08$ [see (122)]. Inflation would take place at the “knee” of the curves, so that small values of ξ , say below 10^2 , seem to be not allowed for the considered values of m_t , α_s and m_H .

In order to have a more detailed picture of the situation, we have to scan also over m_t , α_s and m_H . This is done in Fig. 30, taking, as an example, $\xi = 50$. Fixing $\alpha = 1$, we let vary m_t , α_s and m_H in their experimental ranges (pink, green and blue curves, respectively, among which the long-(short)-dashed ones stand for the highest (lowest) value allowed), bearing in mind that we are still using a lower mass for the

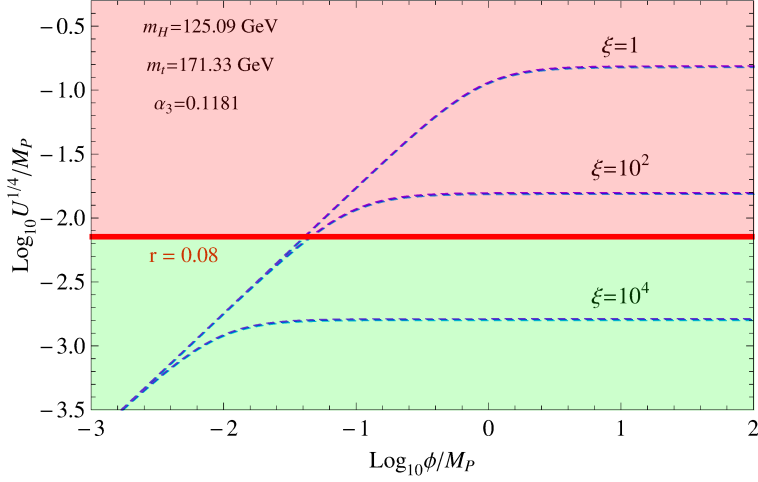


Figure 29: Ensuring stability with a low-valued top quark mass (sticking with the current central experimental values for the Higgs mass and the strong coupling constant), we try to put a weak constraint on the non-minimal coupling in relation to the tensor-to-scalar ratio, dependent in turn on the height of the potential at the inflationary scale. We display with the thick red line the current upper bound on \mathcal{U} , coming, via Eq. (127), from the current limit on the detection of r , already mentioned in (122): within our NNLO analysis, we see that a low value for ξ , namely $\xi \lesssim 10^2$, seems not suitable to explain the current lack of experimental detection of the primordial tensor background.

top quark with respect to its central value: the tuned value used here is, in particular, $m_t = 171.16$ GeV. Our feeling is confirmed here: the knees of the curves, where inflation should take place, are all above the upper limit imposed by the experimental searches of the tensor modes, getting the low- ξ scenario (here represented by a ~ 10 non-minimal coupling) into trouble. The interesting feature developed for the $m_t + \Delta m_t$ curve disappears soon as we vary a little bit the parameters in the game: a proper numerical analysis for such a fine-tuned configuration seems not so reliable to us.

PARTIAL CONCLUSIONS. Summarising, although the plateau position does change a lot, small values of ξ seem to be not allowed, because they would give, assuming to reproduce the correct amount of density perturbations, too large values for r , sticking with the current experimental state of the art.

Models with large values for r , reacting to the detection, later disproved, of a B-mode polarisation signal by the BICEP2 collaboration [135], were proposed, in order to take into account small values for ξ [202] (the motivations for such an investigation will be clear later): we did not manage to find a viable parameter window to match the critical configuration analysed therein. These results are in agreement with the detailed work [8], appeared during the carrying out of this analysis, which is focussed on the analysis of inflation along potential shapes which deviates from plateau.

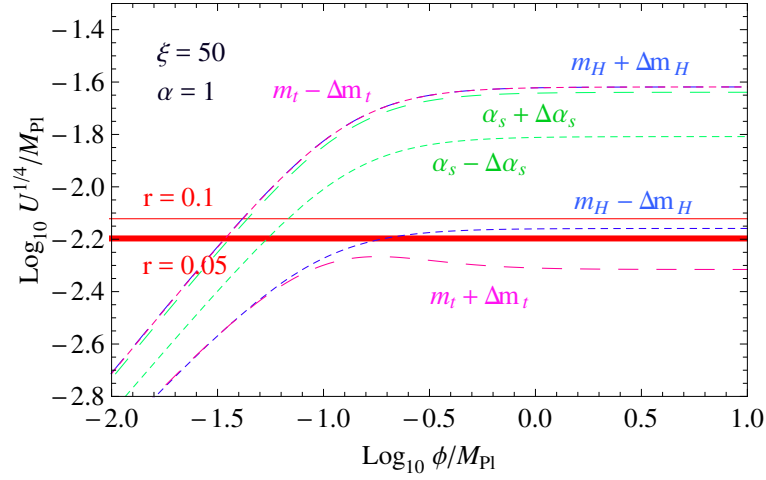


Figure 30: For a fixed $\xi = 50$ scenario and considering, for simplicity, $\alpha = 1$, we let vary m_t , m_H and α_s in their experimental ranges, referring to the updated numerical values used in Sec. 3.2.1: in this case, for the top mass, it was used a value which would have ensured stability, $m_t = 171.16$ GeV. Note that in this figure it was not imposed the constraint coming from the experimental value of the amplitude of scalar perturbations. In red are displayed two particular upper bounds for the potential, related to two peculiar values for r : $r = 0.1$ and $r = 0.05$, reading from top to bottom. In pink we show the variation on m_t , in blue the variation on m_H and in green the variation on α_s . Also in this case, we notice that a value for ξ of order $\xi \sim 10$ would not be allowed, giving rise to a too large amount of primordial gravitational waves. An intriguing feature in the potential is developed in correspondence of the highest edge of our parameter window for m_t : maybe this critical configuration might rely on a low- ξ scenario, reproducing the correct amount of scalar perturbations, but the room of variation of the parameters turned out to be too narrow to carry out a proper numerical analysis.

Now we turn to the explicit derivation of the inflationary observables for the model in exam, wondering if the value for r would be affordable for the near-future CMB experiments (both from the space and the ground): is the (near-future) detection of a sizable tensor-to-scalar ratio a direct motivation for the death of the non-minimally coupled Higgs inflation model?

A tree-level analysis in the slow-roll approximation can be performed for the field χ and the potential $\mathcal{U}(\chi)$. We recall that the slow-roll parameters are defined as in (108), (109) and (110):

$$\epsilon \equiv \frac{M_{\text{p}}^2}{2} \left(\frac{d\mathcal{U}/d\chi}{\mathcal{U}} \right)^2, \quad (193)$$

$$\eta \equiv M_{\text{p}}^2 \left(\frac{d^2\mathcal{U}/d\chi^2}{\mathcal{U}} \right), \quad (194)$$

$$\zeta \equiv M_{\text{p}}^4 \left(\frac{1}{\mathcal{U}^2} \frac{d^3\mathcal{U}}{d\chi^3} \frac{d\mathcal{U}}{d\chi} \right). \quad (195)$$

In the limit $\bar{\phi}_{\text{H}}^2 \gtrsim 1/\xi$, $\xi \gg 1$, they are given by⁵:

$$\epsilon \simeq \frac{4}{3\xi^2\bar{\phi}_{\text{H}}^4} \quad (196)$$

$$\eta \simeq \frac{4}{3\xi^2\bar{\phi}_{\text{H}}^4} (1 - \xi\bar{\phi}_{\text{H}}^2) \quad (197)$$

$$\zeta \simeq \frac{16}{9\xi^3\bar{\phi}_{\text{H}}^6} (\xi\bar{\phi}_{\text{H}}^2 - 3). \quad (198)$$

Slow-roll ends when $\epsilon \simeq 1$ or $|\eta| \simeq 1$, and this occurs, seen (196), at a field value

$$\bar{\phi}_{\text{H, end}} \simeq (4/3)^{1/4}/\sqrt{\xi}. \quad (199)$$

The time duration of the inflationary phase is represented by the number of e-folds (91), given by [204]:

$$N = \int_{\bar{\phi}_{\text{H, end}}}^{\bar{\phi}_{\text{H},*}} \frac{d\bar{\phi}_{\text{H}}}{M_{\text{p}}^2} \frac{\mathcal{U}}{d\mathcal{U}/d\bar{\phi}_{\text{H}}} \left(\frac{d\chi}{d\bar{\phi}_{\text{H}}} \right)^2 \simeq \frac{3}{4} \left[\frac{\bar{\phi}_{\text{H},*}^2 - \bar{\phi}_{\text{H, end}}^2}{M_{\text{p}}^2/\xi} + \ln \left(\frac{1 + \xi\bar{\phi}_{\text{H, end}}^2}{1 + \xi\bar{\phi}_{\text{H},*}^2} \right) \right]. \quad (200)$$

The number of e-folds is fixed independently by the post-inflationary phase of the universe, *i.e.* a matter dominated epoch. The radiation dominated epoch starts at an effective temperature $3.4 \times 10^{13} \text{ GeV} < T_{\text{r}} < 1.1 \times 10^{14} \text{ GeV}$. N is given by [204]:

$$\begin{aligned} N &= 62 - \ln \frac{k}{a_0 H_0} - \ln \frac{10^{16} \text{ GeV}}{\mathcal{U}^{1/4}(\chi_0)} - \ln \frac{\mathcal{U}^{1/4}(\chi_0)}{\mathcal{U}^{1/4}(\chi_{\text{end}})} - \frac{1}{3} \ln \frac{\mathcal{U}^{1/4}(\chi_{\text{end}})}{\rho^{1/4}(T_{\text{max}})} \\ &\simeq 60.4 - \ln \frac{k}{a_0 H_0} - \frac{1}{6} \ln \frac{\chi_{\text{cr}}}{\chi_{\text{r}}}, \end{aligned} \quad (201)$$

where $\rho(T_{\text{max}})$ is the energy density at the beginning of the hot stage, $\chi_{\text{cr}} = \sqrt{2/3}M_{\text{p}}/\xi$ is the critical stage at which the reheating phase ends (here the potential is essentially quadratic) and, for $\chi < \chi_{\text{cr}}$ the radiation-dominated epoch starts. At $3.7(\lambda/0.25)^{1/2}\chi_{\text{cr}} < \chi_{\text{r}} < 40(\lambda/0.25)\chi_{\text{cr}}$ the matter-radiation transition happens. Considering also the spatial curvature $k \simeq 0$, it is found $N \simeq 59$, from which we can say that

$$\bar{\phi}_{\text{H},*} \simeq 9.14/\sqrt{\xi}. \quad (202)$$

⁵ Exact expressions can be found, for instance, in [203].

It is worth-mentioning that the the value of $\phi_{H,\text{end}}$ turns out to be quite insensitive to the particular value of ϵ or η when they approach 1.

The perturbation modes of pivot scale $k_* = 0.002/\text{Mpc}$ left the horizon during inflation when the field value equals $\phi_{H,*}$. At this field value, the potential, in order to generate the correct amount of density perturbations, should satisfy the normalisation condition [133]:

$$\mathcal{U}/\epsilon = 24\pi^2 \Delta_{\mathcal{R}}^2 M_{\text{P}}^4 \simeq (0.0269 M_{\text{P}})^4. \quad (203)$$

This relation, along with the determination of the number of e-folds, fixes the required value of ξ at tree level, which turns out to be of order $\xi \sim \mathcal{O}(10^4)$.

The tree-level predictions for inflationary observables [124, 205] (spectral index n_s , tensor-to-scalar ratio r and the running of the spectral index $dn_s/d \ln k$) for this model, in function of the number of e-folds, are given by:

$$n_s \simeq 1 - \frac{2}{N}, \quad r \simeq 12 \left(1 + \frac{1}{6\xi}\right) \frac{1}{N^2}, \quad (204)$$

where large values of ξ , as already said, are required to match the amount of scalar perturbations. In this limit ($\xi \rightarrow \infty$) the predictions are quite the same of the Starobinsky model [see footnote 1 in this chapter]. Numerically, in the slow-roll approximation, we obtain:

$$n_s \approx 1 - 6\epsilon + 2\eta \simeq 0.967, \quad (205)$$

$$r \approx 16\epsilon \simeq 0.0031 \quad (206)$$

$$\frac{dn_s}{d \ln k} \approx 24\epsilon^2 - 16\epsilon\eta + 2\zeta^2 \simeq 5.4 \times 10^{-4}, \quad (207)$$

where the slow-roll parameters are evaluated at $\phi_{H,*}$. These values are well within the 1σ border of the allowed region of inflationary parameter space, provided by the most up-to-date analyses [134, 136].

Going beyond the tree-level analysis, the procedure adopted for the numerical calculation of the inflationary observables consisted in solving the RGE, with the initial conditions given by the known matching procedure and then in the extrapolation of the physical quantities of interest from the improved effective potential. The first step is to choose a reasonable initial value for ξ and then adjust the top quark mass in order to have the right behaviour of the Higgs quartic coupling at the inflationary scale. Next, we evolve the couplings in the potential up to high energies via the RGE and, from $\mathcal{U}(\chi)$, for prescription I, we obtain the inflationary parameters at a field value corresponding to $N \simeq 60$ e-folds before the end of inflation. We repeated the steps for different initial values of ξ until the correct normalisation (203) was achieved. Finally, we computed the spectral index n_s , the tensor-to-scalar ratio r and the running of the spectral index $dn_s/d \ln k$.

The numbers obtained, displayed in the usual (n_s, r) plane in Fig. 31, are compatible with the tree-level results (205) and very stable with respect to quantum corrections, in agreement with all the existing literature. Furthermore, we verified that the predictions are quite insensitive to any variation of m_t . As we can notice from the figure, the Higgs inflation outcomes are well within the updated experimental constraints given by Planck and BICEP2/Keck Array collaborations: among the *plethora* of (minimal) inflationary models, together with Starobinsky, Higgs inflation provides the lowest

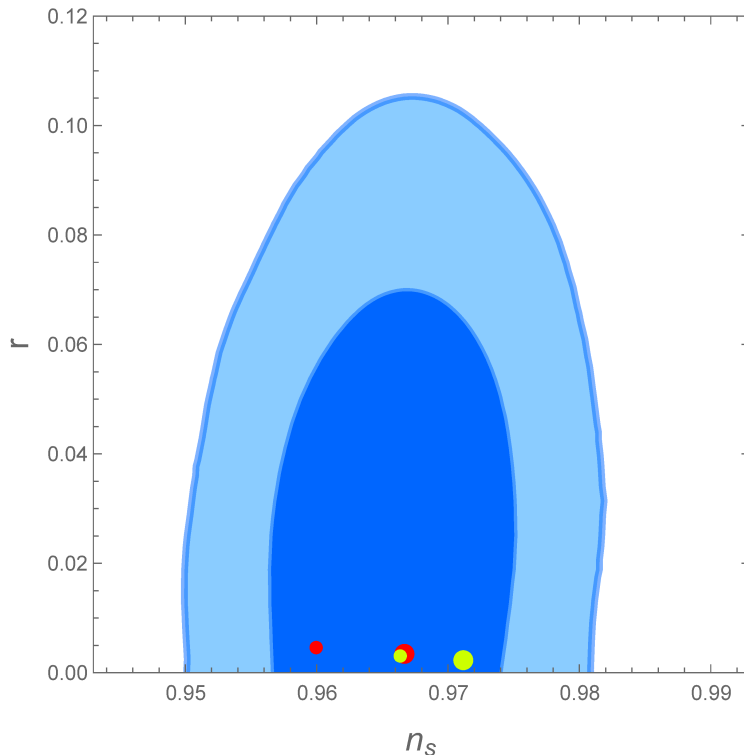


Figure 31: Predictions for inflationary observables (n_s, r): in red are displayed the standard tree-level outcomes for a Starobinsky model, while in yellow the Higgs ξ -inflation model, including quantum corrections. The small (large) point represents the result for $N = 50$ ($N = 60$). In the background we display the 1σ and 2σ contours of the latest constraints put by the joint analysis of the Planck and BICEP2/Keck Array collaborations [134].

values allowed for r , hence a detection of tensor modes in the very next years, given the sensitivity expected for the upcoming CMB experiments, would rule out this approach, pushing the theory community to focus on less minimal constructions.

As briefly anticipated, Higgs inflation and the Starobinsky model are nearly degenerate in predictions: this could be explained investigating the fundamental nature of these two constructions.

The Higgs and Starobinsky models of inflation are attractive because, as we anticipated, are well within the SM physics and they do not need of any new physics extension.

The degeneracy in the inflationary predictions of these two models, which we noticed are in extraordinarily agreement so far with the latest experimental data, is probably due to both their intimate theoretical [206] and phenomenological [207] connection: along with the more general universal attractors models, they share the same nature,

which can be unveiled through some considerations about their large-field behaviour, resumable as a plateau-like configuration.

As we saw in Sec. 4.1.3, during inflation the kinetic terms (very different in our case) are sub-leading with respect to potentials and can be ignored in a first approximation. In this case, the scalar field in Higgs inflation could be treated just as an auxiliary field, which can be integrated out, giving rise to Starobinsky inflation. We can say that Higgs inflation is a sort of descendant of the Starobinsky model, behaving dynamically in exactly the same way during the inflationary phase: their predictions are slightly different, but such differences⁶ turn out to be not measurably in the next future and furthermore, the two models display different UV cutoffs, because of their dissimilar small-field behaviour. This last point could be interesting because of the unitarity issues related to the Higgs inflation model [for more details, see Sec. 6.4]: the cutoff in this model, dependent on the non-minimal coupling, seems to be lower than M_P , while in the Starobinsky theory it is simply the Planck scale, so that inflation can be safely trusted. The reason, again, resides in the role played by the kinetic energy.

For a nice analytical proof of the connection between the two models, see [206].

In a Higgs ξ -inflation scenario, it was pointed out that Starobinsky inflation could be induced by quantum effects related to the large non-minimal coupling: when quantum corrections are taken into account, a large coefficient for the R^2 term can be generated in early Universe. In this way, the problem of a possible metastable vacuum could be escaped, the Higgs field is not forced to have large initial values and the Starobinsky potential would be free of destabilisation sources [208].

6.4 UNITARITY

The non-renormalisable character of gravity could represent a serious issue in the formulation of a self-consistent inflationary model: when we consider a process computed at the lowest order in perturbation theory in the field theory under construction, we usually find an energy Λ at which the cross section of the process hits the unitarity bound [see Sec. 2.2.1]. This UV cutoff, at which the perturbation theory breaks down, inform us that the theory under analysis is not a fundamental theory, but an effective one, valid for momenta up to Λ . Then the fundamental Lagrangian has to be modified by adding all the possible higher-dimensional operators allowed by symmetry, suppressed by the scale Λ : if the coefficients of these operators are of order one, these can spoil the high-energy behavior of our inflationary potential. In this case the realisation of inflation is said to be “unnatural”, while if one finds some mechanism that keeps the undesired higher-dimensional operators effect smaller and negligible, then it is said that the phenomenon is “natural”.

Coming back to Higgs inflation, in the large non-minimal coupling regime, the above mentioned cutoff scale is of order of [209, 210]:

$$\Lambda_{\text{HI}} \sim \frac{M_P}{\xi} \sim 10^{14} \text{ GeV}, \quad (208)$$

⁶ The main phenomenological difference relies on the reheating process after inflation, which results in a 10^{-3} discrepancy in the spectral index and in a variation of one or two units of the e-fold number [207].

lower than M_P , where unitarity would be anyway expected to be lost, and comparable to the scale set by the height of the inflationary potential. This means that new physics, expected to contain new particles and new interactions that affect the potential in an uncontrollable way, should show up at relatively small energies in order to restore unitarity, statement in strong tension with current experimental searches⁷. Hence, introducing a large non-minimal coupling in order to burden the Higgs field also with the role of inflaton, lowers the unitarity cutoff to a value that, in principle, obstructs the predictivity of the model and undermines its self-consistency. In other words, seen that inflation takes place for field values $\phi_H \sim M_P/\sqrt{\xi} \gg M_P/\xi$, above the regime of validity of the theory, the inflationary predictions should depend in a sensitive way on the coefficients with which these operators appear [209, 188, 211, 210].

The dependence of the observables on the RG flow (and so, indirectly, on the higher-order operators) could be considered twofold: from an optimistic point of view, it helps, in principle, to remove the possible degeneracy in the predictions of all these single-field inflationary models, which provide a very tiny amount of primordial gravitational waves. Obviously, this dependence on the unknown UV physics deprives us of all the predictive power of the model under consideration.

A recent analysis [8] stated that the Higgs inflation predictions turn out to be robust in this sense: the threshold corrections induced by the new physics⁸ unavoidably modify the running of the couplings and consequently the shape of the inflationary potential, but the CMB parameters, due to a precise cancellation, remains almost unaffected.

Obviously, the issue could be simply addressed through a sensible reduction of the coupling ξ and hence pushing the scale of perturbative unitarity violation towards the inflationary scale [189]: however, we saw in Sec. 6.3 that, trying to keep a viable inflationary scenario, this configuration is extremely hard to achieve, even though one can consider very critical featured potential configurations.

Another approach, widely followed, is based on a revisited calculation of the cutoff scale: it is found that the domain of validity of the effective theory does depend on the background value of the scalar field ϕ_H and that the value (208) it is an upper bound at $\phi_H = 0$, becoming higher for larger background values of the scalar field [212]. The unitarity cutoff is then dependent on the field regime:

$$\Lambda_{\text{HI}} \sim \left\{ \frac{M_P}{\xi}, \phi_H, \frac{M_P}{\sqrt{\xi}} \right\}, \quad (210)$$

⁷ Another possibility relies on the idea that the model would be strongly interacting at Λ_{HI} , with no need of new degrees of freedom. However, the predictiveness of the model would be lost in any case.

⁸ In the work mentioned are considered also the higher-order operators that affect the effective potential at loop level, leaving the tree-level expression unaltered: this is achieved by adding only the operators that are really necessary for the consistency of the theory. At dimension six, are allowed only operators of the form

$$\mathcal{L} \supset \sum_i c_i \frac{m_H^2}{\Lambda_{\text{HI}}^2} \mathcal{O}_i^4, \quad (209)$$

where the c_i are the unknown Wilson coefficients and the sum is over all the dimension four operators invariant under the SM symmetries. These operators are relevant around the scale $\phi_H \sim M_P/\xi$ and hence they do not affect the tree-level potential, but only the running of the couplings. According to the authors, this choice is not critical to their results and other parametrisation could be used.

where, respectively, we have the value for the small, mid and large field regimes. The field dependence of the cutoff can be understood from integrating out heavy fields with a field-dependent mass. In particular, it is showed that the cutoff, during inflation, coincides with the Planck mass (in the Einstein frame), which is much higher than the Hubble rate at that stage, allowing a semi-classical treatment of the model.

We outlined here the very essential lines of the unitarity problem in Higgs inflation: the full treatment of this issue constitutes a field of research in itself and it is still much debated in literature. All the subtleties and recent developments go beyond the scope of our work.

CONCLUSIONS

At the current stage, the particular near-criticality configuration suggested by experimental data remains unexplained, but the belief that it might be trying to tell us something deep about Nature is perhaps stronger than before. The special nature of the Higgs potential and its stability seem a very good reason to investigate further, both from the experimental and the theoretical side, with particular interest in the determination of the top quark mass, the main parameter in the game, able to control how close we are to the edge.

In Chap. 3, we provided an updated calculation at NNLO of the experimental and theoretical uncertainties on m_t^c , the value of the top mass which ensures absolute stability of the electroweak vacuum. In addition to the uncertainty in the identification of the MC and pole top masses, our results lead us to conclude that the configuration with two degenerate vacua is at present compatible with the experimental data.

Our conclusions are in broad agreement with the previous analyses in literature, where, actually, a light preference in favour of metastability is verifiable. We stressed the technical reasons of the small discrepancies, related mainly to an underestimation of two uncertainties: from the experimental side, in the determination of $\alpha_s^{(5)}$ and from the theoretical one, in the identification of the MC and pole top masses. These two, together with a less conservative interpretation (with respect to ours) of the significance of the results, leaves us not so confident in strongly excluding stability.

It is clear that, in order to discriminate in a robust way between stability and metastability, it would be crucial to reduce the experimental uncertainties for both m_t and $\alpha_s^{(5)}$. A reduction of the theoretical error in the matching would also be welcome.

Throughout our analysis we assumed the SM to be valid all the way up to the Planck scale, albeit we are aware how the stability of the SM can be very sensitive to the higher-order corrections. Near the cutoff of the theory, large Planckian effects are possible, but without a satisfactory comprehension of the UV-completion of the theory there is no hope to evaluate them. The effects of these higher-order operators is dependent on the choice of the free couplings: it is not clear why and how gravitational physics should make the potential more unstable or vice versa. The theory, in addition, when predictions happen to depend on a number of parameters larger than the number of predictions themselves, ceases to be predictive. Furthermore, the use of an effective theory close to its cutoff might not be fully reliable. For these reasons, we choose to ignore the super-Planckian physics and make our studies in minimal frameworks.

In Chap. 4, after a brief introduction of the concept of primordial inflation, we tried to investigate the feasibility of an inflationary model, in which the expansion is driven by the only scalar known so far in Nature: the Higgs field. Being impossible to have inflation in the pure SM framework, we analysed the possibility of a featured SM potential at high energies, in which an inflection point configuration appears in relation to a particular value of the top mass m_t^i . In this way, being in the stability regime, the Higgs scalar could in principle roll down along the potential, passing through a very shallow false vacuum and ends its run in the electroweak minimum. A value for the

tensor-to-scalar ratio r close to 0.2, as claimed by BICEP2 in 2013, would have been compatible at about 2σ with a model based on a shallow false minimum. However, as we know, that detection was mainly related to interstellar dust, and thus, that reference value is now ruled out by observations. With the inclusion of all the theoretical errors and the slight changes in the central values of the input parameters, the present calculation supersedes the results obtained in literature, highlighting the lack of viability of this scenario, sticking with the current experimental state of the art. Thus, the shallow false minimum idea seems in trouble: in order to embed inflation in a SM-like framework, new physics beyond the SM has to be introduced.

The closeness to the stability line can be of course spoiled if we bear in mind that other contributions, besides the SM, are expected in order to explain, among the others, dark matter, dark energy, neutrino masses and the matter-antimatter asymmetry. If new physics beyond the SM appears below M_{P} , the running of λ could be heavily modified: the stability could be worsened, it could remain unaffected, or it can be cured.

Two minimal extension to the SM are then considered here in turn: first, a $U(1)$ extension of the SM gauge group, in order to take into account, together with inflation and stability, the small neutrino masses [see Chap. 6]; second, the very well-known path of a non-minimal coupling between the Higgs field and gravity [see Chap. 5].

The inclusion of new physics beyond SM appears mandatory also if the metastable scenario will be confirmed. The electroweak vacuum stability during (or after) inflation is threatened by the field fluctuations, and so, when the field reaches values above the instability scale, the Higgs evolves to the true minimum at high energy. The consequent evolution of the field should lead to observable effects like the appearance of bubbles or domain walls. For this reason it would be better, in the case of metastable vacuum, to think at some new physics beyond the SM able to stabilise the potential.

We tried to pursue this task, considering in Chap. 6, a possible minimal extension of the SM, adding a $U(1)$ global gauge symmetry, related to the conservation of the $B - L$ quantum number, with an additional gauge boson, three right-handed neutrinos and a new scalar singlet, responsible of the symmetry breaking at a scale not far from the inflationary one.

This is a type I see-saw example, which can be a good representation of the three possible scenarios listed before: the neutrino Yukawa couplings behave like $\sim m_{\nu_R} m_\nu / v^2$, so, with a heavy right-handed neutrino (of order $m_{\nu_R} \sim 10^{15}$ GeV) the effect is destabilising and stability is worsened. If m_{ν_R} is lower than the previous estimation, the Yukawas are too small to interfere with the running of λ and their presence turn out to be irrelevant. Embedding this framework in a larger theoretical background, *i.e.* the $U(1)_{B-L}$ gauge symmetry extension, the see-saw scenario could cure the Higgs potential instability, with the well-known threshold mechanism due to the heavy scalar, coupled to the SM Higgs through a portal coupling, with a non-zero vacuum expectation value, which breaks this larger global symmetry.

Along with this possible source of stabilisation, we wondered if the model could account as a reasonable framework for an inflationary scenario, in which the real part of the additional scalar plays the role of the inflaton. We addressed an analysis of the viable parameter space taking into account both the stability of the SM electroweak

vacuum in the extended model and the inflationary constraints coming from every possible configuration.

The single-field inflationary model we deal with predicts observables within the current experimental bounds in the configuration in which the field starts rolling down from values lower than its vacuum expectation value, which can reach super-Planckian values. In this case, radiative corrections can be safely neglected. In the window $v' \sim 20M_{\text{P}} - 30M_{\text{P}}$, with a scalar self-coupling of order $\lambda_{\chi} \sim 10^{-17} - 10^{-14}$ we can have a suitable inflationary expansion, which lasts enough to solve the early-cosmology problems and reproduces the correct amount of primordial scalar perturbations.

Unfortunately, for the central values of the strong coupling and the top and the Higgs masses, the SM potential can not be stabilised through a threshold mechanism as long as the mass scale of the heavy scalar singlet ($|m_{\chi}|^2 \sim 10^{25} \text{ GeV}^2$) appears beyond Λ_{I}^2 .

We tried to consider a lower value for m_t , in order to push the instability scale towards higher values and make the stabilisation possible. Remaining above the m_t^c which ensures absolute stability [see Chap. 3], we can rely only on an extremely narrow window, and so, a very accurate numerical analysis of stability and running of the couplings is required. Every source of minimal uncertainty could in principle spoil the whole scenario. We then conclude that a minimal extension like this seems not completely satisfying in describing a reasonable inflationary phase, compatible with the stability requirements of the electroweak vacuum. These results turn out to be compatible with the related literature.

Other stabilisation mechanisms in less minimal scenarios seem necessary to solve the issue.

As concerns the non-minimally coupled scenario of Chap. 5, after reviewing the model and all the latest developments related (above all renormalisation prescriptions and UV completion of the model), we focussed on the attempt to lower the ξ coupling value, in order to evade the intrinsic unitarity issues of the theory. We did it in the inflection point configuration, trying to put ourselves in very critical configurations. Summarising, although the plateau position does change a lot, small values of ξ seem to be not allowed, because they would give, assuming to reproduce the correct amount of density perturbations, too large values for r : we did not manage to find a viable parameter window to match the critical configuration analysed. This result is in agreement with the very recent literature on this subject. Lastly, we obtained the inflationary predictions and confirmed their already known robustness against radiative corrections.

A

FORMULÆ FOR THE RG RUNNING AT NNLO

A.1 THE SM GAUGE COUPLINGS β -FUNCTIONS FOR $n_f = 5$

We list here the expressions for the full β -functions for the SM gauge couplings up to three loops for five flavours: referring to the eq. (5) in [49], we consider $n_G = 5/2$, $n_t = 0$ and the rescaling of the definitions of the couplings according to the relation $\alpha_i = g_i^2/(4\pi)$, for $i = 1, 2, 3$. In particular, the following convention is adopted: $g_1 = \sqrt{5/3}g'$. For each coupling we write $dx/dt = \beta_x$, where $t = \ln(\mu/m_Z)$.

At one loop we have:

$$\begin{aligned}\beta_g^{(1)} &= -\frac{23}{6}g(t)^3, \\ \beta_{g'}^{(1)} &= \frac{103}{18}g'(t)^3, \\ \beta_{g_3}^{(1)} &= -\frac{23}{3}g_3(t)^3,\end{aligned}$$

At two loops we have:

$$\begin{aligned}\beta_g^{(2)} &= -\frac{7}{3}g(t)^5 + 10g(t)^3g_3(t)^2 + \frac{4}{3}g(t)^3g'(t)^2, \\ \beta_{g'}^{(2)} &= 4g(t)^2g'(t)^3 + \frac{110}{9}g_3(t)^2g'(t)^3 + \frac{251}{27}g'(t)^5, \\ \beta_{g_3}^{(2)} &= \frac{15}{4}g(t)^2g_3(t)^3 - \frac{116}{3}g_3(t)^5 + \frac{55}{36}g_3(t)^3g'(t)^2.\end{aligned}$$

At three loops we have:

$$\begin{aligned}\beta_g^{(3)} &= \frac{192809}{1728}g(t)^7 + \frac{65}{2}g(t)^5g_3(t)^2 + \frac{1325}{18}g(t)^3g_3(t)^4 \\ &\quad + \frac{821}{96}g(t)^5g'(t)^2 - \frac{5}{18}g(t)^3g_3(t)^2g'(t)^2 - \frac{37333}{5184}g(t)^3g'(t)^4, \\ \beta_{g'}^{(3)} &= \frac{12443}{576}g(t)^4g'(t)^3 - \frac{5}{6}g(t)^2g_3(t)^2g'(t)^3 + \frac{14575}{162}g_3(t)^4g'(t)^3 \\ &\quad + \frac{643}{288}g(t)^2g'(t)^5 - \frac{685}{162}g_3(t)^2g'(t)^5 - \frac{2494397}{46656}g'(t)^7, \\ \beta_{g_3}^{(3)} &= \frac{655}{48}g(t)^4g_3(t)^3 + \frac{35}{2}g(t)^2g_3(t)^5 - \frac{9769}{54}g_3(t)^7 \\ &\quad - \frac{5}{48}g(t)^2g_3(t)^3g'(t)^2 + \frac{385}{54}g_3(t)^5g'(t)^2 - \frac{33175}{3888}g_3(t)^3g'(t)^4.\end{aligned}$$

We provide also the pure QCD term, which is the leading one, of the four-loop contribution for g_3 , again in the five-flavours scenario, initially proposed by [33] and [34]:

$$\beta_{g_3}^{(4)} = \frac{598391}{1458}g_3(t)^9 - \frac{352864}{81}\zeta_3g_3(t)^9,$$

where $\zeta_3 \equiv \zeta(3) \simeq 1.20206$.

A.2 THE SM β -FUNCTIONS FOR $n_f = 6$

Here we provide the full expressions for the β -functions up to three loops for the Higgs quartic coupling λ , the top Yukawa coupling h_t , the gauge couplings g , g' and g_3 , the Higgs anomalous dimension γ , see eq. (29) and, in addition, for the squared Higgs boson mass m_H^2 and the non-minimal coupling ξ . All of these are given in the 6-flavours scenario.

At one loop they are given by [32]:

$$\begin{aligned}
\beta_\lambda^{(1)} &= \frac{27}{4}g(t)^4 + \frac{9}{2}g'(t)^2g(t)^2 - 9\lambda(t)g(t)^2 + \frac{9}{4}g'(t)^4 - 36h_t(t)^4 \\
&\quad + 4\lambda(t)^2 - 3g'(t)^2\lambda(t) + 12h_t(t)^2\lambda(t), \\
\beta_{h_t}^{(1)} &= \frac{9}{2}h_t(t)^3 - \frac{9}{4}g(t)^2h_t(t) - 8g_3(t)^2h_t(t) - \frac{17}{12}g'(t)^2h_t(t), \\
\beta_g^{(1)} &= -\frac{19}{6}g(t)^3, \\
\beta_{g'}^{(1)} &= \frac{41}{6}g'(t)^3, \\
\beta_{g_3}^{(1)} &= -7g_3(t)^3, \\
\beta_\gamma^{(1)} &= -\frac{9}{4}g(t)^2 - \frac{3}{4}g'(t)^2 + 3h_t(t)^2, \\
\beta_{m^2}^{(1)} &= m_H^2 \left(2\lambda(t) + 6h_t(t)^2 - \frac{9}{2}g(t)^2 - \frac{3}{2}g'(t)^2 \right), \\
\beta_\xi^{(1)} &= \left(\xi + \frac{1}{6} \right) \left(-\frac{3}{2}g'(t)^2 - \frac{9}{2}g(t)^2 + 6h_t(t)^2 + 2\lambda(t) \right).
\end{aligned}$$

At two loops they are [32]:

$$\begin{aligned}
\beta_\lambda^{(2)} &= 80g_3(t)^2h_t(t)^2\lambda(t) - 192g_3(t)^2h_t(t)^4 + \frac{915}{8}g(t)^6 - \frac{289}{8}g'(t)^2g(t)^4 \\
&\quad - \frac{27}{2}h_t(t)^2g(t)^4 - \frac{73}{8}\lambda(t)g(t)^4 - \frac{559}{8}g'(t)^4g(t)^2 + 63g'(t)^2h_t(t)^2g(t)^2 \\
&\quad + \frac{39}{4}g'(t)^2\lambda(t)g(t)^2 - 3h_t(t)^4\lambda(t) + \frac{45}{2}h_t(t)^2\lambda(t)g(t)^2 - \frac{379}{8}g'(t)^6 + 180h_t(t)^6 \\
&\quad - 16g'(t)^2h_t(t)^4 - \frac{26}{3}\lambda(t)^3 - \frac{57}{2}g'(t)^4h_t(t)^2 - 24h_t(t)^2\lambda(t)^2 \\
&\quad + 6(3g(t)^2 + g'(t)^2)\lambda(t)^2 + \frac{629}{24}g'(t)^4\lambda(t) + \frac{85}{6}g'(t)^2h_t(t)^2\lambda(t), \\
\beta_{h_t}^{(2)} &= h_t(t) \left[-108g_3(t)^4 + 9g(t)^2g_3(t)^2 + \frac{19}{9}g'(t)^2g_3(t)^2 + 36h_t(t)^2g_3(t)^2 \right. \\
&\quad \left. - \frac{3}{4}g'(t)^2g(t)^2 - \frac{23}{4}g(t)^4 + \frac{1187}{216}g'(t)^4 - 12h_t(t)^4 + \frac{\lambda(t)^2}{6} \right. \\
&\quad \left. + h_t(t)^2 \left(\frac{225}{16}g(t)^2 + \frac{131}{16}g'(t)^2 - 2\lambda(t) \right) \right],
\end{aligned}$$

$$\begin{aligned}\beta_g^{(2)} &= g(t)^3 \left(12g_3(t)^2 + \frac{35}{6}g(t)^2 + \frac{3}{2}g'(t)^2 - \frac{3}{2}h_t(t)^2 \right), \\ \beta_{g'}^{(2)} &= g'(t)^3 \left(\frac{44}{3}g_3(t)^2 + \frac{9}{2}g(t)^2 + \frac{199}{18}g'(t)^2 - \frac{17}{6}h_t(t)^2 \right), \\ \beta_{g_3}^{(2)} &= g_3(t)^3 \left(\frac{9}{2}g(t)^2 - 26g_3(t)^2 + \frac{11}{6}g'(t)^2 - 2h_t(t)^2 \right).\end{aligned}$$

$$\begin{aligned}\beta_\gamma^{(2)} &= -\frac{271}{32}g(t)^4 + \frac{9}{16}g(t)^2g'(t)^2 + \frac{431}{96}g'(t)^4 \\ &\quad + \frac{5}{2} \left(\frac{9}{4}g(t)^2 + \frac{17}{12}g'(t)^2 + 8g_3(t)^2 \right) h_t^2 - \frac{27}{4}h_t^4 + \frac{1}{6}\lambda(t)^2,\end{aligned}$$

$$\begin{aligned}\beta_{m^2}^{(2)} &= m_H^2 \left(-\frac{5}{6}\lambda(t)^2 - 6\lambda(t)h_t(t)^2 + 2\lambda(t)(3g(t)^2 + g'(t)^2) \right. \\ &\quad - \frac{27}{4}h_t(t)^4 + 20g_3(t)^2h_t(t)^2 + \frac{45}{8}g(t)^2h_t(t)^2 + \frac{85}{24}g'(t)^2h_t(t)^2 \\ &\quad \left. - \frac{145}{32}g(t)^4 + \frac{15}{16}g(t)^2g'(t)^2 + \frac{557}{96}g'(t)^4 \right).\end{aligned}$$

$$\begin{aligned}\beta_\xi^{(2)} &= \left(\xi + \frac{1}{6} \right) \left[-\frac{145}{16}g(t)^4 + \frac{15}{8}g(t)^2g'(t)^2 + \frac{557}{48}g'(t)^4 \right. \\ &\quad + \left(\frac{45}{4}g(t)^2 + \frac{85}{12}g'(t)^2 + 40g_3(t)^2 \right) h_t(t)^2 - \frac{27}{2}h_t(t)^4 \\ &\quad \left. + \frac{1}{3}(36g(t)^2 + 12g'(t)^2 - 36h_t(t)^2)\lambda(t) - \frac{5}{3}\lambda(t)^2 \right].\end{aligned}$$

The complete three-loop β -functions for the gauge couplings are [49]:

$$\begin{aligned}\beta_g^{(3)} &= \frac{324953}{1728}g(t)^7 + 39g(t)^5g_3(t)^2 + 81g(t)^3g_3(t)^4 + \frac{291}{32}g(t)^5g'(t)^2 - \frac{1}{3}g(t)^3g_3(t)^2g'(t)^2 \\ &\quad - \frac{5597}{576}g(t)^3g'(t)^4 - \frac{729}{32}g(t)^5h_t(t)^2 - 7g(t)^3g_3(t)^2h_t(t)^2 - \frac{593}{96}g(t)^3g'(t)^2h_t(t)^2 \\ &\quad + \frac{147}{16}g(t)^3h_t(t)^4, \\ \beta_{g'}^{(3)} &= \frac{1315}{64}g(t)^4g'(t)^3 - g(t)^2g_3(t)^2g'(t)^3 + 99g_3(t)^4g'(t)^3 + \frac{205}{96}g(t)^2g'(t)^5 - \frac{137}{27}g_3(t)^2g'(t)^5 \\ &\quad - \frac{388613}{5184}g'(t)^7 - \frac{785}{32}g(t)^2g'(t)^3h_t(t)^2 - \frac{29}{3}g_3(t)^2g'(t)^3h_t(t)^2 - \frac{2827}{288}g'(t)^5h_t(t)^2 \\ &\quad + \frac{315}{16}g'(t)^3h_t(t)^4, \\ \beta_{g_3}^{(3)} &= \frac{109}{8}g(t)^4g_3(t)^3 + 21g(t)^2g_3(t)^5 + \frac{65}{2}g_3(t)^7 - \frac{1}{8}g(t)^2g_3(t)^3g'(t)^2 + \frac{77}{9}g_3(t)^5g'(t)^2 \\ &\quad - \frac{2615}{216}g_3(t)^3g'(t)^4 - \frac{93}{8}g(t)^2g_3(t)^3h_t(t)^2 - 40g_3(t)^5h_t(t)^2 + \frac{101}{24}g_3(t)^3g'(t)^2h_t(t)^2 \\ &\quad + 15g_3(t)^3h_t(t)^4.\end{aligned}$$

The leading terms in the three-loop β -functions of λ and h_t are [50]:

$$\begin{aligned}\beta_\lambda^{(3)} &= 12 \left[\left(-\frac{266}{3} + 32\zeta_3 \right) g_3(t)^4 h_t(t)^4 + (-38 + 240\zeta_3) g_3(t)^2 h_t(t)^6 - \left(\frac{1599}{8} + 36\zeta_3 \right) h_t(t)^8 \right. \\ &\quad + \frac{1}{6} \left(\frac{1244}{3} - 48\zeta_3 \right) g_3(t)^4 h_t(t)^2 \lambda(t) + \frac{1}{6} (895 - 1296\zeta_3) g_3(t)^2 h_t(t)^4 \lambda(t) + \\ &\quad \frac{1}{6} \left(\frac{117}{8} - 198\zeta_3 \right) h_t(t)^6 \lambda(t) + \frac{1}{36} (-1224 + 1152\zeta_3) g_3(t)^2 h_t(t)^2 \lambda(t)^2 + \\ &\quad \left. \frac{1}{36} \left(\frac{1719}{2} + 756\zeta_3 \right) h_t(t)^4 \lambda(t)^2 + \frac{97}{24} h_t(t)^2 \lambda(t)^3 + \frac{1}{1296} (3588 + 2016\zeta_3) \lambda(t)^4 \right], \\ \beta_{h_t}^{(3)} &= 2 \left[\left(-\frac{2083}{3} + 320\zeta_3 \right) g_3(t)^6 + \left(\frac{3827}{12} - 114\zeta_3 \right) g_3(t)^4 h_t(t)^2 - \frac{157}{2} g_3(t)^2 h_t(t)^4 \right. \\ &\quad \left. + \left(\frac{339}{16} + \frac{27}{4}\zeta_3 \right) h_t(t)^6 + \frac{4}{3} g_3(t)^2 h_t(t)^2 \lambda(t) + \frac{33}{2} h_t(t)^4 \lambda(t) + \frac{5}{96} h_t(t)^2 \lambda(t)^2 - \frac{1}{12} \lambda(t)^3 \right].\end{aligned}$$

The three-loop contribution for the β -function of the Higgs anomalous dimension γ is given by [51]:

$$\begin{aligned}\beta_\gamma^{(3)} &= -\frac{1}{6} \lambda(t)^3 - \frac{15}{8} h_t(t)^2 \lambda(t)^2 + \frac{15}{2} h_t(t)^4 \lambda(t) + \left(\frac{789}{16} + 9\zeta_3 \right) h_t(t)^6 \\ &\quad + \left(\frac{15}{2} - 72\zeta_3 \right) g_3(t)^2 h_t(t)^4 + \left(\frac{622}{3} - 24\zeta_3 \right) g_3(t)^4 h_t(t)^2.\end{aligned}$$

Finally we provide the four-loop β -function for g_3 , obtained by Zoller in [56]:

$$\begin{aligned}\beta_{g_3}^{(4)} &= \frac{63559}{18} g_3(t)^9 - \frac{44948}{9} \zeta_3 g_3(t)^9 \\ &\quad - \frac{6709}{9} g_3(t)^7 h_t(t)^2 + 272\zeta_3 g_3(t)^7 h_t(t)^2 \\ &\quad + \frac{1283}{3} g_3(t)^5 h_t(t)^4 - 104\zeta_3 g_3(t)^5 h_t(t)^4 \\ &\quad - \frac{423}{4} g_3(t)^3 h_t(t)^6 - 6\zeta_3 g_3(t)^3 h_t(t)^6 \\ &\quad - 5g_3(t)^2 h_t(t)^4 \lambda(t) + g_3(t)^2 h_t(t)^2 \lambda(t)^2.\end{aligned}$$

This expression is in agreement with [33] for the pure QCD part and with [57] for the top-Yukawa and self-Higgs contributions.

A.3 THE β -FUNCTIONS IN THE $U(1)_{B-L}$ EXTENSION

Here we provide the full expressions for the β -functions up to two loops for the Higgs quartic coupling λ , the scalar singlet quartic coupling λ_χ , the portal coupling $\lambda_{\phi\chi}$, the top Yukawa coupling h_t , the Dirac neutrino Yukawa coupling h_ν and the gauge couplings g , g' and g_3 , with all the relevant terms [167, 170, 171]. All of these are given in the six-flavours scenario. In red we add the relevant contributions (at one loop only) related to the specific $U(1)_{B-L}$ model, studied in Ch. 6, including the g_{B-L} , g'_{B-L} gauge couplings and the Majorana neutrino Yukawa coupling h_{ν_R} [213, 6].

One loop:

$$\begin{aligned}
 \beta_{\lambda}^{(1)} &= \frac{27}{4}g(t)^4 + \frac{9}{2}g'(t)^2g(t)^2 - 9\lambda(t)g(t)^2 + \frac{9}{4}g'(t)^4 - 36h_t(t)^4 \\
 &\quad + 4\lambda(t)^2 - 3g'(t)^2\lambda(t) + 12h_t(t)^2\lambda(t) - 12h_v(t)^4 + 4h_v(t)^2\lambda(t) + 3\lambda_{\phi_X}(t)^2 \\
 &\quad + \frac{9}{2}g'(t)^2g'_{B-L}(t)^2 + \frac{9}{2}g(t)^2g'_{B-L}(t)^2 + \frac{9}{2}g'_{B-L}(t)^4 - 3\lambda(t)g'_{B-L}(t)^2, \\
 \beta_{\lambda_{\phi_X}}^{(1)} &= -\frac{9}{2}g(t)^2\lambda_{\phi_X}(t) + \frac{3}{2}g'(t)^2\lambda_{\phi_X}(t) + 6h_t(t)^2\lambda_{\phi_X}(t) \\
 &\quad + 2\lambda(t)\lambda_{\phi_X}(t) + 4\lambda_{\phi_X}(t)^2 + \lambda_{\phi_X}(t)\lambda_X(t) \\
 &\quad + \frac{3}{2}g'_{B-L}(t)^2\lambda_{\phi_X}(t) + 4\lambda_{\phi_X}(t)h_{\nu_R}(t)^2 - 24g_{B-L}(t)^2 + 12g_{B-L}(t)^2g'_{B-L}(t)^2, \\
 \beta_{\lambda_X}^{(1)} &= 12\lambda_{\phi_X}(t)^2 + \frac{10}{3}\lambda_X(t)^2 - 6h_{\nu_R}(t)^4 + 576g_{B-L}(t)^4 + \frac{4}{3}\lambda_X(t)^2h_{\nu_R}(t)^2 - 48\lambda_X(t)g_{B-L}(t)^2,
 \end{aligned}$$

$$\begin{aligned}
 \beta_{h_t}^{(1)} &= \frac{9}{2}h_t(t)^3 - \frac{9}{4}g(t)^2h_t(t) - 8g_3(t)^2h_t(t) - \frac{17}{12}g'(t)^2h_t(t) + h_t(t)h_v(t)^2 \\
 &\quad - \frac{17}{2}g'_{B-L}(t)^2 - \frac{2}{3}g'_{B-L}(t)^2 - \frac{5}{3}g'_{B-L}(t)g_{B-L}(t), \\
 \beta_{h_v}^{(1)} &= -\frac{9}{4}g(t)^2h_v(t) - \frac{3}{4}g'(t)^2h_v(t) + 3h_t(t)^2h_v(t) + \frac{5}{2}h_v(t)^3 - 6g_{B-L}(t)^2, \\
 \beta_{h_{\nu_R}}^{(1)} &= 4h_{\nu_R}(t)^4 + 2h_{\nu_R}(t)^3 - 6g_{B-L}(t)^2h_{\nu_R}(t),
 \end{aligned}$$

$$\begin{aligned}
 \beta_g^{(1)} &= -\frac{19}{6}g(t)^3, \\
 \beta_{g'}^{(1)} &= \frac{41}{6}g'(t)^3, \\
 \beta_{g_3}^{(1)} &= -7g_3(t)^3, \\
 \beta_{g_{B-L}}^{(1)} &= 12g_{B-L}(t)^3 + \frac{32}{3}g'_{B-L}(t)g_{B-L}(t)^2 + \frac{41}{6}g'_{B-L}(t)^2g_{B-L}(t), \\
 \beta_{g'_{B-L}}^{(1)} &= \frac{41}{6}g'_{B-L}(t)^3 + \frac{41}{3}g'(t)^2g'_{B-L}(t) + \frac{32}{3}g_{B-L}(t)(g'_{B-L}(t)^2 + g'(t)^2) + 12g'_{B-L}(t)^2g_{B-L}(t)^2.
 \end{aligned}$$

Two loops:

$$\begin{aligned}
\beta_\lambda^{(2)} &= \frac{915}{8}g(t)^6 - \frac{289}{8}g(t)^4g'(t)^2 - \frac{559}{8}g(t)^2g'(t)^4 - \frac{379}{8}g'(t)^6 \\
&\quad + \frac{27}{2}g(t)^4h_t(t)^2 + 63g(t)^2g'(t)2h_t(t)^2 - \frac{57}{2}g'(t)^4h_t(t)^2 - 192g_3(t)^2h_t(t)^4 \\
&\quad - 16g'(t)^2h_t(t)^4 + 180h_t(t)^6 + 60h_v(t)^6 \\
&\quad - \frac{9}{2}g(t)^4h_v(t)^2 - 3g(t)^2g'(t)^2h_v(t)^2 - \frac{3}{2}g'(t)^4h_v(t)^2 + 9g(t)^2h_v(t)^4 + 6g'(t)^2h_v(t)^4 \\
&\quad - \frac{73}{8}g(t)^4\lambda(t) + \frac{39}{4}g(t)^2g'(t)^2\lambda(t) + \frac{629}{24}g'(t)^4\lambda(t) + \frac{45}{2}g(t)^2h_t(t)^2\lambda(t) \\
&\quad + 80g_3(t)^2h_t(t)^2\lambda(t) + \frac{85}{6}g'(t)^2h_t(t)^2\lambda(t) \\
&\quad - 3h_t(t)^4\lambda(t) - \frac{15}{2}g(t)^2h_v(t)^2\lambda(t) + \frac{5}{2}g'(t)^2h_v(t)^2\lambda(t) - h_v(t)\lambda(t) \\
&\quad + 18g(t)^2\lambda(t)^2 + 6g'(t)^2\lambda(t)^2 - 24h_t^2\lambda(t)^2 - 8h_v(t)^2\lambda(t)^2 - \frac{26}{3}\lambda(t)^3 \\
&\quad - 5\lambda(t)\lambda_{\phi_X}(t)^2 - 12\lambda_{\phi_X}(t)^3, \\
\beta_{\lambda_{\phi_X}}^{(2)} &= \frac{15}{4}g(t)^2h_v(t)^2 + \frac{5}{4}g'(t)^2h_v(t)^2 \\
&\quad + \lambda_{\phi_X}(t) \left(-\frac{145}{16}g(t)^4 + \frac{15}{8}g(t)^2g'(t)^2 + \frac{557}{48}g'(t)^4 \right. \\
&\quad + \frac{45}{4}g(t)^2h_t(t)^2 + 40g_3(t)^2h_t^2 + \frac{65}{12}g'(t)^2h_t(t)^2 - \frac{27}{2}h_t(t)^4 \\
&\quad - \frac{9}{2}h_v(t)^4 + 12g(t)^2\lambda(t) + 4g'(t)^2\lambda(t) - 12h_t(t)^2\lambda(t) - 4h_v(t)^2\lambda(t) \\
&\quad - \frac{25}{18}\lambda(t)^2 + 3g(t)^2\lambda_{\phi_X}(t) + g'(t)^2\lambda_{\phi_X}(t) - 12h_t(t)^2\lambda_{\phi_X}(t) - 4h_v(t)^2\lambda_{\phi_X}(t) \\
&\quad \left. - 12\lambda(t)\lambda_{\phi_X}(t) - \frac{21}{2}\lambda_{\phi_X}(t)^2 - 6\lambda_{\phi_X}(t)\lambda_X(t) - \frac{25}{6}\lambda(t)^2 \right), \\
\beta_{\lambda_X}^{(2)} &= \lambda_{\phi_X}(t)^2 (24g(t)^2 + 72g'(t)^2 - 72h_t(t)^2 - 24h_v(t)^2 - 48\lambda_{\phi_X}(t) - 20\lambda_X(t)) - \frac{17}{3}\lambda_X(t)^3, \\
\beta_{h_t}^{(2)} &= -\frac{23}{4}g(t)^4 + 9g(t)^2g_3(t)^2 - 108g_3(t)^4 - \frac{3}{4}g(t)^2g'(t)^2 + \frac{19}{9}g_3(t)^2g'(t)^2 + \frac{1187}{216}g'(t)^4 \\
&\quad + \frac{225}{16}g(t)^2h_t(t)^2 + 36g_3(t)^2h_t(t)^2 + \frac{131}{16}g'(t)^2h_t(t)^2 - 12h_t(t)^4 \\
&\quad + \frac{15}{8}g(t)^2h_v(t)^2 + \frac{5}{8}g'(t)^2h_v(t)^2 - \frac{9}{4}h_t(t)^2h_v(t)^2 - \frac{9}{4}h_v(t)^4 \\
&\quad - 2h_t(t)^2\lambda(t) + \frac{1}{6}\lambda(t)^2 + \frac{1}{6}\lambda_{\phi_X}(t)^2, \\
\beta_{h_v}^{(2)} &= h_v(t) \left(-\frac{23}{4}g(t)^4 - \frac{9}{4}g(t)^2g'(t)^2 + \frac{35}{24}g'(t)^4 \right. \\
&\quad + \frac{45}{8}g(t)^2h_t(t)^2 + 20g_3(t)^2h_t(t)^2 + \frac{85}{24}g'(t)^2h_t(t)^2 - 6h_t(t)^4 \\
&\quad + \frac{165}{16}g(t)^2h_v(t)^2 + \frac{51}{8}g'(t)^2h_v(t)^2 - \frac{27}{4}h_t(t)^2h_v(t)^2 - 3h_v(t)^4 \\
&\quad \left. - 2\lambda(t)h_v(t)^2 + \frac{1}{6}\lambda(t)^2 + \frac{1}{4}\lambda_{\phi_X}(t)^4 \right),
\end{aligned}$$

$$\begin{aligned}\beta_g^{(2)} &= g(t)^3 \left(12g_3(t)^2 + \frac{35}{6}g(t)^2 + \frac{3}{2}g'(t)^2 - \frac{3}{2}h_t(t)^2 - \frac{1}{2}h_v(t)^2 \right), \\ \beta_{g'}^{(2)} &= g'(t)^3 \left(\frac{44}{3}g_3(t)^2 + \frac{9}{2}g(t)^2 + \frac{199}{18}g'(t)^2 - \frac{17}{6}h_t(t)^2 - \frac{1}{2}h_v(t)^2 \right), \\ \beta_{g_3}^{(2)} &= g_3(t)^3 \left(\frac{9}{2}g(t)^2 - 26g_3(t)^2 + \frac{11}{6}g'(t)^2 - 2h_t(t)^2 \right).\end{aligned}$$

A.4 THE SM β -FUNCTIONS WITH THE SUPPRESSION FACTOR $s(\phi)$

In this section we list the RGE for the couplings λ , h_t , g , g' , g_3 , ξ and γ in the $\overline{\text{MS}}$ scheme with one suppression factor $s = s(\phi)$ for each off-shell physical Higgs propagator (see section 6.2.1)¹. This procedure was done up to two loops: inserting the suppression factor in the three-loop expressions would mean considering a correction smaller than the uncertainty in the RG equation in the inflationary regime [189]. The SM RG equations of appendix A.2 can be recovered with $s = 1$.

At one loop we have:

$$\begin{aligned}\beta_\lambda^{(1)} &= \frac{27}{4}g(t)^4 + \frac{9}{2}g'(t)^2g(t)^2 - 9\lambda(t)g(t)^2 + \frac{9}{4}g'(t)^4 - 36h_t(t)^4 \\ &\quad + (1 + 3s(\phi))\lambda(t)^2 - 3g'(t)^2\lambda(t) + 12h_t(t)^2\lambda(t), \\ \beta_{h_t}^{(1)} &= \left(\frac{23}{6} + \frac{2}{3}s(\phi) \right) h_t(t)^3 - \frac{9}{4}g(t)^2h_t(t) - 8g_3(t)^2h_t(t) - \frac{17}{12}g'(t)^2h_t(t), \\ \beta_g^{(1)} &= -\frac{39 - s(\phi)}{12}g(t)^3, \\ \beta_{g'}^{(1)} &= \frac{81 + s(\phi)}{12}g'(t)^3, \\ \beta_{g_3}^{(1)} &= -7g_3(t)^3, \\ \beta_\gamma^{(1)} &= -\frac{9}{4}g(t)^2 - \frac{3}{4}g'(t)^2 + 3h_t(t)^2, \\ \beta_\xi^{(1)} &= \left(\xi + \frac{1}{6} \right) \left(-\frac{3}{2}g'(t)^2 - \frac{9}{2}g(t)^2 + 6h_t(t)^2 + (1 + s(\phi))\lambda(t) \right).\end{aligned}$$

¹ The suppression factor $s(\phi)$ was written in terms of μ by inverting the relations between the field and the renormalisation scale, depending on which prescription was used.

At two loops we obtain:

$$\begin{aligned}
\beta_{\lambda}^{(2)} = & 6h_t(t)^6(38 - 8s(\phi)) \\
& + \frac{1}{8} (g(t)^2 g'(t)^4 (-560 + s(\phi)) + g'(t)^6 (-380 + s(\phi)) + g(t)^4 g'(t)^2 (-290 + s(\phi)) \\
& + 3g(t)^6 (304 + s(\phi))) - h_t(t)^4 (192g_3(t)^2 + 16g'(t)^2 + 3\lambda(t)(4 - 39s(\phi) + 36s(\phi)^2)) \\
& - \frac{1}{6} h_t(t)^2 (81g(t)^4 + 171g'(t)^4 - 85g'(t)^2 \lambda(t) - 27g(t)^2 (14g'(t)^2 + 5\lambda(t)) \\
& + 12\lambda(t)(-40g_3(t)^2 + 3\lambda(t) + 9\lambda(t)s(\phi)^2)) \\
& + \frac{1}{24} \lambda(t) (36g'(t)^2 \lambda(t)(1 + s(\phi))^2 + 3g'(t)^4 (-181 - 54s(\phi) + 162s(\phi)^2) \\
& + g'(t)^4 (90 + 377s(\phi) + 162s(\phi)^2) \\
& + 8\lambda(t)^2 (-4 - 24s(\phi) + 27s(\phi)^2 - 52s(\phi)^3 + 27s(\phi)^4) \\
& + 18g(t)^2 (6\lambda(t)(1 + s(\phi))^2 + g'(t)^2 (1 - 6s(\phi) + 18s(\phi)^2))) ,
\end{aligned}$$

$$\begin{aligned}
\beta_{h_t}^{(2)} = & h_t(t) \left[-108g_3(t)^4 + 9g(t)^2 g_3(t)^2 + \frac{19}{9} g'(t)^2 g_3(t)^2 + 36s(\phi) h_t(t)^2 g_3(t)^2 \right. \\
& - \frac{3}{4} g'(t)^2 g(t)^2 - \frac{23}{4} g(t)^4 + \frac{1187}{216} g'(t)^4 - 12s(\phi)^2 h_t(t)^4 + s(\phi)^2 \frac{\lambda(t)^2}{6} \\
& \left. + h_t(t)^2 \left(\frac{225}{16} s(\phi) g(t)^2 + \frac{131}{16} s(\phi) g'(t)^2 - 2s(\phi)^3 \lambda(t) \right) \right] ,
\end{aligned}$$

$$\beta_g^{(2)} = g(t)^3 \left(12g_3(t)^2 + \frac{35}{6} g(t)^2 + \frac{3}{2} g'(t)^2 - \frac{3}{2} s(\phi) h_t(t)^2 \right) ,$$

$$\beta_{g'}^{(2)} = g'(t)^3 \left(\frac{44}{3} g_3(t)^2 + \frac{9}{2} g(t)^2 + \frac{199}{18} g'(t)^2 - \frac{17}{6} s(\phi) h_t(t)^2 \right) ,$$

$$\beta_{g_3}^{(2)} = g_3(t)^3 \left(\frac{9}{2} g(t)^2 - 26g_3(t)^2 + \frac{11}{6} g'(t)^2 - 2s(\phi) h_t(t)^2 \right) .$$

$$\begin{aligned}
\beta_{\gamma}^{(2)} = & -\frac{271}{32} g(t)^4 + \frac{9}{16} g(t)^2 g'(t)^2 + \frac{431}{96} s(\phi) g'(t)^4 \\
& + \frac{5}{2} \left(\frac{9}{4} g(t)^2 + \frac{17}{12} g'(t)^2 + 8g_3(t)^2 \right) h_t^2 \\
& - \frac{27}{4} s(\phi) h_t^4 + \frac{1}{6} s(\phi)^3 \lambda(t)^2 ,
\end{aligned}$$

$$\begin{aligned}
\beta_{\xi}^{(2)} = & \left(\xi + \frac{1}{6} \right) \left[\left(-\frac{199}{16} + \frac{27}{8} s(\phi) \right) g(t)^4 + \left(-\frac{3}{8} + \frac{9}{4} s(\phi) \right) g(t)^2 g'(t)^2 \right. \\
& + \left(\frac{3}{2} + \frac{485}{48} s(\phi) \right) g'(t)^4 + \left(\frac{45}{4} g(t)^2 + \frac{85}{12} g'(t)^2 + 40g_3(t)^2 \right) h_t(t)^2 \\
& + \left(18 - \frac{63}{2} s(\phi) \right) h_t(t)^4 + \frac{1}{6} (1 + s(\phi)) (36g(t)^2 + 12g'(t)^2 - 36h_t(t)^2) \lambda(t) \\
& \left. + \frac{1}{36} (-108 + 126s(\phi) - 144s(\phi)^2 + 66s(\phi)^3) \lambda(t)^2 \right] .
\end{aligned}$$

B | MATCHING PROCEDURES

B.1 STRONG COUPLING MATCHING

Considering the general form of the equation (35):

$$\alpha_s^{(n_l)}(\mu) = \zeta_g^2(\mu, \alpha_s^{(n_f)}(\mu), m(\mu)) \alpha_s^{(n_f)}(\mu),$$

with $n_f = 6$, $n_l = n_f - 1 = 5$ and for the decoupling relations:

$$\zeta_g^2 = 1 + \sum_{i=1}^{\infty} d_i \frac{\alpha_s^{(n_f)}(\mu)}{\pi},$$

we list the coefficients d_i up to three loops [61, 62]:

$$\begin{aligned} d_1 &= -\frac{1}{6} \ln \frac{\mu^2}{m(\mu)^2}, \\ d_2 &= \frac{11}{72} - \frac{11}{24} \ln \frac{\mu^2}{m(\mu)^2} + \frac{1}{36} \ln^2 \frac{\mu^2}{m(\mu)^2}, \\ d_3 &= \frac{564731}{124416} - \frac{82043}{27648} \zeta_3 - \frac{955}{576} \ln \frac{\mu^2}{m(\mu)^2} + \frac{53}{576} \ln^2 \frac{\mu^2}{m(\mu)^2} - \frac{1}{216} \ln^3 \frac{\mu^2}{m(\mu)^2} \\ &\quad + n_l \left(-\frac{2633}{31104} + \frac{67}{576} \ln \frac{\mu^2}{m(\mu)^2} - \frac{1}{36} \ln^2 \frac{\mu^2}{m(\mu)^2} \right). \end{aligned}$$

The mass $m(\mu)$ in the previous equations is the (running) heavy quark mass in the $\overline{\text{MS}}$ -scheme (in our case it corresponds to the top quark mass) and μ , as usual, represents the renormalisation scale.

B.2 HIGGS QUARTIC COUPLING MATCHING

We recall the relation (38):

$$\lambda(\mu) = \sum_{n=1,2,3,\dots} \lambda^{(n)}(\mu) = 3 \frac{m_H^2}{v^2} \left(1 + \delta_t^{(1)}(\mu) + \delta_t^{(2)}(\mu) + \dots \right)$$

where

$$\delta_t^{(2)}(\mu) = \delta_{\text{QCD, lead.}}^{(2)}(\mu) + \delta_{\text{Yukawa, lead.}}^{(2)}(\mu) + \dots$$

According to Sirlin and Zucchini [64], the one-loop matching is given by:

$$\delta_t^{(1)}(\mu) = \frac{G_\mu m_Z^2}{8\sqrt{2}\pi^2} \left(\xi f_1(\mu) + f_0(\mu) + \frac{f_{-1}(\mu)}{\xi} \right),$$

where $\xi = \frac{m_H^2}{m_Z^2}$ and, introducing $c = \frac{m_W}{m_Z}$,

$$\begin{aligned}
f_1(\mu) &= \frac{3}{2} \ln(\xi) - \ln(c^2) + 6 \ln\left(\frac{\mu^2}{m_H^2}\right) - \frac{1}{2} Z\left[\frac{1}{\xi}\right] - Z\left[\frac{c^2}{\xi}\right] + \frac{9}{2} \left(\frac{25}{9} - \frac{\pi}{\sqrt{3}}\right), \\
f_0(\mu) &= \frac{3c^2}{s^2} \ln(c^2) + 12 \ln c^2 (c^2) + \frac{3\xi c^2}{\xi - c^2} \ln\left(\frac{\xi}{c^2}\right) + 4c^2 Z\left[\frac{c^2}{\xi}\right] - \frac{15}{2} (2c^2 + 1) \\
&\quad - 6 \left(2c^2 - \frac{2m_t^2}{m_Z^2} + 1\right) \ln\left(\frac{\mu^2}{m_Z^2}\right) - \frac{3m_t^2}{m_Z^2} \left(4 \ln\left(\frac{m_t^2}{m_Z^2}\right) + 2 Z\left[\frac{m_t^2}{m_Z^2 \xi}\right] - 5\right) \\
&\quad + 2 Z\left[\frac{1}{\xi}\right], \\
f_{-1}(\mu) &= 8(2c^4 + 1) - 12c^4 \ln(c^2) - 12c^4 Z\left[\frac{c^2}{\xi}\right] + 6 \left(2c^4 - \frac{4m_t^4}{m_Z^4} + 1\right) \ln\left(\frac{\mu^2}{m_Z^2}\right) \\
&\quad - 6 Z\left[\frac{1}{\xi}\right] + \frac{24m_t^4}{m_Z^4} \left(\ln\left(\frac{m_t^2}{m_Z^2}\right) + Z\left[\frac{m_t^2}{m_Z^2 \xi}\right] - 2\right), \\
Z[z] &= \begin{cases} 2A(z) \arctan\left(\frac{1}{A(z)}\right) & \text{if } z > \frac{1}{4} \\ A(z) \ln\left(\frac{A(z)+1}{1-A(z)}\right) & \text{if } z < \frac{1}{4} \end{cases}, \\
A(z) &= \sqrt{|1-4z|}.
\end{aligned}$$

We compute the QCD and the Yukawa contribution to $\lambda^{(2)}(\mu)$, following the expressions of [3] (multiplied them by a factor 6 to compensate for the different definition of the quartic coupling). The top QCD contribution is an evaluation of the relevant diagrams via a Taylor series in $x_{Ht} = m_H^2/m_t^2$ up to fourth order (from now on $L_X = \ln(m_X^2/\mu^2)$):

$$\begin{aligned}
\delta_{\text{QCD}}^{(2)}(\mu) &= \frac{6G_\mu m_t^4}{(4\pi)^4} N_c C_F g_3(\mu)^2 [16(-4 - 6L_T + 3L_T^2) \\
&\quad + x_{Ht} \left(35 - \frac{2\pi^2}{3} + 12L_T - 12L_T^2\right) + x_{Ht}^2 \frac{61}{135} + x_{Ht}^3 \frac{1223}{6300} + x_{Ht}^4 \frac{43123}{1323000}],
\end{aligned}$$

where N_c and C_F are colour factors ($N_c = 3$ and $C_F = 4/3$). This equation is in agreement with the respective equation in [63]: the numerical difference for a Higgs mass ~ 125 GeV turns out to be negligible.

The Yukawa contribution is:

$$\begin{aligned}
\delta_{\text{Yukawa}}^{(2)}(\mu) = & \frac{6\sqrt{2}G_\mu^3 m_t^6}{(4\pi)^4} \left\{ N_c^2 \left[16B_0(m_t, m_t, m_H)(-1 + 2L_T) \right. \right. \\
& + x_{Ht}((1 + 4B_0(m_t, m_t, m_H) - 2L_T)(1 - 2L_T))] \\
& + N_c \left[16 + \frac{8}{3}\pi^2 + 32B_0(m_t, m_H, m_t)(1 + 2L_T) - 48L_T + 40L_T^2 \right. \\
& - x_{Ht} \left(\frac{929}{6} + \frac{16}{3}\pi^2 + 48B_0(m_H, m_H, m_H) - 16L_H(1 - L_T) \right. \\
& + B_0(m_t, m_H, m_t) \left(\frac{76}{3} + 32L_T \right) + \frac{190}{3}L_T + 58L_T^2 \left. \right) \\
& + x_{Ht}^2 \left(\frac{17629}{270} + \frac{8}{3}\pi^2 - \frac{2}{3}L_H + B_0(m_H, m_H, m_H)(27 - 18L_T) + 40L_T \right. \\
& + 10L_T L_H + 12L_T^2 + B_0(m_t, m_H, m_t) \left(\frac{13}{3} + 4L_T \right) \left. \right) \\
& + x_{Ht}^3 \left(\frac{1181}{900} - \frac{\pi^2}{2} + \frac{61}{30}B_0(m_H, m_H, m_H) + \frac{59}{90}L_H \right. \\
& \left. \left. - \frac{2}{35}B_0(m_t, m_H, m_t) - \frac{68}{63}L_T \right) \right] \\
& + x_{Ht}^3 \left[\frac{131}{6}\pi^2 + \left(\frac{729}{2} - \frac{135}{4}\sqrt{3}\pi \right) S_2 - 111L_H + 36L_H^2 \right. \\
& \left. + \pi \left(\frac{-225\sqrt{3}}{4} + 18\sqrt{3}L_H \right) + \frac{75 + 72\zeta_3}{4} \right] \left. \right\},
\end{aligned}$$

where

$$\begin{aligned}
B_0(m_H, m_H, m_H) &= 2 - L_H - \pi/\sqrt{3}, \\
B_0(m_t, m_t, m_H) &= 2 - \frac{2}{m_H} \sqrt{4m_t^2 - m_H^2} \arctan \left(\frac{m_H}{\sqrt{4m_t^2 - m_H^2}} \right) - L_T, \\
B_0(m_t, m_H, m_t) &= -\frac{1}{m_t^2} \left[-2m_t^2 + m_H \sqrt{4m_t^2 - m_H^2} \arctan \left(\frac{m_H}{\sqrt{4m_t^2 - m_H^2}} \right) \right. \\
& \quad - m_H \sqrt{4m_t^2 - m_H^2} \arctan \left(\frac{m_H^2 - 2m_t^2}{m_H \sqrt{4m_t^2 - m_H^2}} \right) \\
& \quad \left. + m_H^2 \ln m_H - m_H^2 \ln m_t + 2m_t^2 \ln m_t + m_t^2 \ln \frac{1}{\mu^2} \right],
\end{aligned}$$

and $S_2 = 4/(9\sqrt{3})Cl_2(\pi/3) \simeq 0.26043$, where $Cl_2(x)$ is the Clausen function [214].

B.3 TOP YUKAWA MATCHING

The matching between the top pole mass and the $\overline{\text{MS}}$ Yukawa is given by:

$$h_t(\mu) = 2^{3/4} \sqrt{G_\mu} m_t (1 + \delta_t(\mu)),$$

where

$$\delta_t(\mu) = \delta_t^{\text{QCD}}(\mu) + \delta_t^W(\mu) + \delta_t^{\text{QED}}(\mu).$$

Here $\delta_t^W(\mu) + \delta_t^{\text{QED}}(\mu)$ represent the one-loop electroweak contribution and is given by [67]:

$$\delta_t^W(\mu) + \delta_t^{\text{QED}}(\mu) = -\frac{E(\mu)}{2} + \Re\{\Sigma_V(\mu) + \Sigma_S(\mu)\} - \frac{\Pi(\mu)}{2m_W^2},$$

where

$$\begin{aligned} E(\mu) &= \frac{\alpha_{\text{em}}(m_Z)}{4\pi s^2} \left[\left(\frac{7}{2s^2} - 6 \right) \ln(c^2) - 4 \ln \left(\frac{m_Z^2}{\mu^2} \right) + 6 \right], \\ \Sigma_V(\mu) + \Sigma_S(\mu) &= \frac{\alpha_{\text{em}}(m_Z)}{4\pi} \left[\left(6 - \frac{m_Z^2}{m_t^2} \right) a_f^2 - 4Q_t^2 - \left(\frac{m_Z^2}{m_t^2} + 4 \right) v_f^2 \right. \\ &\quad + \left[a_f^2 \left(4 - \frac{m_Z^2}{m_t^2} \right) - \left(\frac{m_Z^2}{m_t^2} + 2 \right) v_f^2 \right] F(m_t^2, m_t^2, m_Z^2) \\ &\quad - \left[\frac{3}{8s^2} \left(\frac{m_t^2 - m_b^2}{m_W^2} + 1 \right) - 3(Q_t^2 + v_f^2 - a_f^2) + \frac{1}{8c^2} \right] \ln \left(\frac{m_t^2}{\mu^2} \right) \\ &\quad + \frac{1}{4m_W^2 s^2} \left[4m_t^2 - \frac{5m_b^2}{2} + \frac{1}{2}(m_W^2 - m_H^2) + \frac{m_b^4 + m_b^2 m_W^2 - 2m_W^4}{2m_t^2} \right. \\ &\quad + \frac{1}{2m_t^2} \left. \left((m_b^2 + m_t^2)m_W^2 + (m_t^2 - m_b^2)^2 - 2m_W^4 \right) F(m_t^2, m_b^2, m_W^2) \right. \\ &\quad + \left. \left(2m_t^2 - \frac{m_H^2}{2} \right) F(m_t^2, m_t^2, m_H^2) + \left(m_W^2 + \frac{1}{2}(m_t^2 - 3m_b^2) \right) \ln \left(\frac{m_t^2}{m_b^2} \right) \right. \\ &\quad + \left. \frac{1}{2} m_H^2 \left(3 - \frac{m_H^2}{2m_t^2} \right) \ln \left(\frac{m_t^2}{m_H^2} \right) + \frac{1}{4m_t^4} \left(3(m_b^2 + m_t^2)m_W^4 + 4m_t^4 m_W^2 \right. \right. \\ &\quad + \left. \left. (m_t^2 - m_b^2)^3 - 2m_W^6 \right) \ln \left(\frac{m_t^2}{m_Z^2} \right) \right] \\ &\quad + \left[a_f^2 \left(2 - \frac{m_Z^4}{2m_t^4} + \frac{3m_Z^2}{m_t^2} \right) - \frac{m_Z^4 v_f^2}{2m_t^4} \right] \ln \left(\frac{m_t^2}{m_Z^2} \right) \Big], \\ \Pi(\mu) &= \frac{\alpha_{\text{em}}(m_Z)m_W^2}{4\pi s^2} \left[\frac{7}{8c^2} - \frac{17}{4} - \frac{3m_H^2}{4(m_W^2 - m_H^2)} \ln \left(\frac{m_W^2}{m_H^2} \right) - \frac{m_H^2}{8m_W^2} \right. \\ &\quad + \left. \left(2 + \frac{1}{c^2} - \frac{17}{4s^2} \right) \ln(c^2) - \left(\frac{1}{c^2} - 2 \right) \ln \left(\frac{m_W^2}{\mu^2} \right) \right] \\ &\quad + \frac{\alpha_{\text{em}}(m_Z)}{4\pi s^2} \left[\frac{m_b^2 m_t^2}{m_t^2 - m_b^2} \ln \left(\frac{m_t^2}{m_b^2} \right) - \left(\frac{1}{2} - \ln \left(\frac{m_b^2}{\mu^2} \right) \right) m_b^2 \right. \\ &\quad \left. - m_t^2 \left(\frac{1}{2} - \ln \left(\frac{m_t^2}{\mu^2} \right) \right) \right], \end{aligned}$$

with

$$F(x, y, z) = \begin{cases} \frac{\tilde{\lambda}(x, y, z)^{1/2}}{x} \operatorname{arccosh} \left(\frac{-x+y+z}{2\sqrt{yz}} \right) & \text{if } x < (\sqrt{y} - \sqrt{z})^2 \\ -\frac{\tilde{\lambda}(x, y, z)^{1/2}}{x} \arccos \left(\frac{-x+y+z}{2\sqrt{yz}} \right) & \text{if } (\sqrt{y} - \sqrt{z})^2 \leq x \leq (\sqrt{y} + \sqrt{z})^2 \\ \frac{\tilde{\lambda}(x, y, z)^{1/2}}{x} \left[\nu\pi - \operatorname{arccosh} \left(\frac{x-y-z}{2\sqrt{yz}} \right) \right] & \text{if } x > (\sqrt{y} + \sqrt{z})^2 \end{cases},$$

and

$$\tilde{\lambda}(x, y, z) \equiv x^2 + y^2 + z^2 - 2(xy - zy + xz),$$

$$s \equiv \sqrt{1 - \frac{m_W^2}{m_Z^2}}, \quad c \equiv \frac{m_W}{m_Z}, \quad Q_t \equiv \frac{2}{3}, \quad v_f \equiv \frac{1}{4sc} \frac{2s}{3c}, \quad a_f \equiv \frac{1}{4sc}.$$

Concerning the QCD contribution to δ_t , we have (see [67] for the one-loop correction, [68, 69] for two-loop and three-loop corrections and [71, 72] for the four-loop contribution):

$$\begin{aligned} \delta_t^{\text{QCD},(1)}(\mu) &= \left(\frac{\alpha_s(\mu)}{\pi} \right) C_F \left(\frac{3}{4} \ln \frac{m_t^2}{\mu^2} - 1 \right), \\ \delta_t^{\text{QCD},(2)}(\mu) &= \left(\frac{\alpha_s(\mu)}{\pi} \right)^2 \left(C_F^2 z_m^{\text{FF}}(\mu) + C_F C_A z_m^{\text{FA}}(\mu) + C_F T n_l \ln \frac{m_t}{\mu} z_m^{\text{FL}}(\mu) + C_F T z_m^{\text{FH}}(\mu) \right), \\ \delta_t^{\text{QCD},(3)}(\mu) &= \left(\frac{\alpha_s(\mu)}{\pi} \right)^3 \left(z_m^{(3)}(m) + C_F^3 z_m^{\text{FFF}}(\mu) + C_F^2 C_A z_m^{\text{FFA}}(\mu) + C_F^2 T n_l \ln \frac{m_t^2}{\mu^2} z_m^{\text{FFL}}(\mu) \right. \\ &\quad + C_F^2 T z_m^{\text{FFH}}(\mu) + C_F C_A^2 z_m^{\text{FAA}}(\mu) + C_F C_A T n_l \ln \frac{m_t^2}{\mu^2} z_m^{\text{FAL}}(\mu) + C_F C_A T z_m^{\text{FAH}}(\mu) \\ &\quad \left. + C_F T^2 n_l^2 \ln^2 \frac{m_t^2}{\mu^2} z_m^{\text{FLL}}(\mu) + C_F T^2 n_l \ln \frac{m_t^2}{\mu^2} z_m^{\text{FLH}}(\mu) + C_F T^2 z_m^{\text{FHH}}(\mu) \right), \\ \delta_t^{\text{QCD},(4)}(\mu) &= \left(\frac{\alpha_s(\mu)}{\pi} \right)^4 \left(z_m^{(4)}(m) \right), \end{aligned}$$

where n_l represent the number of light quark flavours, $C_A = N_c = 3$ and $C_F = (N_c^2 - 1)/(2N_c) = 4/3$ are the Casimir operators of the adjoint and fundamental representation. The trace of the normalisation of the fundamental representation is $T = 1/2$. The indexes F, A and L shall remind the colour factors C_F , C_A and $T n_l$ respectively. H stands for the colour factor T.

The two-loop contributions are:

$$\begin{aligned} z_m^{\text{FF}}(\mu) &= \frac{7}{128} - \frac{15}{8} \zeta_2 - \frac{3}{4} \zeta_3 + 3 \zeta_2 \ln 2 - \frac{21}{32} \ln \frac{m_t^2}{\mu^2} + \frac{9}{32} \ln^2 \frac{m_t^2}{\mu^2}, \\ z_m^{\text{FA}}(\mu) &= -\frac{1111}{384} + \frac{1}{2} \zeta_2 + \frac{3}{8} \zeta_3 - \frac{3}{2} \zeta_2 \ln 2 + \frac{185}{96} \ln \frac{m_t^2}{\mu^2} - \frac{11}{32} \ln^2 \frac{m_t^2}{\mu^2}, \\ z_m^{\text{FL}}(\mu) &= \frac{71}{96} + \frac{1}{2} \zeta_2 - \frac{13}{24} \ln \frac{m_t^2}{\mu^2} + \frac{1}{8} \ln^2 \frac{m_t^2}{\mu^2}, \\ z_m^{\text{FH}}(\mu) &= \frac{143}{96} - \zeta_2 - \frac{13}{24} \ln \frac{m_t^2}{\mu^2} + \frac{1}{8} \ln^2 \frac{m_t^2}{\mu^2}. \end{aligned}$$

The $z_m^{(3)}(m)$ coefficient reads [215]:

$$\begin{aligned} z_m^{(3)}(m) = & -\frac{9478333}{93312} + \frac{55}{162} \ln^4 2 + \left(-\frac{644201}{6480} + \frac{587}{27} \ln 2 + \frac{44}{27} \ln^2 2 \right) \zeta_2 - \frac{61}{27} \zeta_3 \\ & + \frac{3475}{432} \zeta_4 + \frac{1439}{72} \zeta_2 \zeta_3 - \frac{1975}{216} \zeta_5 + \frac{220}{27} \alpha_4 + n_l \left[\frac{246643}{23328} - \frac{1}{81} \ln^4 2 \right. \\ & + \left. \left(\frac{967}{108} + \frac{22}{27} \ln 2 - \frac{4}{27} \ln^2 2 \right) + \frac{241}{72} \zeta_3 - \frac{305}{108} \zeta_4 - \frac{8}{27} \alpha_4 \right] \\ & + n_l^2 \left[-\frac{2353}{23328} - \frac{13}{54} \zeta_2 - \frac{7}{54} \zeta_3 \right], \end{aligned}$$

where $\alpha_4 = \text{Li}_4(1/2) \simeq 0.517479$, $\zeta_4 \equiv \zeta(4) \simeq 1.08232$ and $\zeta_5 \equiv \zeta(5) \simeq 1.03693$.

While the other three-loop corrections are:

$$\begin{aligned} z_m^{\text{FFF}}(\mu) &= -\frac{9}{128} \ln^3 \frac{m_t^2}{\mu^2} - \frac{27}{128} \ln^2 \frac{m_t^2}{\mu^2} - \left(-\frac{489}{512} + \frac{45}{32} \zeta_2 - \frac{9}{4} \zeta_2 \ln 2 + \frac{9}{16} \zeta_3 \right) \ln \frac{m_t^2}{\mu^2}, \\ z_m^{\text{FFA}}(\mu) &= \frac{33}{128} \ln^3 \frac{m_t^2}{\mu^2} + \frac{109}{64} \ln^2 \frac{m_t^2}{\mu^2} - \left(\frac{5813}{1536} - \frac{61}{16} \zeta_2 + \frac{53}{8} \zeta_2 \ln 2 - \frac{53}{32} \zeta_3 \right) \ln \frac{m_t^2}{\mu^2}, \\ z_m^{\text{FFL}}(\mu) &= -\frac{3}{32} \ln^3 \frac{m_t^2}{\mu^2} - \frac{13}{32} \ln^2 \frac{m_t^2}{\mu^2} - \left(\frac{65}{384} + \frac{7}{8} \zeta_2 - 2\zeta_2 \ln 2 - \frac{1}{4} \zeta_3 \right) \ln \frac{m_t^2}{\mu^2}, \\ z_m^{\text{FFH}}(\mu) &= -\frac{3}{32} \ln^3 \frac{m_t^2}{\mu^2} - \frac{13}{32} \ln^2 \frac{m_t^2}{\mu^2} - \left(-\frac{151}{384} + 2\zeta_2 - 2\zeta_2 \ln 2 - \frac{1}{4} \zeta_3 \right) \ln \frac{m_t^2}{\mu^2}, \\ z_m^{\text{FAA}}(\mu) &= -\frac{121}{576} \ln^3 \frac{m_t^2}{\mu^2} - \frac{2341}{1152} \ln^2 \frac{m_t^2}{\mu^2} - \left(-\frac{13243}{1728} + \frac{11}{12} \zeta_2 - \frac{11}{4} \zeta_2 \ln 2 + \frac{11}{16} \zeta_3 \right) \ln \frac{m_t^2}{\mu^2}, \\ z_m^{\text{FAL}}(\mu) &= \frac{11}{72} \ln^3 \frac{m_t^2}{\mu^2} + \frac{373}{288} \ln^2 \frac{m_t^2}{\mu^2} - \left(\frac{869}{216} + \frac{7}{12} \zeta_2 + \zeta_2 \ln 2 + \frac{1}{2} \zeta_3 \right) \ln \frac{m_t^2}{\mu^2}, \\ z_m^{\text{FAH}}(\mu) &= \frac{11}{72} \ln^3 \frac{m_t^2}{\mu^2} + \frac{373}{288} \ln^2 \frac{m_t^2}{\mu^2} - \left(\frac{583}{108} - \frac{13}{6} \zeta_2 + \zeta_2 \ln 2 + \frac{1}{2} \zeta_3 \right) \ln \frac{m_t^2}{\mu^2}, \\ z_m^{\text{FLL}}(\mu) &= -\frac{1}{36} \ln^3 \frac{m_t^2}{\mu^2} - \frac{13}{72} \ln^2 \frac{m_t^2}{\mu^2} - \left(-\frac{89}{216} - \frac{1}{3} \zeta_2 \right) \ln \frac{m_t^2}{\mu^2}, \\ z_m^{\text{FHL}}(\mu) &= -\frac{1}{18} \ln^3 \frac{m_t^2}{\mu^2} - \frac{13}{36} \ln^2 \frac{m_t^2}{\mu^2} - \left(-\frac{143}{108} + \frac{1}{3} \zeta_2 \right) \ln \frac{m_t^2}{\mu^2}, \\ z_m^{\text{FHH}}(\mu) &= -\frac{1}{36} \ln^3 \frac{m_t^2}{\mu^2} - \frac{13}{72} \ln^2 \frac{m_t^2}{\mu^2} - \left(-\frac{197}{216} + \frac{2}{3} \zeta_2 \right) \ln \frac{m_t^2}{\mu^2}, \end{aligned}$$

where $\zeta_2 \equiv \zeta(2) \simeq 1.64493$.

The four-loop contribution is:

$$z_m^{(4)}(m) = 859.96 + 328.94 \ln \frac{m_t^2}{\mu^2} + 50.856 \ln^2 \frac{m_t^2}{\mu^2} + 6.4922 \ln^3 \frac{m_t^2}{\mu^2} + 0.33203 \ln^4 \frac{m_t^2}{\mu^2}.$$

C

TWO-LOOP EFFECTIVE POTENTIAL

The two-loop correction, in the approximation $\lambda = 0$, is given by [4]:

$$\begin{aligned}
 \lambda_{\text{eff}}^{(2)} = & \frac{1}{(4\pi)^2} \left[8g_3^2 h_t^4 (3r_t^2 - 8r_t + 9) + \frac{1}{2} h_t^6 (-6r_t r_W - 3r_t^2 + 48r_t - 6r_t r_Z - 69 - \pi^2) \right. \\
 & + \frac{3h_t^2 g^4}{16} (8r_W + 4r_Z - 3r_t^2 - 6r_t r_Z - 12r_t + 12r_t r_W + 15 + 2\pi^2) \\
 & + \frac{h_t^2 g'^4}{48} (27r_t^2 - 54r_t r_Z - 68r_t - 28r_Z + 189) + \frac{h_t^2 g^2 g'^2}{8} (9r_t^2 - 18r_t r_Z + 4r_t + 44r_Z - 57) \\
 & + \frac{g^6}{192} (36r_t r_Z + 54r_t^2 - 414r_W r_Z + 69r_W^2 + 1264r_W + 156r_Z^2 + 632r_Z - 144r_t r_W - 2067 + 90\pi^2) \\
 & + \frac{g^4 g'^2}{192} (12r_t r_Z - 6r_t^2 - 6r_W (53r_Z + 50) + 213r_W^2 + 4r_Z (57r_Z - 91) + 817 + 46\pi^2) \\
 & + \frac{g^2 g'^4}{576} (132r_t r_Z - 66r_t^2 + 306r_W r_Z - 153r_W^2 - 36r_W + 924r_Z^2 - 4080r_Z + 4359 + 218\pi^2) \\
 & + \frac{g'^6}{576} (6r_Z (34r_t + 3r_W - 470) - 102r_t^2 - 9r_W^2 + 708r_Z^2 + 2883 + 206\pi^2) \\
 & + \frac{h_t^4}{6} (4g'^2 (3r_t^2 - 8r_t + 9) - 9g^2 (r_t - r_W + 1)) + \frac{3}{4} (g'^6 - 3g^4 h_t^2 + 4h_t^6) \text{Li}_2 \left(\frac{g^2}{2h_t^2} \right) \\
 & + \frac{h_t^2}{48} \psi \left(\frac{g^2 + g'^2}{2h_t^2} \right) \left(9g^4 - 6g^2 g'^2 + 17g'^4 + 2h_t^2 \left(7g'^2 - 73g^2 + \frac{64g^4}{g'^2 + g^2} \right) \right) \\
 & \left. + \frac{g^2}{64} \psi \left(\frac{g^2 + g'^2}{g^2} \right) \left(18g^2 g'^2 + g'^4 - 51g^4 - \frac{48g^6}{g'^2 + g^2} \right) \right],
 \end{aligned}$$

where¹

$$\begin{aligned}
 \psi(z) \equiv & \sqrt{z^2 - 4z} \left[2 \ln^2 \left(\frac{z - \sqrt{z^2 - 4z}}{2z} \right) - \ln^2 z - 4 \text{Li}_2 \left(\frac{z - \sqrt{z^2 - 4z}}{2z} \right) + \frac{\pi^2}{3} \right], \\
 \text{Li}_2(z) \equiv & \int_z^0 \frac{\ln(1-t)}{t} dt,
 \end{aligned}$$

and

$$\begin{aligned}
 r_W & \equiv \ln \left(\frac{2g^2}{4} \right) + 2\Gamma, \\
 r_Z & \equiv \ln \left(\frac{g^2 + g'^2}{4} \right) + 2\Gamma, \\
 r_t & \equiv \ln \left(\frac{h_t^2}{2} \right) + 2\Gamma, \\
 r_{tW} & \equiv (r_t - r_W) \left[\ln \left(\frac{h_t^2}{2} - \frac{g^2}{4} \right) + 2\Gamma \right].
 \end{aligned}$$

¹ Li_2 is the dilogarithmic function, which can be defined by the sum $\text{Li}_2(z) = \sum_k z^k/k^2$, $k = 1, 2, \dots$ [214].

BIBLIOGRAPHY

- [1] G. Jacobellis, I. Masina, Stationary configurations of the Standard Model Higgs potential: electroweak stability and rising inflection point, *Phys. Rev. D* 94 (2016) 073005. [arXiv:1604.06046](#), [doi:10.1103/PhysRevD.94.073005](#).
- [2] A. V. Bednyakov, B. A. Kniehl, A. F. Pikelner, O. L. Veretin, Stability of the Electroweak Vacuum: Gauge Independence and Advanced Precision, *Phys. Rev. Lett.* 115 (20) (2015) 201802. [arXiv:1507.08833](#), [doi:10.1103/PhysRevLett.115.201802](#).
- [3] G. Degrassi, S. Di Vita, J. Elias-Miro, J. R. Espinosa, G. F. Giudice, et al., Higgs mass and vacuum stability in the Standard Model at NNLO, *JHEP* 1208 (2012) 098. [arXiv:1205.6497](#), [doi:10.1007/JHEP08\(2012\)098](#).
- [4] D. Buttazzo, G. Degrassi, P. P. Giardino, G. F. Giudice, F. Sala, A. Salvio, A. Strumia, Investigating the near-criticality of the Higgs boson, *JHEP* 12 (2013) 089. [arXiv:1307.3536](#), [doi:10.1007/JHEP12\(2013\)089](#).
- [5] S. M. Boucenna, S. Morisi, Q. Shafi, J. W. F. Valle, Inflation and majoron dark matter in the seesaw mechanism, *Phys. Rev. D* 90 (5) (2014) 055023. [arXiv:1404.3198](#), [doi:10.1103/PhysRevD.90.055023](#).
- [6] K. Bhattacharya, J. Chakraborty, S. Das, T. Mondal, Higgs vacuum stability and inflationary dynamics after BICEP2 and PLANCK dust polarisation data, *JCAP* 1412 (12) (2014) 001. [arXiv:1408.3966](#), [doi:10.1088/1475-7516/2014/12/001](#).
- [7] G. Ballesteros, C. Tamarit, Higgs portal valleys, stability and inflation, *JHEP* 09 (2015) 210. [arXiv:1505.07476](#), [doi:10.1007/JHEP09\(2015\)210](#).
- [8] J. Fumagalli, M. Postma, UV (in)sensitivity of Higgs inflation, *JHEP* 05 (2016) 049. [arXiv:1602.07234](#), [doi:10.1007/JHEP05\(2016\)049](#).
- [9] **ATLAS**, G. Aad, et al., Observation of a new particle in the search for the Standard Model Higgs boson with the ATLAS detector at the LHC, *Physics Letters B* 716 (2012) 1 – 29. [doi:http://dx.doi.org/10.1016/j.physletb.2012.08.020](#).
- [10] **CMS**, S. Chatrchyan, et al., Observation of a new boson at a mass of 125 GeV with the CMS experiment at the LHC, *Physics Letters B* 716 (2012) 30–61. [doi:http://dx.doi.org/10.1016/j.physletb.2012.08.021](#).
- [11] P. P. Giardino, K. Kannike, I. Masina, M. Raidal, A. Strumia, The universal Higgs fit, *JHEP* 05 (2014) 046. [arXiv:1303.3570](#), [doi:10.1007/JHEP05\(2014\)046](#).
- [12] I. Masina, Higgs boson and top quark masses as tests of electroweak vacuum stability, *Phys. Rev. D* 87 (5) (2013) 053001. [arXiv:1209.0393](#), [doi:10.1103/PhysRevD.87.053001](#).

- [13] A. Kobakhidze, A. Spencer-Smith, Electroweak Vacuum (In)Stability in an Inflationary Universe, *Phys. Lett. B* 722 (2013) 130–134. [arXiv:1301.2846](#), [doi:10.1016/j.physletb.2013.04.013](#).
- [14] J. R. Espinosa, G. F. Giudice, E. Morgante, A. Riotto, L. Senatore, A. Strumia, N. Tetradis, The cosmological Higgstory of the vacuum instability, *JHEP* 09 (2015) 174. [arXiv:1505.04825](#), [doi:10.1007/JHEP09\(2015\)174](#).
- [15] C. Gross, O. Lebedev, M. Zatta, Higgs–inflaton coupling from reheating and the metastable Universe, *Phys. Lett. B* 753 (2016) 178–181. [arXiv:1506.05106](#), [doi:10.1016/j.physletb.2015.12.014](#).
- [16] M. Fairbairn, P. Grothaus, R. Hogan, The Problem with False Vacuum Higgs Inflation, *JCAP* 1406 (2014) 039. [arXiv:1403.7483](#), [doi:10.1088/1475-7516/2014/06/039](#).
- [17] I. Masina, A. Notari, Inflation from the Higgs field false vacuum with hybrid potential, *JCAP* 1211 (2012) 031. [arXiv:1204.4155](#), [doi:10.1088/1475-7516/2012/11/031](#).
- [18] I. Masina, A. Notari, Standard Model False Vacuum Inflation: Correlating the Tensor-to-Scalar Ratio to the Top Quark and Higgs Boson masses, *Phys.Rev.Lett.* 108 (2012) 191302. [arXiv:1112.5430](#), [doi:10.1103/PhysRevLett.108.191302](#).
- [19] I. Masina, A. Notari, The Higgs mass range from Standard Model false vacuum Inflation in scalar-tensor gravity, *Phys.Rev. D* 85 (2012) 123506. [arXiv:1112.2659](#), [doi:10.1103/PhysRevD.85.123506](#).
- [20] F. Bezrukov, M. Shaposhnikov, The Standard Model Higgs boson as the inflaton, *Phys.Lett. B* 659 (2008) 703–706. [arXiv:0710.3755](#), [doi:10.1016/j.physletb.2007.11.072](#).
- [21] S. L. Glashow, Partial-symmetries of weak interactions, *Nuclear Physics* 22 (4) (1961) 579 – 588. [doi:10.1016/0029-5582\(61\)90469-2](#).
- [22] S. Weinberg, A model of leptons, *Phys. Rev. Lett.* 19 (1967) 1264–1266. [doi:10.1103/PhysRevLett.19.1264](#).
- [23] A. Salam, Weak and Electromagnetic Interactions, *Conf. Proc.* C680519 (1968) 367–377.
- [24] F. Halzen, A. D. Martin, *Quarks and Leptons: an introductory course in modern particle physics*, 1984.
- [25] K. A. Olive, et al., Review of Particle Physics, *Chin. Phys.* C38 (2014) 090001. [doi:10.1088/1674-1137/38/9/090001](#).
- [26] P. Higgs, Broken symmetries, massless particles and gauge fields, *Physics Letters* 12 (2) (1964) 132 – 133. [doi:10.1016/0031-9163\(64\)91136-9](#).
- [27] F. Englert, R. Brout, Broken symmetry and the mass of gauge vector mesons, *Phys. Rev. Lett.* 13 (1964) 321–323. [doi:10.1103/PhysRevLett.13.321](#).

- [28] G. Costa, G. Fogli, Symmetries and group theory in particle physics. An introduction to space-time and internal symmetries, *Lect. Notes Phys.* 823 (2012) 1–288. doi:[10.1007/978-3-642-15482-9](https://doi.org/10.1007/978-3-642-15482-9).
- [29] G. 't Hooft, Renormalization of Massless Yang-Mills Fields, *Nucl. Phys.* B33 (1971) 173–199. doi:[10.1016/0550-3213\(71\)90395-6](https://doi.org/10.1016/0550-3213(71)90395-6).
- [30] G. 't Hooft, Renormalizable Lagrangians for Massive Yang-Mills Fields, *Nucl. Phys.* B35 (1971) 167–188. doi:[10.1016/0550-3213\(71\)90139-8](https://doi.org/10.1016/0550-3213(71)90139-8).
- [31] ATLAS, CMS, G. Aad, et al., Combined Measurement of the Higgs Boson Mass in pp Collisions at $\sqrt{s} = 7$ and 8 TeV with the ATLAS and CMS Experiments, *Phys. Rev. Lett.* 114 (2015) 191803. arXiv:[1503.07589](https://arxiv.org/abs/1503.07589), doi:[10.1103/PhysRevLett.114.191803](https://doi.org/10.1103/PhysRevLett.114.191803).
- [32] C. Ford, I. Jack, D. R. T. Jones, The Standard model effective potential at two loops, *Nucl. Phys.* B387 (1992) 373–390, [Erratum: *Nucl. Phys.*B504,551(1997)]. arXiv:[hep-ph/0111190](https://arxiv.org/abs/hep-ph/0111190), doi:[10.1016/0550-3213\(92\)90165-8](https://doi.org/10.1016/0550-3213(92)90165-8).
- [33] T. van Ritbergen, J. A. M. Vermaseren, S. A. Larin, The four loop β -function in quantum chromodynamics, *Phys. Lett.* B400 (1997) 379–384. arXiv:[hep-ph/9701390](https://arxiv.org/abs/hep-ph/9701390), doi:[10.1016/S0370-2693\(97\)00370-5](https://doi.org/10.1016/S0370-2693(97)00370-5).
- [34] M. Czakon, The four-loop QCD β -function and anomalous dimensions, *Nucl. Phys.* B710 (2005) 485–498. arXiv:[hep-ph/0411261](https://arxiv.org/abs/hep-ph/0411261), doi:[10.1016/j.nuclphysb.2005.01.012](https://doi.org/10.1016/j.nuclphysb.2005.01.012).
- [35] D. J. Gross, F. Wilczek, Ultraviolet Behavior of Nonabelian Gauge Theories, *Phys. Rev. Lett.* 30 (1973) 1343–1346. doi:[10.1103/PhysRevLett.30.1343](https://doi.org/10.1103/PhysRevLett.30.1343).
- [36] D. J. Gross, F. Wilczek, Asymptotically Free Gauge Theories, *Phys. Rev.* D8 (1973) 3633–3652. doi:[10.1103/PhysRevD.8.3633](https://doi.org/10.1103/PhysRevD.8.3633).
- [37] H. D. Politzer, Reliable Perturbative Results for Strong Interactions?, *Phys. Rev. Lett.* 30 (1973) 1346–1349. doi:[10.1103/PhysRevLett.30.1346](https://doi.org/10.1103/PhysRevLett.30.1346).
- [38] D. R. T. Jones, Two Loop Diagrams in Yang-Mills Theory, *Nucl. Phys.* B75 (1974) 531. doi:[10.1016/0550-3213\(74\)90093-5](https://doi.org/10.1016/0550-3213(74)90093-5).
- [39] W. E. Caswell, Asymptotic Behavior of Nonabelian Gauge Theories to Two Loop Order, *Phys. Rev. Lett.* 33 (1974) 244. doi:[10.1103/PhysRevLett.33.244](https://doi.org/10.1103/PhysRevLett.33.244).
- [40] O. V. Tarasov, A. A. Vladimirov, Two Loop Renormalization of the Yang-Mills Theory in an Arbitrary Gauge, *Sov. J. Nucl. Phys.* 25 (1977) 585, [*Yad. Fiz.*25, 1104 (1977)].
- [41] O. V. Tarasov, A. A. Vladimirov, A. Yu. Zharkov, The Gell-Mann-Low Function of QCD in the Three Loop Approximation, *Phys. Lett.* B93 (1980) 429–432. doi:[10.1016/0370-2693\(80\)90358-5](https://doi.org/10.1016/0370-2693(80)90358-5).
- [42] M. Fischler, J. Oliensis, Two-loop corrections to the β -function for the Higgs-Yukawa coupling constant, *Physics Letters B* 119 (4) (1982) 385 – 386. doi:[http://dx.doi.org/10.1016/0370-2693\(82\)90695-5](http://dx.doi.org/10.1016/0370-2693(82)90695-5).

- [43] M. E. Machacek, M. T. Vaughn, Two Loop Renormalization Group Equations in a General Quantum Field Theory. 1. Wave Function Renormalization, Nucl. Phys. B222 (1983) 83. doi:[10.1016/0550-3213\(83\)90610-7](https://doi.org/10.1016/0550-3213(83)90610-7).
- [44] M. E. Machacek, M. T. Vaughn, Two Loop Renormalization Group Equations in a General Quantum Field Theory. 2. Yukawa Couplings, Nucl. Phys. B236 (1984) 221. doi:[10.1016/0550-3213\(84\)90533-9](https://doi.org/10.1016/0550-3213(84)90533-9).
- [45] M. E. Machacek, M. T. Vaughn, Two Loop Renormalization Group Equations in a General Quantum Field Theory. 3. Scalar Quartic Couplings, Nucl. Phys. B249 (1985) 70. doi:[10.1016/0550-3213\(85\)90040-9](https://doi.org/10.1016/0550-3213(85)90040-9).
- [46] S. A. Larin, J. A. M. Vermaseren, The three loop QCD β -function and anomalous dimensions, Phys. Lett. B303 (1993) 334–336. arXiv:[hep-ph/9302208](https://arxiv.org/abs/hep-ph/9302208), doi:[10.1016/0370-2693\(93\)91441-0](https://doi.org/10.1016/0370-2693(93)91441-0).
- [47] M.-X. Luo, Y. Xiao, Two loop renormalization group equations in the standard model, Phys. Rev. Lett. 90 (2003) 011601. arXiv:[hep-ph/0207271](https://arxiv.org/abs/hep-ph/0207271), doi:[10.1103/PhysRevLett.90.011601](https://doi.org/10.1103/PhysRevLett.90.011601).
- [48] L. N. Mihaila, J. Salomon, M. Steinhauser, Renormalization constants and β -functions for the gauge couplings of the Standard Model to three-loop order, Phys. Rev. D86 (2012) 096008. arXiv:[1208.3357](https://arxiv.org/abs/1208.3357), doi:[10.1103/PhysRevD.86.096008](https://doi.org/10.1103/PhysRevD.86.096008).
- [49] L. N. Mihaila, J. Salomon, M. Steinhauser, Gauge Coupling β -functions in the Standard Model to Three Loops, Phys. Rev. Lett. 108 (2012) 151602. arXiv:[1201.5868](https://arxiv.org/abs/1201.5868), doi:[10.1103/PhysRevLett.108.151602](https://doi.org/10.1103/PhysRevLett.108.151602).
- [50] K. G. Chetyrkin, M. F. Zoller, Three-loop β -functions for top-Yukawa and the Higgs self-interaction in the Standard Model, JHEP 06 (2012) 033. arXiv:[1205.2892](https://arxiv.org/abs/1205.2892), doi:[10.1007/JHEP06\(2012\)033](https://doi.org/10.1007/JHEP06(2012)033).
- [51] K. G. Chetyrkin, M. F. Zoller, β -function for the Higgs self-interaction in the Standard Model at three-loop level, JHEP 04 (2013) 091, [Erratum: JHEP09,155(2013)]. arXiv:[1303.2890](https://arxiv.org/abs/1303.2890), doi:[10.1007/JHEP04\(2013\)091](https://doi.org/10.1007/JHEP04(2013)091), [10.1007/JHEP09\(2013\)155](https://doi.org/10.1007/JHEP09(2013)155).
- [52] A. V. Bednyakov, A. F. Pikelner, V. N. Velizhanin, Higgs self-coupling β -function in the Standard Model at three loops, Nucl. Phys. B875 (2013) 552–565. arXiv:[1303.4364](https://arxiv.org/abs/1303.4364), doi:[10.1016/j.nuclphysb.2013.07.015](https://doi.org/10.1016/j.nuclphysb.2013.07.015).
- [53] A. V. Bednyakov, A. F. Pikelner, V. N. Velizhanin, Yukawa coupling β -functions in the Standard Model at three loops, Phys. Lett. B722 (2013) 336–340. arXiv:[1212.6829](https://arxiv.org/abs/1212.6829), doi:[10.1016/j.physletb.2013.04.038](https://doi.org/10.1016/j.physletb.2013.04.038).
- [54] A. V. Bednyakov, A. F. Pikelner, V. N. Velizhanin, Three-loop Higgs self-coupling β -function in the Standard Model with complex Yukawa matrices, Nucl. Phys. B879 (2014) 256–267. arXiv:[1310.3806](https://arxiv.org/abs/1310.3806), doi:[10.1016/j.nuclphysb.2013.12.012](https://doi.org/10.1016/j.nuclphysb.2013.12.012).
- [55] A. V. Bednyakov, A. F. Pikelner, V. N. Velizhanin, Three-loop SM β -functions for matrix Yukawa couplings, Phys. Lett. B737 (2014) 129–134. arXiv:[1406.7171](https://arxiv.org/abs/1406.7171), doi:[10.1016/j.physletb.2014.08.049](https://doi.org/10.1016/j.physletb.2014.08.049).

- [56] M. F. Zoller, Top-Yukawa effects on the β -function of the strong coupling in the SM at four-loop level, JHEP 02 (2016) 095. [arXiv:1508.03624](#), [doi:10.1007/JHEP02\(2016\)095](#).
- [57] A. V. Bednyakov, A. F. Pikelner, Four-loop strong coupling β -function in the Standard Model, Phys. Lett. B762 (2016) 151–156. [arXiv:1508.02680](#), [doi:10.1016/j.physletb.2016.09.007](#).
- [58] K. G. Chetyrkin, M. F. Zoller, Leading QCD-induced four-loop contributions to the β -function of the Higgs self-coupling in the SM and vacuum stability, JHEP 06 (2016) 175. [arXiv:1604.00853](#), [doi:10.1007/JHEP06\(2016\)175](#).
- [59] S. Bethke, G. Dissertori, G. P. Salam, Particle Data Group review on Quantum Chromodynamics, revised version of September 2015. .
URL <http://pdg.lbl.gov/2015/reviews/rpp2015-rev-qcd.pdf>
- [60] G. Rodrigo, A. Santamaria, QCD matching conditions at thresholds, Phys. Lett. B313 (1993) 441–446. [arXiv:hep-ph/9305305](#), [doi:10.1016/0370-2693\(93\)90016-B](#).
- [61] Y. Schroder, M. Steinhauser, Four-loop decoupling relations for the strong coupling, JHEP 01 (2006) 051. [arXiv:hep-ph/0512058](#), [doi:10.1088/1126-6708/2006/01/051](#).
- [62] K. G. Chetyrkin, J. H. Kuhn, C. Sturm, QCD decoupling at four loops, Nucl. Phys. B744 (2006) 121–135. [arXiv:hep-ph/0512060](#), [doi:10.1016/j.nuclphysb.2006.03.020](#).
- [63] F. Bezrukov, M. Yu. Kalmykov, B. A. Kniehl, M. Shaposhnikov, Higgs Boson Mass and New Physics, JHEP 10 (2012) 140. [arXiv:1205.2893](#), [doi:10.1007/JHEP10\(2012\)140](#).
- [64] A. Sirlin, R. Zucchini, Dependence of the Quartic Coupling λ_H on M_H and the Possible Onset of New Physics in the Higgs Sector of the Standard Model, Nucl. Phys. B266 (1986) 389. [doi:10.1016/0550-3213\(86\)90096-9](#).
- [65] B. A. Kniehl, A. F. Pikelner, O. L. Veretin, Two-loop electroweak threshold corrections in the Standard Model, Nucl. Phys. B896 (2015) 19–51. [arXiv:1503.02138](#), [doi:10.1016/j.nuclphysb.2015.04.010](#).
- [66] S. Alekhin, A. Djouadi, S. Moch, The top quark and Higgs boson masses and the stability of the electroweak vacuum, Phys. Lett. B716 (2012) 214–219. [arXiv:1207.0980](#), [doi:10.1016/j.physletb.2012.08.024](#).
- [67] R. Hempfling, B. A. Kniehl, On the relation between the fermion pole mass and \overline{MS} Yukawa coupling in the standard model, Phys. Rev. D51 (1995) 1386–1394. [arXiv:hep-ph/9408313](#), [doi:10.1103/PhysRevD.51.1386](#).
- [68] K. G. Chetyrkin, M. Steinhauser, The Relation between the \overline{MS} -bar and the on-shell quark mass at order α_s^3 , Nucl. Phys. B573 (2000) 617–651. [arXiv:hep-ph/9911434](#), [doi:10.1016/S0550-3213\(99\)00784-1](#).

- [69] K. G. Chetyrkin, J. H. Kuhn, M. Steinhauser, RunDec: A Mathematica package for running and decoupling of the strong coupling and quark masses, *Comput. Phys. Commun.* 133 (2000) 43–65. [arXiv:hep-ph/0004189](#), [doi:10.1016/S0010-4655\(00\)00155-7](#).
- [70] K. G. Chetyrkin, M. Steinhauser, Short distance mass of a heavy quark at order α_s^3 , *Phys. Rev. Lett.* 83 (1999) 4001–4004. [arXiv:hep-ph/9907509](#), [doi:10.1103/PhysRevLett.83.4001](#).
- [71] P. Marquard, A. V. Smirnov, V. A. Smirnov, M. Steinhauser, Quark Mass Relations to Four-Loop Order in Perturbative QCD, *Phys. Rev. Lett.* 114 (14) (2015) 142002. [arXiv:1502.01030](#), [doi:10.1103/PhysRevLett.114.142002](#).
- [72] A. L. Kataev, V. S. Molokoedov, On the flavour dependence of the $\mathcal{O}(\alpha_s^4)$ correction to the relation between running and pole heavy quark masses, *Eur. Phys. J. Plus* 131 (8) (2016) 271. [arXiv:1511.06898](#), [doi:10.1140/epjp/i2016-16271-7](#).
- [73] F. Jegerlehner, M. Yu. Kalmykov, $\mathcal{O}(\alpha\alpha_s)$ correction to the pole mass of the t quark within the standard model, *Nucl. Phys. B* 676 (2004) 365–389. [arXiv:hep-ph/0308216](#), [doi:10.1016/j.nuclphysb.2003.10.012](#).
- [74] ATLAS, G. Aad, et al., First combination of Tevatron and LHC measurements of the top-quark mass. [arXiv:1403.4427](#).
- [75] S. Moch, et al., High precision fundamental constants at the TeV scale. [arXiv:1405.4781](#).
- [76] A. H. Hoang, I. W. Stewart, Top Mass Measurements from Jets and the Tevatron Top-Quark Mass, *Nucl. Phys. Proc. Suppl.* 185 (2008) 220–226. [arXiv:0808.0222](#), [doi:10.1016/j.nuclphysbps.2008.10.028](#).
- [77] P. Nason, Theory Summary, *PoS TOP2015* (2016) 056. [arXiv:1602.00443](#).
- [78] G. Corcella, Interpretation of the top-quark mass measurements: a theory overview, in: 8th International Workshop on Top Quark Physics (TOP2015) Ischia, NA, Italy, September 14–18, 2015, 2015. [arXiv:1511.08429](#).
- [79] S. Fleming, A. H. Hoang, S. Mantry, I. W. Stewart, Top Jets in the Peak Region: Factorization Analysis with NLL Resummation, *Phys. Rev. D* 77 (2008) 114003. [arXiv:0711.2079](#), [doi:10.1103/PhysRevD.77.114003](#).
- [80] J. A. Casas, J. R. Espinosa, M. Quiros, Standard model stability bounds for new physics within LHC reach, *Phys. Lett. B* 382 (1996) 374–382. [arXiv:hep-ph/9603227](#), [doi:10.1016/0370-2693\(96\)00682-X](#).
- [81] S. Coleman, E. Weinberg, Radiative corrections as the origin of spontaneous symmetry breaking, *Phys. Rev. D* 7 (1973) 1888–1910. [doi:10.1103/PhysRevD.7.1888](#).
- [82] L. Di Luzio, L. Mihaila, On the gauge dependence of the Standard Model vacuum instability scale, *JHEP* 06 (2014) 079. [arXiv:1404.7450](#), [doi:10.1007/JHEP06\(2014\)079](#).

- [83] R. Jackiw, Functional evaluation of the effective potential, *Phys. Rev. D* 9 (1974) 1686–1701. doi:[10.1103/PhysRevD.9.1686](https://doi.org/10.1103/PhysRevD.9.1686).
- [84] N. K. Nielsen, On the gauge dependence of spontaneous symmetry breaking in gauge theories, *Nucl. Phys. B* 101 (1975) 173 – 188. doi:[10.1016/0550-3213\(75\)90301-6](https://doi.org/10.1016/0550-3213(75)90301-6).
- [85] A. Andreassen, W. Frost, M. D. Schwartz, Consistent Use of Effective Potentials, *Phys. Rev. D* 91 (1) (2015) 016009. arXiv:[1408.0287](https://arxiv.org/abs/1408.0287), doi:[10.1103/PhysRevD.91.016009](https://doi.org/10.1103/PhysRevD.91.016009).
- [86] A. Andreassen, W. Frost, M. D. Schwartz, Consistent Use of the Standard Model Effective Potential, *Phys. Rev. Lett.* 113 (24) (2014) 241801. arXiv:[1408.0292](https://arxiv.org/abs/1408.0292), doi:[10.1103/PhysRevLett.113.241801](https://doi.org/10.1103/PhysRevLett.113.241801).
- [87] M. Quiros, Electroweak vacuum, Lecture presented at the “Niccoló Cabeo school”, Ferrara (Italy), 2014.
- [88] K. G. Wilson, J. B. Kogut, The Renormalization group and the epsilon expansion, *Phys. Rept.* 12 (1974) 75–200. doi:[10.1016/0370-1573\(74\)90023-4](https://doi.org/10.1016/0370-1573(74)90023-4).
- [89] A. Djouadi, The Anatomy of electro-weak symmetry breaking. I: The Higgs boson in the standard model, *Phys. Rept.* 457 (2008) 1–216. arXiv:[hep-ph/0503172](https://arxiv.org/abs/hep-ph/0503172), doi:[10.1016/j.physrep.2007.10.004](https://doi.org/10.1016/j.physrep.2007.10.004).
- [90] T. Hambye, K. Riesselmann, Matching conditions and Higgs mass upper bounds revisited, *Phys. Rev. D* 55 (1997) 7255–7262. arXiv:[hep-ph/9610272](https://arxiv.org/abs/hep-ph/9610272), doi:[10.1103/PhysRevD.55.7255](https://doi.org/10.1103/PhysRevD.55.7255).
- [91] D. Buttazzo, Implications of the discovery of a Higgs boson with a mass of 125 GeV, Ph.D. thesis, Pisa, Scuola Normale Superiore (2014). arXiv:[1403.6535](https://arxiv.org/abs/1403.6535).
- [92] G. 't Hooft, Naturalness, chiral symmetry, and spontaneous chiral symmetry breaking, *NATO Sci. Ser. B* 59 (1980) 135.
- [93] M. J. G. Veltman, The Infrared - Ultraviolet Connection, *Acta Phys. Polon.* B12 (1981) 437.
- [94] G. F. Giudice, R. Rattazzi, Living Dangerously with Low-Energy Supersymmetry, *Nucl. Phys. B* 757 (2006) 19–46. arXiv:[hep-ph/0606105](https://arxiv.org/abs/hep-ph/0606105), doi:[10.1016/j.nuclphysb.2006.07.031](https://doi.org/10.1016/j.nuclphysb.2006.07.031).
- [95] R. Barbieri, G. Giudice, Upper bounds on supersymmetric particle masses, *Nuclear Physics B* 306 (1) (1988) 63 – 76. doi:[doi.org/10.1016/0550-3213\(88\)90171-X](https://doi.org/10.1016/0550-3213(88)90171-X).
- [96] I. Masina, M. Quiros, On the Veltman Condition, the Hierarchy Problem and High-Scale Supersymmetry, *Phys. Rev. D* 88 (2013) 093003. arXiv:[1308.1242](https://arxiv.org/abs/1308.1242), doi:[10.1103/PhysRevD.88.093003](https://doi.org/10.1103/PhysRevD.88.093003).

- [97] J. R. Espinosa, C. Grojean, G. Panico, A. Pomarol, O. Pujolàs, G. Servant, Cosmological Higgs-Axion Interplay for a Naturally Small Electroweak Scale, *Phys. Rev. Lett.* 115 (25) (2015) 251803. [arXiv:1506.09217](#), [doi:10.1103/PhysRevLett.115.251803](#).
- [98] A. Sadeghi, M. Torabian, Emergent Weak Scale from Cosmological Evolution and Dimensional Transmutation. [arXiv:1512.02948](#).
- [99] K. A. Meissner, H. Nicolai, Conformal Symmetry and the Standard Model, *Phys. Lett. B* 648 (2007) 312–317. [arXiv:hep-th/0612165](#), [doi:10.1016/j.physletb.2007.03.023](#).
- [100] J. Elias-Miro, J. R. Espinosa, G. F. Giudice, G. Isidori, A. Riotto, A. Strumia, Higgs mass implications on the stability of the electroweak vacuum, *Phys. Lett. B* 709 (2012) 222–228. [arXiv:1112.3022](#), [doi:10.1016/j.physletb.2012.02.013](#).
- [101] P. Q. Hung, Vacuum Instability and New Constraints on Fermion Masses, *Phys. Rev. Lett.* 42 (1979) 873. [doi:10.1103/PhysRevLett.42.873](#).
- [102] N. Cabibbo, L. Maiani, G. Parisi, R. Petronzio, Bounds on the Fermions and Higgs Boson Masses in Grand Unified Theories, *Nucl. Phys. B* 158 (1979) 295–305. [doi:10.1016/0550-3213\(79\)90167-6](#).
- [103] V. Branchina, E. Messina, Stability, Higgs Boson Mass and New Physics, *Phys. Rev. Lett.* 111 (2013) 241801. [arXiv:1307.5193](#), [doi:10.1103/PhysRevLett.111.241801](#).
- [104] V. Branchina, E. Messina, A. Platania, Top mass determination, Higgs inflation, and vacuum stability, *JHEP* 09 (2014) 182. [arXiv:1407.4112](#), [doi:10.1007/JHEP09\(2014\)182](#).
- [105] V. Branchina, E. Messina, Stability and UV completion of the Standard Model. [arXiv:1507.08812](#).
- [106] C. D. Froggatt, H. B. Nielsen, Standard model criticality prediction: Top mass 173 ± 5 GeV and Higgs mass 135 ± 9 GeV, *Phys. Lett. B* 368 (1996) 96–102. [arXiv:hep-ph/9511371](#), [doi:10.1016/0370-2693\(95\)01480-2](#).
- [107] S. Coleman, Fate of the false vacuum: Semiclassical theory, *Phys. Rev. D* 15 (1977) 2929–2936. [doi:10.1103/PhysRevD.15.2929](#).
- [108] C. G. Callan, S. Coleman, Fate of the false vacuum. ii. first quantum corrections, *Phys. Rev. D* 16 (1977) 1762–1768. [doi:10.1103/PhysRevD.16.1762](#).
- [109] **Planck**, P. A. R. Ade, et al., Planck 2015 results. XIII. Cosmological parameters. [arXiv:1502.01589](#).
- [110] G. Isidori, G. Ridolfi, A. Strumia, On the metastability of the standard model vacuum, *Nucl. Phys. B* 609 (2001) 387–409. [arXiv:hep-ph/0104016](#), [doi:10.1016/S0550-3213\(01\)00302-9](#).

- [111] S. Coleman, F. De Luccia, Gravitational effects on and of vacuum decay, *Phys. Rev. D* 21 (1980) 3305–3315. doi:[10.1103/PhysRevD.21.3305](https://doi.org/10.1103/PhysRevD.21.3305).
- [112] F. Bezrukov, M. Shaposhnikov, Why should we care about the top quark Yukawa coupling?, *J. Exp. Theor. Phys.* 120 (2015) 335–343, [*Zh. Eksp. Teor. Fiz.*147,389(2015)]. arXiv:[1411.1923](https://arxiv.org/abs/1411.1923), doi:[10.1134/S1063776115030152](https://doi.org/10.1134/S1063776115030152).
- [113] M. Bando, T. Kugo, N. Maekawa, H. Nakano, Improving the effective potential, *Phys. Lett. B*301 (1993) 83–89. arXiv:[hep-ph/9210228](https://arxiv.org/abs/hep-ph/9210228), doi:[10.1016/0370-2693\(93\)90725-W](https://doi.org/10.1016/0370-2693(93)90725-W).
- [114] J. Beringer, et al., Review of particle physics*, *Phys. Rev. D* 86 (2012) 010001. doi:[10.1103/PhysRevD.86.010001](https://doi.org/10.1103/PhysRevD.86.010001).
- [115] J. Elias-Miro, J. R. Espinosa, T. Konstandin, Taming Infrared Divergences in the Effective Potential, *JHEP* 08 (2014) 034. arXiv:[1406.2652](https://arxiv.org/abs/1406.2652), doi:[10.1007/JHEP08\(2014\)034](https://doi.org/10.1007/JHEP08(2014)034).
- [116] **CMS**, Combination of the CMS top-quark mass measurements from Run 1 of the LHC (2014). Rep. number: CMS-PAS-TOP-14-015.
- [117] A. Kobakhidze, A. Spencer-Smith, The Higgs vacuum is unstable. arXiv:[1404.4709](https://arxiv.org/abs/1404.4709).
- [118] F. Loebbert, J. Plefka, Quantum Gravitational Contributions to the Standard Model Effective Potential and Vacuum Stability, *Mod. Phys. Lett. A*30 (34) (2015) 1550189. arXiv:[1502.03093](https://arxiv.org/abs/1502.03093), doi:[10.1142/S0217732315501898](https://doi.org/10.1142/S0217732315501898).
- [119] Z. Lalak, M. Lewicki, P. Olszewski, Standard Model vacuum stability in the presence of gauge invariant nonrenormalizable operators, *PoS PLANCK2015* (2015) 076. arXiv:[1510.02797](https://arxiv.org/abs/1510.02797).
- [120] J. R. Espinosa, Implications of the top (and Higgs) mass for vacuum stability, *PoS TOP2015* (2016) 043. arXiv:[1512.01222](https://arxiv.org/abs/1512.01222).
- [121] I. Masina, The Gravitational Wave Background and Higgs False Vacuum Inflation, *Phys.Rev. D*89 (2014) 123505. arXiv:[1403.5244](https://arxiv.org/abs/1403.5244), doi:[10.1103/PhysRevD.89.123505](https://doi.org/10.1103/PhysRevD.89.123505).
- [122] M. Gasperini, *Lezioni di Cosmologia Teorica*, Springer-Verlag, Milano, 2012. doi:[10.1007/9788847024847](https://doi.org/10.1007/9788847024847).
- [123] D. J. Schwarz, C. A. Terrero-Escalante, A. A. Garcia, Higher order corrections to primordial spectra from cosmological inflation, *Phys. Lett. B*517 (2001) 243–249. arXiv:[astro-ph/0106020](https://arxiv.org/abs/astro-ph/0106020), doi:[10.1016/S0370-2693\(01\)01036-X](https://doi.org/10.1016/S0370-2693(01)01036-X).
- [124] A. H. Guth, The Inflationary Universe: A Possible Solution to the Horizon and Flatness Problems, *Phys.Rev. D*23 (1981) 347–356. doi:[10.1103/PhysRevD.23.347](https://doi.org/10.1103/PhysRevD.23.347).
- [125] A. H. Guth, Eternal inflation and its implications, *J. Phys. A*40 (2007) 6811–6826. arXiv:[hep-th/0702178](https://arxiv.org/abs/hep-th/0702178), doi:[10.1088/1751-8113/40/25/S25](https://doi.org/10.1088/1751-8113/40/25/S25).

- [126] A. D. Linde, Chaotic Inflation, *Phys.Lett. B*129 (1983) 177–181. doi:[10.1016/0370-2693\(83\)90837-7](https://doi.org/10.1016/0370-2693(83)90837-7).
- [127] R. Allahverdi, R. Brandenberger, F.-Y. Cyr-Racine, A. Mazumdar, Reheating in Inflationary Cosmology: Theory and Applications, *Ann. Rev. Nucl. Part. Sci.* 60 (2010) 27–51. arXiv:[1001.2600](https://arxiv.org/abs/1001.2600), doi:[10.1146/annurev.nucl.012809.104511](https://doi.org/10.1146/annurev.nucl.012809.104511).
- [128] A. A. Penzias, R. W. Wilson, A Measurement of excess antenna temperature at 4080-Mc/s, *Astrophys. J.* 142 (1965) 419–421. doi:[10.1086/148307](https://doi.org/10.1086/148307).
- [129] S. Dodelson, *Modern Cosmology*, Academic Press, Amsterdam, 2003.
- [130] V. F. Mukhanov, H. Feldman, R. H. Brandenberger, Theory of cosmological perturbations. Part 1. Classical perturbations. Part 2. Quantum theory of perturbations. Part 3. Extensions, *Phys.Rept.* 215 (1992) 203–333. doi:[10.1016/0370-1573\(92\)90044-Z](https://doi.org/10.1016/0370-1573(92)90044-Z).
- [131] V. F. Mukhanov, G. V. Chibisov, Quantum Fluctuation and Nonsingular Universe. (In Russian), *JETP Lett.* 33 (1981) 532–535.
- [132] M. Scalisi, Inflation, Universality and Attractors, Ph.D. thesis, Groningen U. (2016). arXiv:[1607.01030](https://arxiv.org/abs/1607.01030).
- [133] **Planck**, P. A. R. Ade, et al., Planck 2015 results. XX. Constraints on inflation. arXiv:[1502.02114](https://arxiv.org/abs/1502.02114).
- [134] **Planck**, **BICEP2/Keck Array**, P. Ade, et al., Joint Analysis of BICEP2/KeckArray and Planck Data, *Phys. Rev. Lett.* 114 (2015) 101301. arXiv:[1502.00612](https://arxiv.org/abs/1502.00612), doi:[10.1103/PhysRevLett.114.101301](https://doi.org/10.1103/PhysRevLett.114.101301).
- [135] **BICEP2**, P. Ade, et al., Detection of B-Mode Polarization at Degree Angular Scales by BICEP2, *Phys.Rev.Lett.* 112 (2014) 241–101. arXiv:[1403.3985](https://arxiv.org/abs/1403.3985), doi:[10.1103/PhysRevLett.112.241101](https://doi.org/10.1103/PhysRevLett.112.241101).
- [136] **BICEP2**, **Keck Array**, P. A. R. Ade, et al., Improved Constraints on Cosmology and Foregrounds from BICEP2 and Keck Array Cosmic Microwave Background Data with Inclusion of 95 GHz Band, *Phys. Rev. Lett.* 116 (2016) 031302. arXiv:[1510.09217](https://arxiv.org/abs/1510.09217), doi:[10.1103/PhysRevLett.116.031302](https://doi.org/10.1103/PhysRevLett.116.031302).
- [137] D. H. Lyth, What would we learn by detecting a gravitational wave signal in the cosmic microwave background anisotropy?, *Phys. Rev. Lett.* 78 (1997) 1861–1863. arXiv:[hep-ph/9606387](https://arxiv.org/abs/hep-ph/9606387), doi:[10.1103/PhysRevLett.78.1861](https://doi.org/10.1103/PhysRevLett.78.1861).
- [138] G. Isidori, V. S. Rychkov, A. Strumia, N. Tetradis, Gravitational corrections to standard model vacuum decay, *Phys.Rev. D*77 (2008) 025034. arXiv:[0712.0242](https://arxiv.org/abs/0712.0242), doi:[10.1103/PhysRevD.77.025034](https://doi.org/10.1103/PhysRevD.77.025034).
- [139] A. De Simone, A. Riotto, Cosmological Perturbations from the Standard Model Higgs, *JCAP* 1302 (2013) 014. arXiv:[1208.1344](https://arxiv.org/abs/1208.1344), doi:[10.1088/1475-7516/2013/02/014](https://doi.org/10.1088/1475-7516/2013/02/014).

- [140] A. Notari, Higgs Mass and Gravity Waves in Standard Model False Vacuum Inflation, *Phys. Rev. D*91 (2015) 063527. [arXiv:1405.6943](#), [doi:10.1103/PhysRevD.91.063527](#).
- [141] F. Bezrukov, J. Rubio, M. Shaposhnikov, Living beyond the edge: Higgs inflation and vacuum metastability, *Phys. Rev. D*92 (8) (2015) 083512. [arXiv:1412.3811](#), [doi:10.1103/PhysRevD.92.083512](#).
- [142] M. Quiros, Finite temperature field theory and phase transitions, in: *Proceedings, Summer School in High-energy physics and cosmology: Trieste, Italy, June 29–July 17, 1998, 1999*, pp. 187–259. [arXiv:hep-ph/9901312](#).
- [143] M. Gell-Mann, P. Ramond, R. Slansky, Complex Spinors and Unified Theories, *Conf. Proc. C*790927 (1979) 315–321. [arXiv:1306.4669](#).
- [144] T. Yanagida, proceedings of the workshop on unified theories and baryon number in the universe, tsukuba, 1979, eds. a. sawada, a. sugamoto, Tech. rep., KEK Report.
- [145] R. N. Mohapatra, G. Senjanović, Neutrino mass and spontaneous parity nonconservation, *Phys. Rev. Lett.* 44 (1980) 912–915. [doi:10.1103/PhysRevLett.44.912](#).
- [146] S. Weinberg, *The quantum theory of fields. Vol. 2: Modern applications*, Cambridge University Press, 2013.
- [147] J. A. Casas, V. Di Clemente, A. Ibarra, M. Quiros, Massive neutrinos and the Higgs mass window, *Phys. Rev. D*62 (2000) 053005. [arXiv:hep-ph/9904295](#), [doi:10.1103/PhysRevD.62.053005](#).
- [148] I. Gogoladze, N. Okada, Q. Shafi, Higgs Boson Mass Bounds in the Standard Model with Type III and Type I Seesaw, *Phys. Lett. B*668 (2008) 121–125. [arXiv:0805.2129](#), [doi:10.1016/j.physletb.2008.08.023](#).
- [149] S. Iso, N. Okada, Y. Orikasa, The minimal $B - L$ model naturally realized at TeV scale, *Phys. Rev. D*80 (2009) 115007. [arXiv:0909.0128](#), [doi:10.1103/PhysRevD.80.115007](#).
- [150] W. Rodejohann, H. Zhang, Impact of massive neutrinos on the Higgs self-coupling and electroweak vacuum stability, *JHEP* 06 (2012) 022. [arXiv:1203.3825](#), [doi:10.1007/JHEP06\(2012\)022](#).
- [151] J. Chakraborty, M. Das, S. Mohanty, Constraints on TeV scale Majorana neutrino phenomenology from the Vacuum Stability of the Higgs, *Mod. Phys. Lett. A*28 (2013) 1350032. [arXiv:1207.2027](#), [doi:10.1142/S0217732313500326](#).
- [152] W. Chao, M. Gonderinger, M. J. Ramsey-Musolf, Higgs Vacuum Stability, Neutrino Mass, and Dark Matter, *Phys. Rev. D*86 (2012) 113017. [arXiv:1210.0491](#), [doi:10.1103/PhysRevD.86.113017](#).
- [153] A. Datta, A. Elsayed, S. Khalil, A. Moursy, Higgs vacuum stability in the $B - L$ extended standard model, *Phys. Rev. D*88 (5) (2013) 053011. [arXiv:1308.0816](#), [doi:10.1103/PhysRevD.88.053011](#).

- [154] J. Chakraborty, P. Konar, T. Mondal, Constraining a class of $b - l$ extended models from vacuum stability and perturbativity, *Phys.Rev. D*89 (2014) 056014. [arXiv:1308.1291](#), [doi:10.1103/PhysRevD.89.056014](#).
- [155] S. Khalil, Low scale $B - L$ extension of the Standard Model at the LHC, *J. Phys. G*35 (2008) 055001. [arXiv:hep-ph/0611205](#), [doi:10.1088/0954-3899/35/5/055001](#).
- [156] W. Emam, S. Khalil, Higgs and Z-prime phenomenology in $B - L$ extension of the standard model at LHC, *Eur. Phys. J. C*52 (2007) 625–633. [arXiv:0704.1395](#), [doi:10.1140/epjc/s10052-007-0411-7](#).
- [157] L. Basso, A. Belyaev, S. Moretti, C. H. Shepherd-Themistocleous, Phenomenology of the minimal $B - L$ extension of the Standard model: Z' and neutrinos, *Phys. Rev. D*80 (2009) 055030. [arXiv:0812.4313](#), [doi:10.1103/PhysRevD.80.055030](#).
- [158] L. Basso, S. Moretti, G. M. Pruna, A Renormalisation Group Equation Study of the Scalar Sector of the Minimal $B - L$ Extension of the Standard Model, *Phys. Rev. D*82 (2010) 055018. [arXiv:1004.3039](#), [doi:10.1103/PhysRevD.82.055018](#).
- [159] S. Khalil, TeV-scale gauged $B - L$ symmetry with inverse seesaw mechanism, *Phys. Rev. D*82 (2010) 077702. [arXiv:1004.0013](#), [doi:10.1103/PhysRevD.82.077702](#).
- [160] A. Kobakhidze, A. Spencer-Smith, Neutrino Masses and Higgs Vacuum Stability, *JHEP* 08 (2013) 036. [arXiv:1305.7283](#), [doi:10.1007/JHEP08\(2013\)036](#).
- [161] N. Okada, Q. Shafi, Observable Gravity Waves From $U(1)_{B-L}$ Higgs and Coleman-Weinberg Inflation. [arXiv:1311.0921](#).
- [162] D. Raut, N. Okada, Running Non-Minimal Inflation with Stabilized Inflation Potential, *PoS DSU2015* (2016) 013. [arXiv:1509.04439](#).
- [163] S.-M. Choi, H. M. Lee, Inflection point inflation and reheating, *Eur. Phys. J. C*76 (6) (2016) 303. [arXiv:1601.05979](#), [doi:10.1140/epjc/s10052-016-4150-5](#).
- [164] L. Basso, Minimal Z' models and the 125 GeV Higgs boson, *Phys. Lett. B*725 (2013) 322–326. [arXiv:1303.1084](#), [doi:10.1016/j.physletb.2013.07.025](#).
- [165] N. Okada, S. Okada, Z'_{BL} portal dark matter and LHC Run-2 results, *Phys. Rev. D*93 (7) (2016) 075003. [arXiv:1601.07526](#), [doi:10.1103/PhysRevD.93.075003](#).
- [166] R. N. Mohapatra, A. Y. Smirnov, Neutrino Mass and New Physics, *Ann. Rev. Nucl. Part. Sci.* 56 (2006) 569–628. [arXiv:hep-ph/0603118](#), [doi:10.1146/annurev.nucl.56.080805.140534](#).
- [167] J. Elias-Miro, J. R. Espinosa, G. F. Giudice, H. M. Lee, A. Strumia, Stabilization of the Electroweak Vacuum by a Scalar Threshold Effect, *JHEP* 06 (2012) 031. [arXiv:1203.0237](#), [doi:10.1007/JHEP06\(2012\)031](#).
- [168] G. Ballesteros, C. Tamarit, Radiative plateau inflation. , *JHEP* 02 (2016) 153. [arXiv:1510.05669](#), [doi:10.1007/JHEP02\(2016\)153](#).

- [169] G. Ballesteros, J. Redondo, A. Ringwald, C. Tamarit, Standard Model-Axion-Seesaw-Higgs Portal Inflation. Five problems of particle physics and cosmology solved in one stroke [arXiv:1610.01639](#).
- [170] Y. Hamada, H. Kawai, K.-Y. Oda, Predictions on mass of Higgs portal scalar dark matter from Higgs inflation and flat potential, *JHEP* 1407 (2014) 026. [arXiv:1404.6141](#), [doi:10.1007/JHEP07\(2014\)026](#).
- [171] N. Haba, H. Ishida, R. Takahashi, Higgs inflation and Higgs portal dark matter with right-handed neutrinos, *PTEP* 2015 (5) (2015) 053B01. [arXiv:1405.5738](#), [doi:10.1093/ptep/ptv053](#).
- [172] L. Boubekeur, D. Lyth, Hilltop inflation, *JCAP* 0507 (2005) 010. [arXiv:hep-ph/0502047](#), [doi:10.1088/1475-7516/2005/07/010](#).
- [173] A. R. Liddle, D. H. Lyth, *Cosmological inflation and large scale structure*, 2000.
- [174] G. F. Giudice, E. W. Kolb, A. Riotto, Largest temperature of the radiation era and its cosmological implications, *Phys. Rev. D* 64 (2001) 023508. [arXiv:hep-ph/0005123](#), [doi:10.1103/PhysRevD.64.023508](#).
- [175] P. F. de Salas, M. Lattanzi, G. Mangano, G. Miele, S. Pastor, O. Pisanti, Bounds on very low reheating scenarios after Planck, *Phys. Rev. D* 92 (12) (2015) 123534. [arXiv:1511.00672](#), [doi:10.1103/PhysRevD.92.123534](#).
- [176] Y. Chikashige, R. Mohapatra, R. Peccei, Are there real goldstone bosons associated with broken lepton number?, *Physics Letters B* 98 (4) (1981) 265 – 268. [doi:10.1016/0370-2693\(81\)90011-3](#).
- [177] V. Berezhinsky, J. W. F. Valle, The KeV majoron as a dark matter particle, *Phys. Lett. B* 318 (1993) 360–366. [arXiv:hep-ph/9309214](#), [doi:10.1016/0370-2693\(93\)90140-D](#).
- [178] M. Lattanzi, J. W. F. Valle, Decaying warm dark matter and neutrino masses, *Phys. Rev. Lett.* 99 (2007) 121301. [arXiv:0705.2406](#), [doi:10.1103/PhysRevLett.99.121301](#).
- [179] M. Lattanzi, S. Riemer-Sorensen, M. Tortola, J. W. F. Valle, Updated CMB and x - and γ -ray constraints on Majoron dark matter, *Phys. Rev. D* 88 (6) (2013) 063528. [arXiv:1303.4685](#), [doi:10.1103/PhysRevD.88.063528](#).
- [180] M. Frigerio, T. Hambye, E. Masso, Sub-GeV dark matter as pseudo-Goldstone from the seesaw scale, *Phys. Rev. X* 1 (2011) 021026. [arXiv:1107.4564](#), [doi:10.1103/PhysRevX.1.021026](#).
- [181] G. Lazarides, Q. Shafi, Origin of matter in the inflationary cosmology, *Physics Letters B* 258 (3) (1991) 305 – 309. [doi:10.1016/0370-2693\(91\)91090-I](#).
- [182] A. A. Starobinsky, Spectrum of relict gravitational radiation and the early state of the universe, *JETP Lett.* 30 (1979) 682–685.

- [183] A. A. Starobinsky, A New Type of Isotropic Cosmological Models Without Singularity, *Phys.Lett. B*91 (1980) 99–102. doi:[10.1016/0370-2693\(80\)90670-X](https://doi.org/10.1016/0370-2693(80)90670-X).
- [184] N. Birrell, P. Davies, *Quantum Fields in Curved Space*, Cambridge Monogr.Math.Phys., 1982. doi:doi.org/10.1017/CB09780511622632.
- [185] M. Atkins, X. Calmet, Bounds on the Nonminimal Coupling of the Higgs Boson to Gravity, *Phys. Rev. Lett.* 110 (5) (2013) 051301. arXiv:[1211.0281](https://arxiv.org/abs/1211.0281), doi:[10.1103/PhysRevLett.110.051301](https://doi.org/10.1103/PhysRevLett.110.051301).
- [186] A. De Simone, M. P. Hertzberg, F. Wilczek, Running Inflation in the Standard Model, *Phys.Lett. B*678 (2009) 1–8. arXiv:[0812.4946](https://arxiv.org/abs/0812.4946), doi:[10.1016/j.physletb.2009.05.054](https://doi.org/10.1016/j.physletb.2009.05.054).
- [187] F. Bezrukov, M. Shaposhnikov, Standard Model Higgs boson mass from inflation: Two loop analysis, *JHEP* 0907 (2009) 089. arXiv:[0904.1537](https://arxiv.org/abs/0904.1537), doi:[10.1088/1126-6708/2009/07/089](https://doi.org/10.1088/1126-6708/2009/07/089).
- [188] R. N. Lerner, J. McDonald, Distinguishing Higgs inflation and its variants, *Phys.Rev. D*83 (2011) 123522. arXiv:[1104.2468](https://arxiv.org/abs/1104.2468), doi:[10.1103/PhysRevD.83.123522](https://doi.org/10.1103/PhysRevD.83.123522).
- [189] K. Allison, Higgs xi-inflation for the 125-126 GeV Higgs: a two-loop analysis, *JHEP* 1402 (2014) 040. arXiv:[1306.6931](https://arxiv.org/abs/1306.6931), doi:[10.1007/JHEP02\(2014\)040](https://doi.org/10.1007/JHEP02(2014)040).
- [190] F. Bezrukov, A. Magnin, M. Shaposhnikov, Standard Model Higgs boson mass from inflation, *Phys.Lett. B*675 (2009) 88–92. arXiv:[0812.4950](https://arxiv.org/abs/0812.4950), doi:[10.1016/j.physletb.2009.03.035](https://doi.org/10.1016/j.physletb.2009.03.035).
- [191] A. Barvinsky, A. Y. Kamenshchik, A. Starobinsky, Inflation scenario via the Standard Model Higgs boson and LHC, *JCAP* 0811 (2008) 021. arXiv:[0809.2104](https://arxiv.org/abs/0809.2104), doi:[10.1088/1475-7516/2008/11/021](https://doi.org/10.1088/1475-7516/2008/11/021).
- [192] V. Faraoni, E. Gunzig, Einstein frame or Jordan frame?, *Int.J.Theor.Phys.* 38 (1999) 217–225. arXiv:[astro-ph/9910176](https://arxiv.org/abs/astro-ph/9910176), doi:[10.1023/A:1026645510351](https://doi.org/10.1023/A:1026645510351).
- [193] M. Shaposhnikov, D. Zenhausern, Scale invariance, unimodular gravity and dark energy, *Phys. Lett. B*671 (2009) 187–192. arXiv:[0809.3395](https://arxiv.org/abs/0809.3395), doi:[10.1016/j.physletb.2008.11.054](https://doi.org/10.1016/j.physletb.2008.11.054).
- [194] M. Shaposhnikov, D. Zenhausern, Quantum scale invariance, cosmological constant and hierarchy problem, *Phys. Lett. B*671 (2009) 162–166. arXiv:[0809.3406](https://arxiv.org/abs/0809.3406), doi:[10.1016/j.physletb.2008.11.041](https://doi.org/10.1016/j.physletb.2008.11.041).
- [195] A. Salvio, A. Strumia, Agravity, *JHEP* 06 (2014) 080. arXiv:[1403.4226](https://arxiv.org/abs/1403.4226), doi:[10.1007/JHEP06\(2014\)080](https://doi.org/10.1007/JHEP06(2014)080).
- [196] K. Kannike, G. Hutsi, L. Pizza, A. Racioppi, M. Raidal, A. Salvio, A. Strumia, Dynamically Induced Planck Scale and Inflation, *JHEP* 05 (2015) 065. arXiv:[1502.01334](https://arxiv.org/abs/1502.01334), doi:[10.1007/JHEP05\(2015\)065](https://doi.org/10.1007/JHEP05(2015)065).

- [197] R. Catena, M. Pietroni, L. Scarabello, Einstein and Jordan reconciled: a frame-invariant approach to scalar-tensor cosmology, *Phys. Rev. D* 76 (2007) 084039. [arXiv:astro-ph/0604492](#), [doi:10.1103/PhysRevD.76.084039](#).
- [198] T. Prokopec, J. Weenink, Frame independent cosmological perturbations, *JCAP* 1309 (2013) 027. [arXiv:1304.6737](#), [doi:10.1088/1475-7516/2013/09/027](#).
- [199] A. Yu. Kamenshchik, C. F. Steinwachs, Question of quantum equivalence between Jordan frame and Einstein frame, *Phys. Rev. D* 91 (8) (2015) 084033. [arXiv:1408.5769](#), [doi:10.1103/PhysRevD.91.084033](#).
- [200] D. P. George, S. Mooij, M. Postma, Quantum corrections in Higgs inflation: the Standard Model case, *JCAP* 1604 (04) (2016) 006. [arXiv:1508.04660](#), [doi:10.1088/1475-7516/2016/04/006](#).
- [201] A. Salvio, Higgs Inflation at NNLO after the Boson Discovery, *Phys.Lett. B* 727 (2013) 234–239. [arXiv:1308.2244](#), [doi:10.1016/j.physletb.2013.10.042](#).
- [202] F. Bezrukov, M. Shaposhnikov, Higgs inflation at the critical point, *Phys. Lett. B* 734 (2014) 249–254. [arXiv:1403.6078](#), [doi:10.1016/j.physletb.2014.05.074](#).
- [203] D. I. Kaiser, Primordial spectral indices from generalized Einstein theories, *Phys.Rev. D* 52 (1995) 4295–4306. [arXiv:astro-ph/9408044](#), [doi:10.1103/PhysRevD.52.4295](#).
- [204] F. Bezrukov, D. Gorbunov, M. Shaposhnikov, On initial conditions for the Hot Big Bang, *JCAP* 0906 (2009) 029. [arXiv:0812.3622](#), [doi:10.1088/1475-7516/2009/06/029](#).
- [205] A. D. Linde, A New Inflationary Universe Scenario: A Possible Solution of the Horizon, Flatness, Homogeneity, Isotropy and Primordial Monopole Problems, *Phys.Lett. B* 108 (1982) 389–393. [doi:10.1016/0370-2693\(82\)91219-9](#).
- [206] A. Kehagias, A. M. Dizgah, A. Riotto, Remarks on the Starobinsky model of inflation and its descendants, *Phys. Rev. D* 89 (4) (2014) 043527. [arXiv:1312.1155](#), [doi:10.1103/PhysRevD.89.043527](#).
- [207] F. Bezrukov, D. Gorbunov, Distinguishing between R^2 -inflation and Higgs-inflation, *Phys.Lett. B* 713 (2012) 365–368. [arXiv:1111.4397](#), [doi:10.1016/j.physletb.2012.06.040](#).
- [208] X. ysis, I. Kuntz, Higgs Starobinsky Inflation, *Eur. Phys. J. C* 76 (5) (2016) 289. [arXiv:1605.02236](#), [doi:10.1140/epjc/s10052-016-4136-3](#).
- [209] C. Burgess, H. M. Lee, M. Trott, Comment on Higgs Inflation and Naturalness, *JHEP* 1007 (2010) 007. [arXiv:1002.2730](#), [doi:10.1007/JHEP07\(2010\)007](#).
- [210] J. Barbon, J. Espinosa, On the Naturalness of Higgs Inflation, *Phys.Rev. D* 79 (2009) 081302. [arXiv:0903.0355](#), [doi:10.1103/PhysRevD.79.081302](#).
- [211] M. Atkins, X. Calmet, Remarks on Higgs Inflation, *Phys.Lett. B* 697 (2011) 37–40. [arXiv:1011.4179](#), [doi:10.1016/j.physletb.2011.01.028](#).

- [212] F. Bezrukov, A. Magnin, M. Shaposhnikov, S. Sibiryakov, Higgs inflation: consistency and generalisations, *JHEP* 1101 (2011) 016. [arXiv:1008.5157](#), [doi:10.1007/JHEP01\(2011\)016](#).
- [213] F. del Aguila, G. D. Coughlan, M. Quiros, Gauge Coupling Renormalization With Several U(1) Factors, *Nucl. Phys. B*307 (1988) 633, [Erratum: *Nucl. Phys. B*312,751(1989)]. [doi:10.1016/0550-3213\(88\)90266-0](#).
- [214] M. Abramowitz, I. Stegun, *Handbook of Mathematical Functions*, Dover Publications, 1965.
- [215] K. Melnikov, T. van Ritbergen, The Three loop on-shell renormalization of QCD and QED, *Nucl. Phys. B*591 (2000) 515–546. [arXiv:hep-ph/0005131](#), [doi:10.1016/S0550-3213\(00\)00526-5](#).

This thesis was created using \LaTeX and edited in the Windows 8.1 environment. The typesetting software used is the MiKTeX distribution, while the style package adopted is "Tesi Classica" by Lorenzo Pantieri, with some minor adjustments.

Giuseppe Iacobellis: *Higgs connections: Electroweak Vacuum Stability and Cosmology*,
Ph.D. Thesis, © march 2017.